U.PORTO

FEUP FACULDADE DE ENGENHARIA
UNIVERSIDADE DO PORTO

Multistage treatment system for leachates from industrial hazardous and non-hazardous waste landfills

Thesis submitted in partial fulfilment of the requirements for the degree of Doctor of Philosophy in Environmental Engineering at the Faculty of Engineering, University of Porto

Inalmar Dantas Barbosa Segundo

Supervisor: Vítor Jorge Pais Vilar, Ph.D.
Co-Supervisors: Maria Francisca da Costa Moreira, Ph.D.
Tânia Filomena Castro Valente Silva, Ph.D.

Laboratory of Separation and Reaction Engineering – Laboratory of Catalysis and Materials (LSRE-LCM)
Department of Chemical Engineering
Faculty of Engineering
University of Porto
January 2021

This work was financially supported by: (i) Base Funding - UIDB/50020/2020 of the Associate Laboratory LSRE-LCM - funded by national funds through *Fundação para a Ciência e a Tecnologia*, (FCT) and *Ministério da Ciência, Tecnologia e Ensino Superior* (MCTES) - *Programa de Investimento e Despesas de Desenvolvimento da Administração Central* (PIDDAC), (ii) Project AIProcMat@N2020 - Advanced Industrial Processes and Materials for a Sustainable Northern Region of Portugal 2020, with the reference NORTE-01-0145-FEDER-000006, supported by Norte Portugal Regional Operational Programme (NORTE 2020), under the Portugal 2020 Partnership Agreement, through the European Regional Development Fund (ERDF); and (iii) *Conselho Nacional de Desenvolvimento Científico e Tecnológico* (CNPq), Brazil, through Inalmar Dantas Barbosa Segundo's doctoral fellowship (reference 205715/2014-1).

LSRE - LCM - FEUP

Acknowledgments

Firstly, it would not have been possible to meet all the objectives of this work without the constant assistance of my supervisors, Dr. Vítor Vilar, Dr. Francisca Moreira, and Dr. Tânia Silva. Thank you so much for your patience, contribution, and encouragement to this work happens.

I would like to thank Marta Costa, Manuela Dinis, and Mariana Abreu, which were responsible for allowing the collection of the leachate from both industrial landfills studied in this work.

I am very grateful to Dr. Alberto Webler and Dr. Ana Isabel Gomes, for all the collaboration and support during these years working together with landfill leachate. The days, nights, and even weekends at the lab, working hard in experiments, solving equipment problems, and taking care of sometimes bipolar and unthankful bacteria, were sufficient to reveal a memorable friendship. Thank you so much for sharing your knowledge with me.

Special thanks to those who shared good moments with me in many refreshing coffees, lunches, lab routines, conferences and also in moments outside the University: Batuíra Filho and Jonathan Cawettiere, who spent all four years along with me, in the happiest times, but in the bad ones too; and also Ana Araújo, Bárbara Araújo, Belisa Marinho, Carolina Ferreira, David Guimarães, Eliamin Rosendo, Luciana Prazeres, Paulo Mazur, and Raíssa Atzingen. You all made it so much easier, "malta". An extended greeting goes to all colleagues from Lab. E404 for the partnership and good work environment: Aida Díez, Ana Caseiro, Ana Ferraz, Ariana Pintor, Bárbara Vieira, Bruna Porto, Daniela Morais, Danieli Brandler, Deborah Cordeiro, Diego Todescato, Elvira Bocos, Gustavo Cunha, Joana Monteiro, João Miller, José Ramos, Jennyfer Diaz, Karyn Nathally, Lais Silva, Larissa Paulista, Maria Vidales, Marlon Caianelo, Patricia Peri, Pedro Presumido, Pello Alfonso, Ridha Djellabi, Salvador Cotillas, Sandra Miranda, Sara Santos, Sílvia Santos and Srikanth Vuppala.

Without the dedication of my ex-wife, Gabriela, and my daughter, Alice, born on this long journey, these years would be more difficult and solitary. Thank you so much for being always with me. Also, I would like to express my genuine acknowledgment to the family that I left in Brazil. Thank you for all the unconditional support and love.

Finally, I am very thankful to the foremost Brazilian ex-presidents, Luís Inácio Lula da Silva and Dilma Rousseff, for the economic investments in superior education that make possible all this work

With love to my daughter, Alice

“We can judge our progress by the courage of our questions and the depth of our answers, our willingness to embrace what is true rather than what feels good.”

Carl Sagan

Abstract

Population growth and global development of industrial activity have been contributing to the severe increase of the generated municipal and industrial solid waste. In developed countries, the deposition of solid waste into landfills is a common practice that leads to the production of large amounts of a highly contaminated liquid stream called leachate. There has been a world-wide effort to develop cost-effective treatment solutions for leachates from municipal solid waste landfills (MSWLs) but the lack of proper treatments for leachates from industrial solid waste landfills (ISWLs), either from non-hazardous ISWLs (NHISWLs) or hazardous ISWLs (HISWLs), is an unavoidable fact. The current thesis aimed at tackling the lack of cost-effective treatment solutions for ISWL leachates by developing multistage treatment strategies for two ISWL leachates: one from a HISWL and another from a NHISWL. The HISWL leachate was characterized by a high/moderate content of organics with low biodegradability and a defiant high salinity mainly due to sulphur compounds (sulphide, sulphite and sulphate) and chloride ions. The NHISWL leachate had a moderate content of organics and salts and low biodegradability.

As regards the treatment of the HISWL leachate, the removal of sulphur compounds was the primary challenge to be overcome in order to get a more biodegradable effluent. This was achieved by the application of a two-stage pre-treatment: (i) catalytic oxidation of sulphide (0.5 g L^{-1}) and sulphite (2.5 g L^{-1}) ions to sulphate ions, followed by (ii) chemical precipitation of sulphates (13 g L^{-1}). Two oxidant agents were tested in the catalytic oxidation: air and hydrogen peroxide (H_2O_2). The transition metals available in the leachate were used as catalysts. Concentrations of sulphide and sulphite lower than 1.0 mg L^{-1} (emission limit value - ELV) were obtained after 5-h oxygenation or 1-min peroxidation under the best conditions, i.e. natural pH, air flow rate of 1 L_{air} $L_{leachate}^{-1}$ min^{-1} and H_2O_2:sulphur stoichiometric molar ratio. Aeration was considered unsafe since more than 33 volatile organic compounds (VOCs) and hydrogen sulphide (H_2S) were released into the atmosphere. Hereafter, the removal of sulphates from the pre-oxidised leachate was assessed by applying chemical precipitation as ettringite ($Ca_6Al_2(SO_4)_3(OH)_{12}\cdot 26H_2O$) or barite ($BaSO_4$) mineralogical phases at distinct pH values and reactants concentration. At natural pH, sulphate contents below 2.0 g L^{-1} (ELV) were achieved using a $[Ca^{2+}]$:$[Al^{3+}]$:$[SO_4^{2-}]$ molar ratio of 12:4:3 (2-fold stoichiometry) and a $[Ba^{2+}]$:$[SO_4^{2-}]$ molar ratio of 1.0:1.0 (1-fold stoichiometry). The analysis of precipitates by X-ray diffraction (XRD) showed a three-phase ettringite (only 67% corresponding to ettringite itself) and single-phase barite. Barite precipitation proved to be more appealing since a value-added product was obtained and, furthermore, fewer reactants were required.

After sulphur compounds removal using (i) H_2O_2-driven catalytic oxidation and (ii) chemical precipitation through barite, the following treatment technologies were applied to the HISWL leachate: biological oxidation, coagulation, and different advanced oxidation processes (AOPs)/electrochemical AOPs (EAOPs), such as H_2O_2 photolysis with ultraviolet C (UVC) radiation (H_2O_2/UVC), anodic oxidation (AO), photo-Fenton oxidation with ultraviolet A (UVA) radiation (PF-UVA) or UVC radiation (PF-UVC), and photoelectro-Fenton oxidation with UVA radiation (PEF-UVA). These technologies were incorporated into three different treatment trains. From the various tested technologies and strategies, the best treatment line for the HISWL leachate counted on four more stages, with a total of six stages: (iii) 1st biological oxidation for removal of biodegradable organic compounds and nitrogen species, (iv) coagulation with ferric chloride (coagulant dose of 100 mg Fe L^{-1}, pH 2.8) for removal of a fraction of recalcitrant organics and suspended solids, (v) PF-UVA process with 4-h duration (pH 2.8, initial total dissolved iron content of 140 mg L^{-1}) for recalcitrant organics degradation and biodegradability improvement, and (vi) 2nd biological oxidation for removal of the biodegradable organic matter resulting from the PF-UVA process. The use of AO instead of the PF-UVA process demonstrated to be unfeasible mainly due to the release of high amounts of the hazardous chlorine gas, as a consequence of the high content of chloride, and generation of high amounts of foam. The PEF-UVA process also revealed some important operational drawbacks related to the deposition of particles on the cathode surface that inhibited the electrochemical generation of H_2O_2. The discharge of the final effluent directly in a waterbody was not possible due to the unfeasibility of reaching a chemical oxygen demand (COD) below the ELV imposed by legislation (125 or 150 mg O_2 L^{-1} according to the European or Portuguese legislation, respectively). However, it was possible to achieve a COD below 1000 mg O_2 L^{-1}, which is a common limit imposed by municipal wastewater treatment plants (MWWTPs) to effluents discharged into the municipal sewer.

Focusing on the possibility of fulfilling the COD ELV for the discharge of treated effluents into waterbodies, the HISWL leachate was collected for a second time (leachate with some different characteristics mainly as regards the organic matter) and the impact of ozonation and ozone (O_3)-based AOPs as a stage (iii) after chemical precipitation or as a stage (iv) after chemical precipitation followed by coagulation was assessed. This HISWL leachate did not contain organic biodegradable compounds to justify the application of biological oxidation after chemical precipitation. O_3-based AOPs encompassed: perozonation (O_3/H_2O_2), photo-assisted ozonation (O_3/UVC), photo-assisted perozonation (O_3/H_2O_2/UVC) and O_3/H_2O_2/UVC system after Fe-mediated coagulation targeting photo-Fenton-assisted ozonation (O_3/PF). The best treatment train excluded a coagulation stage and included an O_3/H_2O_2 process for ~2.1 h (natural pH; room temperature; 3.5 kg O_3 per m^3 leachate; 1.1 kg H_2O_2

per m^3 leachate) as a stage (iii), followed by biological oxidation for removal of the biodegradable organic matter resulting from the O_3/H_2O_2 process. This gave rise to a four-stage treatment. Once again, it was not reached COD values able to discharge the leachate to water bodies.

Regarding the NHISWL leachate, the application of coagulation and biological processes were appraised as well as of the following AOPs/EAOPs: PF-UVA, PF-UVC, AO, and ozonation and O_3-based technologies, such as O_3/H_2O_2, O_3/UVC and O_3/PF. The best multistage treatment strategy included the following three stages: (i) coagulation with ferric chloride (coagulant dose of 300 mg Fe L^{-1}, pH 4.0) for partial removal of organics and phosphorous, (ii) PF-UVC process with 4-h duration (pH 4.0, initial total dissolved iron content of 115 mg L^{-1}) for recalcitrant organics oxidation, and (iii) biological process for removal of the generated biodegradable organics and of nitrogen compounds in the case of optimized operational conditions. The application of coagulation prior to the AOP/EAOP stage has proved indispensable for the fulfilment of legislation demands. Upon treatment, the NHISWL leachate fulfilled European and Portuguese requirements for discharge into aquatic systems, except for ammonium and consequently for total nitrogen.

The treatment of ISWL leachates proved to be a big challenge, in special the treatment of HISWL leachates.

Resumo

O crescimento populacional e o desenvolvimento global da atividade industrial têm contribuído para o crescimento acentuado da geração de resíduos sólidos urbanos e industriais. Nos países desenvolvidos, a deposição de resíduos sólidos em aterros é uma prática comum que leva a produção de grandes quantidades de uma corrente líquida altamente contaminada chamada de lixiviado. Tem havido um esforço à escala mundial para que se desenvolvam soluções de tratamento de lixiviados de aterros de resíduos sólidos urbanos (ARSUs) com bom custo-benefício, mas a falta de tratamentos adequados para os lixiviados de aterros de resíduos sólidos industriais (ARSIs), quer ARSIs não perigosos (ARSINPs) quer ARSIs perigosos (ARSIPs), é um fato inquestionável. A presente tese visou combater a falta de soluções viáveis de tratamento de lixiviados de ARSIs através do desenvolvimento de estratégias integradas de tratamento para dois lixiviados de ARSIs: um proveniente de um ARSIP e outro oriundo de um ARSINP. O lixiviado do ARSIP caracterizou-se por um conteúdo moderado/alto de compostos orgânicos com baixa biodegradabilidade e uma salinidade desafiadora, principalmente devido a compostos de enxofre (sulfuretos, sulfitos e sulfatos) e a iões cloreto. O lixiviado do ARSINP possuía um conteúdo moderado de compostos orgânicos e de sais, além de uma baixa biodegradabilidade.

No que diz respeito ao tratamento do lixiviado do ARSIP, a remoção de compostos de enxofre foi o primeiro desafio a ser superado na busca por um efluente mais biodegradável. Isso foi alcançado através da aplicação de um pré-tratamento de dois estágios: (i) oxidação catalítica dos iões sulfureto (0,5 g L^{-1}) e sulfito (2,5 g L^{-1}) a iões sulfato, seguida por (ii) precipitação química dos sulfatos (13 g L^{-1}). Dois agentes oxidantes foram testados na oxidação catalítica: ar e peróxido de hidrogênio (H_2O_2). Os metais de transição disponíveis no lixiviado foram usados como catalisadores. Concentrações de sulfuretos e sulfitos abaixo de 1,0 mg L^{-1} (valor limite de emissão – VLE) foram obtidos após 5 h de oxigenação ou 1 min de peroxidação nas melhores condições, isto é, pH natural, caudal de ar de 1 L_{ar} $L_{lixiviado}^{-1}$ min^{-1}, e razão molar estequiométrica entre H_2O_2:enxofre. A aeração foi considerada insegura uma vez que mais de 33 compostos orgânicos voláteis (COVs) e sulfureto de hidrogénio (H_2S) foram libertados para a atmosfera. De seguida, a remoção dos sulfatos do lixiviado foi avaliada através da aplicação da precipitação química como etringita ($Ca_6Al_2(SO_4)_3(OH)_{12}\cdot 26H_2O$) ou barita ($BaSO_4$) a distintos valores de pH e concentração de reagentes. Ao pH natural, concentrações de sulfato abaixo do VLE (2.0 g L^{-1}) foram alcançadas usando uma razão molar de 12:4:3 para a etringita ($[Ca^{2+}]$:$[Al^{3+}]$:$[SO_4^{2-}]$) e de 1,0:1,0 ($[Ba^{2+}]$:$[SO_4^{2-}]$) para a barita. A análise dos precipitados por difração de raios-X (DRX) revelou uma etringita com três fases (somente 67% correspondia à etringita propriamente dita), e uma barita com uma

única fase. A precipitação dos sulfatos na forma de barita provou ser mais apelativa uma vez que se obteve um produto com valor acrescentado e foram necessários menos reagentes.

Após remoção dos compostos de enxofre usando (i) oxidação catalítica com H_2O_2 e (ii) precipitação química de barita, as seguintes tecnologias de tratamento foram aplicadas para o lixiviado do ARSIP: oxidação biológica, coagulação, e diferentes processos de oxidação avançados (POAs) e processos eletroquímicos de oxidação avançados (PEOAs), como a fotólise do H_2O_2 com radiação ultra-violeta C (H_2O_2/UVC), oxidação anódica (OA), foto-Fenton com ultra-violeta A (FF-UVA) ou radiação UVC (FF-UVC), e foto-eletro-Fenton com radiação UVA (FEF-UVA). Estas tecnologias foram incorporadas em três estratégias integradas de tratamento. De acordo com as diferentes tecnologias e estratégias testadas, a melhor linha de tratamento para o lixiviado do ARSIP contou com mais quatro estágios, num total de seis estágios: (iii) 1ª oxidação biológica para remoção do material orgânico biodegradável e espécies de azoto, (iv) coagulação com cloreto férrico (dose de coagulante de 100 mg Fe L^{-1}, pH 2,8) para remoção de uma fração dos compostos orgânicos recalcitrantes e sólidos suspensos, (v) FF-UVA com 4 h de duração (pH 2,8, ferro total dissolvido inicial de 140 mg L^{-1}) para degradação dos compostos orgânicos recalcitrantes e melhoria da biodegradabilidade, e (vi) 2ª oxidação biológica para remoção da matéria orgânica biodegradável resultante do processo FF-UVA. O uso da OA ao invés do FF-UVA demonstrou ser inviável principalmente devido à libertação de grandes quantidades do perigoso gás cloro, em virtude do elevado teor de cloretos no lixiviado, assim como à geração de grande quantidade de espuma. O processo FEF-UVA também revelou alguns problemas operacionais relevantes relacionados com a deposição de partículas na superfície do cátodo e consequente interrupção da geração eletroquímica de H_2O_2. A descarga do efluente final diretamente em meio hídrico não foi possível devido à impraticabilidade de se alcançar uma carência química de oxigénio (CQO) abaixo dos valores impostos pela legislação (125 ou 150 mg O_2 L^{-1} de acordo com a legislação Europeia e Portuguesa, respetivamente). No entanto, foi possível chegar a uma CQO abaixo de 1000 mg O_2 L^{-1}, valor que corresponde a um limite frequentemente imposto por estações de tratamento de águas residuais (ETARs) para efluentes descarregados na rede de esgostos municipal.

Direcionando o foco para a possibilidade de enquadramento da CQO no VLE para a descarga de efluentes tratados em meio hídrico, o lixiviado do ARSIP foi coletado por uma segunda vez (lixiviado com algumas características diferentes, principalmente no que diz respeito ao conteúdo orgânico), e o impacto da ozonização e de outros POAs baseados no ozono (O_3) aplicados como estágio (iii) após precipitação química dos sulfatos ou como estágio (iv) após precipitação química seguida por coagulação, foram investigadas. O lixiviado não continha um conteúdo orgânico biodegradável

suficiente para justificar a aplicação de uma oxidação biológica após a precipitação química. Os POAs com ozono envolveram: ozonização com peróxido de hidrogénio (O_3/H_2O_2), ozonização foto-assistida (O_3/UVC), ozonização foto-assistida com peróxido de hidrogénio (O_3/H_2O_2/UVC) e O_3/H_2O_2/UVC após coagulação com ferro, culminando em ozonização assistida pelo processo de foto-Fenton (O_3/FF). A melhor estratégia de tratamento excluiu o estágio de coagulação e incluiu no seu lugar o processo de O_3/H_2O_2 por ~2,1 h (pH natural; temperatura ambiente; 3,5 kg O_3 por m^3 de lixiviado; 1,1 kg H_2O_2 por m^3 de lixiviado), seguido por uma segunda oxidação biológica para remoção de matéria orgânica biodegradável resultante do processo O_3/H_2O_2. Isto deu origem a um tratamento composto por quatro estágios. Mais uma vez, foi impossível cumprir o VLE da CQO para descarga no meio hídrico.

No que respeita ao lixiviado do ARSINP, foi avaliada a aplicação da coagulação e de processos biológicos, bem como dos seguintes POAs/PEOAs: FF-UVA, FF-UVC, OA, e ozonização e tecnologias baseadas em O_3, tais como O_3/ H_2O_2, O_3/UVC e O_3/FF. A melhor estratégia de tratamento incluiu os três estágios seguintes: (i) coagulação com cloreto férrico (dose do coagulante de 300 mg Fe L^{-1}, pH 4,0) para remoção parcial de compostos orgânicos e fósforo, (ii) processo FF-UVC com 4 h de duração (pH 4,0, teor inicial de ferro dissolvido total de 115 mg L^{-1}) para oxidação de compostos orgânicos recalcitrantes, e (iii) processo biológico para remoção da matéria orgânica biodegradável gerada, assim como de compostos azotados no caso de se terem condições operacionais otimizadas. A aplicação da coagulação antes do POA/PEOA mostrou-se indispensável para o cumprimento das exigências da legislação. Após o tratamento, o lixiviado do ARSINP cumpriu os requisitos Europeus e Portugueses para descarga em sistemas aquáticos, exceto para o amónio e, consequentemente, para o azoto total.

O tratamento dos lixiviados de ARSI provou ser um grande desafio, em especial o tratamento de lixiviados de ARSIP.

Table of Contents

List of Figures

List of Tables

Notation

Acronyms

AnMBR	Anaerobic Membrane BioReactor
AOB	Ammonia-Oxidising Bacteria
AO	Anodic Oxidation
AOP	Advanced Oxidation Process
BDD	Boron-Doped Diamond electrode
BOD_5	5-day Biochemical Oxygen Demand
BRICS	Brazil, Russia, India, China and South Africa economic block
CEC	Contaminant of Emerging Concern
COD	Chemical Oxygen Demand
COVID-19	Coronavirus disease – 19
CPC	Compound Parabolic Collector
DIC	Dissolved Inorganic Carbon
DPD	Dipropyl-p-PhenyleneDiamine
DO	Dissolved Oxygen
DOC	Dissolved Organic Carbon
EGSB	Expanded Granular Sludge Blanket
EAOPs	Electrochemical Advanced Oxidation Processes
EDS	Energy Dispersive X-ray Spectrometry
EEM	Excitation-Emission Matrix
ELV	Emission Limit Value
EPDM	Ethylene Propylene Diene Monomer
FTIR	Fourier-Transform Infrared Spectroscopy
GC	Gas Chomatograph
GDP	Gross Domestic Product
HISW	Hazardous Industrial Solid Waste
HISWL	Hazardous Industrial Solid Waste Landfill
HPLC	High-Performance Liquid Chromatography
IS	Ionic Strength
ISWL	Industrial Solid Waste Landfill
MBR	Membrane BioReactors
MLVSS	Mixed Liquor Volatile Suspended Solids
MSD	Mass Spectrometer Detector
MSW	Municipal Solid Waste
MSWL	Municipal Solid Waste Landfill
MWWTP	Municipal Wastewater Treatment Plant
NDIR	NonDispersive Infrared Detector
NF	Nanofiltration
NHISW	Non-Hazardous Industrial Solid Waste
NHISWL	Non-Hazardous Industrial Solid Waste Landfill
NIOSH	National Institute for Occupational Safety and Health
OCD	Organic Carbon Detection
PE	Population Equivalent
PEF	Photoelectro-Fenton
PF	Photo-Fenton
PTFE	PolyTetraFluoroEthylene

RO	Reverse Osmosis
SBR	Sequencing Batch Reactor
SEM	Scanning Electron Microscopy
SHE	Standard Hydrogen Electrode
SMEWW	Standard Methods for the Examination of Water and Wastewater
SOS	Sulphur Oxidation State
STEL	Short-Term Exposure Limit
$SUVA_{254}$	Specific UltraViolet Absorbance at 254 nm
SVI	Sludge Volume Index
TAN	Total Ammonia Nitrogen
TDC	Total Dissolved Carbon
TDI	Total Dissolved Iron
TDS	Total Dissolved Solids
TSP	TetraSulfoPhthalocyanine
TSS	Total Suspended Solids
TWA	Time Weighted Average
UASB	Up-flow Anaerobic Sludge Blanket
UV	UltraViolet
UVA	UltraViolet A
UVC	UltraViolet C
UV-Vis	UltraViolet-Visible
UWW	Urban WasteWater
VOCs	Volatile Organic Compounds
VSS	Volatile Suspended Solids
WWTP	Wastewater Treatment Plant
XRD	X-ray Diffraction

Chemical names

$(CH_3CH_2)_2O$	Diethyl ether
Ag_2SO_4	Silver sulphate
Al	Aluminium
Al^{3+}	Aluminium ion
$AlCl_3$	Aluminium chloride
$Al_2(SO_4)_3$	Aluminium sulphate
As	Arsenic
Au	Gold
Ba	Barium
Ba^{2+}	Barium ion
$BaCl_2$	Barium chloride
$BaSO_4$	Barium sulphate
CH_3CN	Acetonitrile
CH_3OH	Metranol
CH_3SO_3H	Methanesulfonic acid
CH_5NO_3S	Aminomethanesul-fonic acid
$C_2H_4O_2$	Acetic acid
$C_2H_5KO_4$	Potassium hydrogen phthalate
$C_2H_7NO_2$	Ammonium acetate
C_3H_6O	Acetone
C_3H_8S	2-Propanethiol
C_4H_8O	2-Butanone
$C_4H_8N_2S$	N-Allythiourea
C_4H_9NO	2-Ethoxy-2-methylpropane
$C_4H_{10}S$	Butanethiol
$C_5H_{10}O$	2-Pentanone
$C_5H_{12}O$	2-Methoxy-2-methylpropane
C_6H_6	Benzene
C_6H_7N	Aniline
$C_6H_8O_6$	L-ascorbic acid
$C_6H_{10}O$	Cyclohexanone
$C_6H_{12}O$	Cyclohexanol
$C_6H_{12}O$	Methyl isobutyl ketone
$C_6H_{12}O_6$	Alpha-D-glucose
$C_6H_{14}O$	2-Ethoxy-2-methylpropane
C_7H_8	Toluene
$C_7H_{14}O$	2,4-Dimethyl-3-pentanone
$C_8H_5F_3O_3$	HTB
C_8H_{10}	Ethylbenzene
$C_8H_5KO_4$	Potassium hydrogen
C_9H_8	3-Phenyl-1-propyne
C_9H_{12}	2-Ethyltoluene
$C_{10}H_8$	Naphthalene
$C_{10}H_{16}$	Alpha-Pinene
$C_{10}H_{18}O$	Borneol
$C_{10}H_{22}$	Decane
$C_{11}H_{10}$	1-Methylnaphthalene

$C_{11}H_{24}$	Undecane
$C_{13}H_{28}$	Tridecane
$C_{10}H_{16}O$	Camphor
$C_{12}H_8N_2$	1,10-phenanthroline
Ca^{2+}	Calcium ion
$CaCO_3$	Calcite
$Ca_6Al_2(SO_4)_3(OH)_{12}.26H_2O$	Ettringite
CaCl	Calcium chloride
Cd	Cadmium
Cl^-	Chloride ion
Cl_2	Molecular chlorine
ClO^-	Hypochorite
ClO_2^-	Chlorite ion
ClO_3^-	Chlorate ion
ClO_4^-	Perchlorate ion
CO_3^{2-}	Carbonate ion
Cr	Chromium
Cu	Copper
e^-	Electron
Fe	Iron
Fe^{2+}	Ferrous ion
Fe^{3+}	Ferric ion
$FeCl_3$	Ferric chloride
$FeOH^{2+}$	Iron hydroxide
$FeSO_4$	Ferrous sulphate
H^+	Hydrogen ion
HCO_3^-	Hydrogen carbonate ion
HCl	Hydrochloric acid
HClO	Hypochlorous acid
H_2O	Water
HO^-	Hydroxyl ion
$HO^\bullet$	Hydroxyl radical
$HO_2^\bullet$	Hydroperoxyl radical
HS^-	Bisulfide ion
HSO_3^-	Hydrogen sulphite ion
H_2S	Hydrogen sulphide
H_2SO_4	Sulphuric acid
H_2O_2	Hydrogen peroxide
H_2SO_4	Sulfuric acid
$K_2Cr_2O_7$	Potassium dichromate
KH_2PO_4	Monopotassium phosphate
K_2HPO_4	Dipotassium hydrogen phosphate
KI	Potassium iodide
$MgSO_4$	Magnesium sulphate
Mn	Manganese
N	Nitrogen
Na_2CO_3	Sodium carbonate
Na_2HPO_4	Disodium hydrogen phosphate
NaOH	Sodium hydroxide
Nb	Niobium

NH_3	Ammonia
NH_4^+	Ammonium ion
NH_4VO_3	Ammonium monovanadate
Ni	Nickel
NO	Nitrogen monoxide
NO_2^-	Nitrite
NO_3^-	Nitrate
O_2	Molecular oxygen
$O_2^{\bullet-}$	Superoxide radical
O_3	Ozone
$O_3^{\bullet-}$	Trioxidanidyl
P	Phosphorus
Pb	Lead
PbO_2	Lead oxide anode
Pd	Palladium
S^0	Elemental sulphur
S^{2-}	Sulphide
$S_2O_3^{2-}$	Thiosulphate ion
SO_3^{2-}	Sulphite
SO_4^{2-}	Sulphate
$TiRuSnO_2$	Ti–Ru–Sn ternary oxide anode
Zn	Zinc

Symbols

A	Ampere
C	Concentration (mg L^{-1} or mM)
C_A	DOC content in sample at time *t* (Zahn-Wellens test)
C_B	DOC content in blank at time t (Zahn-Wellens test)
C_{BA}	DOC content in blank after 3 h of the test beginning (Zahn-Wellens test)
C_T	DOC content in sample at time t (Zahn-Wellens test)
d	Diameter (m)
D_t	Percentage of biodegradation (Zahn-Wellens test)
e^-	Electron
E^o	Hydrogen standard electrode potential
EC	Specific energy consumption for electrochemical cell operation
E_{cell}	Average cell voltage
hv	Incident radiation
I	Applied current intensity
kDa	1000 daltons (unit of molecular mass)
MΩ	Milliohm
MPa	Megapascal
$[O_3]_{in}$	Inlet concentrations of O_3 in the gas phase
$[O_3]_{out}$	Outlet (off-gas) concentrations of O_3 in the gas phase
pKa	Value used to indicate the strength of an acid
Q	Flow rate (L h^{-1})
R^2	Coefficient of determination
t	Time (min, h)
T	Temperature (ºC)
V	Voltage
V_S	Solution volume (mL, L)
λ	Wavelength (nm)
k_{DOC}	Pseudo-first-order kinetic constants for DOC removal
S^2_R	Residual variance
W	Watts

1 Introduction

This first chapter presents an overview of the problems associated with the increase of industrial solid waste, the established and emerging treatment technologies for wastewaters with focus on leachates from industrial solid waste landfills, and the legislation covering the discharge of treated effluents. The objectives and the thesis outline are also provided at the end of the chapter.

1.1 Industrial solid waste

The onset of urbanization and the globalization of informatics and other technologies did accelerate the pace of mechanical development and growth of industrial activity, as well as the waste generation. In this way, it is ironic to point that a pandemic with immeasurable aftereffects as the COVID-19, induced the Earth to take a brief breath. Populations around the world had to stop their way of life because of this novel disease, and the benefits of the abrupt decrease in anthropogenic activities to the environment are visible [1, 2]. However, it is still unclear how the industrial activity will be affected during this pandemic break, but certainly, the gross domestic product (GDP) of all countries will be seriously affected, and so the waste generation. By analysing Figure 1.1 it is possible to notice that the economy develops proportionally to an increasing in industrial waste, and, in this way, the income level of a country is expected to affect solid waste generation, as well as the standard of living of its population.

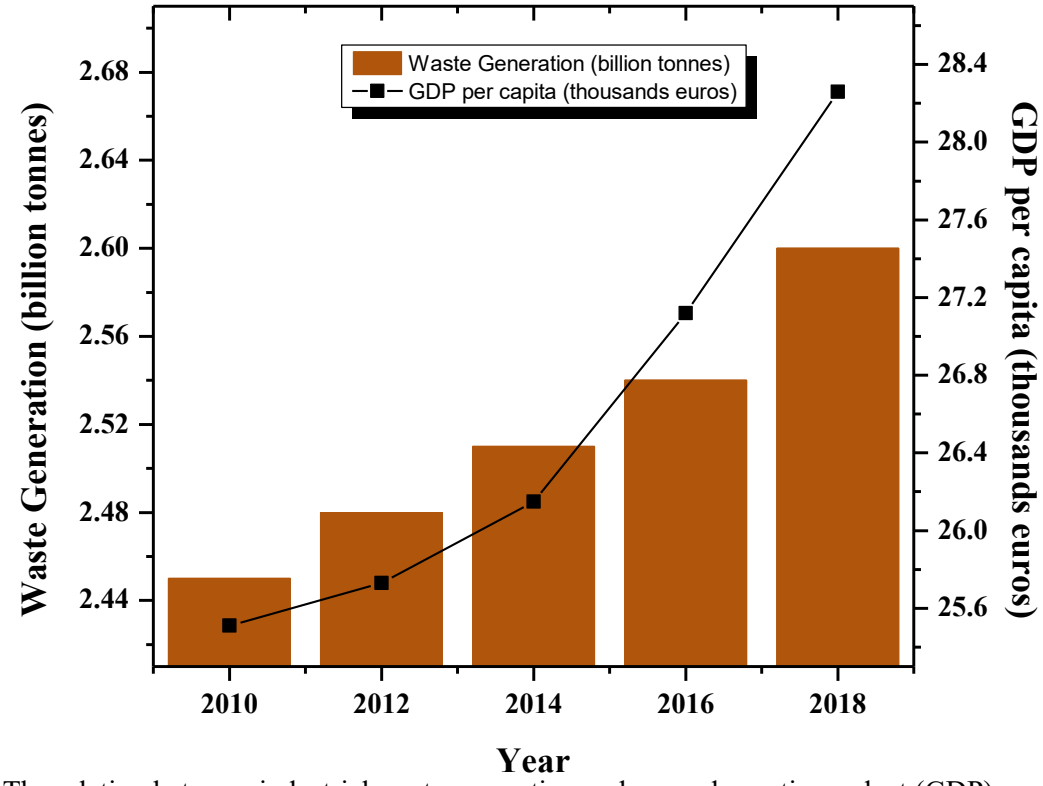

Figure 1.1 The relation between industrial waste generation and gross domestic product (GDP) per capita at the 28 countries of the European Union from 2010 until 2018 (Source: [3, 4]).

High-income countries have the concern to face this rise, but the evolution of methods and technologies to properly treat and manage these residues not always follow the same velocity and the necessities of the financial market. This happens because there are distinct interests involved: (i) the capital, here represented by the industries, their owners and actionists, and (ii) the overall civil society, which can be represented by the research centers since usually, they are responsible for studying and analysing the

social and technical waste management parameters. The first is guided by the winnings and the development at any cost, so they are usually associated only with their benefits, with big publicity around their production. The second retains less interest for society, once the waste is not an enjoyable product, but a reject that remains hidden from the populations' eyes. The government is in the middle of these and has an ambiguous function since it is responsible throughout specific legislation for leveraging the economy and improve the industry activity, balancing economic growth, but also have to do and to apply the law, controlling the anthropogenic activities responsible for environmental deterioration.

In this way, it is clear that industrial waste generation is a global concern, and the research centers are the main devices that society has to guarantee less harmful economic development. In the countries where specific data are available, the industrial waste generation is eighteen times greater than municipal solid waste (MSW) and rises significantly as the income level of the countries also increases [5]. Despite these numbers and their wide diversity, the number of researches focused on the management or treatment of industrial waste (non-hazardous and hazardous) is lower than that addressing MSW. The difference is even higher if one only considers the studies concerning hazardous industrial waste. Even though the volume per capita of hazardous waste be quite lesser when compared to non-hazardous (4 to 96% [3]), the potential damages to the environmental and human health are meaningful.

A massive structure to attend an economy that avoids waste generation in urban space did increase in the last years, with a focus on recycling and recovering. However, a huge change in this perspective has also to attain the logic of industry, throughout a source reduction in the waste management hierarchy, once it is the larger waste producer, including harmful and toxic substances.

From this perspective, Figure 1.2 presents the number of works available at the Science Direct scientific database, separated by year and according to the following keywords: "Industrial Waste", "Municipal Solid Waste", "Industrial Solid Waste", "Hazardous Industrial Waste" and "Hazardous Industrial Solid Waste", all of these keywords searched together with the keyword "Treatment". Note that the term "Waste" includes any type of waste (solid, liquid and gaseous) and the term "Solid Waste" only refers to waste in solid form.

The treatment of industrial waste is an old concern for researchers, appearing even before the '70s and increasing until the "boom" in the '90s. Studies regarding the treatment of MSW appeared in a meaningful and continuous way after 1975. Later, in the middle of the '80s, research on the treatment of industrial solid waste started appearing and was intensified in the final of the '90s / beginning of the

‘00s. Insights on the remediation of hazardous industrial waste appeared in the '90s, albeit modest, and the study of hazardous industrial solid waste (HISW) has been negligible up to now.

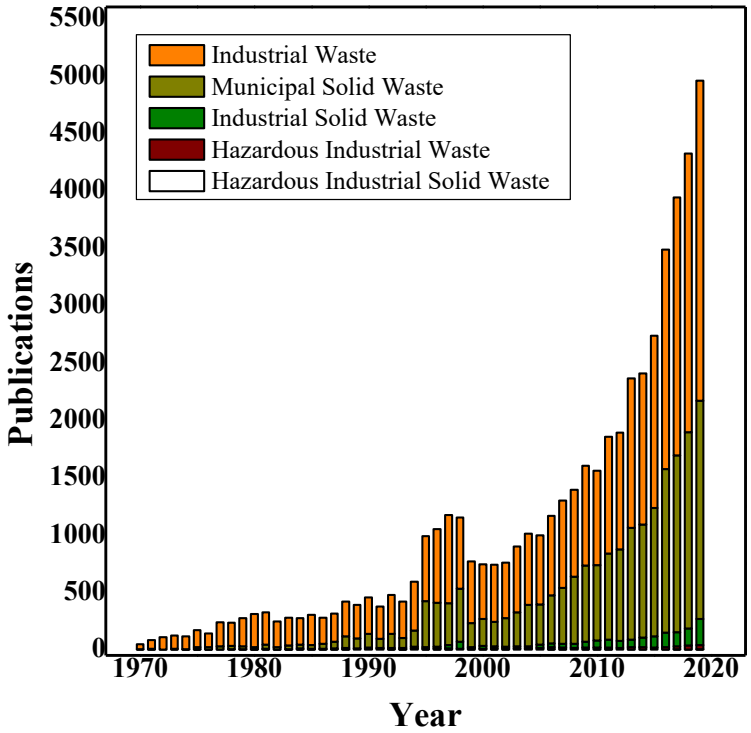

Figure 1.2 Evolution in the number of publications focused directly or indirectly on the treatment of distinct types of waste (Source: Science Direct).

There is a perceptible increase in the number of publications focused on industrial solid waste in the last decade, whereas the transportation to a formal hazardous or non-hazardous waste treatment center coupling a combination of incineration and landfilling is commonly the first step toward sustainable waste management. In general terms, industrial waste has more attention than MSW due to the waste diversity and industrial activities, demanding different approaches for each one. While liquid industrial waste is usually treated in situ, with different and particular treatment methods, industrial solid waste is stored in landfills, and the leachate is generally treated using a single technology or a combination of the following technologies: (i) biological treatment, where bacteria degrade the biodegradable organic fraction; (ii) separation method, which generally is coagulation/flocculation or precipitation, but more recently membranes and other technologies have been commonly used; and/or (iii) advanced oxidation processes (AOPs), which are capable of overcoming barriers in the removal of recalcitrant compounds. It is important mentioning that when compared with incineration, in terms of exploitation and capital costs, landfilling is the cheapest method [6].

It is true that as nations prosper economically, waste is managed using more sustainable and safe methods. Nevertheless, sometimes the liquid reject is simply collected and stored for a long time, with the risk of mine waste spill and other accidents, posing several impacts on nature, as the incidents with

cyanide in Omai (Guyana, 1995, [7]); fly ash slurry from a coal-fired power plant in Kingston (United States, 2008, [8]); iron-rich sludge at Ajka (Hungary, 2010, [9]), Mariana (Brazil, 2011, [10, 11]), and Brumadinho (Brazil, 2019, [12]), or metals-laden sludge in Mount Polley (Canada, 2014, [13]). These accidents demonstrate that effluent storage is responsible for large-scale catastrophes everywhere, always due to the improper storage of large quantities of waste.

In landfills, the leachate generated by the percolated mixture of industrial solid waste inside the landfill is more complex and less studied than the accrued into MSW landfill (MSWL), demanding more efforts for their characterization and posterior treatment.

A major deficiency in the industrial solid waste narrative is the lack of scientific data concerning its generation and management, mainly in the developing countries, where solid waste management issue is a challenging topic to the authorities [14]. In BRICS economic block, composed of Brazil, Russia, India, China, and South Africa, the countries size is a relevant barrier to achieve better sanitation and management of waste. Sanitary sewages are not a reality for the major of the population in developing countries, and most of the cities still dumping the waste in unprepared land. Furthermore, effective waste management is expensive, often comprising 10% of municipal budgets in middle-income countries, and can attain 20% in low-income ones [5]. Operating this essential service in industrial countries also requires integrated systems that are efficient, sustainable, and socially supported.

1.1.1 Non-hazardous and hazardous industrial solid waste

Definition of non-hazardous industrial solid waste (NHISW) varies from jurisdiction to jurisdiction, but always fits in the role between the mixed refuse from homes and industry, i.e. MSW and the materials that are regulated owing to their toxicity and related public health concerns, i.e. HISW [15]. Thus, it is widely reported that NHISW can consist of some manufacturing industrial wastes as organic and inorganic chemicals, mining, construction, wood product, resin and plastics, stone, clay, glass, concrete and kindred products, pulp, paper, electronic manufacturing, sludge from waste industries, etc.

The term hazardous is an inherent property of something. Nonetheless, from a scientific perspective, there is a need to prove through research that the chemical compound concentration is sufficiently high to justify its hazardousness. In this way, the difference between NHISW and HISW can be scientific or legal, i.e. arguably situational [16]. Most of the countries consider HISW as a waste that presents a threat to human health and the environment when it is improperly managed.

Generation of the complex organic liquids in landfills, called leachates, remains inevitable due to rainwater percolation and the decomposition of the wastes themselves. Considering the temporal variability of leachate quantity and composition (depending on the age of the landfills, climatic conditions, soil properties, waste type and composition), reinforced by the high concentration of recalcitrant substances, such as humic [17-19] and fulvic substances [20], xenobiotics [21], pesticides [22], heavy metals [23], and inorganic macrocomponents [24], there is no universal and cost-effective treatment solution to ensure water resources protection [25, 26].

Table 1.1 displays the physicochemical characteristics of various leachates from different solid waste landfills in terms of dissolved organic carbon (DOC), chemical oxygen demand (COD), 5-day biochemical oxygen demand (BOD_5), BOD_5/COD ratio, pH, alkalinity and amount of chloride and ammonium. It is visible the large diversity of wastes coming from MSWLs and from NHISW landfills (NHISWLs) and HISW landfills (HISWLs). Important parameters have a huge difference between them, like pH (from 5.1 to 9.6), COD (from 480 to 54454 mg O_2 L^{-1}), and BOD_5 (from 25 to 16996 mg O_2 L^{-1}). This variety makes each landfill leachate very particular, requiring specific treatment solutions.

1.1.2 Treatment technologies for leachates

The selection of an appropriate treatment method is strictly dependent upon the leachate composition and characteristics. Despite the world-wide effort to develop treatment solutions for leachates from MSWLs [27], little has been done with regard to the treatment of leachates from ISWLs, either NHISWLs or HISWLs. If one looks further at the successful development of cost-effective treatment solutions for ISWL leachates that allows meeting European regulations for the discharge of treated effluents, the lack is even more tangible. One-stage treatments have been in general ineffective. For example, Gotvajn et al. [28] tested distinct one-stage treatments for a NHISWL leachate, including aerobic biological oxidation, air stripping, activated carbon adsorption, coagulation/flocculation and Fenton oxidation, and found that no method alone was effective enough to meet the European discharge limits, suggesting the need for the integration of several technologies.

Regarding leachates from HISWLs, Kattel et al. [29] studied the remediation of a leachate from a semicoke landfill of an oil-shale thermal treatment plant. This leachate exhibited a moderate content of organic compounds (COD of 851–2040 mg O_2 L^{-1} and DOC of 243–463 mg L^{-1}), moderate biodegradability (7-day biochemical oxygen demand (BOD_7)/COD ratio 0.25–0.39), very low concentration of solids (total suspended solids (TSS) of 21–24 mg L^{-1}), residual nitrogen content, and moderate conductivity of 6.0–9.0 mS cm^{-1}. The authors assessed the use of an activated sludge process

combined with Fenton's oxidation either as pre- or post-treatment stage. Both strategies were able to provide a leachate complying with the Estonian regulations for the discharge of industrial effluents (COD of 250 mg O_2 L^{-1}) but incapable of giving a leachate in compliance with European legislation (COD of 125 mg O_2 L^{-1}), according to the Directive 91/271/CEE [30].

Besides the use of combined treatments, Kattel et al. [29] tested the application of single treatments for partial HISWL leachate remediation, such as coagulation, ozonation, Fenton treatment and activated sludge biological process. The use of one-stage treatments for HISWLs leachates was also evaluated in other studies: Morgan [31], Dollerer and Wilderer [32], and Setiadi and Fairus [33] applied biological treatments and Šír et al. [34] employed reverse osmosis. Below, established and emerging technologies for the treatment of wastewaters will be described, with focus on their application to the remediation of leachates from ISWLs.

1.1.2.1 Separation technologies

Colloidal particles (from 1 to 1000 nm), particulate materials (> 1000 nm) [35] and some dissolved matter (any matter that is able to pass through a filter with pore size ranging from 0.2 to 0.7 μm but can still be separated from the solution through various separation techniques [36]) are pollutants that can be easily removed at initial stages of the treatment process by conventional coagulation/flocculation, electrocoagulation, precipitation or even through membranes technologies. These pollutants can be responsible for the absorption of UV light, decreasing the efficiency of light assisted treatment methods [37]. Separation technologies have as a major drawback the fact that there is a reject (retentate stream) to be handled. Thereby, despite the necessity of these processes in some stage of a wastewater treatment-line, other technologies that really reach the mineralization of organic matter should be preferred over separation processes.

1.1.2.1.1 Coagulation/flocculation

Colloids are very small particles that cannot settle naturally due to electrostatic repulsions between the particles (usually negatively charged), which is a barrier to aggregation and subsequent sedimentation [38]. Coagulants can neutralize the colloids charges and aggregate them, and the flocculants promote the agglomeration of the aggregated colloids, transforming them into bigger structures through gentle stirring, posteriorly settled by gravity in the form of sludge [39].

Table 1.1 Characterization of leachates from different solid waste landfills and applied treatment strategy.

	DOC[a]	COD[a]	BOD_5[a]	BOD_5/COD	pH	Alkalinity[a]	Chloride[a]	Ammonium[a]	Treatment Strategy	Ref.
MISWLs		2500			8.5	1547		2917	Electro-Fenton with Fe^0	[40]
		7184	220	0.03	8.3	6375	6000		Electro-Fenton and biological process	[41]
		3626			8.7			375	Ultrasonic and anaerobic digestion	[42]
		19814	1325	0.07	8.2	23250	6551	2925	Combined sodium persulfate/hydrogen peroxide	[43]
		5216	2949	0.56	8.2		9853	1997	Garbage enzyme	[44]
		5927	3995	0.67	7.9		8574	721	Garbage enzyme	[44]
		7693	7455	0.96	9.2		9269	829	Garbage enzyme	[44]
	1152	4976			8.4				Sonolytic and sonocatalytic processes	[45]
HISWLs		3715	960	0.26	9.5				Fenton process	[46]
		4123	890	0.21	9.7				Electro-Fenton	[47]
		3783	955	0.25	8.1			165	Baffled constructed wetland system	[48]
NHISWLs	5244	19900	4000	0.20	8.0		45772	491	Evaporation and reverse osmosis	[49]
	181							95	Biological process	[50]
		6900	3220	0.47	8.1	1690	5200	215[b]	Biological process	[51]
		14420			5.1	3750	7090		Electrocoagulation and biological processes	[52]
	170	480	25	0.05	7.7		405		Ozone-based processes, hydrogen peroxide and biological process	[53]
	13966	54454	16996	0.31	8.6	28800	6751	8403	Biological process, coagulation, Fenton, photo-Fenton, anodic oxidation and photoelectro-Fenton	[54]
	955	2462	601	0.24	8.2		1844	2184	Air stripping, activated carbon adsorption, aerobic biological treatment, coagulation-flocculation and Fenton	[28]

[a] All values in mg L^{-1} (COD in mg O_2 L^{-1});
[b] Total Kjeldahl nitrogen.

Other mechanisms available in coagulation/flocculation processes are: (i) the sorption of oppositely charged ions, which causes destabilization of surface charge, reducing it, (ii) the formation of particle bridging, with consequent molecular weight increase, and (iii) precipitation and enmeshment mechanism, where colloidal particles can be enmeshed into insoluble flocs of hydrolysis products [55].

In landfill leachates treatment lines, coagulation/flocculation can be fitted in different stages of the process. Coagulation is a highly pH-dependent process [56], and acidic to neutral pH usually achieves better results when metal salts are used as coagulants [57]. Hence, this fact should be always taken into consideration, since it can include additional acidification/neutralization stages, which has a cost. Jar-tests assays are essential to obtain the optimum operational parameters (pH, coagulant type, and dosage), aiming to improve water characteristics and decrease settling time and so the cost involved.

The most commonly used metal salts are aluminium and iron sulphates and chlorides, which can form multivalent ions (Al^{3+}, Fe^{2+}, Fe^{3+}) and various hydrolysis products through a series of hydrolytic reactions depending on the solution pH (Eq. 1.1) [55]. Among these products, the neutral amorphous metal hydroxides as $Al(OH)_3$ and $Fe(OH)_3$ are the poorly soluble species [55].

$$Me^{3+} + nH_2O \leftrightarrow Me(OH)_3^{3-n} + nH^+ \quad 1.1$$

Besides a large amount of sludge as a result of coagulated substances, the metal residuals in the finished water is also a big issue derivative of the use of these metal salts as aggregation agents. Hence, their removal is mandatory before the final discharge of the effluent since the limit of Al and Fe discharge are usually stringent.

A typical flocculant is a polymer with long and repetitive chain hydrocarbons, with molecular weights up to 100 times higher than those of coagulants. Also, during manufacturing, a variety of different functional groups can be attached to the backbone of a flocculant to give it different and specific properties and charges (neutral, anionic or cationic), resulting in synthetic polymers that are much more active than natural polymers. Most studies use anionic flocculants, formed by negatively charged carboxylate groups of acrylamide-acrylate copolymers [58].

Landfill leachates present a myriad of pollutants with positive and negative charges. For instance, some heavy metal ions are positively-charged, whilst humic acids are negative. In this way, flocculants with higher contents of positively-charged groups into its molecular chain will result in a higher efficiency for humic acids removal, and contrariwise for heavy metal cations [59].

From the nine works analysed in Table 1.2, whenever comparable, $FeCl_3$ coagulant always reached better COD removal than $Al_2(SO_4)_3$ coagulants but at more acidic pH values. It is important to mention that coagulant dosage is very variable, inferring the importance of the jar-tests to each specific leachate. Only one work attained good results with the addition of a flocculant (COD removal from 34% only with $FeCl_3$ to 51% when an anionic polyelectrolyte flocculant was added) [28]. Other two studies tested the addition of flocculants but no improvement was achieved [54] or only faster settling was observed [60].

Table 1.2 Performance of $FeCl_3$ and $Al_2(SO_4)_3$ coagulation for different landfill leachates.

Coagulant	pH	[Coag.] (g L^{-1})	COD (g O_2 L^{-1})	[Coag.]/COD	COD removal (%)	Flocculant (mg L^{-1})	Ref.
$FeCl_3$	3.2	2	5.7	0.35	63	-	[57]
$Al_2(SO_4)_3$	7.3	2	5.7	0.35	39		
$FeCl_3$	4.2	8	2.2	3.63	71[a]	-	[61]
$FeCl_3$	5.2	10	2.3	4.34	68[a]		
$FeCl_3$	4.2	5	2.9	1.72	45[a]		
$FeCl_3$	6.9	7	3.15	2.22	49.3	-	[62]
$FeCl_3$	2.8	0.3	8.36	0.03	66	4.0[b]	[54]
$FeCl_3$	6.0	1	1.2	0.83	51	2.5[c]	[28]
$Al_2(SO_4)_3$	6.9	1	1.2	0.83	25	-	
$FeCl_3$	6.0	1.4	1.1	1.3	72	-	[63]
$FeCl_3$	3.2	0.4	19.2	0.02	28	5.0[d]	[60]
$Al_2(SO_4)_3$	5.1	0.8	19.2	0.04	27	5.0[d]	
$Al_2(SO_4)_3$	7.0	1	4.97	0.20	25	-	[64]
$Al_2(SO_4)_3$	6.0	0.6	2.81	0.21	53	-	[65]
$FeCl_3$	5.5	0.6	2.81	0.21	68	-	

[a] DOC removal;
[b] Flocculants: Ambifloc C 58 (cationic) and Magnafloc 155 polyacrylamide (anionic) = no improvement;
[c] Flocculant: anionic polyelectrolyte (unreported brand) = +17% in COD removal;
[d] Flocculants (commercialised by Brenntag): anionic (A-401, A-352, A-1849) and cationic polyelectrolytes (C-472 and C-421) = no improvement.

1.1.2.1.2 Electrocoagulation

A conventional coagulation process requires the addition of chemical reagents and pH adjustments for an effective treatment, resulting in an expensive and labor-intensive process. Contrary to this, electrocoagulation usually does not require external chemicals since the coagulants are generated *in situ*. Furthermore, this process can remove any size of suspended solids, oil and grease, as well as heavy metals, and produces about half the sludge of chemical coagulation [66].

Similar to conventional coagulation, iron and aluminium are the main elements in the electro technology because of the surface complexation and electrostatic attraction of these compounds [67]. Electrocoagulation mechanism also depends on metal dissolution and consists basically of two processes:

anodic metal dissolution while applying electric current (Eqs. 1.2 and 1.3), and chemical dissolution due to the metal interaction with the medium (Eqs. 1.4 and 1.5 [67]). Thus, the interaction of generated metal hydroxides leads to the oxidation of toxic pollutants to lesser toxic species, or their charge neutralization followed by (i) sorption on the metal hydroxides and removal by sweep coagulation, and (ii) the gas produced at the cathode assists in bringing the floc to the surface of the water by sweep flotation [68]. Beyond this, the final quality of treated wastewater during electrocoagulation is influenced by the anode material, distance between electrodes, anionic and cationic composition of the solution, flow rate of water in the interelectrode space, pH, current density, etc. [69]. Current density depends on the amount of electricity passed through the electrolytic solution and is the most important factor in the process, once it can govern the performance directly, affecting the coagulant dose [70]. Table 1.3 shows the efficiency of electrocoagulation for the remediation of various landfill leachates.

Table 1.3 Performance of electrocoagulation for different landfill leachates.

Electrode	Inter electrode gap (cm)	Surface area (cm^2)	pH	Current density ($mA\ cm^{-2}$)	Time (min)	$[COD]_0$ ($mg\ O_2\ L^{-1}$)	COD removal (%)	Ref.
Fe	2	40	6	-	20	14420	15	[52]
Al							30	
SS[a]							40	
Al	2	42	6.3	25	50	8580	51	[70]
Fe							60	
Al	2	120	5	21	35	1530	37	[71]
Fe	1	38	6.4	100	60	44900	22	[72]
Al	2	-	5.4	5	180	2520	64	[73]
Fe							60	
Al	-	476	8.6	10	30	596	70	[74]
Fe			8.9	8			65	
Fe	1.16	42	7.7	25	60	7230	45	[75]

[a] Stainless steel.

Electrocoagulation was able to promote COD removals in the same order of magnitude as conventional coagulation. Highlight can be given to the operation at near-neutral pH values. Time (20 to 180 min), current density (5 to 100 $mA\ cm^{-2}$) and the electrode surface area (38 to 476 cm^2) are divergent in the different studies as a result of the different characteristics of the leachates. So far, only one research has covered the application of electrocoagulation to the treatment of an ISWL leachate [52]. In this study, aluminium and stainless steel electrodes achieved better results in terms of organics removal, whereas iron electrodes provided improved metals removal.

$$Fe \rightarrow Fe^{2+} + 2e^- \quad (1.2)$$

$$Al \rightarrow Al^{3+} + 3e^- \quad (1.3)$$

$$Fe^{2+} + 2OH^- \rightarrow Fe(OH)_{2(s)} + 2e^- \quad 1.4$$

$$Al^{3+} + 3OH^- \rightarrow Al(OH)_{3(s)} + 3e^- \quad 1.5$$

1.1.2.1.3 Chemical precipitation

Chemical precipitation involves the addition of chemical reagents and then separation of precipitates from the solution throughout their conversion into solid, by converting the substance into an insoluble form or by making the solution a supersaturated one [76]. It is widely used as a treatment for industrial wastewater since it can remove a large amount of specifics contaminants in loco at a relatively low cost. A sole chemical precipitation treatment for landfill leachates is not useful due to their contaminant variety, but when allied to other techniques, it can be highly recommended.

Chemical precipitation can also be used to recover compounds from landfill leachates and sometimes generate value-added compounds. Table 1.4 collects some studies on compounds recovery from landfill leachates through the application of chemical precipitation.

Table 1.4 Chemical precipitation for compounds recovery in landfill leachates.

Compound	Precipitated as	pH	Concentration of recovered compound (g L^{-1})	Compound removal (%)	Ref.
Magnesium	Struvite	9.5	0.72	98.6	[77]
Phosphate	Struvite	9	9.1	77.0	[78]
Ammonium	Struvite	8.8	5.61	96.2	[79]
Ammonium	Struvite	9.5	2.52	85.5	[80]
Ammonium	Struvite	10	0.64	88.0	[81]
Ammonium	Struvite	9	1.75	82.0	[82]
Ammonium	Struvite	9	1.57	83.0	[83]
Sulphate	Ettringite	11	1.08	61.6	[84]

1.1.2.1.4 Membrane separation processes

Membrane separation processes are based on selective barriers capable of promoting the removal of certain components present in a solution by the action of a driving force [85]. These barriers are generally formed by porous solids, which size can be distributed in different classes: nanopore (0.1 to 100 nm), micropore (0.1 to 100 μm), and millipore (0.1 to 100 mm) [86].

Highlight can be given to nanofiltration (NF) and reverse osmosis (RO) technologies. Both have the same separation mechanism, but while RO is a pressure-driven membrane separation process with an operating

pressure of 1.5–12 MPa and a cut-off limit of 0.1–1 nm molecular size of the dissolved components, the NF cut-off limit is only about 1 nm and has a low operating pressure (below 2.5 MPa). In this way, RO is the most sophisticated membrane liquid separation technology, which can block all the suspended solids, dissolved matters, colloids, dissolved salts, and organic matters with a molecular weight greater than 100 Da [87]. Depending on the pore size and effluent characteristics, fouling is a main limiting factor in membrane applications, caused by pore-clogging or sorption of solutes on the membrane surface, decreasing their efficiency [88]. Therefore, appropriate pre-treatment has to be used aiming to reduce different types of membrane fouling (Figure 1.3), which explains the use of these technologies mainly as tertiary treatment, including the removal of contaminants of emerging concern (CECs) [89].

RO and ultrafiltration (UF) are used for landfill leachate treatment since the ’80s, but only properly analysed in literature in the late ’90s [90]. Table 1.5 evidences the possibility of treating landfill leachates by membrane technologies, with some studies achieving almost total COD removal even in leachates with high organic matter content. However, better attention is necessary to know the real applicability of the membranes, regarding mostly the membrane fouling and reuse.

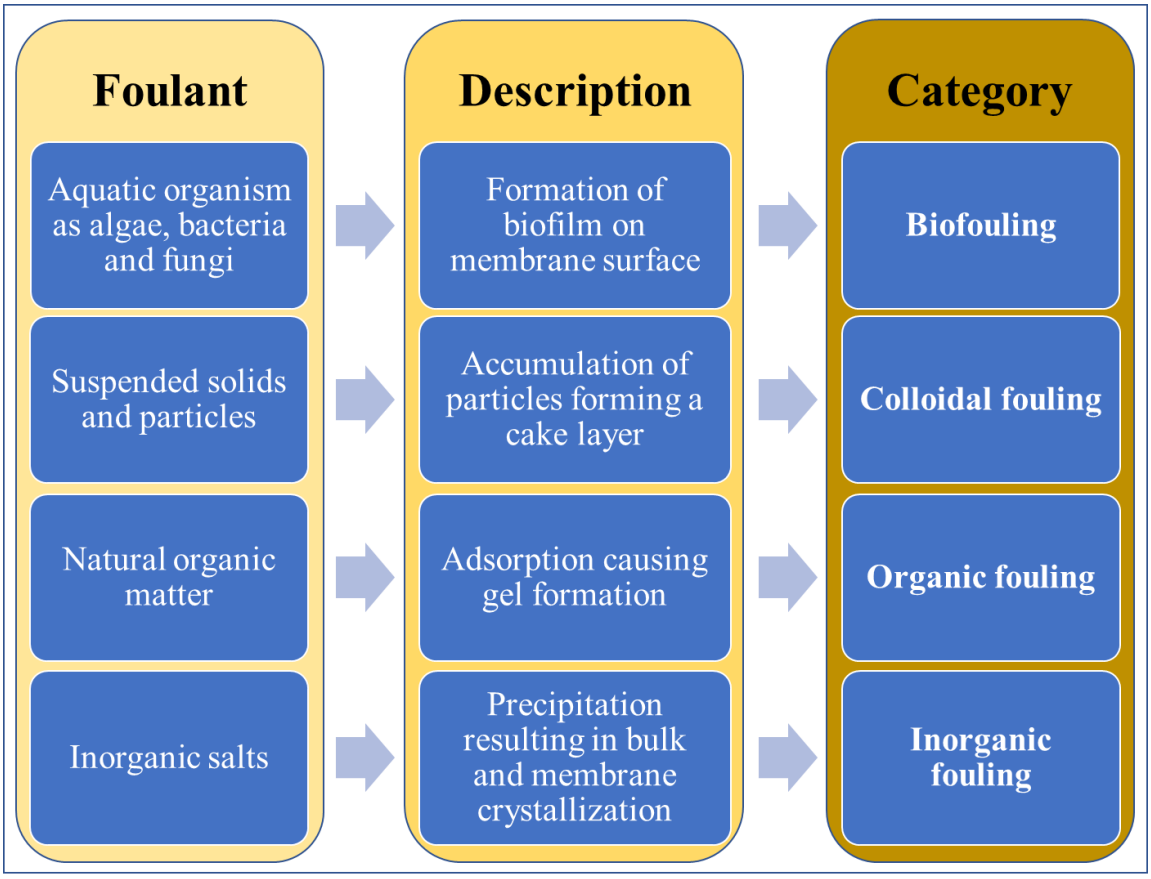

Figure 1.3 Fouling categories in membrane technologies for wastewater treatment. Adapted from Abuabdou et al. [91].

Table 1.5 Performance of membrane separation processes for different landfill leachates.

Membrane technology	Transmembrane pressure (MPa)	Molecular weight *cut-off* (kDa)	$[COD]_0$ (mg O_2 L^{-1})	COD removal (%)	Ref.
RO	-	-	1797	99.2	[90]
RO	-	-	718	98.6	[92]
UF	0.3	300	788	71.3	[93]
Fine-UF	0.8	5.0	788	86.3	[93]
UF	-	-	1780	89	[94]
RO	-	-	1780	97	[94]
UF	1.0	1.0	1339	66	[95]
UF	0.16	150	3960	49.6	[96]
UF	0.16	150	5548	48	[96]

1.1.2.2 Oxidation technologies

Oxidation technologies cover the degradation of organic compounds to form simpler compounds and ultimately to provide their mineralization, i.e. their conversion into carbon dioxide, water and, depending on the composition of the compounds, other minerals such as sulphate, ammonia, nitrate, phosphate and chloride. These technologies can be divided into two main categories relating to the nature of the treatment: biological or chemical.

1.1.2.2.1 Biological treatment

Biological methods are based on the metabolic activity of bacteria and fungi that live in natural environments. They are widely used for treating wastewaters, including landfill leachates, due to their ability for removing biodegradable organics and nitrogen species, relative simplicity and cost-effectiveness. Biological oxidation can be performed under aerobic, anaerobic, and anoxic conditions.

Aerobic biological processes, using sequencing batch reactors (SBRs), membrane bioreactors (MBRs) and biofilm reactors, generally achieve good removal rates for COD, with a total consumption of biodegradable organics, and are also able to promote nitrification. Dissolved oxygen is the key factor in aerobic biological processes and highly responsible for total costs.

Anaerobic/anoxic biological processes, using up-flow anaerobic sludge blanket reactor (UASB), anaerobic membrane bioreactor (AnMBR) and expanded granular sludge blanket reactor (EGSB), can also promote good organics removal and promotes denitrification [97].

Note that systems could not always be characterized as completely aerobic, anaerobic or anoxic due to the fact that most of them apply a combination of different regimes to achieve the optimal treatment efficiency [98]. It happens due to the wide number of existing bacteria, which sometimes is very dependent on a good interaction with specific groups of pollutants, temperature, pH and all the

environmental inside the reactor. Thus, the substrate affinity of nutrient-removing bacteria determines their bacteria species composition [99]. Abatenh et al. [100] show a review where these affinity interactions and the main bacteria group for each kind of pollutant are demonstrated.

In recent years, fungal-based processes have been applied to wastewater since they can mineralize humic acids through the production of powerful oxidative and non-specific extracellular enzymes, peroxidases, and laccases [101]. Fungi represent a kingdom of heterotrophic eukaryotes that grow individually (yeasts) or forming hyphae and mycelium (molds) and can be used in leachate treatment using the fungal cells or only the isolated enzymes from them [102].

1.1.2.2.2 Catalytic oxidation processes

Due to the ability of the transition-metal ions and their complexes to alter the electronic structure of both reductants and oxidants species, they can be used as effective catalysts, overcoming the activation energy barrier imposed by the spin-state symmetry restrictions [103]. In this way, wastewaters relatively rich in transition-metal ions and their complexes, such as leachates from HISWLs and NHISWLs, can take advantage of them to support the oxidation of several compounds when applying air (oxidant: oxygen) and other reactants, including hydrogen peroxide (H_2O_2), peroxymonosulphate, chlorine and potassium permanganate.

Webler et al. [54] successfully conducted an aeration stage in the treatment of a NHISWL leachate to oxidize nitrite to nitrate before the application of an AOP/EAOP and then avoid an induction period where the oxidants of the AOP/EAOP would be wasted for this conversion. The use of H_2O_2 as an oxidant has several advantages: (i) its decomposition results in oxygen and water, (ii) it is safe and easy to handle, and (iii) it is economically competitive [104]. Beyond the oxidation of nitrite to nitrate, catalytic oxidation processes can be used to convert, for example, sulphites and sulphides into sulphates [105].

1.1.2.2.3 Advanced oxidation processes

Chemical advanced oxidation processes (AOPs) and electrochemical AOPs (EAOPs) are recognized as a superior technology because they are able to oxidize recalcitrant organic compounds, contrary to biological treatments. They involve the formation of strong oxidants, mainly hydroxyl radicals ($HO^{\bullet}$) (E^{o} of 2.730 V/SHE) [106]), which react with organic contaminants present in the wastewater, converting them into biodegradable compounds until the complete mineralization in water, carbon dioxide and inorganic salts [107]. AOPs/EAOPs proved to be efficient in the removal of persistent organic pollutants

that remain in the water for a long time, such as pharmaceuticals [108, 109], pesticides [110], dyes [111] and humic substances [112].

Among the various AOPs/EAOPs, one can highlight the photolysis of H_2O_2 under ultraviolet C (UVC) radiation (H_2O_2/UVC), anodic oxidation (AO), Fenton's reaction based processes such as Fenton, photo-Fenton (PF), electro-Fenton [57] and photoeletro-Fenton (PEF), and ozonation and ozone (O_3)-based processes.

1.1.2.2.3.1 Photolysis of H_2O_2 under UVC radiation

H_2O_2/UVC process is a simple AOP based on the $HO^{\bullet}$ formation thought the homolytic cleavage of the peroxide bond (–O–O–) under UVC radiation via Eq. 1.6 [113].

$$H_2O_2 \xrightarrow{hv} 2HO^{\bullet} \quad 1.6$$

Despite the good performance of the H_2O_2/UVC process for less complex effluents, landfill leachates generally show dark colour and high turbidity, decreasing the process efficiency due to the occurrence of inner filter effects, i.e. competition for photons between photo-activators and light-absorbing compounds, and/or light attenuation thought the optical pathlength of the photoreactor. Nevertheless, a study with a biologically pre-treated MSWL leachate showed an improvement in COD and colour removal from 67% and 61% to 89% and 95%, respectively, when UVC irradiation was coupled to the H_2O_2 oxidation during 180 minutes of reaction [114]. Also, COD and colour removal of 65% and 72%, respectively, were demonstrated in another MSWL leachate after 300 min of reaction, with COD removal proportionally dependent on the UV power [115].

1.1.2.2.3.2 Anodic oxidation

AO is recognized as the simplest and most popular EAOP. In AO, organics can be (i) directly oxidized at the anode surface by electron transfer, (ii) indirectly oxidized by intermediates of oxidation of water to oxygen, including the powerful physisorbed $HO^{\bullet}$ at the anode surface, denoted $M(HO^{\bullet})$, generated via Eq. 1.7, and weaker oxidants like H_2O_2 produced from $M(HO^{\bullet})$ dimerization by Eq. 1.8 and O_3 formed from water discharge at the anode surface by Eq. 1.9, and/or (iii) other oxidant agents electrochemically produced from some ions [116].

$$M + H_2O \rightarrow M(HO^{\bullet}) + H^+ + e^- \quad 1.7$$

$$2M(HO^{\bullet}) \rightarrow 2MO + H_2O_2 \quad 1.8$$

$$3H_2O \rightarrow O_3 + 6H^+ + 6e^- \quad (1.9)$$

Oxidants electrochemically generated from ions include active chlorine species, persulfate, perphosphate, percarbonate and H_2O_2 generated from chloride, sulphate (or hydrogen sulphate), phosphate, carbonate (or hydrogen carbonate) and oxygen, respectively, existing in the bulk. While active chlorine species, persulfate, perphosphate and percarbonate are produced from ions oxidation at the anode, the H_2O_2 is generated from oxygen reduction at the cathode. Ions can already compose the effluent matrix or be externally added. Active chlorine species are the most important indirect oxidation agents. Their generation comprises direct oxidation of chloride ions at the anode to yield chlorine (Cl_2) via Eq. 1.10, which disproportionated to hypochlorous acid (HClO) and chloride via Eq. 1.11 [117]. HClO is in equilibrium with hypochlorite ion (ClO^-) according to Eq. 1.12 [118].

$$2Cl^- \rightarrow Cl_2 + 2e^- \quad (1.10)$$

$$Cl_2 + H_2O \leftrightarrow HClO + Cl^- + H^+ \quad (1.11)$$

$$HClO \leftrightarrow ClO^- + H^+ \quad (1.12)$$

The predominant active chlorine species is Cl_2 for pH below 3, from pH 3 to 8 the dominant species is HClO and the ClO^- prevails for pH above 8 [119]. HClO (E^o = 1.49 V/SHE) and Cl_2 (E^o = 1.36 V/SHE) exhibit higher redox potentials than ClO^- (E^o = 0.89 V/SHE), and so the oxidation of organics should be faster at acidic pH. HClO content can be converted into chlorate ion (ClO_3^-) according to Eq. 1.13, which is a poor oxidant. For some electrodes, namely boron-doped diamond (BDD), perchlorate ion (ClO_4^-) is also formed via Eqs. 1.14-1.17 [120], which corresponds to the least reactive oxidant of the chloro-oxoanions and it is known for its hazardousness for human health [121]. Hazardous organochlorinated species, including chloramines, trihalomethanes, haloacetonitriles and haloketones, have also been detected during AO as a result of active chlorine species reaction with different functional groups of organic matter [122].

$$6HClO + 3H_2O \rightarrow 2ClO_3^- + 4Cl^- + 12H^+ + 1.5O_2 + 6e^- \quad (1.13)$$

$$Cl^- + HO^\bullet \rightarrow ClO^- + H^+ + e^- \quad (1.14)$$

$$ClO^- + HO^\bullet \rightarrow ClO_2^- + H^+ + e^- \quad (1.15)$$

$$ClO_2^- + HO^\bullet \rightarrow ClO_3^- + H^+ + e^- \quad (1.16)$$

$$ClO_3^- + HO^\bullet \rightarrow ClO_4^- + H^+ + e^- \quad (1.17)$$

The efficiency of the process is highly dependent on the mass transfer of contaminants from the bulk to the anode surface [117], and also on the nature of the anode material. Several anodes have been tested with the purpose to find the best performance for landfill leachate treatment. Ti–Ru–Sn ternary oxide anode ($TiRuSnO_2$), lead oxide anode (PbO_2), and BDD anodes were compared in the treatment of an old age MSWLL, demonstrating a faster oxidation rate and lower specific energy consumption using the BDD anode, consequently resulting in a minor price of treatment [123]. Generally, BDD shows the best organics removal rates. This anode has the better potential for O_2 evolution (2.2 to 2.6 V/SHE) and was widely used for the treatment of leachates. By analysing Table 1.6, it is clear to notice the BDD superiority in COD removal efficiency in comparison with other anodes. The efficacy of treatment is very dependent on the leachate matrix, which can also explain the wide difference in current density values used in the studies. Low pH generally is the best option, but complete COD removal was achieved with BDD anode even at high pH [123]. Only one study applied AO to a NHISWL leachate, achieving approximately 50% of COD removal, which is a reasonable abatement and instigates the use of this technology also for industrial solid waste [54].

Table 1.6 Performance of AO for different landfill leachates.

Anode	Current density (mA cm^{-2})	Time (min)	pH	COD (mg O_2 L^{-1})	COD removal (%)	Ref.
BDD	300	360	2.8	897[a]	~ 50[a]	[54]
$TiRuSnO_2$	2000	480	8.2	780	35	[123]
PbO_2	2000	480	8.2	780	85.2	
BDD	2000	480	8.2	780	100	
Ti/BDD	40	480	2	652	95.2	[124]
Ti/RuO_2	40	480	2	652	92.8	
BDD/Nb	50	360	5.16	3779	87.5	[125]
BDD	~ 260	480	5	3385	51	[126]

[a] DOC (in mg L^{-1}) instead of COD.

1.1.2.2.3.3 Fenton's reaction based processes

Fenton, PF, EF, and PEF processes are based on Fenton's reaction (Eq. 1.18), in which H_2O_2 and Fe^{2+} are the reagents and powerful $HO^{\bullet}$ are generated [127].

$$Fe^{2+} + H_2O_2 \rightarrow Fe^{3+} + HO^{\bullet} + OH^{-} \quad 1.18$$

In the classical Fenton process, H_2O_2 is added to the solution and Fe^{2+} is also added to the solution or is already part of the effluent matrix. This process can be efficiently applied at acidic pH of 2.8-3.0 since precipitation does not take place yet for most of the wastewaters [128]. The major limiting step of the Fenton process is the unavailability of Fe^{2+}. In the case of excess of H_2O_2, Fe^{3+} can be reduced to Fe^{2+} via

Eqs. 1.19 and 1.20 [128], which, against all expectations, can be regarded as parasitic reactions competing with Fenton's reaction since these two reactions are much slower than the Fenton's reaction and $HO_2^{\bullet}$ is a weak oxidant. Note that other parasitic reactions can also occur in the presence of H_2O_2 and Fe^{2+} in excess, such as Eqs. 1.21 and 1.22 [129].

$$Fe^{3+} + H_2O_2 \rightarrow Fe^{2+} + HO_2^{\bullet} + H^+ \quad 1.19$$

$$Fe^{3+} + HO_2^{\bullet} \rightarrow Fe^{2+} + O_2 + H^+ \quad 1.20$$

$$H_2O_2 + HO^{\bullet} \rightarrow H_2O + HO_2^{\bullet} \quad 1.21$$

$$Fe^{2+} + HO^{\bullet} \rightarrow Fe^{3+} + OH^- \quad 1.22$$

An efficient way to promote Fe^{3+} regeneration to Fe^{2+} and thus increase the rate of Fenton's reaction relies on the use of UV irradiation. In the presence of UV light, two main mechanisms occur: (i) the photoreduction of Fe(III)-hydroxy complexes, namely the photoreduction of the most photoactive $FeOH^{2+}$ at pH near 3 according to Eq. 1.23 [128], leading not only to Fe^{3+} regeneration to Fe^{2+} but also to the production of extra $HO^{\bullet}$, and (ii) the direct photolysis by ligand-to-metal charge transfer excitation of complexes formed between Fe^{3+} and some organics, including carboxylic acids, via the general Eq. 1.24 [130], promoting the regeneration of Fe^{2+} and the formation of weak oxidizing species (superoxide anion radical, carbon dioxide anion radical, H_2O_2, etc.).

$$FeOH^{2+} + h\nu \rightarrow Fe^{2+} + HO^{\bullet} \quad 1.23$$

$$Fe^{3+}(L)_n + h\nu \rightarrow Fe^{2+}(L)_{n-1} + (L)^{\bullet}{}_{(ox)} \quad 1.24$$

Usually, artificial ultraviolet A (UVA) or UVC radiation is employed, but the scientific community has also been resorting to solar radiation (UV-Vis) as a green alternative. In the presence of UVC light, the homolytic cleavage of the peroxide (–O–O–) bond via Eq. 1.6 also occurs, improving the production of $HO^{\bullet}$.

EF and PEF processes have also reached attention due to the efficacy of the in-loco generation of H_2O_2 from the two-electron reduction of O_2 (directly injected as a pure gas or bubbled air) at the cathode surface in acidic/neutral media, according to Eq. 1.25 (E^o = 0.68 V/SHE) [131].

$$O_{2\,(g)} + 2\,H^+ + 2e^- \rightarrow H_2O_2 \quad 1.25$$

Furthermore, the Fe^{3+} regeneration to Fe^{2+} is also promoted by cathodic reduction via Eq. 1.26 [132], leading to the continuous production of Fenton's reagent.

$$Fe^{3+} + e^- \rightarrow Fe^{2+} \quad 1.26$$

Hence, the cathode plays an essential role in these processes and can be the reason for the treatment success or failure. Two main cathode materials have been applied, namely carbon-polytetrafluoroethylene (PTFE) gas (O_2 or air) diffusion electrodes and carbon felts. The former cathodes provide large amounts of H_2O_2 and low Fe^{2+} cathodic regeneration, whereas the latter cathodes promote Fe^{3+} continuous cathodic conversion into Fe^{2+} and low H_2O_2 electrogeneration [133].

Table 1.7 summarizes the main results of the utilization of Fenton's reaction based processes along the last years in the treatment of leachates from different kind of landfills. By analysing the literature, is it clear that the PEF process usually is the most powerful Fenton's reaction based process, followed by the PF process.

Table 1.7 Performance of Fenton's reaction based processes for different landfill leachates.

Process	pH	[Fe] (mg L^{-1})	[Fe]:[H_2O_2]	COD (mg O_2 L^{-1})	COD removal (%)	Ref.
Fenton	2.8	60	1:6.6	384[a]	~ 22[a]	[134]
PF	2.8	60	1:6.6	384[a]	~ 68[a]	
Solar PF	2.8	60	1:6.6	384[a]	~ 75[a]	
EF	2.8	60	-	384[a]	~ 42[a]	
PEF	2.8	60	-	384[a]	~ 73[a]	
Solar PEF	2.8	60	-	384[a]	~ 78[a]	
Fenton	3	439	1:5	2540	19	[135]
Solar PF	3	439	1:5	2540	78	
Fenton	3	386	1:5	1962	53	
Solar PF	3	386	1:5	1962	84	
Solar PF	2.8 – 3	30	1:6.6	1302[a]	43	[136]
PEF	4 – 5	81	1:3.7	6924	48	[137]
PF	3	-	-	2000	70	[138]
PEF	3	-	-	2000	97	
PEF	2.8	150	1:2.6	2820	92	[54]
Fenton	3	634	1:4.75	10516	81	[139]

[a] DOC (in mg L^{-1}) instead of COD.

1.1.2.2.3.4 Ozonation and O_3-based processes

Ozonation process is a classical AOP based on two main mechanisms: (i) direct reaction pathway involving O_3 on account of its high redox potential (E^o of 2.076 V/SHE) [140]), which preferentially impacts unsaturated electron-rich bonds of specific functional groups (e.g. aromatics, olefins and amines) [141], and (ii) indirect route involving various highly reactive species generated by O_3 decomposition at alkaline pH via Eqs. 1.27-1.40 [142], among which the powerful $HO^{\bullet}$ and also H_2O_2.

$$O_3 + HO^- \rightarrow HO_2^- + O_2 \quad (1.27)$$

$$HO_2^- + O_3 \rightarrow O_3^{\bullet -} + HO_2^{\bullet} \quad (1.28)$$

$$HO_2^{\bullet} \rightarrow O_2^{\bullet -} + H^+ \quad 1.29$$

$$O_2^{\bullet -} + H^+ \leftrightarrow HO_2^{\bullet} \quad 1.30$$

$$O_2^{\bullet -} + O_3 \rightarrow O_3^{\bullet -} + O_2 \quad 1.31$$

$$O_3^{\bullet -} + H_2O \rightarrow HO^{\bullet} + O_2 + HO^- \quad 1.32$$

$$O_3^{\bullet -} + HO^{\bullet} \rightarrow HO_2^{\bullet} + O_2^{\bullet -} \quad 1.33$$

$$O_3^{\bullet -} + HO^{\bullet} \rightarrow O_3 + HO^- \quad 1.34$$

$$HO^{\bullet} + O_3 \rightarrow HO_2^{\bullet} + O_2 \quad 1.35$$

$$HO_2^- + H^+ \rightarrow H_2O_2 \quad 1.36$$

$$H_2O_2 \rightarrow HO_2^- + H^+ \quad 1.37$$

$$O_3 + H_2O_2 \rightarrow HO_2^{\bullet} + OH^{\bullet} + O_2 \quad 1.38$$

$$HO^{\bullet} + H_2O_2 \rightarrow HO_2^{\bullet} + H_2O \quad 1.39$$

$$HO^{\bullet} + HO_2^- \rightarrow HO_2^{\bullet} + HO^- \quad 1.40$$

O_3-based processes mainly include ozonation with H_2O_2 (O_3/H_2O_2), with UVC radiation (O_3/UVC) and with H_2O_2 and UVC radiation (O_3/H_2O_2/UVC). In the O_3/H_2O_2 process, the rate of Eqs. 1.37 and 1.38 is improved. Researchers agree that O_3/H_2O_2 system is highly effective in achieving fast mineralization of recalcitrant organic from landfill leachates [143, 144]. In the O_3/UVC process, UVC light itself can effectively degrade some compounds by direct photolysis or also excite the organic molecules of the pollutant, increasing their susceptibility towards an attack by the $HO^{\bullet}$ [145]. Moreover, the formation of H_2O_2 is instigated via Eq. 1.41 [146] and the homolytic cleavage of the peroxide bond (–O–O–) under UVC radiation via Eq. 1.6 [113] can occur, with consequent generation of more $HO^{\bullet}$.

$$O_3 + H_2O + h\nu \rightarrow H_2O_2 + O_2 \quad 1.41$$

In the O_3/H_2O_2/UVC process, the concomitant presence of UVC radiation and high amounts of H_2O_2 promotes the occurrence in a high extent of the homolytic cleavage of the peroxide bond (–O–O–) via Eq. 1.6 [113] and the consequent production of high amounts of $HO^{\bullet}$.

Table 1.8 collects some studies on the treatment of landfill leachates by ozonation and O_3-based processes. Few works are available as regards the leachate treatment by these processes. Until now, only one publication has focused on the treatment of an ISWL leachate with ozonation technology, with an abatement of 50% of COD [53]. From Table 1.8, one can highlight the high efficiency of O_3/H_2O_2 and O_3/UVC processes and the inability of the O_3/H_2O_2/UVC process to provide a much better efficiency

compared to these processes. High pH is chosen in all works, proving the preference and benefits of $HO^{\bullet}$ oxidation power (indirect reaction) instead of dissolved O_3 attack (direct reaction).

Table 1.8 Performance of ozonation and O_3-based processes for different landfill leachates.

Process	pH	Volume (L)	Time (min)	Gas flow rate (L O_2 min^{-1})	[O_3] (g L^{-1})	COD (g O_2 L^{-1})	[O_3]:[H_2O_2]	COD removal (%)	Ref.
Ozonation	9	1.5	180	0.1	0.18	1.07	1:2.8	53	[147]
O_3/H_2O_2								57	
O_3/UVC								66	
O_3/H_2O_2/UVC							1:2.8	67	
Ozonation	8.1	4	30	1	1.2	6.50	1:1	~ 15[a]	[77]
O_3/H_2O_2								~ 22[a]	
O_3/UVC								~ 25[a]	
Ozonation	9	9	-	7.5	5	0.48	1:2	50	[53]
O_3/H_2O_2								40[a]	
Ozonation	9.3	0.4	180	0.19	1.2	11.4		39	[148]
Ozonation	9	0.5	180	0.5	3.6	1.88	1:1.1	34	[143]
O_3/H_2O_2								44	
Ozonation	9	1	60	0.83	0.11	0.74	1:5.3	30	[144]
O_3/H_2O_2								63	
Ozonation	10	10	60	1	0.09	1.39		16	[149]

[a] TOC (in mg L^{-1}) instead of COD.

1.2 Legislation

Countries across the globe have their own laws as regards the discharge of treated wastewaters into aquatic systems, as the landfills leachates. Table 1.9 evidences the pluralism of regulatory parameters among some countries.

COD is usually used to assess the organic content and it varies from very stringent values of 45 and 60 mg O_2 L^{-1} in Switzerland and Singapore and much higher values of 200 mg O_2 L^{-1} in Germany. The legislation of the United States and Brazil ignores this parameter. The content of organics is only assessed in terms of BOD_5. BOD_5 analysis is very important since it rates the necessary oxygen quantity to oxidize the biodegradable organic matter present in water. However, there is a huge lack of information if the COD is not measured, once only with this parameter is possible to analyse the non-biodegradable organic matter, which sometimes can be much higher than biodegradable ones, mainly in industrial wastewater.

Germany and United Kingdom do not include the total suspended solids in their legislation, but these solids can absorb light in superficial water, causing increased water temperature and decreased oxygen,

which creates an unfavourable environment for aquatic life and decreases the natural capacity for water depuration.

Table 1.9 Main limit emission values for effluents discharge into waterbodies according to the legislation of European Union and different countries.

Country	COD (mg O_2 L^{-1})	BOD_5 (mg O_2 L^{-1})	TSS (mg L^{-1})	Total phosphorous (mg P L^{-1})	Ammonia (mg NH_3-N L^{-1})	Total nitrogen (mg N L^{-1})	Ref.
European Union	125	25	35	1	-	10	[30]
Brazil	-	> 60 %[a]	1[b]	-	20	-	[150]
Germany	200	20	-	3	-	70	[151]
Portugal	150	40	60	3[c] or 0.5[d]	8	15	[152]
Singapore	100[e] or 60[f]	50[e] or 20[f]	50[e] or 30[f]	-	-	-	[153]
South Africa	75	-	25	-	6	-	[154]
Switzerland[g]	60[h] or 45[i]	20[h] or 15[i]	20[h] or 15[i]	0.8[j]	2[k]	-	[155]
United Kingdom	125	25	-	2[l] or 1[m]	-	15[l] or 10[m]	[156]
United States	-	37[n] or 140[o]	27[n] or 88[o]	-	4.9[n] or 10[o]	-	[157]

[a] At least 60% of BOD_5 removal;
[b] 1 mL L^{-1} after 1 h in an Inhoff test (sedimentable materials);
[c] In waters that feed lake or reservoir;
[d] In lake or reservoir;
[e] Not controlled watercourse;
[f] Controlled watercourse;
[g] For landfill leachate there is a regulation that limits the DOC to 10 mg L^{-1};
[h] For wastewater from plants of less than 10000 population equivalent;
[i] For wastewater plants from 10000 population equivalent or over;
[j] Only if discharged in sensitive waters as lakes or watercourses downstream of lakes;
[k] Ammonium (sum of NH_4^+-N and NH_3-N);
[l] In eutrophic sensitive area, from 10000 - 100000 population equivalent;
[m] In eutrophic sensitive area, over 100000 population equivalent;
[n] Maximum monthly average;
[o] Maximum daily average.

Switzerland is recognized as a country that imposes more stringent wastewater effluent standards, as organic trace contaminants, and includes, exclusively, limits for DOC for landfill leachates discharge. Higher discharge limits force the industries and landfills to improve their liquid effluent treatments, triggering a more sustainable environment.

Phosphorus and nitrogen contents are important parameters to be measured since if excessively found in waterbodies they could cause alteration and degradation of freshwater, through eutrophication, because of large nutrient inputs. The United States and Brazil do not have specific legislation for total phosphorus, while Singapore does not require any limit value for ammonia or total nitrogen discharge. In Germany, the required limit of total nitrogen for discharge in waterbodies is 70 mg L^{-1}, which can be an input value

high above the recommended, since waterbodies with values upper than 2 mg N L^{-1} are already considered hypertrophic [158]. It is clear that legislation for phosphorus and nitrogen discharge in waterbodies is very variable.

In the impossibility of reducing the effluents pollutant load up to the imposed discharge limits, effluents are generally sent to a wastewater treatment plant (WWTP), where they are diluted before treatment. Each WWTP defines its admission criteria.

1.3 Definition of a treatment strategy

The selection of an appropriate treatment solution for a leachate is strictly dependent on its characteristics. Some of the main characteristics that should always be considered include soluble organics responsible for oxygen consumption; solids and/or colloidal material in suspension; substances that have a hazardous environmental impact due to their persistency, toxicity, and bioaccumulation potential; heavy metals; refractory substances; phosphorous and nitrogen content; and volatile compounds. A wide characterization of the leachate is always very recommendable, once it can support the choice of appropriate treatment and improve the landfill leachate management [159]. However, even publications in scientific journals with high impact factors sometimes do not show a satisfactory characterization, making it impossible to perform a proper comparison between different leachates, their characteristics and treatment.

Figure 1.4 indicates usual routes that can be useful when a multistage treatment is indicated for leachate treatment. Table 1.10 displays the advantages and drawbacks of some of the processes described in this work. It is important to notice that it is crucial to consider the purpose of a wastewater treatment when selecting a treatment, i.e. the desired quality of the treated water.

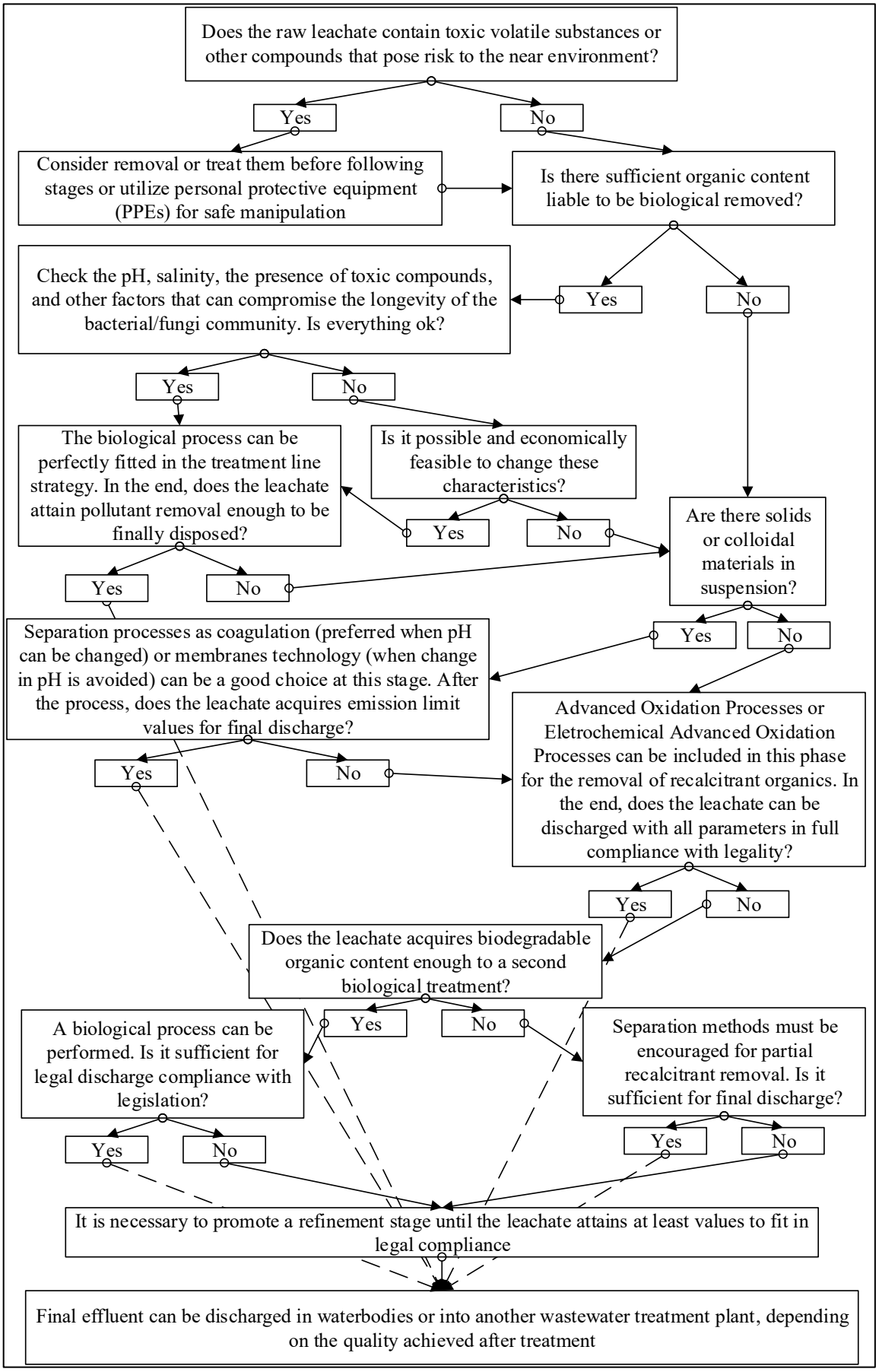

Figure 1.4 Pathways for landfill leachate treatment: from raw leachate to a proper discharge.

Table 1.10 Main advantages and disadvantages of some treatment technologies.

Technology	Advantages	Disadvantages
Coagulation/flocculation	Cheap and easy to operate Fast removal of contaminants	Necessity of a final deposition of the sludge Very pH dependent Necessity of pH adjustments, before and after the treatment Increase in salinity
Electrocoagulation	Simple and easy to operate Fast removal of contaminants Less sludge formation if compared to traditional coagulation No external chemicals are needed	Necessity of a final deposition of the sludge Anodes has to be changed frequently High energy consumption
Chemical precipitation	Simple and easy to operate Selectivity: can be used to removal specific compounds	Necessity of a final deposition of the precipitated pH dependent Demands large addition of chemicals (possibility of increase in salinity)
Membrane separation processes	Easy to operate and scalabe capacities Small footprint	Membranes fouling Limited pollutant degradation Inadequate separation of low molecular sized compounds
Biological treatment	Cheap and easy to operate Usually, no chemicals are needed	Acclimatation of biomass is often required in high polluted wastewaster High retention time It is limited to those organics compounds that are biodegradable. Not all organic compounds are susceptible to rapid and complete degradation

Technology	Advantages	Disadvantages
Catalytic oxidation processes	Easy to operate Reduction of costs since catalysts are already in the effluent Reduction of reagents consumption and reaction time in posterior stages	When aeration is applied, volatile organic compounds (VOCs) and/or other toxic compounds can be released
UVC/H_2O_2	Efficient in a wide range of pH Simple and easy to operate	Efficiency decreases in coloured/turbid effluents Demands large quantities of H_2O_2 Longer time required if compared to other AOPs
AO	Efficient in a wide range of pH Less or none chemicals are necessary for operation No catalyst is necessary	Requires expensive electrodes material High energy consumption Hazardous by-products
Fenton's reaction based processes	Cheaper catalyst source Easy to operate (if compared to heterogenous photocatalysis)	Higher efficiency only at acidic pH Sludge formation Necessity of post-treatment (neutralization) Reutilization of catalyst is not possible or very limited
Ozonation and O_3-based processes	Relatively simple installations, requiring little space No chemicals are needed on-site once O_3 is generated in situ The volume remains constant and sludge is not formed Remanescent dissolved O_3 can be eliminated since it tends to decompose into oxygen Fluctuations in flow rate and composition are not limiting factors	Relatively high cost of equipment and maintenance High requirements of energy for O_3 generator Off-gas O_3 must be destructed

1.4 Aim of the work and thesis outline

The present thesis focuses on the treatment of leachates from ISWLs by applying multistage treatment strategies that comprise various technologies, including coagulation/flocculation, chemical precipitation, biological oxidation, catalytic oxidation and various AOPs/EAOPs, such as H_2O_2/UVC, AO, Fenton's reaction based processes, and ozonation and O_3-based processes. Two ISWL leachates were covered: one from a HISWL and another from a NHISWL.

Two main objectives were addressed:

(i) To define treatment trains for the two ISWL leachates that allow achieving final effluents fulfilling European and Portuguese requirements for discharge into aquatic systems;

(ii) To tackle the lack of effective treatment solutions for ISWL leachates.

In addition, other objectives were covered:

(iii) To detail the physicochemical characteristics of the leachates;

(iv) To assess the influence of various operational variables on processes efficiency;

(v) To assess the possibility of recovering some added-value compounds from the leachates.

The thesis is structured into 7 chapters:

Chapter 1 corresponds to the present introductory section, wherein the problem of industrial solid waste pollution is covered as well as the available treatment technologies for landfill leachates and legislation covering the discharge of treated effluents. The objectives and the thesis outline are also provided at the end of the chapter.

Chapter 2 presents a description of all chemicals, experimental units and procedures, as well as the employed analytical determinations used within this thesis.

Chapter 3 focuses on the removal of sulphur compounds from the HISWL leachate by catalytic oxidation and chemical precipitation along with the formation of value-added products.

Chapter 4 discloses the complete treatment strategy for the HISWL leachate of Chapter 3. Various processes were covered: biological oxidation, coagulation/flocculation and various AOPs/EAOPs, such as H_2O_2/UVC, AO, PF and PEF.

Chapter 5 shows a new approach for the treatment of the HISWL leachate focused on the ozonation process and O_3-based processes, attempting to attain better results.

Chapter 6 focuses on the definition of a complete treatment train for the NHISWL leachate. The following processes were covered: coagulation/flocculation, biological oxidation, and AOPs/EAOPs, including PF, AO, ozonation and O_3-based technologies.

Finally, Chapter 7 displays a discussion of the most relevant results and conclusions of this thesis as well as some suggestions for future work.

1.5 References

[1] I. Chakraborty, P. Maity, COVID-19 outbreak: Migration, effects on society, global environment and prevention, Science of The Total Environment, 728 (2020) 138882.

[2] M.A. Zambrano-Monserrate, M.A. Ruano, L. Sanchez-Alcalde, Indirect effects of COVID-19 on the environment, Science of The Total Environment, 728 (2020) 138813.

[3] Eurostat, Generation of waste by waste category, hazardousness and NACE Rev. 2 activity, 2019.

[4] Eurostat, Real GDP per capita, 2020.

[5] W. Silpa Kaza Lisa Yao Perinaz Bhada-Tata Frank Van, What a Waste 2.0: A Global Snapshot of Solid Waste Management to 2050, The World Bank, 2018.

[6] S. Renou, J.G. Givaudan, S. Poulain, F. Dirassouyan, P. Moulin, Landfill leachate treatment: Review and opportunity, Journal of Hazardous Materials, 150 (2008) 468-493.

[7] S. Henderson, Environmental disaster declared after cyanide spill, Marine Pollution Bulletin, 30 (1995) 630.

[8] A.B. Ramsey, A.M. Faiia, A. Szynkiewicz, Eight years after the coal ash spill – Fate of trace metals in the contaminated river sediments near Kingston, eastern Tennessee, Applied Geochemistry, 104 (2019) 158-167.

[9] D. Winkler, A. Bidló, B. Bolodár-Varga, Á. Erdő, A. Horváth, Long-term ecological effects of the red mud disaster in Hungary: Regeneration of red mud flooded areas in a contaminated industrial region, Science of The Total Environment, 644 (2018) 1292-1303.

[10] F.R. Segura, E.A. Nunes, F.P. Paniz, A.C.C. Paulelli, G.B. Rodrigues, G.Ú.L. Braga, W. dos Reis Pedreira Filho, F. Barbosa, G. Cerchiaro, F.F. Silva, B.L. Batista, Potential risks of the residue from Samarco's mine dam burst (Bento Rodrigues, Brazil), Environmental Pollution, 218 (2016) 813-825.

[11] F.F.d. Carmo, L.H.Y. Kamino, R.T. Junior, I.C.d. Campos, F.F.d. Carmo, G. Silvino, K.J.d.S.X.d. Castro, M.L. Mauro, N.U.A. Rodrigues, M.P.d.S. Miranda, C.E.F. Pinto, Fundão tailings dam failures: the environment tragedy of the largest technological disaster of Brazilian mining in global context, Perspectives in Ecology and Conservation, 15 (2017) 145-151.

[12] F. Thompson, B.C. de Oliveira, M.C. Cordeiro, B.P. Masi, T.P. Rangel, P. Paz, T. Freitas, G. Lopes, B.S. Silva, A. S. Cabral, M. Soares, D. Lacerda, C. dos Santos Vergilio, M. Lopes-Ferreira, C. Lima, C. Thompson, C.E. de Rezende, Severe impacts of the Brumadinho dam failure (Minas Gerais, Brazil) on the water quality of the Paraopeba River, Science of The Total Environment, 705 (2020) 135914.

[13] P. Byrne, K.A. Hudson-Edwards, G. Bird, M.G. Macklin, P.A. Brewer, R.D. Williams, H.E. Jamieson, Water quality impacts and river system recovery following the 2014 Mount Polley mine tailings dam spill, British Columbia, Canada, Applied Geochemistry, 91 (2018) 64-74.

[14] H.I. Abdel-Shafy, M.S.M. Mansour, Solid waste issue: Sources, composition, disposal, recycling, and valorization, Egyptian Journal of Petroleum, 27 (2018) 1275-1290.

[15] M. Chertow, J. Park, Chapter 18 - Reusing Nonhazardous Industrial Waste Across Business Clusters, in: T.M. Letcher, D.A. Vallero (Eds.) Waste (Second Edition), Academic Press, 2019, pp. 353-363.

[16] D.A. Vallero, Chapter 31 - Hazardous Wastes, in: T.M. Letcher, D.A. Vallero (Eds.) Waste (Second Edition), Academic Press, 2019, pp. 585-630.

[17] X. Liu, J.T. Novak, Z. He, Removal of landfill leachate ultraviolet quenching substances by electricity induced humic acid precipitation and electrooxidation in a membrane electrochemical reactor, Science of The Total Environment, 689 (2019) 571-579.

[18] S.M. Iskander, J.T. Novak, Z. He, Reduction of reagent requirements and sludge generation in Fenton's oxidation of landfill leachate by synergistically incorporating forward osmosis and humic acid recovery, Water Research, 151 (2019) 310-317.

[19] M. Morozesk, M.M. Bonomo, I.d.C. Souza, L.D. Rocha, I.D. Duarte, I.O. Martins, L.B. Dobbss, M.T.W.D. Carneiro, M.N. Fernandes, S.T. Matsumoto, Effects of humic acids from landfill leachate on plants: An integrated approach using chemical, biochemical and cytogenetic analysis, Chemosphere, 184 (2017) 309-317.

[20] J. Zhang, J.-L. Gong, G.-M. Zenga, X.-M. Ou, Y. Jiang, Y.-N. Chang, M. Guo, C. Zhang, H.-Y. Liu, Simultaneous removal of humic acid/fulvic acid and lead from landfill leachate using magnetic graphene oxide, Applied Surface Science, 370 (2016) 335-350.

[21] A. Baun, A. Ledin, L.A. Reitzel, P.L. Bjerg, T.H. Christensen, Xenobiotic organic compounds in leachates from ten Danish MSW landfills—chemical analysis and toxicity tests, Water Research, 38 (2004) 3845-3858.

[22] I. Brás, L. Santos, A. Alves, Monitoring organochlorine pesticides from landfill leachates by gas chromatography–electron-capture detection after solid-phase microextraction, Journal of Chromatography A, 891 (2000) 305-311.

[23] S. Bilardi, P.S. Calabrò, R. Greco, N. Moraci, Selective removal of heavy metals from landfill leachate by reactive granular filters, Science of The Total Environment, 644 (2018) 335-341.

[24] T. Kawanishi, S. Matsumoto, Y. Horii, M. Masuzaki, Desalination for landfill leachates containing condensed inorganic salts, Desalination, 97 (1994) 415-425.

[25] V.J.P. Vilar, T.F.C.V. Silva, M.A.N. Santos, A. Fonseca, I. Saraiva, R.A.R. Boaventura, Evaluation of solar photo-Fenton parameters on the pre-oxidation of leachates from a sanitary landfill, Solar Energy, 86 (2012) 3301-3315.

[26] T.F.C.V. Silva, M.E.F. Silva, A. Cristina Cunha-Queda, A. Fonseca, I. Saraiva, R.A.R. Boaventura, V.J.P. Vilar, Sanitary landfill leachate treatment using combined solar photo-Fenton and biological oxidation processes at pre-industrial scale, Chemical Engineering Journal, 228 (2013) 850-866.

[27] H. Luo, Y. Zeng, Y. Cheng, D. He, X. Pan, Recent advances in municipal landfill leachate: A review focusing on its characteristics, treatment, and toxicity assessment, Science of The Total Environment, 703 (2020) 135468.

[28] A.Ž. Gotvajn, T. Tišler, J. Zagorc-Končan, Comparison of different treatment strategies for industrial landfill leachate, Journal of Hazardous Materials, 162 (2009) 1446-1456.

[29] E. Kattel, A. Kivi, K. Klein, T. Tenno, N. Dulova, M. Trapido, Hazardous waste landfill leachate treatment by combined chemical and biological techniques, Desalination and Water Treatment, 57 (2016) 13236-13245.

[30] T.C.o.t.E. Union, Council Directive 91/271/EEC of 21 May 1991 concerning urban waste-water treatment, Official Journal of the European Communities (1991).

[31] W.E. Morgan, Anaerobic/aerobic treatment of hazardous waste leachate, Journal of Hazardous Materials, 24 (1990) 279-310.

[32] J. Dollerer, P.A. Wilderer, Biological treatment of leachates from hazardous waste landfills using SBBR technology, Water Science and Technology, 34 (1996) 437-444.

[33] T. Setiadi, S. Fairus, Hazardous waste landfill leachate treatment using an activated sludge-membrane system, Water Science and Technology, 48 (2003) 111-117.

[34] M. Šír, M. Podhola, T. Patočka, Z. Honzajková, P. Kocurek, M. Kubal, M. Kuraš, The effect of humic acids on the reverse osmosis treatment of hazardous landfill leachate, Journal of Hazardous Materials, 207-208 (2012) 86-90.

[35] M. Baalousha, J.R. Lead, Y. Ju-Nam, 3.05 - Natural Colloids and Manufactured Nanoparticles in Aquatic and Terrestrial Systems, in: P. Wilderer (Ed.) Treatise on Water Science, Elsevier, Oxford, 2011, pp. 89-129.

[36] H.E. Hartnett, Dissolved Organic Matter (DOM), in: W.M. White (Ed.) Encyclopedia of Geochemistry: A Comprehensive Reference Source on the Chemistry of the Earth, Springer International Publishing, Cham, 2017, pp. 1-3.

[37] V.I. Haltrin, Absorption and scattering of light in natural waters, in: A.A. Kokhanovsky (Ed.) Light Scattering Reviews: Single and Multiple Light Scattering, Springer Berlin Heidelberg, Berlin, Heidelberg, 2006, pp. 445-486.

[38] K. Scott, WATER PURIFICATION, in: K. Scott (Ed.) Handbook of Industrial Membranes, Elsevier Science, Amsterdam, 1995, pp. 521-572.

[39] A.F. Ismail, K.C. Khulbe, T. Matsuura, Chapter 8 - RO Membrane Fouling, in: A.F. Ismail, K.C. Khulbe, T. Matsuura (Eds.) Reverse Osmosis, Elsevier, 2019, pp. 189-220.

[40] Z. Wang, J. Li, W. Tan, X. Wu, H. Lin, H. Zhang, Removal of COD from landfill leachate by advanced Fenton process combined with electrolysis, Separation and Purification Technology, 208 (2019) 3-11.

[41] A. Baiju, R. Gandhimathi, S.T. Ramesh, P.V. Nidheesh, Combined heterogeneous Electro-Fenton and biological process for the treatment of stabilized landfill leachate, Journal of Environmental Management, 210 (2018) 328-337.

[42] G. Nazimudheen, K. Roy, T. Sivasankar, V.S. Moholkar, Mechanistic investigations in ultrasonic pretreatment and anaerobic digestion of landfill leachates, Journal of Environmental Chemical Engineering, 6 (2018) 1690-1701.

[43] A.H. Hilles, S.S. Abu Amr, R.A. Hussein, O.D. El-Sebaie, A.I. Arafa, Performance of combined sodium persulfate/H2O2 based advanced oxidation process in stabilized landfill leachate treatment, Journal of Environmental Management, 166 (2016) 493-498.

[44] A. Rani, S. Negi, A. Hussain, S. Kumar, Treatment of urban municipal landfill leachate utilizing garbage enzyme, Bioresource Technology, 297 (2020) 122437.

[45] N. Kocakaplan, N. Ertugay, E. Malkoç, The degradation of landfill leachate in the presence of different catalysts by sonolytic and sonocatalytic processes, Particulate Science and Technology, 36 (2018) 734-741.

[46] P.K. Singa, M.H. Isa, Y.C. Ho, J.-W. Lim, Treatment of hazardous waste landfill leachate using Fenton oxidation process, E3S Web of Conferences, 34 (2018) 02034.

[47] P.K. Singa, M.H. Isa, Y.C. Ho, J.-W. Lim, Kinects and optmization of electro-Fenton process for COD removal from hazardous waste landfill Leachate, International Journal of Civil Engineering and Technology (IJCIET), 9 (2018) 8.

[48] N. Meky, M. Fujii, A. Tawfik, Treatment of hypersaline hazardous landfill leachate using a baffled constructed wetland system: effect of granular packing media and vegetation, Environmental Technology, 40 (2019) 518-528.

[49] L. Di Palma, P. Ferrantelli, C. Merli, E. Petrucci, Treatment of industrial landfill leachate by means of evaporation and reverse osmosis, Waste Management, 22 (2002) 951-955.

[50] D. Hira, N. Aiko, Y. Yabuki, T. Fujii, Impact of aerobic acclimation on the nitrification performance and microbial community of landfill leachate sludge, Journal of Environmental Management, 209 (2018) 188-194.

[51] M.S. Sung, D. Chang, H.Y. Lee, Performance improvement of an unstable anaerobic leachate treatment system in an industrial waste landfill, Water Science and Technology, 36 (1997) 333-340.

[52] D. Bhagawan, S. Poodari, N. Chaitanya, S. Ravi, Y.M. Rani, V. Himabindu, S. Vidyavathi, Industrial solid waste landfill leachate treatment using electrocoagulation and biological methods, Desalination and Water Treatment, 68 (2017) 6.

[53] P. Haapea, S. Korhonen, T. Tuhkanen, Treatment of industrial landfill leachates by chemical and biological methods: ozonation, ozonation + hydrogen peroxide, hydrogen peroxide and biological post-treatment for ozonated water, ozone: Science & Engineering, 24 (2002) 369-378.

[54] A.D. Webler, F.C. Moreira, M.W.C. Dezotti, C.F. Mahler, I.D.B. Segundo, R.A.R. Boaventura, V.J.P. Vilar, Development of an integrated treatment strategy for a leather tannery landfill leachate, Waste Management, 89 (2019) 114-128.

[55] M. Vepsäläinen, M. Sillanpää, Chapter 1 - Electrocoagulation in the treatment of industrial waters and wastewaters, in: M. Sillanpää (Ed.) Advanced Water Treatment, Elsevier2020, pp. 1-78.

[56] T.T. Teng, S. San Wong, L. Wei Low, Chapter 10 - Coagulation–Flocculation Method for the Treatment of Pulp and Paper Mill Wastewater, in: M. Fanun (Ed.) The Role of Colloidal Systems in Environmental Protection, Elsevier, Amsterdam, 2014, pp. 239-259.

[57] C. Amor, E.D. Torres-Socías, J.A. Peres, M.I. Maldonado, I. Oller, S. Malato, M.S. Lucas, Mature landfill leachate treatment by coagulation/flocculation combined with Fenton and solar photo-Fenton processes, Journal of Hazardous Materials, 286 (2015) 261-268.

[58] J. Pillai, Flocculants and Coagulants: The Keys to Water and Waste Management in Aggregate Production, Estadísticas de la Industria Química.

[59] Z. Tian, L. Zhang, X. Sang, G. Shi, C. Ni, Preparation and flocculation performance study of a novel amphoteric alginate flocculant, Journal of Physics and Chemistry of Solids, 141 (2020) 109408.

[60] E. Marañón, L. Castrillón, Y. Fernández-Nava, A. Fernández-Méndez, A. Fernández-Sánchez, Coagulation–flocculation as a pretreatment process at a landfill leachate nitrification–denitrification plant, Journal of Hazardous Materials, 156 (2008) 538-544.

[61] S.K. Singh, T.G. Townsend, T.H. Boyer, Evaluation of coagulation ($FeCl_3$) and anion exchange (MIEX) for stabilized landfill leachate treatment and high-pressure membrane pretreatment, Separation and Purification Technology, 96 (2012) 98-106.

[62] V. Oloibiri, S. De Coninck, M. Chys, K. Demeestere, S.W.H. Van Hulle, Characterisation of landfill leachate by EEM-PARAFAC-SOM during physical-chemical treatment by coagulation-flocculation, activated carbon adsorption and ion exchange, Chemosphere, 186 (2017) 873-883.

[63] A.R. Ishak, F.S. Hamid, S. Mohamad, K.S. Tay, Stabilized landfill leachate treatment by coagulation-flocculation coupled with UV-based sulfate radical oxidation process, Waste Management, 76 (2018) 575-581.

[64] Z.J. Yong, M.J.K. Bashir, C.A. Ng, S. Sethupathi, J.-W. Lim, A sequential treatment of intermediate tropical landfill leachate using a sequencing batch reactor (SBR) and coagulation, Journal of Environmental Management, 205 (2018) 244-252.

[65] W. Li, T. Hua, Q. Zhou, S. Zhang, F. Li, Treatment of stabilized landfill leachate by the combined process of coagulation/flocculation and powder activated carbon adsorption, Desalination, 264 (2010) 56-62.

[66] C.E. Barrera-Díaz, P. Balderas-Hernández, B. Bilyeu, Chapter 3 - Electrocoagulation: Fundamentals and Prospectives, in: C.A. Martínez-Huitle, M.A. Rodrigo, O. Scialdone (Eds.) Electrochemical Water and Wastewater Treatment, Butterworth-Heinemann, 2018, pp. 61-76.

[67] C. Espinoza-Cisternas, R. Salazar, Chapter 15 - Application of Electrochemical Processes for Treating Effluents From Landfill Leachate as Well as the Agro and Food Industries, in: C.A. Martínez-Huitle, M.A. Rodrigo, O. Scialdone (Eds.) Electrochemical Water and Wastewater Treatment, Butterworth-Heinemann, 2018, pp. 393-419.

[68] P.V. Nidheesh, J. Scaria, D.S. Babu, M.S. Kumar, An overview on combined electrocoagulation-degradation processes for the effective treatment of water and wastewater, Chemosphere, 263 (2021) 127907.

[69] M. Sillanpää, M. Shestakova, Chapter 2 - Electrochemical Water Treatment Methods, in: M. Sillanpää, M. Shestakova (Eds.) Electrochemical Water Treatment Methods, Butterworth-Heinemann2017, pp. 47-130.

[70] F. Ghanbari, J. Wu, M. Khatebasreh, D. Ding, K.-Y.A. Lin, Efficient treatment for landfill leachate through sequential electrocoagulation, electrooxidation and PMS/UV/$CuFe_2O_4$ process, Separation and Purification Technology, 242 (2020) 116828.

[71] N. Muhammad Niza, M.S. Yusoff, M.A.A. Mohd Zainuri, M.I. Emmanuel, A. Mohamed Hussen Shadi, M.A. Kamaruddin, Performance of batch electrocoagulation with vibration-induced electrode plates for landfill leachate treatment, Journal of Water Process Engineering, 36 (2020) 101282.

[72] B. Xu, S.M. Iskander, Z. He, Dominant formation of unregulated disinfection by-products during electrocoagulation treatment of landfill leachate, Environmental Research, 182 (2020) 109006.

[73] G.S. Soomro, C. Qu, N. Ren, S. Meng, X. Li, D. Liang, S. Zhang, Y. Li, Efficient removal of refractory organics in landfill leachate concentrates by electrocoagulation in tandem with simultaneous electro-oxidation and in-situ peroxone, Environmental Research, 183 (2020) 109249.

[74] O. Dia, P. Drogui, G. Buelna, R. Dubé, B.S. Ihsen, Electrocoagulation of bio-filtrated landfill leachate: Fractionation of organic matter and influence of anode materials, Chemosphere, 168 (2017) 1136-1141.

[75] N. Huda, A.A.A. Raman, M.M. Bello, S. Ramesh, Electrocoagulation treatment of raw landfill leachate using iron-based electrodes: Effects of process parameters and optimization, Journal of Environmental Management, 204 (2017) 75-81.

[76] G. Sharma, A. Kumar, S. Sharma, M. Naushad, R. Prakash Dwivedi, Z.A. Alothman, G.T. Mola, Novel development of nanoparticles to bimetallic nanoparticles and their composites: A review, Journal of King Saud University - Science, 31 (2019) 257-269.

[77] J.J. Wu, C.C. Wu, H.W. Ma, C.C. Chang, Treatment of landfill leachate by ozone-based advanced oxidation processes, Chemosphere, 54 (2004) 997-1003.

[78] A. Podder, D. Reinhart, R. Goel, Integrated leachate management approach incorporating nutrient recovery and removal, Waste Management, 102 (2020) 420-431.

[79] X.Z. Li, Q.L. Zhao, X.D. Hao, Ammonium removal from landfill leachate by chemical precipitation, Waste Management, 19 (1999) 409-415.

[80] T. Zhang, L. Ding, H. Ren, Pretreatment of ammonium removal from landfill leachate by chemical precipitation, Journal of Hazardous Materials, 166 (2009) 911-915.

[81] Y.-n. Chen, C.-h. Liu, J.-x. Nie, X.-p. Luo, D.-s. Wang, Chemical precipitation and biosorption treating landfill leachate to remove ammonium-nitrogen, Clean Technologies and Environmental Policy, 15 (2013) 395-399.

[82] H. Huang, D. Xiao, Q. Zhang, L. Ding, Removal of ammonia from landfill leachate by struvite precipitation with the use of low-cost phosphate and magnesium sources, Journal of Environmental Management, 145 (2014) 191-198.

[83] H. Huang, J. Liu, C. Xu, F. Gao, Recycling struvite pyrolysate obtained at negative pressure for ammonia nitrogen removal from landfill leachate, Chemical Engineering Journal, 284 (2016) 1204-1211.

[84] A. Aygun, S. Dogan, M. Argun, H. Ates, Removal of sulphate from landfill leachate by crystallization, Environmental Engineering Research, 24 (2018).

[85] A.V. Santos, L.H.d. Andrade, M.C.S. Amaral, L.C. Lange, Integration of membrane separation and Fenton processes for sanitary landfill leachate treatment, Environmental Technology, 40 (2019) 2897-2905.

[86] T.J. Mays, A new classification of pore sizes, in: P.L. Llewellyn, F. Rodriquez-Reinoso, J. Rouqerol, N. Seaton (Eds.) Studies in Surface Science and Catalysis, Elsevier, 2007, pp. 57-62.

[87] Z. Youcai, Chapter 5 - Leachate Treatment Engineering Processes, in: Z. Youcai (Ed.) Pollution Control Technology for Leachate from Municipal Solid Waste, Butterworth-Heinemann, 2018, pp. 361-522.

[88] L. Malaeb, G.M. Ayoub, Reverse osmosis technology for water treatment: State of the art review, Desalination, 267 (2011) 1-8.

[89] J.C. Espíndola, V.J.P. Vilar, Innovative light-driven chemical/catalytic reactors towards contaminants of emerging concern mitigation: A review, Chemical Engineering Journal, 394 (2020) 124865.

[90] T.A. Peters, Purification of landfill leachate with reverse osmosis and nanofiltration, Desalination, 119 (1998) 289-293.

[91] S.M.A. Abuabdou, W. Ahmad, N.C. Aun, M.J.K. Bashir, A review of anaerobic membrane bioreactors (AnMBR) for the treatment of highly contaminated landfill leachate and biogas production: Effectiveness, limitations and future perspectives, Journal of Cleaner Production, 255 (2020) 120215.

[92] W. Chen, X. Zhuo, C. He, Q. Shi, Q. Li, Molecular investigation into the transformation of dissolved organic matter in mature landfill leachate during treatment in a combined membrane bioreactor-reverse osmosis process, Journal of Hazardous Materials, 397 (2020) 122759.

[93] M. Zielińska, D. Kulikowska, M. Stańczak, Adsorption – Membrane process for treatment of stabilized municipal landfill leachate, Waste Management, 114 (2020) 174-182.

[94] J. Bohdziewicz, Treatment of landfill leachate by means of pressure driven membrane operations, Architecture Civil Engineering Environment, 1 (2008) 123-132.

[95] S. Renou, S. Poulain, J.G. Givaudan, P. Moulin, Amelioration of ultrafiltration process by lime treatment: Case of landfill leachate, Desalination, 249 (2009) 72-82.

[96] S. Collado, D. Núñez, P. Oulego, F.A. Riera, M. Díaz, Effect of landfill leachate ageing on ultrafiltration performance and membrane fouling behaviour, Journal of Water Process Engineering, 36 (2020) 101291.

[97] K. Wang, L. Li, F. Tan, D. Wu, Treatment of Landfill Leachate Using Activated Sludge Technology: A Review, Archaea (Vancouver, B.C.), 2018 (2018) 1039453-1039453.

[98] A.Ž. Gotvajn, A. Pavko, Wastewater Treatment Engineering: Perspectives on Biological Treatment of Sanitary Landfill Leachate, Intech Open, 2015.

[99] A. Cydzik-Kwiatkowska, M. Zielińska, Bacterial communities in full-scale wastewater treatment systems, World J Microbiol Biotechnol, 32 (2016) 66-66.

[100] E. Abatenh, B. Gizaw, Z. Tsegaye, M. Wassie, Open Journal of Environmental Biology The Role of Microorganisms in Bioremediation-A Review, Open Journal of Environmental Biology, 1 (2017) 038-040.

[101] P. Ghosh, I.S. Thakur, Treatment of Landfill Leachate Using Fungi: An Efficient and Cost-Effective Strategy, in: T. Satyanarayana, S.K. Deshmukh, B.N. Johri (Eds.) Developments in Fungal Biology and Applied Mycology, Springer Singapore, Singapore, 2017, pp. 341-357.

[102] S. Collado, P. Oulego, O. Suárez-Iglesias, M. Díaz, Leachates and natural organic matter. A review of their biotreatment using fungi, Waste Management, 96 (2019) 108-120.

[103] A. Kotronarou, M.R. Hoffmann, Catalytic autoxidation of hydrogen sulfide in wastewater, Environmental Science & Technology, 25 (1991) 1153-1160.

[104] M.R. Hoffmann, Kinetics and mechanism of oxidation of hydrogen sulfide by hydrogen peroxide in acidic solution, Environmental Science & Technology, 11 (1977) 61-66.

[105] N. Ahmad, S. Maitra, B.K. Dutta, F. Ahmad, Remediation of sulfidic wastewater by catalytic oxidation with hydrogen peroxide, Journal of Environmental Sciences, 21 (2009) 1735-1740.

[106] D.A. Armstrong, R.E. Huie, W.H. Koppenol, S.V. Lymar, G. Merényi, P. Neta, B. Ruscic, D.M. Stanbury, S. Steenken, P. Wardman, Standard electrode potentials involving radicals in aqueous solution: Inorganic radicals (IUPAC Technical Report), Pure Appl. Chem., 87 (2015) 1139-1150.

[107] S.C. Ameta, Chapter 1 - Introduction, in: S.C. Ameta, R. Ameta (Eds.) Advanced Oxidation Processes for Waste Water Treatment, Academic Press, 2018, pp. 1-12.

[108] D. Kanakaraju, B.D. Glass, M. Oelgemöller, Advanced oxidation process-mediated removal of pharmaceuticals from water: A review, Journal of Environmental Management, 219 (2018) 189-207.

[109] J. Wang, R. Zhuan, Degradation of antibiotics by advanced oxidation processes: An overview, Science of The Total Environment, 701 (2020) 135023.

[110] M. Malakootian, A. Shahesmaeili, M. Faraji, H. Amiri, S. Silva Martinez, Advanced oxidation processes for the removal of organophosphorus pesticides in aqueous matrices: A systematic review and meta-analysis, Process Safety and Environmental Protection, 134 (2020) 292-307.

[111] S. Samsami, M. Mohamadi, M.-H. Sarrafzadeh, E.R. Rene, M. Firoozbahr, Recent advances in the treatment of dye-containing wastewater from textile industries: Overview and perspectives, Process Safety and Environmental Protection, 143 (2020) 138-163.

[112] S. Liu, M. Lim, K. Chiang, R. Amal, R. Fabris, C. Chow, M. Drikas, A study on the removal of humic acid using advanced oxidation processes, Separation Science and Technology, 42 (2007) 1391-1404.

[113] J.H. Baxendale, J.A. Wilson, The photolysis of hydrogen peroxide at high light intensities, Transactions of the Faraday Society, 53 (1957) 344-356.

[114] G. Del Moro, A. Mancini, G. Mascolo, C. Di Iaconi, Comparison of UV/H_2O_2 based AOP as an end treatment or integrated with biological degradation for treating landfill leachates, Chemical Engineering Journal, 218 (2013) 133-137.

[115] H.-Y. Shu, H.-J. Fan, M.-C. Chang, W.-P. Hsieh, Treatment of MSW landfill leachate by a thin gap annular UV/H2O2 photoreactor with multi-UV lamps, Journal of Hazardous Materials, 129 (2006) 73-79.

[116] F.C. Moreira, R.A.R. Boaventura, E. Brillas, V.J.P. Vilar, Electrochemical advanced oxidation processes: A review on their application to synthetic and real wastewaters, Applied Catalysis B: Environmental, 202 (2017) 217-261.

[117] M. Panizza, G. Cerisola, Direct And Mediated Anodic Oxidation of Organic Pollutants, Chemical Reviews, 109 (2009) 6541-6569.

[118] D.C. Harris, Exploring Chemical Analysis, 4rd edition, W. H. Freeman and Company, New York, 2009.

[119] C. Boxall, G.H. Kelsall, Hypochlorite Electrogeneration. 2. Thermodynamics and Kinetic-model of the Anode Reaction Layer, Symposium on Electrochemical Engineering and the EnvironmentInstitution of Chemical Engineers, Rugby, United Kingdom, 1992, pp. 59-70.

[120] A. Sánchez-Carretero, C. Sáez, P. Cañizares, M.A. Rodrigo, Electrochemical production of perchlorates using conductive diamond electrolyses, Chemical Engineering Journal, 166 (2011) 710-714.

[121] G.M. Brown, B. Gu, The Chemistry of Perchlorate in the Environment, in: B. Gu, J.B. Coates (Eds.) Perchlorate. Environmental Occurrence, Interactions and Treatment, Chapter 2, Springer, New York, United States, 2006, pp. 17-47.

[122] L.-C. Chiang, J.-E. Chang, T.-C. Wen, Indirect oxidation effect in electrochemical oxidation treatment of landfill leachate, Water Research, 29 (1995) 671-678.

[123] M. Panizza, C.A. Martinez-Huitle, Role of electrode materials for the anodic oxidation of a real landfill leachate – Comparison between Ti–Ru–Sn ternary oxide, PbO2 and boron-doped diamond anode, Chemosphere, 90 (2013) 1455-1460.

[124] T.L. Luu, Post treatment of ICEAS-biologically landfill leachate using electrochemical oxidation with Ti/BDD and Ti/RuO_2 anodes, Environmental Technology & Innovation, 20 (2020) 101099.

[125] B. Zhou, Z. Yu, Q. Wei, H. Long, Y. Xie, Y. Wang, Electrochemical oxidation of biological pretreated and membrane separated landfill leachate concentrates on boron doped diamond anode, Applied Surface Science, 377 (2016) 406-415.

[126] Á. Anglada, A. Urtiaga, I. Ortiz, D. Mantzavinos, E. Diamadopoulos, Boron-doped diamond anodic treatment of landfill leachate: Evaluation of operating variables and formation of oxidation by-products, Water Research, 45 (2011) 828-838.

[127] F. Haber, J. Weiss, The catalytic decomposition of hydrogen peroxide by iron salts, Proceedings of the Royal Society of London. Series A, Mathematical and Physical Sciences, 147 (1934) 332-351.

[128] Y. Sun, J.J. Pignatello, Photochemical reactions involved in the total mineralization of 2,4-D by $Fe^{3+}/H_2O_2/UV$, Environmental Science & Technology, 27 (1993) 304-310.

[129] S. Bouafia-Chergui, N. Oturan, H. Khalaf, M.A. Oturan, Parametric study on the effect of the ratios $[H_2O_2]/[Fe^{3+}]$ and $[H_2O_2]$/[substrate] on the photo-Fenton degradation of cationic azo dye Basic Blue 41, Journal of Environmental Science and Health - Part A Toxic/Hazardous Substances and Environmental Engineering, 45 (2010) 622-629.

[130] O. Horváth, K.L. Stevenson, Charge Transfer Photochemistry of Coordination Compounds, VCH, New York, 1992.

[131] P.C. Foller, R.T. Bombard, Processes for the production of mixtures of caustic soda and hydrogen peroxide via the reduction of oxygen, Journal of Applied Electrochemistry, 25 (1995) 613-627.

[132] J.-J. Aaron, M. Oturan, New photochemical and electrochemical methods for the degradation of pesticides in aqueous media. Environmental applications, Turkish Journal of Chemistry, 25 (2001) 509-520.

[133] I. Sirés, J.A. Garrido, R.M. Rodríguez, E. Brillas, N. Oturan, M.A. Oturan, Catalytic behavior of the Fe^{3+}/Fe^{2+} system in the electro-Fenton degradation of the antimicrobial chlorophene, Applied Catalysis B: Environmental, 72 (2007) 382-394.

[134] F.C. Moreira, J. Soler, A. Fonseca, I. Saraiva, R.A.R. Boaventura, E. Brillas, V.J.P. Vilar, Incorporation of electrochemical advanced oxidation processes in a multistage treatment system for sanitary landfill leachate, Water Research, 81 (2015) 375-387.

[135] F.M. da Costa, S.D.A. Daflon, D.M. Bila, F.V. da Fonseca, J.C. Campos, Evaluation of the biodegradability and toxicity of landfill leachates after pretreatment using advanced oxidative processes, Waste Management, 76 (2018) 606-613.

[136] A. Ruiz-Delgado, P. Plaza-Bolaños, I. Oller, S. Malato, A. Agüera, Advanced evaluation of landfill leachate treatments by low and high-resolution mass spectrometry focusing on microcontaminant removal, Journal of Hazardous Materials, 384 (2020) 121372.

[137] L. Pellenz, F.H. Borba, D.J. Daroit, M.F.M. Lassen, S. Baroni, C.F. Zorzo, R.E. Guimarães, F.R. Espinoza-Quiñones, D. Seibert, Landfill leachate treatment by a boron-doped diamond-based photo-electro-Fenton system integrated with biological oxidation: A toxicity, genotoxicity and by products assessment, Journal of Environmental Management, 264 (2020) 110473.

[138] P. Asaithambi, R. Govindarajan, M.B. Yesuf, E. Alemayehu, Removal of color, COD and determination of power consumption from landfill leachate wastewater using an electrochemical advanced oxidation processes, Separation and Purification Technology, 233 (2020) 115935.

[139] A.M. Roudi, H. Kamyab, S. Chelliapan, V. Ashokkumar, A. Kumar, K.K. Yadav, N. Gupta, Application of response surface method for total organic carbon reduction in leachate treatment using Fenton process, Environmental Technology & Innovation, 19 (2020) 101009.

[140] D.R. Lide, Handbook of Chemistry and Physics, 84th edition, CRC Press, Boca Raton, 2004.

[141] J. Hoigné, H. Bader, Rate constants of reactions of ozone with organic and inorganic compounds in water-II: Dissociating organic compounds, Water Res., 17 (1983) 185-194.

[142] H. Tomiyasu, H. Fukutomi, G. Gordon, Kinetics and mechanism of ozone decomposition in basic aqueous solution, Inorganic Chemistry, 24 (1985) 2962-2966.

[143] N. Amaral-Silva, R.C. Martins, S. Castro-Silva, R.M. Quinta-Ferreira, Ozonation and perozonation on the biodegradability improvement of a landfill leachate, Journal of Environmental Chemical Engineering, 4 (2016) 527-533.

[144] S. Cortez, P. Teixeira, R. Oliveira, M. Mota, Ozonation as polishing treatment of mature landfill leachate, Journal of Hazardous Materials, 182 (2010) 730-734.

[145] E.M. Cuerda-Correa, M. Alexandre-Franco, G. Fernández, Advanced Oxidation Processes for the Removal of Antibiotics from Water. An Overview, Water, 12 (2019) 102.

[146] F.J. Beltran, Ozone–UV radiation–hydrogen peroxide oxidation technologies, in: M.A. Tarr (Ed.) Chemical Degradation Methods for Wastes and Pollutants - Environmental and Industrial Applications, Marcel Dekker, Inc., New York, 2003, pp. 1-77.

[147] A.I. Gomes, T.F. Soares, T.F.C.V. Silva, R.A.R. Boaventura, V.J.P. Vilar, Ozone-driven processes for mature urban landfill leachate treatment: Organic matter degradation, biodegradability enhancement and treatment costs for different reactors configuration, Science of The Total Environment, 724 (2020) 138083.

[148] M. Ghahrchi, A. Rezaee, Electro-catalytic ozonation for improving the biodegradability of mature landfill leachate, Journal of Environmental Management, 254 (2020) 109811.

[149] M. Chys, V.A. Oloibiri, W.T.M. Audenaert, K. Demeestere, S.W.H. Van Hulle, Ozonation of biologically treated landfill leachate: efficiency and insights in organic conversions, Chemical Engineering Journal, 277 (2015) 104-111.

[150] National Environmental Council, Resolução nº 430, de 13 de maio de 2011, Brazil, 2011.

[151] Ministry for the Environment, Nature, Conservation and Nuclear Safety, Promulgation of the New Version of the Ordinance on Requirements for the Discharge of Waste Water into Waters, Germany, 2004.

[152] Ministry of the Environment, Decreto-Lei nº 236/98 de 1 de Agosto, in: Diário da República, Portugal, 1998.

[153] Environmental Protection and Management, (Trade Effluent) Regulations 160/1999, Singapure, 2008.

[154] Ministry of Water and Environmental Affairs, Revision of General Authorisations in terms of section 39 of the National Water Act, 1998, South Africa, University of Pretoria, 2013.

[155] The Swiss Federal Council, 814.201 Waters Protections Ordinance of 28 October 1998 (WPO), Switzerland, 1998.

[156] United Kingdom Environmental Agency, Waste water treatment works: treatment monitoring and compliance limits, United Kingdom, 2019.

[157] Environmental Protection Agency, Effluent limitations attainable by the application of the best practicable control technology currently available (BPT), in: 40 CFR Parts 136 and 445, Federal Register, National Archives and Records Administration, United States, 2000, pp. 3050.

[158] B. Bhagowati, K.U. Ahamad, A review on lake eutrophication dynamics and recent developments in lake modeling, Ecohydrology & Hydrobiology, 19 (2019) 155-166.

[159] E. Caroline Baettker, C. Kozak, H.G. Knapik, M.M. Aisse, Applicability of conventional and non-conventional parameters for municipal landfill leachate characterization, Chemosphere, 251 (2020) 126414.

2 Materials and methods

This chapter presents a detailed description of all chemicals, experimental setups and procedures, and analytical determinations used in the work developed within this thesis.

The experimental work was mostly developed at the Laboratory of Separation and Reaction Engineering – Laboratory of Catalysis and Materials (LSRE-LCM), Department of Chemical Engineering, Faculty of Engineering of University of Porto, Portugal

2.1 Chemicals

Table 2.1 shows a brief description of all chemicals employed in the different reactions and analytical methods. Demineralized and ultrapure water used for analyses were obtained from a reverse osmosis system (Panice) and a Millipore® Direct-Q system (18.2 MΩ cm resistivity at 25 °C), respectively.

2.2 Experimental setups and procedures

Experimental units and respective experimental procedures for the various processes carried out within this thesis are described below.

2.2.1 Catalytic oxidation process

In Chapter 3, oxygen in the air supplied by an air pump (Aqua Medic, Mistral 2000) at different flow rates (0, 0.2, 0.3, 0.4, 0.5, and 0.75 L min^{-1}) or H_2O_2 at different contents (18%, 30%, 42%, 60%, 81% and 100% of the stoichiometric molar amount) were added to a glass vessel under magnetic stirring at ca. 100 rpm (Fisher Scientific, model FB15011) containing 500 mL of raw HISWL leachate. These trials were conducted at room temperature and without pH correction. Samples were taken every 30 min, during 120 min, for the aeration tests, and at 1-, 2.5-, 5-, 10- and 30-min for peroxidation tests. Sulphides and sulphites contents and pH were monitored. It should be noted that there was no significant difference in the sulphur compounds concentration after 1-min reaction, using H_2O_2. Accordingly, the results were presented for this reaction time. Under the best conditions, the experiments with air and H_2O_2 were replicated for 6- and 1-hour, respectively, and, at predefined times, the sulphides, sulphites, sulphates, dissolved oxygen and H_2O_2 concentrations were monitored as well as the presence of H_2S (g) in the surrounding interface gas-liquid. Given the complexity of the effluent and the compounds that could be released into the atmosphere, a sample of the gas-phase generated during the air oxidation process under the best conditions was also collected in a Tedlar bag (232-05SKC, SKC Inc.) for volatile VOCs analysis.

To generate high amounts of HISWL leachate free of sulphides and sulphites in Chapters 3 and 5, about 80 L of raw HISWL leachate (collected at different times for each chapter) were introduced into a 100 L stirred tank reactor, where the sulphide and sulphite ions were catalytically oxidised (5-min stirring time, natural pH and room temperature) by the addition of H_2O_2 as oxidant agent, using $[H_2O_2]:[S^{2-}]$ and $[H_2O_2]:[SO_3^{2-}]$ molar proportions of 4:1 and 1:1, respectively. After the settling of the chemical sludge overnight, leachate containing oxidised sulphur species, including sulphate, was then withdraw from the reactor.

Table 2.1 Chemicals.

Chemical	Molecular formula	Molecular weight (g mol^{-1})	Purity	Density (g cm^{-3})	Supplier	Purpose
Hydrogen peroxide	H_2O_2	34.02	30% (w/v)	1.10	Labkem	Oxidant
Barium chloride dihydrate	$BaCl_2.2H_2O$	244.28	≥ 99.0% (w/w)	-	PanReac	Sulphate chemical precipitation
Aluminium chloride hexahydrate	$AlCl_3.6H_2O$	241.43	≥ 99.0% (w/w)	2.398	Alfa Aesar	
Calcium hydroxide	$Ca(OH)_2$	74.10	83% (w/w)	2.24	VWR-Prolabo	
Ferric chloride	$FeCl_3$	162.2	-	-	Quimitécnica	Coagulation/flocculation experiments
Aluminium sulphate	$Al_2(SO_4)_3$	342.131	-	1.3	Rivaz Química	
Anionic flocculant Magnafloc 155	-	-	-	-	Tratamento de Águas Ltd.	
Cationic flocculant Ambifloc C 58	-	-	-	-	Tratamento de Águas Ltd.	
Ferrous sulphate heptahydrate	$FeSO_4.7H_2O$	278.05	98% (w/w)	-	PanReac	Catalyst
Pure and dry oxygen O_2 (HiQ® Oxygen 4.5)	O_2	32.00	≥ 99.995%	-	Linde	O_3 experiments
Potassium iodide	KI	166.00	-	3.23	Merck	
Ammonium monovanadate	NH_4VO_3	116.97	≥ 99.0% (w/w)	2.3	Merck	H_2O_2 analysis
1,10-phenanthroline 1-hydrate	$C_{12}H_8N_2.H_2O$	198.23	≥ 99.0% (w/w)	1.10	Panreac	Dissolved iron analysis
Acetic acid	$C_2H_4O_2$	60.05	100%	1.05	Fisher	
Ammonium acetate	$C_2H_7NO_2$	77.08	≥ 97% (w/w)	1.07	Fisher	
L-ascorbic acid	$C_6H_8O_6$	176.13	≥ 99% (w/w)	1.65	Acrós Organics	
Potassium dichromate	$K_2Cr_2O_7$	294.19	-	2.7	Merck	COD analysis
Potassium hydrogen phthalate	$C_2H_5KO_4$	204.22	-	1.636	Merk	

Table 2.1 Chemicals.

Chemical	Molecular formula	Molecular weight (g mol^{-1})	Purity	Density (g cm^{-3})	Supplier	Purpose
Silver sulphate	Ag_2SO_4	311.80	-	5.45	Merk	
Sulphuric acid	H_2SO_4	98.08	96%	1.84	Pronalab	
Sulphuric acid	H_2SO_4	98.08	96% (w/w)	1.84	Merck	pH adjustment (pure or diluted solutions)
Hydrochloric acid	HCl	36.46	33%	1.16	PanReac	
Sodium hydroxide	NaOH	40.00	98.5% (w/w)	2.13	Merck	
Potassium hydrogen	$C_8H_5KO_4$	204.22	-	-	ISAZA	Standard solutions for TC-IC-TN analyser calibration
Hydrogen carbonate	HCO_3^-	61.02	-	-	ISAZA	
Sodium carbonate	Na_2CO_3	105.99	-	-	ISAZA	
N-Allythiourea	$C_4H_8N_2S$	116.19	-	-	Merck	BOD_5 analysis
Sodium hydroxide pellets	NaOH	40.00	-	-	Merk	
Alpha-D-glucose	$C_6H_{12}O_6$	180.16	-	-	Fisher	Zahn-Wellens test

Table 2.1 Chemicals.

Chemical	Molecular formula	Molecular weight (g mol^{-1})	Purity	Density (g cm^{-3})	Supplier	Purpose
Chloride	NaCl	58.44	1000[a]	1.00	Merck	Standard solutions for anion chromatography analysis
Nitrate	$NaNO_3$	84.99	1000[a]	1.00	Merck	
Sulphate	Na_2SO_4	142.04	1000[a]	1.00	Merck	
Fluoride	NaF	41.99	1000[a]	1.00	Merck	
Phosphate	KH_2PO_4	136.09	1000[a]	1.00	Merck	
Bromide	NaBr	102.89	1000[a]	1.00	Merck	
Nitrite	$NaNO_2$	68.98	999[a]	1.00	Merck	
Sodium hydroxide	NaOH	40.00	100% (w/w)	1.04	Merck	Eluent for anion chromatography analysis
Ammonium	NH_4Cl	53.49	1000[a]	1.00	Merck	Standard solutions for cation chromatography analysis
Calcium	$CaCl_2$	110.98	1000[a]	1.00	Merck	
Magnesium	$MgCl_2.6H_2O$	203.31	1000[a]	1.00	Merck	
Potassium	KCl	74.55	1000[a]	1.00	Merck	
Sodium	NaCl	58.44	1000[a]	1.00	Merck	
Lithium	LiCl	42.39	1000[a]	1.00	Merck	
Methanesulfonic acid	CH_3SO_3H	96.11	> 99% (w/w)	1.48	Merck	Eluent for cation chromatography analysis
Ammonium chloride	NH_4Cl	53.49	> 95% (w/w)	1.9	VWR	Mineral medium for Zahn-Wellens and BOD_5 tests
Calcium chloride dihydrate	$CaCl.2H_2O$	147.02	> 95% (w/w)	-	VWR	
Dipotassium hydrogen phosphate	K_2HPO_4	174.18	-	2.44	Merck	
Disodium hydrogen phosphate dihydrate	$Na_2HPO_4.2H_2O$	178.00	-	-	Merck	
Iron (III) chloride hexahydrate	$FeCl_3.6H_2O$	270.30	-	-	Chem-lab	

Table 2.1 Chemicals.

Chemical	Molecular formula	Molecular weight (g mol^{-1})	Purity	Density (g cm^{-3})	Supplier	Purpose
Magnesium sulphate heptahydrate	$MgSO_4.7H_2O$	246.47	> 99% (w/w)	-	Panreac	
Potassium dihydrogen phosphate	KH_2PO_4	136.09	-	2.3	VWR	
Acetonitrile	CH_3CN	41.05	-	0.79	Merck	Humic substances analysis
Hydrochloric acid	HCl	36.46	37	1.16	Fisher	
Diethyl ether	$(CH_3CH_2)_2O$	74.12	-	0.71	Sigma-Aldrich	
Supelite DAX-8	-	-	-	-	Supelco	
Metranol	CH_3OH	32.04	-	0.79	Basic	
Sodium hydroxide	NaOH	40.00	-	-	Merck	

[a] Concentration expressed in mg L^{-1}.

2.2.2 Chemical precipitation process

In Chapter 3, chemical precipitation of sulphate as ettringite ($Ca_6Al_2(SO_4)_3(OH)_{12}.26H_2O$) and barite ($BaSO_4$) minerals was carried out using 250 mL of leachate previously subjected to oxidation with H_2O_2. For ettringite precipitation, aluminium chloride and calcium hydroxide were added at different initial pH values (9, 11, 11.5, 12 and 12.5) and different $[Ca^{2+}]$:$[Al^{3+}]$:$[SO_4^{2-}]$ molar ratios (6:2:3; 8:2.7:3, 9:3:3, 10:3.3:3, 12:4:3 and 14:4.7:3). For barite precipitation, barium chloride was added, varying the initial pH values (3, 5, 7, 8.5, 10 and 12) and the $[Ba^{2+}]$:$[SO_4^{2-}]$ molar ratios (0.5:1, 0.75:1, 1:1, 1.5:1 and 2:1). After chemicals addition, leachate samples were mixed for 30 min at 150 rpm, followed by a settling period of 30 min. Then, a sample of the supernatant was collected to measure the pH and the concentration of sulphates, aluminium, calcium and barium. Surface morphology and chemical composition of ettringite and barite precipitates (generated using the best operational conditions) were characterized by FTIR, SEM-EDS and XRD. Before analysis, ettringite and barite precipitates were washed with pure water and dried at 50 °C.

To produce high amounts of HISWL leachate free of sulphates in Chapters 3 and 5, the clarified pre-oxidised HISWL leachate (about 77 L) was placed into another 100 L stirred tank reactor, where the sulphate ions were chemically precipitated as barite (30-min stirring time, natural pH and room temperature) by the addition of $BaCl_2.2H_2O$, using a $[Ba^{2+}]$:$[SO_4^{2-}]$ molar ratio of 1:1. Finally, about 75 L of the desulphurised HISWL leachate was withdrawn from the reactor, after the sedimentation of the barite mineral overnight, and stored at 4 °C until its use in the subsequent trials.

2.2.3 Biological oxidation

In Chapter 4, biological oxidation was carried out in the biological system of Figure 2.1, which was composed of a 40 L capacity tank equipped with a mechanical stirrer (Ingenieurbüro CAT Scientific, model R50D) and an air pump (Aqua Medic, model Mistral 4000) connected to a flow controller and to an air diffuser placed at the tank bottom. Initially, 0.6 L of centrifuged activated sludge from a biological reactor used to treat another ISWL leachate was placed into the tank. Then, 10 L of pre-treated HISWL leachate were added to contact with the activated sludge for 6 days. The operational conditions were as follows: pH 8.4-8.7, with no need for pH control during the treatment, ambient temperature (21.1-22.2 ºC), and dissolved oxygen (DO) of ~2 mg L^{-1}. The DOC decreased during the first 4 days of treatment and remained similar in the next 2 days. The leachate was then withdrawn from the reactor after sludge settling for 2 h. Thereafter, 30 L of pre-treated HISWL leachate were added to the reactor and treated for 9 days under the above-mentioned operational conditions. The water lost by evaporation was restored

during treatments. The bio-treated HISWL leachate was finally withdrawn from the reactor after sludge settling for 2 h and used in subsequent trials.

In Chapter 6, the performance of a biological process was assessed by means of a Zahn-Wellens test executed according to the Test Guideline no. 302 B [1]. NHISWL leachate samples of 240 mL at neutral pH were added to magnetically stirred open glass vessels together with: (i) centrifuged activated sludge from a MWWTP of Northern mainland Portugal, previously adapted to the NHISWL leachate, and (ii) mineral nutrients (KH_2PO_4, K_2HPO_4, Na_2HPO_4, NH_4Cl, $CaCl_2$, $MgSO_4$ and $FeCl_3$).

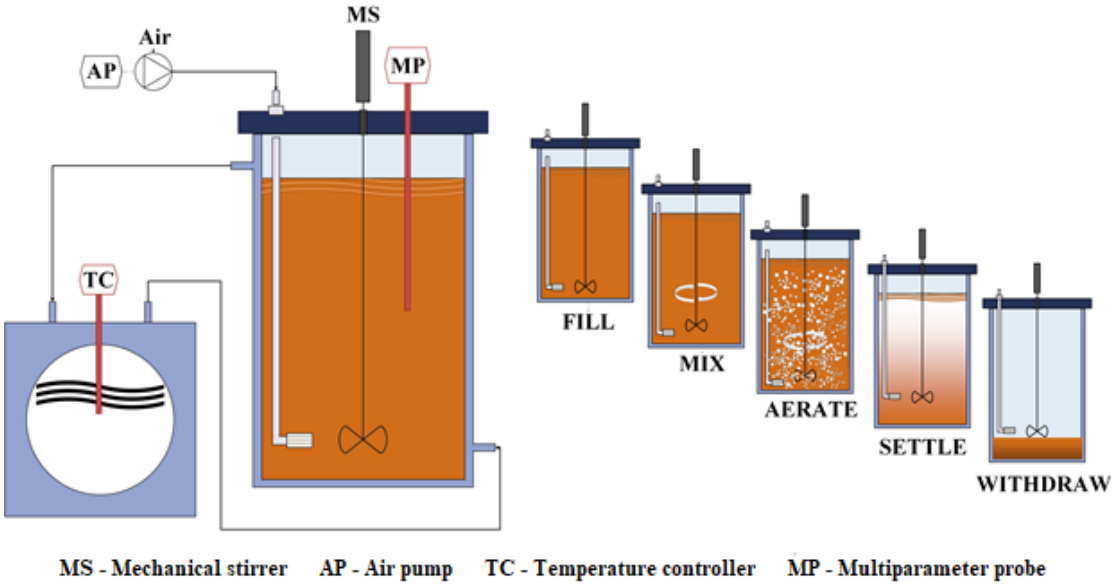

Figure 2.1 Sketch of the biological system used in Chapter 4.

Vessels were kept in the dark at 25 ºC for 28 days. Blank and control experiments were prepared using demineralized water and glucose (highly biodegradable) as carbon sources instead of samples, respectively. The percentage of biodegradation [2] was determined via Eq. 2.1 [1]:

$$D_t = \left[1 - \frac{C_T - C_B}{C_A - C_{BA}}\right] \times 100 \qquad 2.1$$

where C_T and C_B are sample and blank DOC contents (mg L^{-1}), respectively, at the sampling time t, and C_A and C_{BA} are the corresponding sample and blank DOC contents, respectively, measured 3 h after the test beginning.

2.2.4 Coagulation/flocculation process

Coagulation/flocculation trials were carried out in 500 mL capacity beakers under mechanical stirring (Jar Tester, Velp Scientifica, model JLT6). A volume of 200 mL (Chapter 4) or 250 mL (Chapters 5 and 6) of leachate was placed inside the beakers, the pH was adjusted to a given value (when required) and

a given coagulant ($FeCl_3$ or $Al_2(SO_4)_3$) dosage was added. Afterward, mechanical stirring was provided for 3 min at 120 rpm (rapid mixing) followed by 20 min at 20 rpm (slow mixing). The effect of solution pH and coagulant dosage was assessed. For the best pH and coagulant dosage, the use of a flocculant (cationic polyacrylamide flocculant Ambifloc C 58 or anionic polyacrylamide flocculant Magnafloc 155) was tested by adding a given flocculant dosage after the rapid mixing. The resulting sludge was settled for 2 h and the clarified leachate was analysed.

To generate coagulated leachate for subsequent trials, coagulation was performed at one go in a 30 L vessel using 9 L (Chapter 4), 5 L (Chapter 5) or 20 L (Chapter 6) of the leachate and the best pH and coagulant/flocculant type and dosage. Mechanical stirring was provided for 6 min (Chapters 4 and 5) or 7 min (Chapter 6) at 120 rpm (rapid mixing) followed by 40 min (Chapters 4 and 5) or 45 min (Chapter 6) at 20 rpm (slow mixing). Sedimentation was carried out for 2 h and the clarified leachate was carefully withdrawn and then refrigerated until the start of each assay.

In Chapter 5, in order to assess the influence of the pre-treatment type in a downstream O_3-based process, coagulation of the near-sulphur-free HISWL leachate was performed using: (i) ferric salts ($FeCl_3$) at acidic medium, under the best conditions reported in Chapter 3 (dose of 100 mg Fe^{3+} L^{-1}; pH of 2.8), using a leachate from the same HISWL; and (ii) aluminium salts ($Al_2(SO_4)_3$) at free near-neutral pH conditions, whose dose was optimized in a jar-test apparatus. Following this general procedure, the optimization of the coagulation process was divided into two parts. Firstly, in the presence of 300 mg Al^{3+} L^{-1} of coagulant, the effect of pH was evaluated according to three approaches: (i) coagulation at natural pH, without further correction after the coagulant addition; (ii) coagulation at natural pH, with further correction to its initial value after the coagulant addition; and (iii) coagulation with initial pH adjustment to 6 and further correction to its initial value after the coagulant addition. Secondly, for the best pH condition, the influence of the $Al_2(SO_4)_3$ dose was assessed between 100 and 400 mg Al^{3+} L^{-1}. The addition of flocculants to the coagulated leachate showed no improvements.

2.2.5 AOPs/EAOPs

2.2.5.1 H_2O_2/UVC, PF, AO and PEF

H_2O_2/UVC, PF, AO and PEF processes were carried out in a lab-scale flow system (Figure 2.2a) operated in semi-batch mode, with continuous solution recirculation throughout the system. The system was mainly composed of: (i) a 680 mL capacity photoreactor - FluHelik, (ii) a 1.5 L recirculation cylindrical glass vessel magnetically stirred and thermostatically controlled, (iii) a gear pump (Ismatec, model BVP-Z), and (iv) an electrochemical filter-press cell for AO and PEF processes.

The FluHelik photoreactor mainly consisted of: (i) a cylindrical shell of polished stainless steel (Chapter 4) or borosilicate glass (Chapter 6) with inlet and outlet pipes located perpendicularly to the fluid flow direction and tangentially to the shell, in horizontal plane and at the top in opposite sides, and (ii) a concentric inner quartz tube filled with an UVC or an UVA lamp. It is detailed characterized elsewhere [3]. Two UVC low-pressure mercury lamps were employed: 6 W power (Chapter 4 and 6) - Philips TUV G6T5 (radiant power of ~1.7 W determined by H_2O_2 actinometry [164]) and 11 W power (Chapter 6) - Philips TUV G11T5 (radiant power of ~2.5 W determined by H_2O_2 actinometry [3]). One UVA fluorescent blacklight blue lamp was used (Chapters 4 and 6): 6 W power - Philips TL 6W/08 (radiant power of ~0.6 W determined by 2-nitrobenzaldehyde actinometry [3]).

The electrochemical cell was a MicroFlowCell from ElectroCell (Tarm, Denmark) and corresponded to a one-compartment filter-press reactor. It was equipped with a BDD electrode working as an anode. The BDD electrode had 10 cm^2 of active area and comprised a conductive 2 mm thickness niobium sheet coated with approximately 5 μm BDD thin film. Two different electrodes were used as cathode: (i) a platinum (Pt) electrode of 10 cm^2 active area, consisting of a conductive 2 mm thickness titanium sheet coated with 2.5 μm pure Pt layer (Chapters 4 and 6 for AO process), and (ii) a carbon- polytetrafluoroethylene (PTFE) air-diffusion electrode of 10 cm^2 active area, compressed onto a 2 mm thickness nickel frame, which acted as an electrical connector (Chapter 4 for PEF process). All electrodes were supplied by ElectroCell. The anode and the cathode were separated by a 2 mm thickness PTFE flow frame filled with a polypropylene turbulence for solution circulation. When using the carbon-PTFE air-diffusion electrode, an identical frame was put in contact with the outer face of the electrode and fed with compressed air at a flow rate of ca. 5 L min^{-1} supplied by an air pump (Aqua Medic, model Mistral 2000). All the electrochemical reactor components were divided by 1 mm thickness peroxide-cured ethylene propylene diene monomer (EPDM) gaskets in order to avoid leakages. An Agilent E3634A 200W power supply (7 A, 25 V or 4 A, 50 V) was responsible to provide constant current density during trials. The applied potential of the cell was directly displayed. All system units were connected by PTFE tubing.

To perform H_2O_2/UVC, PF, AO, and PEF processes, a volume of ISWL leachate of 1.090 L or 1.100 L (Chapter 4 for trials without or with iron addition, respectively) or 1.080 L (Chapter 6) was added to the system and recirculated during 10-20 min in the dark at 50 L h^{-1} (Chapter 4) or 75 L h^{-1} (Chapter 6) until reaching a temperature of 20±1 ºC (good hydrodynamic conditions occur inside the FluHelik photoreactor for flow rates ≥ 50 L h^{-1} according to Webler et al., [4]). A control sample was taken. In Chapter 4, in PF-UVA trials using the acidified HISWL leachate and the coagulated HISWL leachate

with different total dissolved (TDI) contents, a given amount of $FeSO_4.7H_2O$ was added taking into account the iron content of the HISWL leachate, the leachate was recirculated for 10 min in the dark and a second control sample was taken.

Reactions were started-up by: (i) the addition of 400 mg L^{-1} of H_2O_2 together with the lamp switch on for H_2O_2/UVC and PF trials, (ii) the provision of a constant current density for the AO process, and (iii) the supply of a constant current density simultaneously with the UVA lamp switch on for the PEF-UVA process. H_2O_2 was continuously added in PF trials to maintain the oxidant content in the range ~100-500 mg L^{-1} since Bacardit et al., [5] reported that quite similar approaches improved the oxidation rate by ensuring the presence of H_2O_2 while minimising its consumption. The thermostatic bath temperature was continuously adjusted during reactions to keep the leachate at 20±1 ºC. In Chapter 4, the pH was controlled during PF, AO, and PEF-UVA trials at pH 2.8 and remained constant in the other trials. In Chapter 6, the pH was not controlled during reactions, suffering some changes. In AO and PEF-UVA trials, the specific energy consumption per unit volume for electrochemical cell operation (EC, kWh m^{-3}) was calculated via Eq. 2.2 [6]:

$$EC = \frac{E_{cell}\, I\, t}{V_s} \qquad 2.2$$

where E_{cell} is the average cell voltage (V), I is the applied current intensity (A), t is the reaction time (h) and V_s is the solution volume (L).

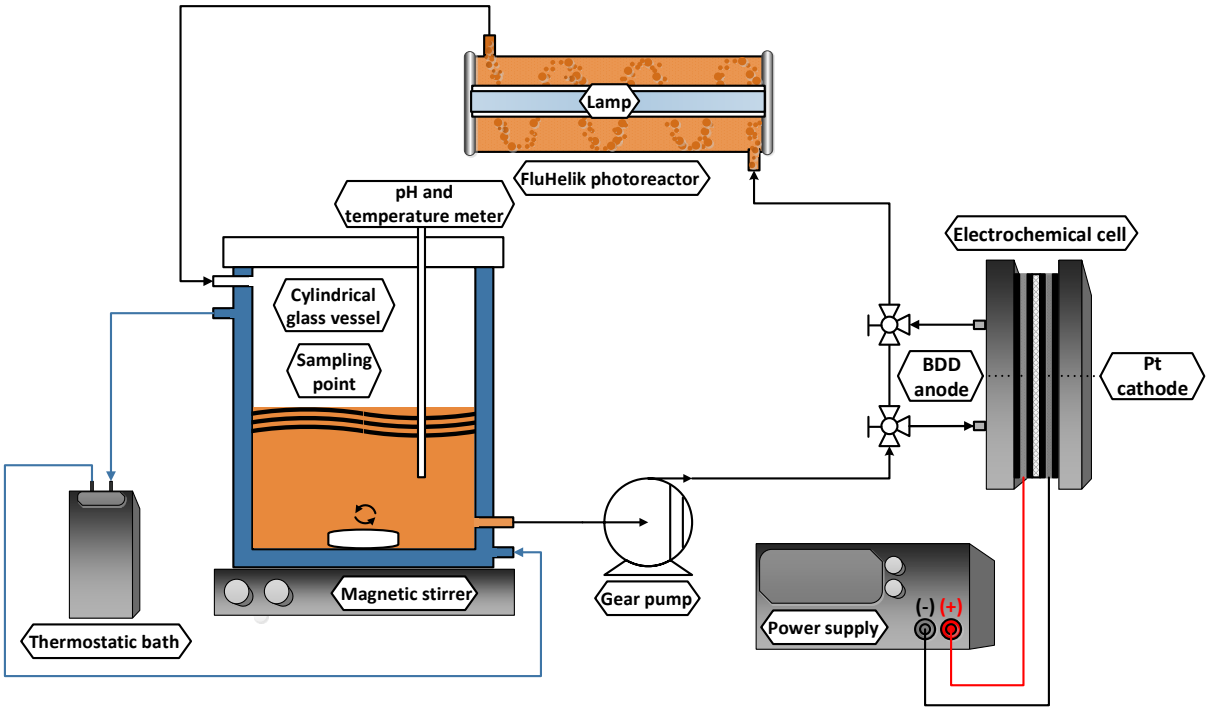

(a)

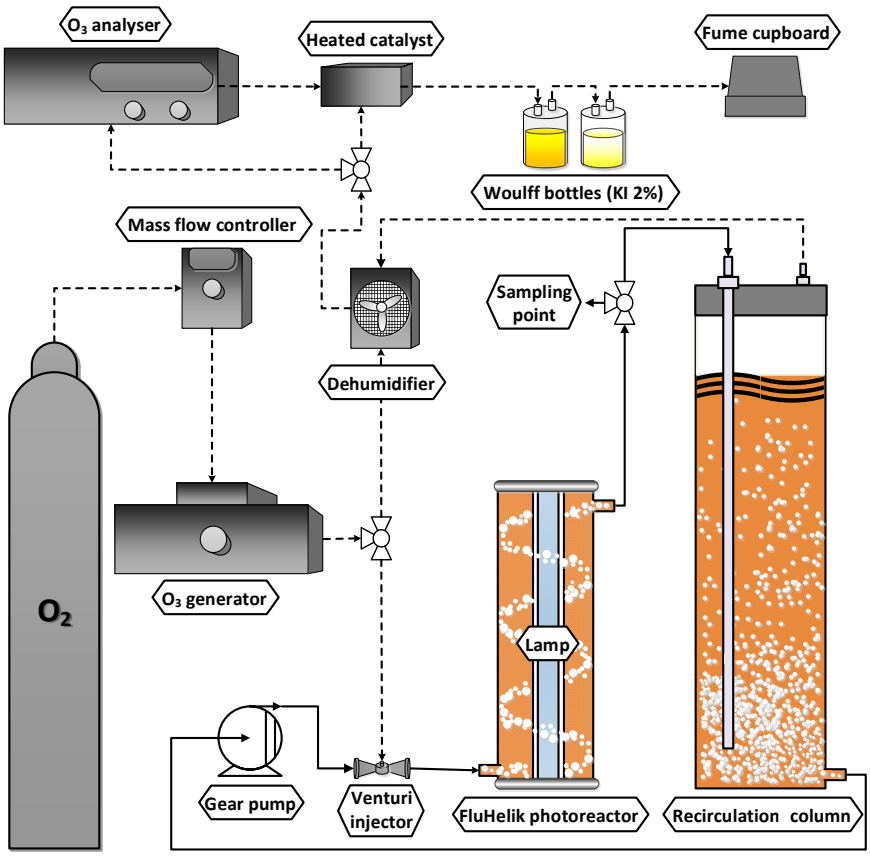

(b)

Figure 2.2 Sketch of lab-scale flow systems for H_2O_2/UVC, PF, AO and PEF processes (a) and ozonation and O_3-based processes (b).

2.2.5.2 Ozonation and O_3-based processes

Ozonation and O_3-based processes (O_3/H_2O_2, O_3/UVC, and O_3/H_2O_2/UVC) were carried in the lab-scale flow system of (Figure 2.2b), operated in semi-batch mode. It was mainly composed of: (i) an O_3 generator (BMT, model 802 N) fed by pure and dry O_2 at a constant flow rate regulated by a digital mass flow controller, able to produce up to 4 g O_3 h^{-1}, (ii) a recirculation column (BMT, model 4.1) made of glass and cylindrical in shape (internal diameter of 73 mm, maximum fluid column height of 370 mm, volume capacity of ~1.5 L), (iii) a 680 mL capacity FluHelik photoreactor, coupled in series to the column and filled with an 11 W UVC lamp in O_3/UVC and O_3/H_2O_2/UVC trials (photoreactor and UVC lamp described in Section 2.3.1), (iv) a gear pump (Ismatec, model BVP-Z), (v) a Venturi injector placed at the FluHelik inlet to inject a continuous flow of an O_3/O_2 gaseous mixture into the recirculating liquid stream, (vi) an UV-based O_3 analyser (BMT, model 964) coupled to a dehumidifier (BMT, model DH3b), and (vii) an O_3 destroyer unit (Heated Catalytic BMT) and Woulff bottles filled with 2% potassium iodide (KI) solution to safely deal with unreacted O_3 gas leaving the system. All system units were connected by PTFE tubing and the system was placed inside a fume cupboard to avoid O_3 exposure. More detailed information regarding this system can be accessed in Gomes et al. [7].

To perform ozonation and O_3-based processes, the O_3 gas stream was firstly diverted to the O_3 analyser until complete stabilization of the O_3 generation process. Meanwhile, the recirculation column was filled with 1.5 L of leachate, which was recirculated at 75 L h^{-1} for 10-20 min in the dark. After the stabilization period, a control sample was taken at a sampling point located between the FluHelik reactor and the column. The start of the reactions was marked by the O_3/O_2 gas stream forwarding to the Venturi injector for the ozonation process, simultaneously with the following procedures for O_3-based processes: (i) addition of 500 or 400 mg L^{-1} of H_2O_2 for the O_3/H_2O_2 process (Chapters 5 and 6, respectively), (ii) UVC lamp switch on for the O_3/UVC process, and (iii) addition of H_2O_2 together with UVC lamp switch on for the O_3/H_2O_2/UVC process. H_2O_2 was continuously added in O_3/H_2O_2 and O_3/H_2O_2/UVC methods to maintain the oxidant content in the range ~100-500 mg L^{-1} and thus enhance the oxidation rate [7], with the exception of one test in Chapter 5 where it was added all at once for comparison purposes. Temperature and pH were not controlled during reactions. The monitoring of injected, exhausted, and dissolved O_3 during reactions was done. The amount of O_3 consumed at each treatment time was estimated as the transferred O_3 dose (TOD, g O_3 L^{-1}), which depicts the accumulated amount of O_3 in the gas phase that is transferred to the liquid phase per unit of volume and time, according to Eq. 2.3.

$$TOD = \int_{o}^{t} \frac{Q_{gas}}{V_s} ([O_3]_{in} - [O_3]_{out}) dt \qquad 2.3$$

where t is the contact time (min), Q_{gas} is the gas flow rate (L min^{-1}), V_s is the solution volume (liquid phase) (L), and $[O_3]_{in}$ and $[O_3]_{out}$ are the inlet and outlet (off-gas) concentrations of O_3 in the gas phase (g L^{-1}), respectively.

2.3 Analyical determinations

Table 2.2 presents the analytical determinations carried out during the experimental work developed within this thesis.

2.4 Modeling of removal kinetics

A pseudo-first-order kinetic model was fitted to DOC, sulphides, and sulphites data obtained along the various processes as a simple mathematical model to quantitatively compare the processes efficiency. The kinetic model was adjusted by a nonlinear regression method using Fig.P software for Windows from Biosoft. The pseudo-first-order kinetic constants for DOC removal (k_{DOC}) and for sulphides and sulphites removal (k), in min^{-1}, were calculated from Eq. 2.4:

$$[X]_t = [X]_0 \times e^{-k_X \times t} \quad 2.4$$

where $[X]_t$ is the DOC, sulphides or sulphites content after time t and $[X]_0$ is the DOC, sulphides or sulphites content just before the reaction beginning.

The fitting was performed by minimizing the sum of the squared deviations between experimental and predicted values. The goodness of fitting was assessed by calculating the relative standard deviations, the coefficient of determination (R^2), and the residual variance (S^2_R).

Table 2.2 Analytical determinations.

Parameter	Methodology
5-day biochemical oxygen demand	BOD_5 was measured according to the Standard Methods for the Examination of Water and Wastewater (SMEWW) [8], 5210-B test, using an OxiTop® system (manometric respirometry).
Alkalinity	Alkalinity measurement was performed according to SMEWW [8], 2320 B test, using titration.
Ammonium, calcium, lithium, magnesium, potassium and sodium[a]	NH_4^+, Ca^{2+}, Li^+, Mg^{2+}, K^+ and Na^+ inorganic cations were determined by ion chromatography injecting 25 µL of sample in a Dionex DX-120 device equipped with a IonPac® CS12A (4 × 250 mm) column at ambient temperature and a cation self-regenerating (CSRS® Ultra II, 4 mm) suppressor, under isocratic elution of 20 mM methanesulphonic acid at a flow rate of 1.0 mL min^{-1} during 12 min.
Aromatic compounds[a]	The presence and content of aromatic compounds was qualitatively evaluated by UV spectrometry at 254 nm using a Merck Spectroquant® Prove 300 UV/Vis spectrophotometer.
Biodegradability – Zahn-Wellens test	Zahn-Wellens test was carried out as described in Section 2.2.3.
Chemical oxygen demand[b]	COD was measured according to the SMEWW [8], 5220-D test, through oxidation with potassium dichromate followed by photometric measuring, using using a WTW CR4200 thermoreactor and a Merck Spectroquant® Prove 300 UV/Vis spectrophotometer.
Chloride, nitrate, nitrite and sulphate[a]	Cl^-, NO_3^-, NO_2^- and SO_4^{2-} inorganic anions were quantified by ion chromatography injecting 10 µL of sample in a Dionex ICS-2100 apparatus, equipped with a IonPac® AS11-HC (4 × 250 mm) column at 30 ºC and an anion self-regenerating suppressor (ASRS® 300, 4 mm), under isocratic elution of 30 mM NaOH at a flow rate of 1.5 mL min^{-1} during 12 min.
Colour[a]	Colour was assessed by measuring the absorbance at 400 nm in a Merck Spectroquant® Prove 300 UV/Vis spectrophotometer and converting the data into the Platinum-Cobalt (Pt-Co) scale, according to NP 627:1972 [9].
Dissolved oxygen, conductivity and redox potential	DO, conductivity and ORP were measured by a HANNA Instruments HI 9828 Multiparameter analyser.
Dissolved O_3	Dissolved O_3 concentration was determined by reaction with dipropyl-*p*-phenylenediamine (DPD), according to DIN 38408-3, using Merck Spectroquant® kits Cat. No. 100607 and a Merck Spectroquant® Prove 300 UV/Vis spectrophotometer.
Fluorescence spectra[a]	Fluorescence spectra were measured using a Horiba Aqualog fluorometer by scanning with excitation wavelengths from 225 to 450 nm in 5 nm increments and emission wavelengths from 250 to 580 nm in 1 nm increments. The normalized methods for total fluorescence and regional integration were performed as described by Chen and Westerhoff [10].
Humic substances	HS extraction from leachate samples was performed by the acid-base treatment method, according to the SMEWW [8]. Shortly, leachate was filtered through a 0.45 µm cellulose membrane filter and acidified to pH 2.0. Acidified samples were percolated through a Supelite DAX-8 (Supelco) resin column. The preparative cleaning procedure of the resin is described by Friedrich et al. [11]. After percolating the whole sample through the adsorption column, HS were eluted from the DAX-8 resin using 0.1 M NaOH, in reverse flow, and measured as DOC.
Hydrogen peroxide[a]	H_2O_2 concentration was determined by the colourimetric vanadate method [12], measuring the absorbance at 450 nm in a Merck Spectroquant® Prove 300 UV/Vis spectrophotometer.

Table 2.2 Analytical determinations.

Parameter	Methodology
Hydrogen sulphide and nitrogen monoxide [165]	H_2S and NO were analysed by a multi-gas monitor MultiRAE Lite, from RAE systems.
pH and temperature	pH and temperature were measured by a multiparameter meter HI9828, from Hanna Instruments, and pH meter VWR symphony - SB90M5.
Salinity	Salinity was estimated by the formula [13]: $\text{Salinity (\%)} = 0.4665 \times \text{Conductivity (mS cm}^{-1}\text{)}^{1.097}$ (2.5)
Settled sludge volume	SSV_{30} was measured according to SMEWW [167], 2710 C test.
Size distributions of dissolved organic compounds[a]	Size distributions of dissolved organic compounds were determined by size exclusion chromatography (SEC) separation using a hydroxylated methacrylic polymer column (TOYOPEARL® HW-50S, Tosoh Bioscience LLC; 21 mm × 250 mm) combined with organic carbon detection (OCD) using a high-performance liquid chromatography (HPLC) (Agilent 1290) hyphenated with an organic carbon detector (Suez GE Sievers M9 TOC analyser).
Sludge volume index	SVI was determined according to the SMEWW [8], 2710 D test, which uses 30-min settled sludge volume (SSV_{30}) and TSS values.
Specific ultraviolet absorbance at 254 nm	$SUVA_{254}$ (L mg^{-1} m^{-1}) was obtained by dividing the UV absorbance at 254 nm (m^{-1}) of filtered samples by DOC (mg L^{-1}).
Solid-phase characterization	Surface morphology and chemical composition of minerals was assessed by scanning electron microscopy [14] coupled with energy dispersive X-ray (EDS) analysis, using a high resolution (Schottky) Environmental Scanning Electron Microscope with X-Ray Microanalysis and Electron Backscattered Diffraction analysis (Quanta 400 FEG ESEM/EDAX Genesis X4M). Samples were coated with an Au/Pd thin film, by sputtering, using the SPI Module Sputter Coater equipment. Functional groups on the surface of the precipitates were identified by infrared spectrometry (4000-400 cm^{-1}) using a Shimadzu FTIR IRAffinity spectrometer and analysed using KBr pellets and a diffuse reflectance accessory (Pike Technologies Inc., model TM EasiDiff). Crystaline nature of materials was investigated and quantified by x-ray diffraction (XRD) using a PANalytical Empyrean diffractometer. Phase identification from power diffraction was accomplished by using Match! Software (version 3.6.1.115), with FullProf and Crystallography Open Database [15].
Sulphide[a]	Total dissolved free sulphides (H_2S, HS^- and S^{2-}) were measured as S^{2-}, according to SMEWW [8], 4500-S^{2-} D test, by reaction with dimethyl-*p*-phenylenediamine and iron(III) (Merck Spectroquant® kits Cat. No. 114779 and Merck Spectroquant® Prove 300 UV/Vis spectrophotometer).
Sulphite[a]	SO_3^{2-} analysis was performed based on the reaction with 2,2'-dinitro-5,5'-dithiodibenzoic acid (Spectroquant® kits Cat. No. 101746 and Merck Spectroquant® Prove 300 UV/Vis spectrophotometer).
Total aluminium, barium, cadmium, chromium, copper, iron, lead, manganese, nickel and zinc[c]	Total concentration of Al, Ba, Cd, Cr, Cu, Fe, Pb, Mn, Ni and Zn was analysed by atomic absorption spectrometry in a 932 plus atomic absorption spectrometer from GBC Scientific Equipment.
Total arsenic[c]	Total As was measured by graphite furnace atomic absorption spectrometry (GF-AAS, GBC GF 3000, SenAA Dual).
Total dissolved carbon, dissolved inorganic carbon and dissolved organic carbon[a]	Total dissolved carbon and dissolved inorganic carbon were separately determined by catalytic combustion at 680 ºC and acidification, respectively, using a nondispersive infrared detector (NDIR) in a Shimadzu TOC-VCSN

Table 2.2 Analytical determinations.

Parameter	Methodology
	analyser equipped with ASI-V autosampler (Shimadzu, model TOC-V_{CSN}), after calibration with standard solutions of potassium hydrogen phthalate (total carbon) and a mixture of sodium hydrogen carbonate/sodium carbonate (inorganic carbon). DOC was given by the difference between. DOC was given by the difference between TDC and DIC (DOC = TDC - DIC).
Total nitrogen	N_T was determined by digestion with peroxodisulfate standardized procedure ISO 11905-1 followed by colorimetry based on reaction with 2,6-dimethylphenol (Merck Spectroquant® kits Cat. No. 114763, WTW CR4200 thermoreactor and Merck Spectroquant® Prove 300 UV/Vis spectrophotometer).
Total phosphorous	P_T was measured based on SMEWW [8], 4500-P E test, using colorimetry based on ascorbic acid (Merck Spectroquant® kits Cat. No. 114543, WTW CR4200 thermoreactor and Merck Spectroquant® Prove 300 UV/Vis spectrophotometer).
Total suspended solids and volatile suspended solids	TSS was measured by gravimetry, drying the solid residue at 105 °C, according to SMEWW [167], 2540-D test. VSS was determined by gravimetry, after suspended solids oxidation at 550 °C, according to SMEWW [8], 2540-E test.
Transmittance[a]	Transmittance was obtained from the UV absorbance at 254 nm (m^{-1}), according to: $\text{Transmittance (\%)} = 10^{(2 - \text{UV absorbance at 254 nm } (m^{-1}))}$ (2.6)
Turbidity	Turbidity was determined according to SMEWW [8], 2130 B test, using a HANNA HI 88703 turbidity meter.
Volatile organic compounds	VOCs were identifying using a GC/MSD device (gas chromatograph GC 6890N coupled to a mass spectrometer detector MSD 5973, Agilent Technologies, Inc.).

[a] Samples were filtered through 0.45 μm Nylon membrane filters before analysis.
[b] For samples with H_2O_2, the excess of H_2O_2 was previously removed by adding a small volume of 0.1 g L^{-1} catalase solution (2500 U mg^{-1} bovine liver) at neutral pH.
[c] Samples acidified with nitric acid and digested, and further filtered thought 0.45 μm cellulose acetate membrane before analysis.

2.5 References

[1] OECD, Test No. 302B: Inherent Biodegradability: Zahn-Wellens/ EVPA Test, Organisation for Economic Cooperation and Development (OECD) Guidelines for the Testing of Chemicals, (1992).

[2] Y. Deng, J.D. Englehardt, Treatment of landfill leachate by the Fenton process, Water Research, 40 (2006) 3683-3694.

[3] F.C. Moreira, E. Bocos, A.G.F. Faria, J.B.L. Pereira, C.P. Fonte, R.J. Santos, J.C.B. Lopes, M.M. Dias, M.A. Sanromán, M. Pazos, R.A.R. Boaventura, V.J.P. Vilar, Selecting the best piping arrangement for scaling-up an annular channel reactor: An experimental and computational fluid dynamics study, Science of The Total Environment, 667 (2019) 821-832.

[4] A.D. Webler, F.C. Moreira, M.W.C. Dezotti, C.F. Mahler, I.D.B. Segundo, R.A.R. Boaventura, V.J.P. Vilar, Development of an integrated treatment strategy for a leather tannery landfill leachate, Waste Management, 89 (2019) 114-128.

[5] J. Bacardit, I. Oller, M.I. Maldonado, E. Chamarro, S. Malato, S. Esplugas, Simple models for the control of photo-Fenton by monitoring H_2O_2, Journal of Advanced Oxidation Technologies, 10 (2007) 219-228.

[6] C. Flox, P.-L. Cabot, F. Centellas, J.A. Garrido, R.M. Rodríguez, C. Arias, E. Brillas, Solar photoelectro-Fenton degradation of cresols using a flow reactor with a boron-doped diamond anode, Applied Catalysis B: Environmental, 75 (2007) 17-28.

[7] A.I. Gomes, T.F. Soares, T.F.C.V. Silva, R.A.R. Boaventura, V.J.P. Vilar, Ozone-driven processes for mature urban landfill leachate treatment: Organic matter degradation, biodegradability enhancement and treatment costs for different reactors configuration, Science of The Total Environment, 724 (2020) 138083.

[8] A.D. Eaton, L.S. Clesceri, M.A.H. Franson, E.W. Rice, A.E. Greenberg, Standard Methods for Examination of Water and Wastewater, 21st Edition, American Public Health Association (APHA), American Water Works Association (AWWA), Water Environment Federation (WEF), United States of America, 2005.

[9] N. 627:1972, Portuguese Standard 627:1972, Water; Determinarion of true colour, Instituto Português da Qualidade, 1972.

[10] W. Chen, P. Westerhoff, J.A. Leenheer, K. Booksh, Fluorescence Excitation-Emission matrix regional integration to quantify spectra for dissolved organic matter, Environmental Science & Technology, 37 (2003) 5701-5710.

[11] L.C. Friedrich, M.A. Mendes, V.O. Silva, C.L.P.S. Zanta, A. Machulek Jr., F.H. Quina, Mechanistic implications of zinc(II) ions on the degradation of phenol by the fenton reaction, Journal of the Brazilian Chemical Society, 23 (2012) 1372-1377.

[12] R.F.P. Nogueira, M.C. Oliveira, W.C. Paterlini, Simple and fast spectrophotometric determination of H_2O_2 in photo-Fenton reactions using metavanadate, Talanta, 66 (2005) 86-91.

[13] W.D. Williams, Conductivity and salinity of Australian salt lakes, Marine and Freshwater Research, 37 (1986) 177-182.

[14] G. Sharma, A. Kumar, S. Sharma, M. Naushad, R. Prakash Dwivedi, Z.A. Alothman, G.T. Mola, Novel development of nanoparticles to bimetallic nanoparticles and their composites: A review, Journal of King Saud University - Science, 31 (2019) 257-269.

[15] COD, Crystallography Open Database, http://www.crystallography.net/cod/, http://www.crystallography.net/cod/.

3 Sulphur Compounds Removal from a Hazardous Industrial Solid Waste Landfill Leachate by Catalytic Oxidation and Chemical Precipitation

This chapter presents the removal of sulphur compounds from a high-strength leachate of a hazardous industrial solid waste landfill. Firstly, sulphides (0.5 g L^{-1}) and sulphites (2.5 g L^{-1}) were catalytic oxidised at natural pH (8.7). Air or H_2O_2 were applied as oxidants and metals present in the leachate were used as catalysts. Distinct air flow rates and H_2O_2:sulphur molar ratios were tested. Concentrations of sulphide and sulphite lower than 1.0 mg L^{-1} (emission limit value - ELV) were obtained after 5-hour oxygenation or 1-min peroxidation under the best conditions, i.e. air flow rate of 1 L_{air} $L_{leachate}^{-1}$ min^{-1} and H_2O_2:sulphur stoichiometric molar ratio. Aeration was considered unsafe since more than 33 volatile organic compounds (VOCs) and hydrogen sulphide (H_2S) were released into the atmosphere. Sulphates (13 g L^{-1}) were removed by chemical precipitation as ettringite or barite applying different reactants contents and pH values. Without pH correction, sulphate contents below 2.0 g L^{-1} (ELV) were achieved using a [Ca^{2+}]:[Al^{3+}]:[SO_4^{2-}] molar ratio of 12:4:3 (2-fold stoichiometry) and a [Ba^{2+}]:[SO_4^{2-}] molar ratio of 1.0:1.0 (1-fold stoichiometry). The analysis of precipitates by X-ray diffraction (XRD) showed a three-phase ettringite (only 67% corresponding to ettringite itself) and single-phase barite. Barite precipitation proved to be more appealing since a value-added product was obtained and, furthermore, fewer reactants were required. After sulphur compounds removal using H_2O_2-driven catalytic oxidation and chemical precipitation through barite, the leachate was suitable for biological treatment, despite the high salinity, and a high fraction of the organic load (46%) could be biologically oxidised.

This chapter is based on the following research article: "Barbosa Segundo, I.D., Silva, T.F.C.V., Moreira, F.C., Gabriela V.S., Boaventura, R.A.R., Vilar, V.J.P., Sulphur compounds removal from an industrial landfill leachate by catalytic oxidation and chemical precipitation: From a hazardous effluent to a value-added product, Science of The Total Environment, 655 (2019) 1249-1260, DOI: 10.1016/j.scitotenv.2018.11.274".

3.1 Introduction

Leachates from ISWLs, either NHISWLs or HISWLs, can contain high amounts of sulphur compounds, namely sulphides, sulphites and sulphates, which have been showing inhibitory/recalcitrant characteristics for the common biological treatments [1, 2]. For these effluents, the direct application of biological treatments is not feasible. Furthermore, these leachates can contain very high loads of organic compounds, rendering the direct application of the costly AOPs unfeasible. This contrasts with the effective symbiosis between biological and chemical/physical processes, including AOPs, already demonstrated elsewhere for different types of leachates [3-6].

Sulphide and sulphite ions have been successfully oxidised, catalytically or not, by air and several reactants such as H_2O_2, peroxymonosulphate, chlorine and potassium permanganate [7-21]. However, when comparing H_2O_2 to other chemicals, several advantages can be itemised: (i) its decomposition results in oxygen and water; (ii) it is safe and easy to handle; and (iii) it is economically competitive [16]. As regards sulphates removal from aqueous solution, several technologies have been proposed, such as chemical precipitation, reverse osmosis, nanofiltration and electrodialysis [2, 22]. Chemical precipitation as ettringite ($Ca_6Al_2(SO_4)_3(OH)_{12}\cdot 26H_2O$) or barite ($BaSO_4$), through the use of calcium/aluminium or barium salts, respectively, seems to be a good alternative, especially when exists the perspective of valorisation of those precipitates [22, 23].

Accordingly, the work developed within this chapter was mainly focused on the application of a 2-stage pre-treatment to a sulphur-rich HISWL leachate aiming at the removal of sulphur compounds. In a first stage, catalytic oxidation of sulphide and sulphite ions was carried out. Two oxidant agents were tested: air at different flow rates and H_2O_2 at different concentrations. The transition metals available in the leachate were used as catalysts. Gas-phase generated during the catalytic oxidation step was evaluated in terms of volatile organic compounds (VOCs) and gaseous hydrogen sulphide (H_2S). In a second stage, the removal of sulphates from the pre-oxidised leachate (with the best oxidant) was assessed by using chemical precipitation as ettringite or barite mineralogical phases. Chemical precipitation was assessed as a function of leachate pH and reactants concentration (calcium/aluminium and barium). Surface morphology and chemical composition of ettringite and barite precipitates were characterized by Fourier Transform Infrared Spectroscopy (FTIR), Scanning Electron Microscopy (SEM), Energy Dispersive X-ray (EDS) and X-ray diffractometry (XRD), in order to evaluate its potential use as value-added products.

3.2 Materials and methods

All the chemicals, experimental units and procedures, analytical determinations and modeling of removal kinetics used within this chapter are described in Chapter 2.

The raw leachate was collected in March 2016 from the stabilization lagoon (2800 m^3) of a HISWL located in the Central Region of Portugal, operating since June 2008. This HISWL mostly accepts sludge from wastewater treatment plants (WWTPs), waste from steelworks and mining and metallurgical industries, as well as soils contaminated with heavy hydrocarbons. Table 3.1 displays the physicochemical characteristics of the raw HISWL leachate.

3.3 Results and discussion

3.3.1 Characterization of the HISWL leachate

The raw HISWL leachate presents the following main characteristics: (i) moderate brown colour (Figure 3.1), most likely related to the presence of humic substances (300 mg C L^{-1} and $2 < SUVA_{254} < 4$, indicating that the natural organic matter is composed by a mixture of humic and non-humic matter [24, 25]); (ii) very pungent odour, associated with the existence of hydrogen sulphide (0.5 g L^{-1}) and VOCs; (iii) slightly alkaline pH; (iv) high conductivity (62.4 mS cm^{-1}), with a calculated ionic strength (IS) of 1.05 M based on the available information; (v) high alkalinity (5.7 g $CaCO_3$ L^{-1}), mostly in the form of bicarbonate (about 98%), as pH is slightly higher than 8.3 [26]; (vi) high organic matter content (DOC = 2.3 g L^{-1}, COD = 7.1 g L^{-1}); (vii) low biodegradability (Zhan-Wellens test= 15%, BOD_5/COD = 0.16); (viii) moderate total nitrogen content (540 mg N L^{-1}), mainly in the forms of ammonium (60%) and organic nitrogen (> 37%); (ix) high sulphur content ($[SO_4^{2-}]$ = 13 g L^{-1}, $[SO_3^{2-}]$ = 2.5 g L^{-1}, $[S^{2-}]$ = 0.5 g L^{-1}); and (x) high content of light metals ($[Ca^{2+}]+[Li^{+}]+[Mg^{2+}]+[K^{+}]+[Na^{+}]+[Al^{3+}]+[Ba^{2+}]$ ~ 818 mM) and low content of heavy metals (53 μM < [As]+[27]+[Cr]+[Cu]+[Fe]+[Pb]+[Mn]+[Ni]+[Zn] < 61 μM).

Figure 3.1 HISWL leachate samples: raw (a) and after treatment by catalytic oxidation H_2O_2 and chemical precipitation as barite under stoiciometric conditions at the natural effluent pH (b).

Table 3.1 Physicochemical characterization of the raw HISWL leachate and of the HISWL leachate along the various treatment stages.

Parameter (unit)	Raw	After catalytic oxidation		After chemical precipitation		ELV[e]
		With air[a]	With H_2O_2[b]	As ettringite[c]	As barite[d]	
Colour	Brown	Dark brown	Light brown	Light yellow	Light Brown	
Colour (diluted 1:20)	d.	d.	d.	n.d.	d.	n.d. (diluted 1:20)
Colour (Pt-Co units)	2000	4000	2000	660	1300	
Odour	Very strong	Strong	Strong	Very Low	Low	
Odour (diluted 1:20)	d.	d.	d.	d.	d.	n.d. (diluted 1:20)
pH	8.7	9.4	8.5	10.8	8.4	6.0-9.0
Conductivity (mS cm^{-1})	62.4	64.7	53.6	79.0	70.1	
Alkalinity (mg $CaCO_3$ L^{-1})	5707	5792	5112	194	3936	
Redox potential (mV)	-94.6	-10.7	-10.0	-6.1	-7.5	
Turbidity (NTU)	260	550	37	45	80	
Total dissolved carbon – TDC (mg L^{-1})	3670	3562	3472	1920	3971	
Dissolved inorganic carbon – DIC (mg L^{-1})	1352	1363	1246	27	953	
Dissolved organic carbon – DOC (mg L^{-1})	2318	2199	2226	1893	2107	
Chemical oxygen demand – COD (mg O_2 L^{-1})	7063	6050	6038	6200	6100	150 or 125
COD/DOC	3.0	2.8	2.7	3.3	2.9	
Biochemical oxygen demand - BOD_5 (mg O_2 L^{-1})	1100	600	700	2100	2200	40 or 25
BOD_5/COD	0.16	0.10	0.12	0.34	0.36	
Biodegradability - Zhan-Wellens test (%)	15	n.m.	6.3	42	46	
Humic substances (mg C L^{-1})	300	n.m.	n.m.	n.m.	n.m.	
Absorbance at 254 nm (AU) (diluted 1:50)	1.21	1.29	1.24	1.08	1.30	
$SUVA_{254}$ (L mg^{-1} m^{-1})	2.6	2.9	2.9	2.8	3.1	
Total suspended solids – TSS (mg L^{-1})	128	n.m.	n.m.	406	607	60 or 35
Total volatile solids – VSS (mg L^{-1})	80	n.m.	n.m.	74	67	
Total nitrogen - N_T (mg L^{-1})	540	379	451	346	427	15 or 10
Ammonium – N-NH_4^+ (mg L^{-1})	326	181	302	245	323	7.8
Nitrite – N-NO_2^- (mg L^{-1})	<4.9[h]	<4.9[h]	<4.9[h]	<4.9[h]	<4.9[h]	
Nitrate – N-NO_3^- (mg L^{-1})	<8.0[h]	<8.0[h]	<8.0[h]	<8.0[h]	<8.0[h]	11
Sulphate – SO_4^{2-} (g L^{-1})	12.7	14.0	13.9	0.4	0.3	2

Table 3.1 Physicochemical characterization of the raw HISWL leachate and of the HISWL leachate along the various treatment stages.

Parameter (unit)	Raw	After catalytic oxidation		After chemical precipitation		ELV[e]
		With air[a]	With H_2O_2[b]	As ettringite[c]	As barite[d]	
Sulphite[f] – SO_3^{2-} (mg L^{-1})	2500	< 1	< 1	< 1	< 1	1.0
Sulphide[g] – S^{2-} (mg L^{-1})	500	< 0.1	< 0.1	< 0.1	< 0.1	1.0
Chloride – Cl^- (g L^{-1})	15.4	15.0	15.4	34.8	25.6	
Total phosphorous (mg L^{-1})	10	4.5	8	<0.05	5	10 or 1
Calcium – Ca^{2+} (mg L^{-1})	<32[h]	<32[h]	<32[h]	61	<32[h]	
Lithium – Li^+ (mg L^{-1})	<3.3[h]	<3.3[h]	<3.3[h]	<3.3[h]	<3.3[h]	
Magnesium – Mg^{2+} (mg L^{-1})	<12[h]	<12[h]	<12[h]	<12[h]	<12[h]	
Potassium – K^+ (g L^{-1})	3.6	3.7	3.5	3.3	3.1	
Sodium – Na^+ (g L^{-1})	16.7	16.1	16.9	17.2	17.6	
Total Aluminium – Al (mg L^{-1})	< 0.6[h]	< 0.6[h]	< 0.6[h]	19	< 0.6[h]	10
Total Barium – Ba (mg L^{-1})	< 0.61[h]	< 0.61[h]	< 0.61[h]	< 0.61[h]	< 0.61[h]	
Total arsenic – As (mg L^{-1})	< 0.03[h]	n.m.	n.m.	n.m.	n.m.	1.0
Total cadmium – Cd (mg L^{-1})	< 0.05[h]	n.m.	n.m.	n.m.	n.m.	0.2
Total chromium – Cr (mg L^{-1})	0.14	n.m.	n.m.	n.m.	n.m.	2.0
Total copper – Cu (mg L^{-1})	0.09	n.m.	n.m.	n.m.	n.m.	1.0
Total iron – Fe (mg L^{-1})	1.9	n.m.	n.m.	n.m.	n.m.	2.0
Total lead – Pb (mg L^{-1})	<0.21[h]	n.m.	n.m.	n.m.	n.m.	1.0
Total manganese – Mn (mg L^{-1})	< 0.35	n.m.	n.m.	n.m.	n.m.	
Total nickel – Ni (mg L^{-1})	0.63	n.m.	n.m.	n.m.	n.m.	
Total zinc – Zn (mg L^{-1})	0.24	n.m.	n.m.	n.m.	n.m.	2.0

d. – detected; n.d. – not detected; n.m. – not measured;

[a] Aeration for 6 hours with an air flow rate of 0.5 L min^{-1};

[b] Oxidation adding the stoichiometric amount of H_2O_2 at the natural effluent pH;

[c] Sulphates precipitation using the leachate after H_2O_2-driven oxidation with a $[Ca^{2+}]:[Al^{3+}]:[SO_4^{2-}]$ molar ratio of 12:4:3 without pH correction;

[d] Sulphates precipitation using the leachate after H_2O_2-driven oxidation with a $[Ba^{2+}]:[SO_4^{2-}]$ molar ratio of 1:1 without pH correction;

[e] ELV - Emission Limit Value according to Decree-Law no. 236/98 or Directive no. 91/271/CEE;

[f] Total dissolved free sulphites ($SO_2.H_2O + HSO_3^- + SO_3^{2-}$);

[g] Total dissolved free sulphides ($H_2S + HS^- + S^{2-}$); [h] Limit of detection; [i] Limit of quantification.

According to the leachate classification presented by Renou et al. [28], this effluent displays, for the most part, the characteristics of an intermediate leachate, and as such there is no technology that, acting alone, is capable to treat it at reasonable costs. So, the treatment should be based on combined systems that allow the best cost/effective solution complying with the local legislation in force. Looking at the leachate physicochemical characteristics and emission limit values (ELV) imposed by the Decree-Law no. 236/98 or European Directive no. 91/271/CEE (Table 3.1), three major concerns are notorious: (i) high organic matter content, with COD and BOD values 47- or 57- and 28- or 44- fold higher than ELV, respectively; (ii) high nitrogen content, with total and ammonium nitrogen concentration 36- or 54- and 42-fold higher than ELV, respectively; and (iii) high sulphur content, with sulphates, sulphites and sulphides concentration 6.6-, 2500- and 500-fold higher than ELV, respectively. Previous studies, with stabilized leachate from urban sanitary landfill [4, 6, 29], showed that the nitrogen and organic matter content could be successfully removed by combining biological and chemical oxidation processes, and the use of biological technologies should be prioritized to achieve the most economical treatment methodology. However, the high sulphur content exhibited by this leachate, in addition to being well above the ELVs, is inhibitory for the common biological processes [1, 2]. Thus, the treatment strategy adopted consisted of the preliminary removal of (i) sulphites and sulphides by catalytic oxidation, using the leachate metals themselves as catalysts, and (ii) sulphates by chemical precipitation. At the end of this preliminary treatment, the leachate should be ready to undergo a biological process.

3.3.2 Catalytic oxidation processes

3.3.2.1 Liquid-phase reactions

In the absence of catalysts, the chemical oxidation of reductant species is a slow process due to the adverse spin-state symmetries caused by differences in the reactants electronic configuration. In virtue of their ability to alter the electronic structure of both oxidants and reductants species, transition-metal ions and their complexes are usually used as effective catalysts, overcoming the activation energy barrier imposed by the spin-state symmetry restrictions [14]. Attending to the fact that the industrial leachate studied in this work already presented a total transition metals concentration of at least 53 μM (considering the sum of Cr, Cu, Fe, Ni and Zi, Table 3.1), only the effect of the oxidant type (O_2 and H_2O_2) was assessed on the catalytic oxidation of sulphide and sulphite ions.

Chemical oxidation kinetics is also affected by reactant concentration, sulphur to oxidant ratio, ionic strength, temperature, presence of inhibitors and pH [10, 11, 21]. In aqueous solution, dissolved free sulphides can exist as (i) molecular hydrogen sulphide (H_2S, pKa_1 = 7.00 for IS = 0 M [19], and pKa_1 =

7.37 for IS = 1.0 M, with p*Ka* value corrected for the leachate IS through the Truesdell-Jones model [30, 31]), which can easily volatize, (ii) bisulphide ion (HS^-, pKa_2 = 14.0 for IS = 0 M [19] and pKa_2 = 14.7 for IS = 1.0 M) and (iii) sulphide (S^{2-}) [14, 19]. In turn, sulphite ion (SO_3^{2-}) can exist in equilibrium with the volatile sulphur dioxide ($SO_2.H_2O$, pKa_1 = 1.86 for IS = 0 M [32] and pKa_1 = 2.20 for IS = 1.0 M) and bisulphite anion (HSO_3^-, pKa_2 = 7.15 for IS = 0 M [32] and pKa_2 = 7.89 for IS = 1.0 M) [17]. Taking into account the leachate pH (Table 3.1) and calculated IS, it was possible to foresee that the distribution of sulphide (sulphur oxidation state (SOS): -2) and sulphite (SOS: +4) species, in solution, were, respectively: (i) 4% H_2S and 96% HS^-; and (ii) 14% HSO_3^- and 86% SO_3^{2-}. So, the oxidation by air injection or H_2O_2 addition can led to the main following chemical reactions (Eqs. 3.1– 3.8) [9, 10, 12, 17]:

$$2HS^- + O_2 \rightarrow 2S^0 + 2OH^- \quad (3.1)$$

$$2HS^- + 2O_2 \rightarrow S_2O_3^{2-} + H_2O \quad (3.2)$$

$$2HS^- + 3O_2 \rightarrow 2SO_3^{2-} + 2H^+ \quad (3.3)$$

$$2HS^- + 4O_2 \rightarrow 2SO_4^{2-} + 2H^+ \quad (3.4)$$

$$2SO_3^{2-} + O_2 \rightarrow 2SO_4^{2-} \quad (3.5)$$

$$HS^- + H_2O_2 + H^+ \rightarrow S^0 + 2H_2O \quad (3.6)$$

$$HS^- + 4H_2O_2 \rightarrow SO_4^{2-} + 4H_2O + H^+ \quad (3.7)$$

$$SO_3^{2-} + H_2O_2 \rightarrow SO_4^{2-} + H_2O \quad (3.8)$$

Sulphur compounds are generally very reactive, and they can exist in many oxidation states. Consequently, their oxidation, especially sulphide (represented by S^{2-}) since it presents the lower sulphur oxidation state, can result in a large variety of products, ranging from elemental sulphur to sulphate, which is the sulphur species with higher oxidation state (SOS: +6) [9, 10, 12, 17].

Regardless of the air flow rate applied, and sulphur species oxidised, Figure 3.2 and Table 3.2 show that the oxidation reactions followed a pseudo-first-order kinetic model (determination coefficient (R^2) $\geq$ 0.99 and residual variance (S^2_R) $\leq$ 0.8 mM^2). Statistically, with a confidence level of 95%, it can be verified that: (i) there is no difference between the kinetic constants of sulphides and sulphites and the initial reaction rate of sulphites is on average 2-fold higher than of sulphides, for each air flow rate applied; (ii) from the flow rate of 0.5 L min^{-1} (1 L_{air} $L_{leachate}^{-1}$ min^{-1}) forward, the reaction rate becomes independent of the air flow rate, indicating that the oxygen diffusion rate, in this operating conditions, was enough for the reaction needs.

Using an air flow rate of 0.5 L min^{-1}, the aeration process led to sulphide ($[S^{2-}]_0$ = 14 mM) and sulphite ($[SO_3^{2-}]_0$ = 28 mM) removal efficiencies of 99% and 94%, after 2-hours, respectively, accompanied by an increase on the leachate pH value from 8.5 to 9.2. The kinetic parameters for sulphide removal obtained under these conditions are in very good agreement with those reported by Fischer et al. [18]. An initial reaction rate of 0.33 mM min^{-1} was obtained by the authors when applying an O_2-driven oxidation to a solution of 14.3 mM sulphides (in borate buffer) at pH 9 and in the presence of 1.8 μM cobalt as a homogenous catalyst. On the other hand, by increasing the catalyst concentration to 17.6 μM (ca. 10-fold), these authors were able to reach an initial reaction rate 3.5-fold higher. Thus, taking into account that the leachate total transition metals concentration was 53 μM (considering Cr, Cu, Fe, Ni, and Zn), it would be expectable that the reaction rate achieved in this work was even higher. The slower kinetics can potentially be explained by: (i) usage of air instead of pure oxygen; (ii) presence of sulphites, which were simultaneously oxidised with the sulphides; (iii) ability that each transition metal has to catalyse chemical reactions (for instance, Hoffmann and Lim [15] showed that the catalytic activity of metal-tetrasulfophthalocyanine (TSP) complexes followed the apparent order of CoTSP > NiTSP > CuTSP, over the entire pH range); and (iv) presence of inhibitory compounds, which is more than probable in such high-complex effluents like the leachates. In fact, Chen and Morris [7] have found that the oxygenation of industrial wastewater containing sulphides can be inhibited by compounds presenting basic nitrogen with a free electron pair.

After 2-hour aeration, despite the high removal efficiencies obtained (see Table 3.2 and Figure 3.2), especially for flow rates higher than 0.3 L min^{-1}, both sulphite and sulphide concentrations still remain above the ELVs (1.0 mg L^{-1}), and the variation on the sulphate anions content was negligible. Replicating the assay at 0.5 L min^{-1} for 6-hour (data not shown), it was possible to observe that the: (i) dissolved oxygen content was null until 2.5-hour, then increasing to 6 mg L^{-1} until 3.5-hour, and after that remained constant, never achieving the concentration of saturation (0.26 mmol O_2 L^{-1}, considering the Henry´s law constant (1.26×10^{-3} M atm^{-1} [32]), at 25 ºC and 1 atm, and the oxygen molar fraction); (ii) concentration of sulphur reduced species achieved values in compliance with the legislation (~5-hour); (iii) sulphates amount increased from 133 to 146 mM, which means that, according to the stoichiometry of the Eq. 3.4 and Eq. 3.5, only 31% of sulphur (S^{2-}+SO_3^{2-}) was totally oxidised into sulphate; and (iv) leachate's pH raised from 8.6 to 9.4, suggesting that elemental sulphur was also generated as reaction product (see Eq. 3.1), which is expected in reactions where sulphide is in excess [14]. If total oxidation had occurred, 28 mM of sulphates (SOS: +6) should have been generated only considering sulphite (SOS: +4) oxygenation. So, it can be concluded that at least 54% sulphite was converted into dithionate ($S_2O_6^{2-}$, SOS: +5), which even being usually a low-yield reaction product is frequently detected [20].

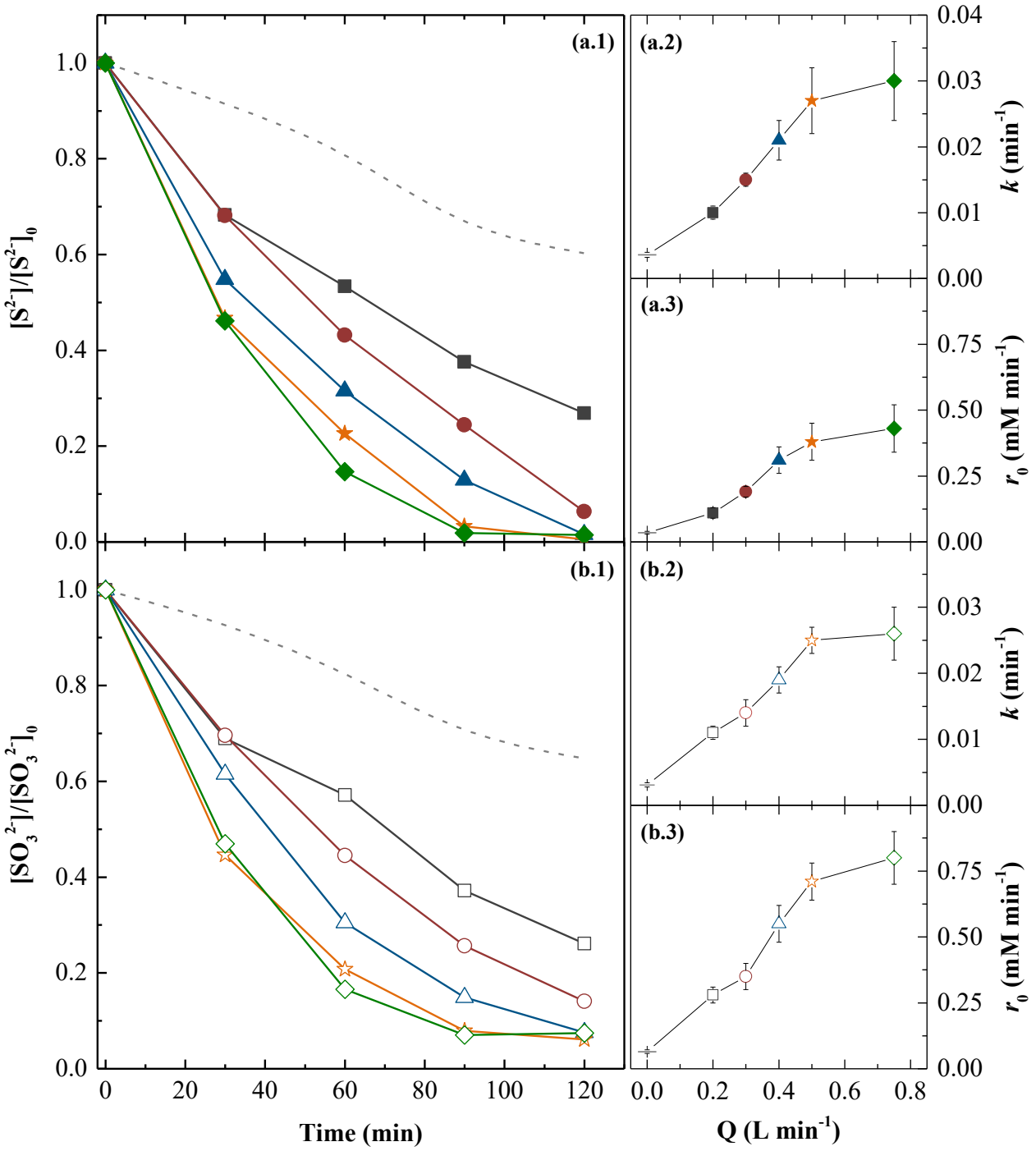

Figure 3.2 Representation of the normalized concentration of sulphide ($[S^{2-}]0$ = 13±2 mM) (a.1) and sulphite ($[SO_3^{2-}]_0$ = 28±3 mM) (b.1) as a function of time, during oxidation tests with air, and the respective pseudo-first-order kinetic constants (.2) and initial reaction rates (.3) for the different air flow rates: 0 (---); 0.2 (■,□), 0.3 (●,○), 0.4 (▲,△), 0.5 (★,☆) and 0.75 (◆,◇) L min^{-1} (Operating conditions: room temperature, stirring speed of 100 rpm, pH_0 = 8.5±0.1).

Table 3.2 Summary of the main experimental results obtained for the chemical oxidation of sulphides and sulphites using different air flow rates.

Parameter	Q_{air} (L min^{-1})					
	0.0	**0.2**	**0.3**	**0.4**	**0.5**	**0.75**
pH$_m$	8.83	8.90	8.97	8.89	8.98	8.98
ΔpH	8.49 - 9.05	8.48 - 9.09	8.50 - 9.16	8.40 - 9.09	8.50 - 9.18	8.40 - 9.21
Sulphides – $[S^{2-}]_0$ = 13±2 mM						
1-h Removal	18.0%	41.4%	56.8%	68.4%	77.3%	85.3%
2-h Removal	36.7%	71.2%	84.1%	96.9%	98.9%	98.5%
k [a] **(min^{-1})**	0.0036 ± 0.0004	0.010 ± 0.001	0.015 ± 0.001	0.021 ± 0.003	0.027 ± 0.005	0.030 ± 0.006
***r*$_0$** [b] **(mM min^{-1})**	0.28 ± 0.03	0.11 ± 0.02	0.19 ± 0.02	0.31 ± 0.05	0.38 ± 0.07	0.43 ± 0.09
R^2 [c]	0.990	0.990	0.995	0.993	0.992	0.992
***S*^2_R** [d] **(mM^2)**	0.021	0.098	0.104	0.224	0.257	0.299
Sulphites - $[SO_3^{2-}]_0$ = 28±3 mM						
1-h Removal	17.0%	46.6%	55.5%	69.5%	79.2%	83.4%
2-h Removal	32.0%	75.5%	85.9%	92.4%	93.9%	92.5%
k [a] **(min^{-1})**	0.0031 ± 0.0003	0.011 ± 0.001	0.014 ± 0.002	0.019 ± 0.002	0.025 ± 0.002	0.026 ± 0.004
***r*$_0$** [b] **(mM min^{-1})**	0.28 ± 0.03	0.28 ± 0.03	0.35 ± 0.05	0.55 ± 0.07	0.71 ± 0.07	0.8 ± 0.1
***R*^{2}** [c]	0.992	0.995	0.993	0.994	0.998	0.994
***S*^2_R** [d] **(mM^2)**	0.057	0.252	0.547	0.727	0.231	0.804

[a] Pseudo-first-order kinetic constant for sulphide and sulphite removal;
[b] Initial reaction rate for sulphide and sulphite removal;
[c] Coefficient of determination;
[d] Residual variance.

While the O_2 content was controlled by the diffusion of the air into the wastewater, for each oxidation experiment mediated by H_2O_2, the oxidant dose added was determined as a function of the stoichiometric amount needed to achieve complete oxidation of sulphide and sulphite ions into sulphates, according to Eq. 3.7 and Eq. 3.8, i.e., $[H_2O_2]_{stoic.} = 4[S^{2-}]_0 + [SO_3^{2-}]_0$. Contrary to the air-driven oxidation, the reaction using H_2O_2 was practically instantaneous, occurring within 1-min (minimum time required to homogenization and sample collection), showing itself a stronger oxidant as expected [13, 19]. However, in spite of the lower reaction times expected when comparing to oxygenation, these results go also against the literature, where the sulphites and sulphides oxidation with H_2O_2 is described as a slow process following a pseudo-first-order kinetic [16, 17, 19]. This increment in the reaction rate can be explained by the presence of transition metals working as catalysts.

From Figure 3.3 it is possible to verify that: (i) the oxidant stoichiometric amount was enough to remove almost 100% of both sulphur species; (ii) using H_2O_2 concentrations equal to or more than 60% of the stoichiometric amount, sulphide and sulphite removal efficiencies higher than 96% were achieved; and (iii) although for sulphides, concentrations below the ELV were attained using only 42% of the H_2O_2 stoichiometric content, for sulphites, this was only true when the stoichiometric quantity was added. Accordingly, Cadena and Peters [19] reported sulphide removals of 79% and 99% from a typical wastewater, using 44% and 58% of the H_2O_2 stoichiometric amount, respectively, after 30-min at 25 ºC and in absence of catalyst. It is worth to mention that, even under stoichiometric conditions, only 12 mM of sulphates were generated, instead of the expected 46 mM, and just 66% of H_2O_2 was consumed with no changes on pH. This suggests, likewise as in the aeration trials, the production of elemental sulphur and dithionate as intermediates. Even extending the reaction for 1-hour, sulphate concentration did not increase further.

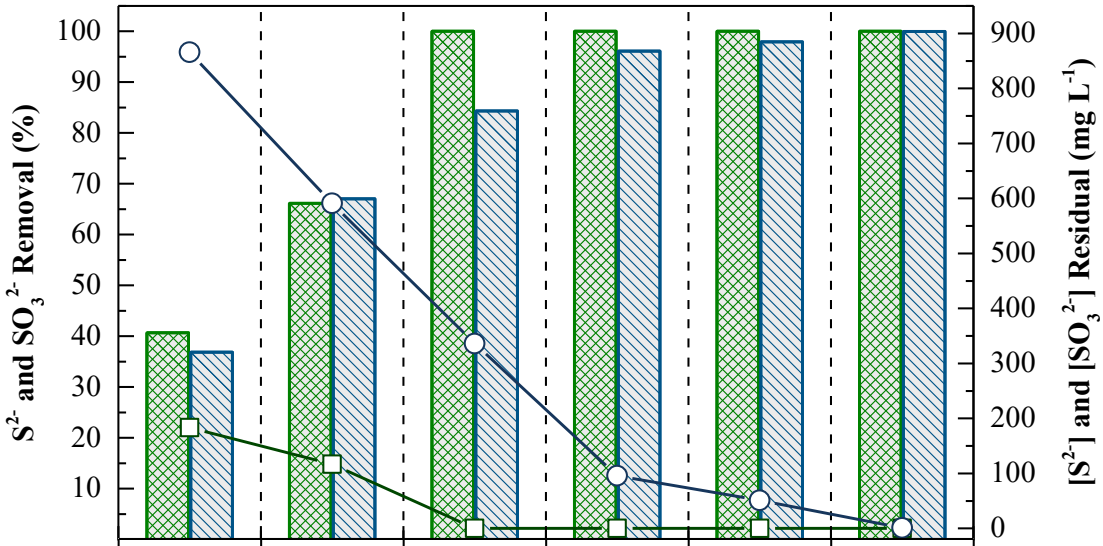

$[H_2O_2]_{add}/[H_2O_2]_{stoic.}$	0.18	0.30	0.42	0.60	0.81	1.00
$1 - [S^{2-}]_R / [S^{2-}]_0$	40.7%	66.1%	> 99.9%	> 99.9%	> 99.9%	> 99.9%
$1 - [SO_3^{2-}]_R / [SO_3^{2-}]_0$	36.9%	67.1%	84.3%	96.1%	97.9%	> 99.9%
$[S^{2-}]_R$ (mg L^{-1})	183	117	< 0.1	< 0.1	< 0.1	< 0.1
$[SO_3^{2-}]_R$ (mg L^{-1})	866	591	336	95.9	50.9	< 1

Figure 3.3 Illustration of the removal (bars) and the residual concentrations (points) of sulphides ($[S^{2-}]_0$ = 14±2 mM, ▨, □) and sulphites ($[SO_3^{2-}]_0$ = 29±5 mM, ▨, ○) as a function of the H_2O_2 concentration, represented as the ratio between the amount of H_2O_2 added o over the stoichiometric (Operating conditions: room temperature, stirring speed of 100 rpm for 1 min, pH_0 = 8.5±0.2).

3.3.2.2 Gas-phase characterization

Besides the lower residence times required for the H_2O_2-driven catalytic oxidation, this reaction also stood out since it is experimentally "cleaner". In other words, when H_2O_2 was used, the industrial leachate became clearer and few/uniform foam was formed, while when the air was used, the effluent became darker, large amounts of irregular foam and precipitate were generated and a strong odour of "rotten egg" was felt. This smell is generally associated with the gaseous H_2S [16]. In fact, during the extended experiments in the best conditions (addition of the H_2O_2 stoichiometric amount and injection of 0.5 L min^{-1} of air), the presence of H_2S in the gas stream was evaluated (data not shown) and it was found that: (i) before the oxidant addition, the H_2S concentration in the gas-liquid interface was already higher than 90 ppm; (ii) using H_2O_2, the H_2S content was 28 ppm in 1 min and became zero in less than 10 min; and (iii) applying air, 28 and 0 ppm of H_2S was only reached after ca. 1-hour and 4-hour, respectively. It should be noted that the European Commission, through the Directive 2009/161/EU [33], has established indicative occupational exposure limit values to H_2S of 5 and 10 ppm, for a reference period of 8-hour time weighted average (TWA) and a short-term period (STEL) of 15 minutes, respectively. The American Conference of Governmental Industrial Hygienists is even more restrictive and, currently, its recommendation for airborne H_2S exposure is a TWA of 1 ppm and a STEL of 5 ppm [34]. In this work, while the oxidation process with H_2O_2 led to H_2S concentrations in compliance with both organizations (STEL = 3.7 ppm), the use of air led to a significant exceedance of the recommended values (TWA = 8.6 ppm and STEL = 85 ppm), making this technology extremely unsafe for a full-scale implementation, unless a gas-stream treatment step is added.

In addition to H_2S, VOCs in the gas-stream generated during the leachate aeration were assessed. Figure 3.4 and Table 3.3 display the distribution of the identified VOCs (84%) by GC-MS within the respective reactive groups, where the total content could be arranged in the order Ketones (73.8%) > Hydrocarbons (11.1%, comprising 6.6% Aromatics, 4.0% Aliphatic Saturated and 0.5% Aliphatic Unsaturated) > Alcohols (4.7%) > Ethers (4.0%) > Amines (3.3%) > Amides (1.7%) > Organic sulphides (0.9%) > Acids (0.5%). With no doubt, the reactive group that stood out was ketones, within which just the acetone (1324 ppb), 2-butanone (1049 ppb) and methyl isobutyl ketone (387 ppb) represented more than 68% of the whole gas-sample. Following these species, the five most abundant compounds, with concentrations between 200 and 100 ppb, were cyclohexanol, decane, aniline, cyclohexanone and benzene, belonging to the group of alcohols, aliphatic saturated hydrocarbons, amines, ketones and aromatic hydrocarbons, respectively. The presence of such airborne pollutants in landfills, including H_2S, is in agreement with the outcomes from some authors [34-36]. All these VOCs have in common the fact that they can be used as industrial solvents for production and/or cleaning purposes. In fact, methyl isobutyl ketone is amongst

the top ten most popular organic solvents used in industry [35], which is consistent with a leachate from a HISWL. According to the National Institute for Occupational Safety and Health (NIOSH), from the Centers for Disease Control and Prevention (CDC) [36], and considering that the gas-stream was collected during the first 15-min of the experiment, it could be concluded that all of these compounds were below the STEL. However, the three main substances and benzene are considered highly flammable and the remaining ones are categorized as flammable and combustible.

Given all the above considerations, H_2O_2 was selected as the best oxidant for sulphides and sulphites removal.

3.3.3 Chemical precipitation processes

3.3.3.1 Liquid-phase reactions

Due to its relatively low cost, initially, lime was tested to precipitate sulphate anions. However, the results were not favourable, only removal efficiencies lesser than 10% were reached even above stoichiometric proportions. Thus, chemical precipitation of sulphate after H_2O_2-driven catalytic oxidation was performed using calcium/aluminium and barium ions aiming at the formation of ettringite ($[Ca_3Al(OH)_6]_2(SO_4)_3.26H_2O$) and barite ($BaSO_4$) minerals. As ettringite is usually stable in the pH range 10.5-13.0 [37] and barite growth and nucleation are not meaningfully affected by pH in the interval 3-9 [38], precipitation experiments were initiated by changing the reactants content at pH 11 and 8.5 (resulting from the previous step), respectively (Figure 3.5a.1-b.1). Afterward, knowing the best molar ratio of reactants over sulphate, the solution pH was varied (Figure 3.5a.2-b.2).

As regards the sulphate removal ($[SO_4^{2-}]_0$ = 147±5 mM) via ettringite formation (Figure 3.5a), we concluded that for pH 11: (i) increasing the calcium and aluminium concentration from 1-fold to 2-fold the stoichiometric ratio ($[Ca^{2+}]:[Al^{3+}]:[SO_4^{2-}]$ = 6:2:3-12:4:3), the efficiency increased from 27% to a maximum of 91% and the residual sulphate content decreased from 10.2 to a minimum of 1.3 g L^{-1}, which is below the ELV (2 g L^{-1}); (ii) a molar ratio of $[Ca^{2+}]:[SO_4^{2-}]$ and $[Al^{3+}]:[SO_4^{2-}]$ higher than 4 and 1.33, respectively, did not improve the process performance; and (iii) the residual aluminium content was in average 435 mg L^{-1}, which is more than 40 times the ELV. These results were close to the optimized conditions obtained by Dou et al. [23] for a synthetic wastewater containing 24.0 and 57.6 mM of calcium and sulphate, respectively. They reported a sulphate removal of 99.7% using molar ratios of $[Ca^{2+}]:[SO_4^{2-}]$ and $[Al^{3+}]:[SO_4^{2-}]$ equal to 3.20 and 1.25, respectively, at pH 11.3. The slightly lower efficiency observed in this work can be attributed to the higher initial sulphate concentration and the

leachate sample matrix, taking into account that the presence of foreign substances can inhibit the ettringite crystallization [37].

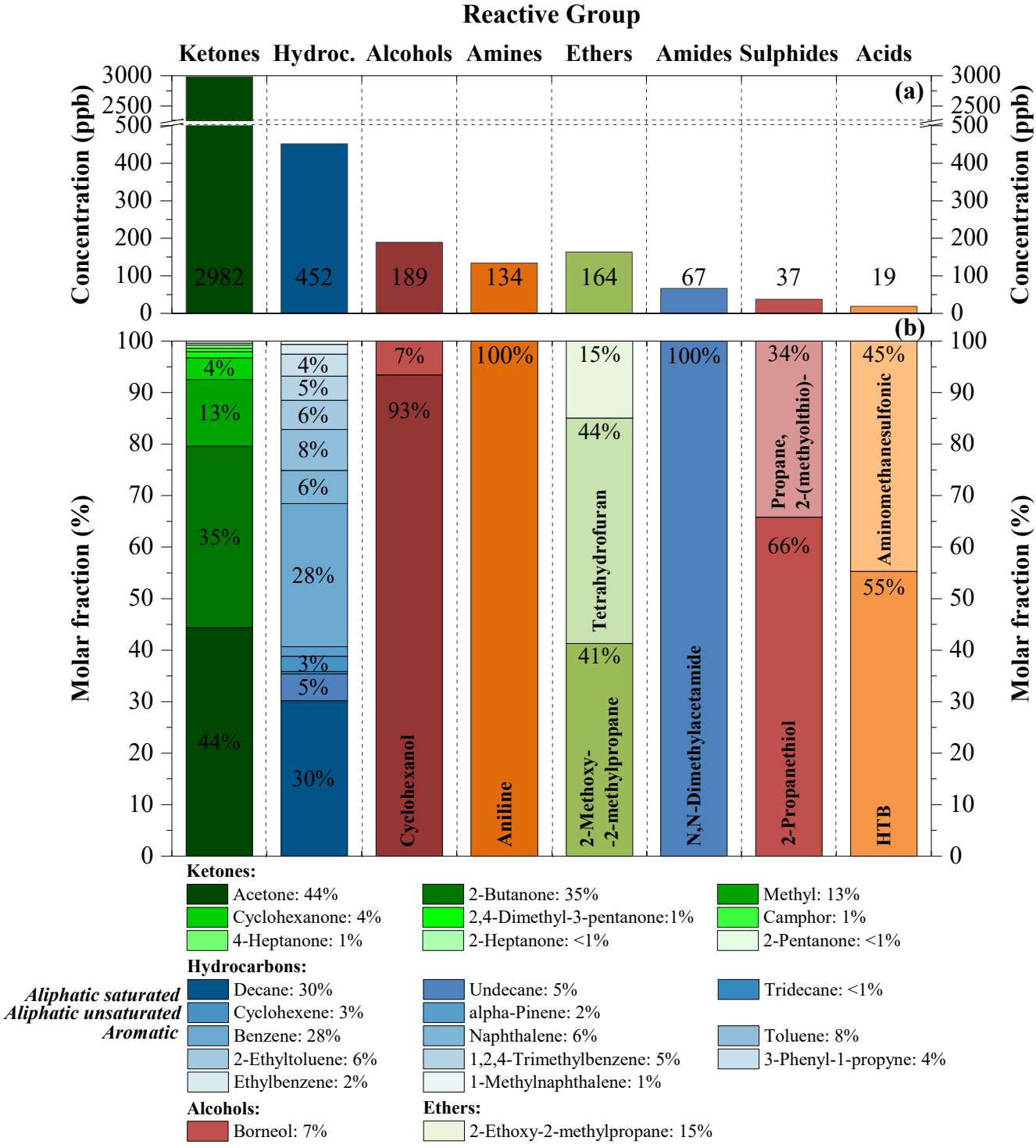

Figure 3.4 Representation of the VOCs identified in the gas-stream generated during the air-driven catalytic oxidation (at a flow rate of 1 L_{air} $L_{leachate}$ min^{-1}): total concentration of each reactive group (a) molar fraction of each compound within the respective group (b).

Table 3.3 VOCs identified and quantified in the gas-phase generated during the sulphide and sulphite catalytic oxidation process by aeration.

Contaminant	IUPAC name	Reactive Group	Molecular Weight (g mol^{-1})	CAS no.	Molecular Formula	Structural Formula	Concentration (ppb)
Acetone	Propan-2-one	Ketones	58.08	67-64-1	C_3H_6O	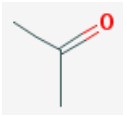	1324
2-Butanone	Butan-2-one	Ketones	72.11	78-93-3	C_4H_8O	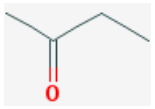	1049
Methyl isobutyl ketone	4-Methylpentan-2-one	Ketones	100.16	108-10-1	$C_6H_{12}O$	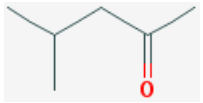	387
Cyclohexanone	Cyclohexanone	Ketones	98.15	108-94-1	$C_6H_{10}O$	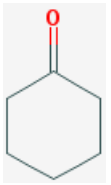	126
2,4-Dimethyl-3-pentanone	2,4-Dimethylpentan-3-one	Ketones	114.19	565-80-0	$C_7H_{14}O$	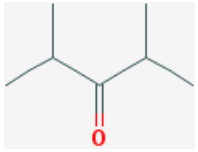	36
Camphor	4,7,7-Trimethylbicyclo[2.2.1]heptan-3-one	Ketones	152.24	76-22-2	$C_{10}H_{16}O$	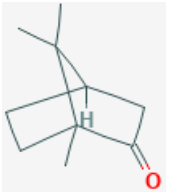	19
4-Heptanone	Heptan-4-one	Ketones	114.19	123-19-3	$C_7H_{14}O$	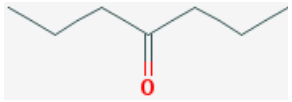	18

Table 3.3 VOCs identified and quantified in the gas-phase generated during the sulphide and sulphite catalytic oxidation process by aeration.

Contaminant	IUPAC name	Reactive Group	Molecular Weight (g mol^{-1})	CAS no.	Molecular Formula	Structural Formula	Concentration (ppb)
2-Heptanone	Heptan-2-one	Ketones	114.19	110-43-0	$C_7H_{14}O$	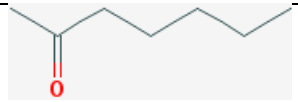	12
2-Pentanone	Pentan-2-one	Ketones	86.13	107-87-9	$C_5H_{10}O$	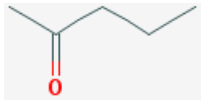	12
Decane	Decane	Hydrocarbons, Aliphatic Saturated	142.29	124-18-5	$C_{10}H_{22}$		136
Undecane	Undecane	Hydrocarbons, Aliphatic Saturated	156.31	1120-21-4	$C_{11}H_{24}$		24
Tridecane	Tridecane	Hydrocarbons, Aliphatic Saturated	184.37	629-50-5	$C_{13}H_{28}$		2
Cyclohexene, 1-methyl-4-(1-methylethylidene)-	1-Methyl-4-propan-2-ylidenecyclohexene	Hydrocarbons, Aliphatic Unsaturated	136.23	586-62-9	$C_{10}H_{16}$	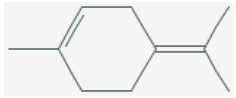	13
alpha-Pinene	4,6,6-Trimethylbicyclo[3.1.1]hept-3-ene	Hydrocarbons, Aliphatic Unsaturated	136.24	80-56-8	$C_{10}H_{16}$	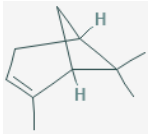	8
Benzene	Benzene	Hydrocarbons, Aromatic	78.11	71-43-2	C_6H_6	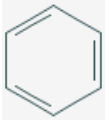	125
Naphthalene	Naphthalene	Hydrocarbons, Aromatic	128.17	91-20-3	$C_{10}H_8$	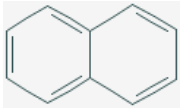	29

Table 3.3 VOCs identified and quantified in the gas-phase generated during the sulphide and sulphite catalytic oxidation process by aeration.

Contaminant	IUPAC name	Reactive Group	Molecular Weight (g mol^{-1})	CAS no.	Molecular Formula	Structural Formula	Concentration (ppb)
Toluene	Toluene	Hydrocarbons, Aromatic	92.14	108-88-3	C_7H_8	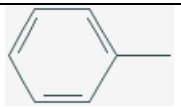	36
2-Ethyltoluene	1-Ethyl-2-methylbenzene	Hydrocarbons, Aromatic	120.20	611-14-3	C_9H_{12}	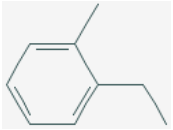	26
1,2,4-Trimethylbenzene	1,2,4-Trimethylbenzene	Hydrocarbons, Aromatic	120.20	95-63-6	C_9H_{12}	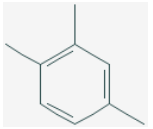	21
3-Phenyl-1-propyne	Prop-2-ynylbenzene	Hydrocarbons, Aromatic	116.16	10147-11-2	C_9H_8	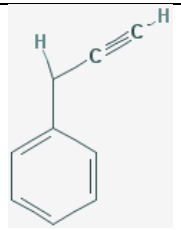	19
Ethylbenzene	Ethylbenzene	Hydrocarbons, Aromatic	106.17	100-41-4	C_8H_{10}	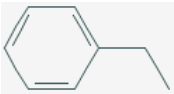	9
1-Methylnaphthalene	1-Methylnaphthalene	Hydrocarbons, Aromatic	142.20	1321-94-4	$C_{11}H_{10}$	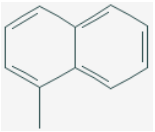	3

Table 3.3 VOCs identified and quantified in the gas-phase generated during the sulphide and sulphite catalytic oxidation process by aeration.

Contaminant	IUPAC name	Reactive Group	Molecular Weight (g mol^{-1})	CAS no.	Molecular Formula	Structural Formula	Concentration (ppb)
Cyclohexanol	Cyclohexanol	Alcohols and Polyols	100.16	108-93-0	$C_6H_{12}O$	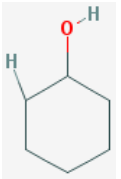	177
Borneol	4,7,7-Trimethylbicyclo[2.2.1]heptan-3-ol	Alcohols and Polyols	154.25	507-70-0	$C_{10}H_{18}O$	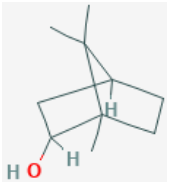	12
Aniline	Aniline	Amines, Aromatic	93.13	62-53-3	C_6H_7N	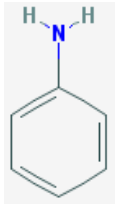	134
2-Methoxy-2-methylpropane	2-Methoxy-2-methylpropane	Ethers	88.15	1634-04-4	$C_5H_{12}O$	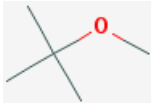	68
Tetrahydrofuran	Oxolane	Ethers	72.11	109-99-9	C_4H_8O	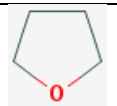	72
2-Ethoxy-2-methylpropane	2-Ethoxy-2-methylpropane	Ethers	102.18	637-92-3	$C_6H_{14}O$	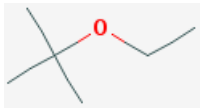	24

Table 3.3 VOCs identified and quantified in the gas-phase generated during the sulphide and sulphite catalytic oxidation process by aeration.

Contaminant	IUPAC name	Reactive Group	Molecular Weight (g mol^{-1})	CAS no.	Molecular Formula	Structural Formula	Concentration (ppb)
N,N-Dimethylacetamide	N,N-Dimethylacetamide	Amides and Imides	87.12	127-19-5	C_4H_9NO	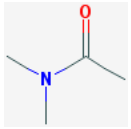	67
2-Propanethiol	Propane-2-thiol	Sulfides, Orhanic	76.16	75-33-2	C_3H_8S	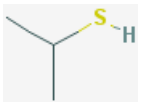	25
Propane, 2-(methylthio)-	2-Methylsulfanylpropane	Sulfides, Orhanic	90.19	1551-21-9	$C_4H_{10}S$	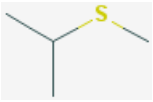	13
HTB	2-Hydroxy-4-(trifluoromethyl)benzoic acid	Acids	206.12	328-90-5	$C_8H_5F_3O_3$	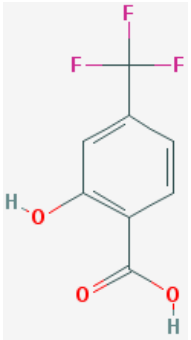	8
Aminomethanesul-fonic acid	Aminomethanesulfonic acid	Acids	111.12	6939-85-1	CH_5NO_3S	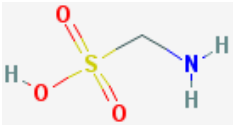	10

Since the maximum sulphate removal efficiency was obtained using a double reagents stoichiometric amount, pH variation tests were performed under these conditions. It was observed that the higher the pH the lower the process efficiency. Thus, contrary to expected, the highest sulphate abatement (97%) was obtained using the natural pH (8.7), which turns out to be advantageous since a cost reduction with reactants for pH correction could be achieved. On the other hand, while the residual concentration of sulphates (0.4 g L^{-1}) fulfilled the legal requirements, aluminium still remained above the ELV (ca. 2 times), requiring an additional step for the removal of residual aluminium. Additional tests (data not shown), with the supernatant resultant from ettringite precipitation in the best conditions ($[Ca^{2+}]$:$[Al^{3+}]$:$[SO_4^{2-}]$ molar ratio of 12:4:3 without pH correction), showed aluminium removal efficiencies of 97% or ~100% at pH values of 7.5 or 6.0, respectively. The addition of a further treatment step makes this process less and less appealing when thinking about its large-scale implementation.

In the case of experiments aiming at sulphate removal through precipitation as barite (Figure 3.5b), it was verified that: (i) at pH 8.5 (i.e. without pH correction), increasing the barium concentration until a $[Ba^{2+}]$:$[SO_4^{2-}]$ molar ratio of 1:1, sulphates removal increased proportionally up to 98%, in accordance with the reaction theoretical stoichiometry (i.e. $BaSO_4$ (s) = Ba^{2+} (aq) + SO_4^{2-} (aq)), and, after that, the performance did not improve, moreover, residual barium content increased to 14 g L^{-1} when $[Ba^{2+}]$:$[SO_4^{2-}]$ molar ratio of 2:1 is tested; and (ii) under stoichiometric conditions, for pH ≥ 7.0, sulphate precipitation was not significantly affected (97-99% removal and residual sulphate concentration of 0.2-0.4 g L^{-1}, and residual barium < 1 mg L^{-1}) and, for pH values below 7.0, the efficiency was slightly lesser (in average <7%), with residual sulphates concentration always complying with the ELV, (but residual barium above ELV). Similarly, even using barium chloride concentrations well below the stoichiometric, Benatti et al. [22] did not find a significant influence of the pH (in the range 2-8) on the residual sulphate concentration after treating a synthetic wastewater with more than 152 g SO_4^{2-} L^{-1}. Furthermore, for a $[Ba^{2+}]$:$[SO_4^{2-}]$ molar ratio of ca. 0.4:1, they reported sulphate removals between 52% and 61%, which were slightly higher than the predicted by the reaction requirements. Oppositely, Kartic et al. [39] verified that sulphate removal from a pigment industry effluent ($[SO_4^{2-}]_0$ = 729±3 mM) was only nearly 100% using barium in excess, and when the stoichiometric amount was applied the efficiency was around 90%. These marginal disparities among works could be related to the matrices of the different wastewaters treated. It is worth mentioning that barium is toxic for human beings and, as such, adequate effluent monitoring is imposed. Actually, according to the Portuguese Decree-Law no. 236/98, barium is considered a “dangerous substance” and the maximum value allowed upstream the treatment plants for drinking water is 0.1 or 1.0 mg L^{-1}, depending on the treatment type. In view of the foregoing, removal of sulphates by the addition of barium can be safely and efficiently applied to the industrial

leachate if both stoichiometric requirements and pH ≥ 7 is assured, thus keeping residual sulphate and barium below 2000 and 1 mg L^{-1}, respectively.

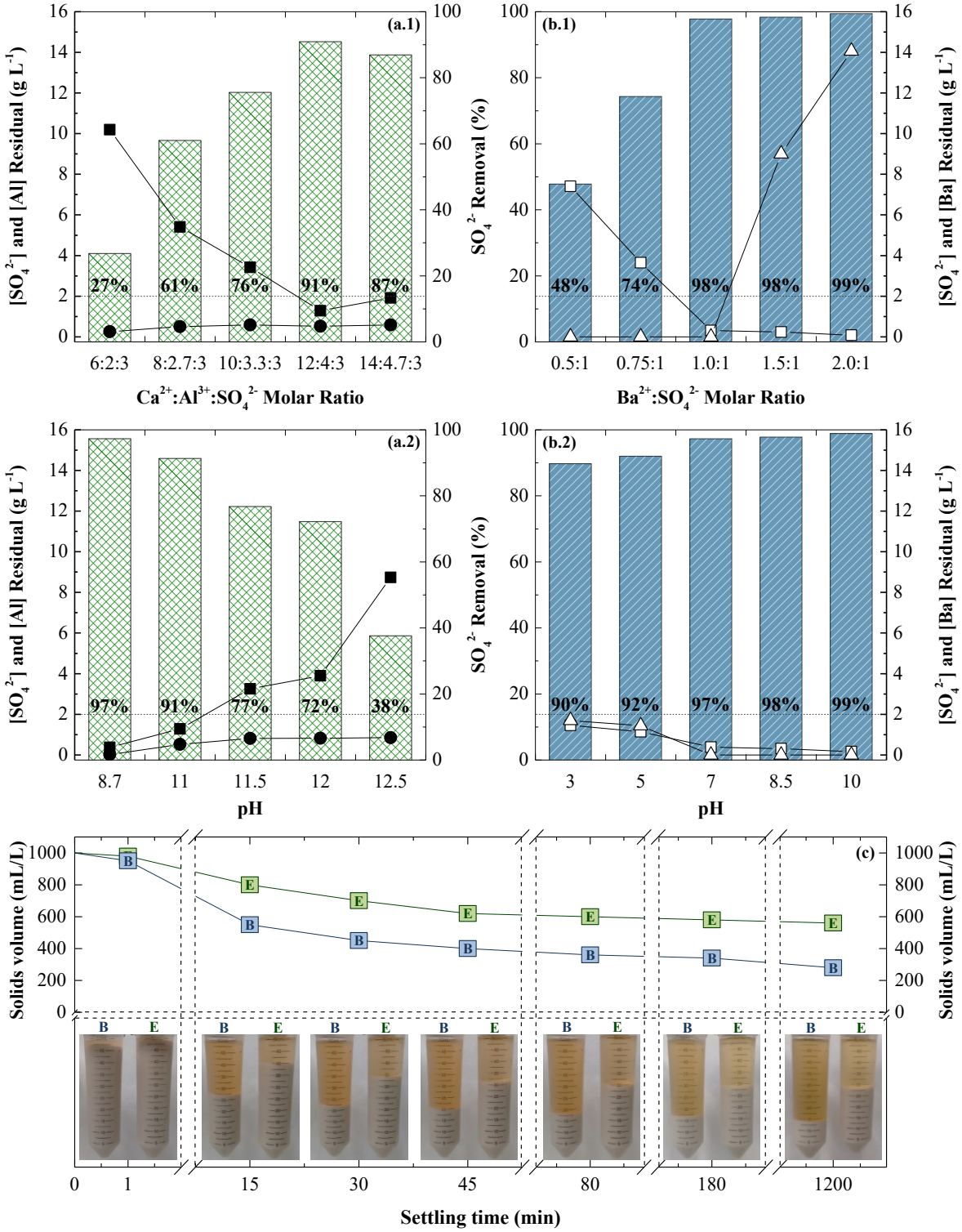

Figure 3.5 Evaluation of: influence of the reactants molar ratio (.1) at pH 11 (a) and pH 8.5 (b), and initial pH (.2) using $[Ca^{2+}]:[Al^{3+}]:[SO_4^{2-}]$ = 12:4:3 (a) and $[Ba^{2+}]:[SO_4^{2-}]$ = 1:1 (b) on the sulphates removal (▨, ▬), by chemical precipitation as ettringite (a.) and barite (b.), and the residual concentrations of sulphate (■,□), aluminium (●) and barium (△); and solids volume as a function of the settling time in the best conditions (c) (pH 8.7 and 8.5 and molar ratios of $[Ca^{2+}]:[Al^{3+}]:[SO_4^{2-}]$ and $[Ba^{2+}]:[SO_4^{2-}]$ equal to 12:4:3 and 1:1 for ettringite (E) and barite (B), respectively).

Additionally, comparing the chemical precipitation via ettringite and barite formation, in the best conditions, it was inferred that: (i) a larger amount of reagents was required (1.7 g Ca^{2+} + 0.4 g Al^{3+} instead of 1.4 g Ba^{2+}, per gram of SO_4^{2-}), resulting in an increase of the treatment cost and chlorides content (which may affect the performance of a downstream advanced oxidation process) of 2.3- and 1.9-fold, respectively (Table 3.1); (ii) pH rose to about 11 instead of remain approximately constant (Table 3.1); (iii) residual aluminium persisted in solution while almost no barium was detected (Table 3.1 and Figure 3.5); (iv) solids settling velocity was slower and its volume was 56 and 100% higher, at 0.5- and 20-h sedimentation time, respectively (see Figure 3.5c); and (v) precipitate presented lesser quality, as will be discussed in the next section. Leachate aspect at the end of chemical precipitation as barite is displayed in Figure 3.1. It should also be noted that, once sulphur compounds were removed, the leachate was not inhibitory to activated sludge, and biodegradability increased from 15% to 42-46% (see Table 3.1), making this effluent suitable to be treated by biological processes aiming the removal of the residual organic matter (Table 3.1).

3.3.3.2 Solid-phase characterization

In order to assess the main characteristics of the minerals resulting from the chemical precipitation as ettringite and barite, SEM-EDS (Figure 3.6), FTIR (Figure 3.7) and XRD (Figure 3.8) analysis were performed in the best conditions (i.e. without pH correction and using molar ratios of $[Ca^{2+}]$:$[Al^{3+}]$:$[SO_4^{2-}]$ and $[Ba^{2+}]$:$[SO_4^{2-}]$ equal to 12:4:3 and 1:1, respectively).

The SEM micrographs (Figure 3.6) show that the agglomerates of uneven sized ettringite and barite particles present a six-sided needle-like and spherical-like morphology, respectively, which is consistent with the observations reported by Cody et al. [39]. As expected, EDS spectra (Figure 3.6) indicate that ettringite and barite crystals were mainly composed of Ca-O-S-Al and Ba-O-S atoms, respectively. Trace amounts of Na-Cl and Na-Si-K were also found, maybe due to an ineffective washing. The presence of Au-Pd atoms was associated with the thin film used to coat the samples. On both samples, C atoms were identified, which can possibly be attributed to the carbon adhesive tap used for fixation and/or carbon which has been adsorbed on the surface of the crystals or precipitated as carbonate, since there is a loss in the leachate alkalinity (see Table 3.1).

In general, FTIR analysis results (Figure 3.7) are in good agreement with the ettringite and barite spectra reported by Dou et al. [23] and Zhang et al. [40], respectively. So, as regards ettringite spectrum, the major vibrational bands can be related to [23]: OH^- stretching and H_2O (3478 cm^{-1}); H_2O (1620 cm^{-1}); CO_3^{2-} (1472 cm^{-1}); SO_4^{2-} (1130 and 600 cm^{-1}) and Al-O-H bending vibration (876 and 521 cm^{-1}). Besides that, the band at 2133 cm^{-1} can be explained as a combination of SO_4^{2-} [41], and the detected peaks at

1796 and 2513 cm^{-1} can also be associated with the presence of calcium carbonate [42]. As a matter of fact, during the ettringite precipitation, the leachate alkalinity was almost all depleted (Table 3.1) and, as shown from the XRD analysis, beyond ettringite, phases containing carbonated compounds were also identified (Figure 3.8). Concerning the barite spectrum, the major vibrational bands can be assigned to [40]: H_2O stretching (3412 cm^{-1}), COO^- and OH^- (1655 and 1437-1400 cm^{-1}), adsorbed on the $BaSO_4$ surface; and $BaSO_4$ stretching characteristic (1192, 1086, 984 and 611 cm^{-1}).

On the basis of the XRD characterization (Figure 3.8), and considering the good Rietveld Refinement obtained, it could be inferred that while the addition of barium to the sulphate-containing pre-oxidised leachate resulted in a precipitate composed only by one phase (2.4% unidentified peak area, Bragg R-factor = 4.0%, χ^2 = 1.6), barite ($BaSO_4$, COD ID: 9004122 [45, 46]**)**, the use of calcium and aluminium led to the formation of a multiphasic precipitate (4.5% unidentified peak area, Bragg R-factor = 6.5%, χ^2 = 1.6**)** constituted by: (i) 68.3% ettringite ($Ca_6Al_2(SO_4)_3(OH)_{12}(H_2O)_{26}$-ph1, COD ID: 9015084 [43, 44]); (ii) 17.2% calcite ($CaCO_3$-ph2, COD ID: 4502443 [45, 48]); and (iii) 14.5% carbonated calcium hemicarboaluminate ($C_{0.4}AlCa_2O_{9.2}$-ph3, COD ID: 2105251 [45, 49]).

These results were found to be in good agreement with the ones reported in the literature [23, 42] and with the liquid-phase characteristics (Table 3.1): (i) almost complete removal of alkalinity; and (ii) low amounts of calcium and aluminium remained in solution despite they had been added in excess regarding ettringite stoichiometry. Furthermore, from the Rietveld refinement, the ettringite and barite reflection peaks were also indexed to the following crystal systems, respectively: (i) trigonal (hexagonal lattice system, with unit-cell parameters of $a = b =$ 1.12344/0.499474/0.574338 and c = 2.14439/1.71098/4.71366 nm, for ph1/ph2/ph3) and (ii) orthorhombic (unit-cell parameters; a = 0.887193, b = 0.544149 and c = 0.716039 nm). Within the XRD equipment limits, it can be concluded that only the chemical precipitation with barium led to a production of a pure phase without secondary phases, increasing the commercial interest of this product.

Taking all of these results into consideration, it can be assumed that the best option to remove the sulphate ions from the leachate is through its precipitation as barite, which can be further purified and utilized, for instance, as a component of oil well drilling fluid, filler in adhesives, plastics, paints and rubber, and improver of polymers mechanical proprieties [45].

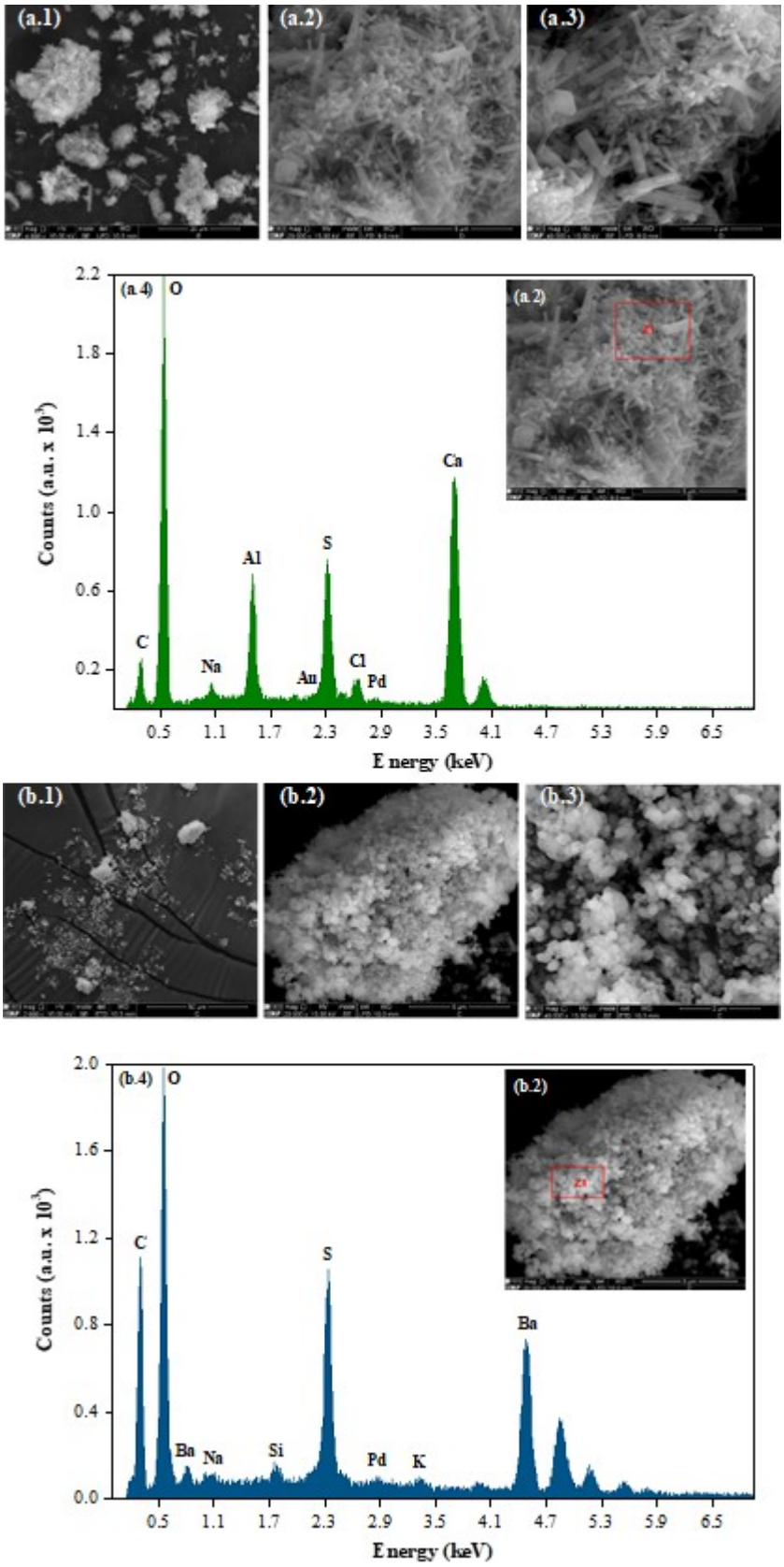

Figure 3.6 SEM micrographs (.1-.3) and EDS spectra (.4) for sulphate precipitates as ettringite (a) and barite (b). (Magnifications: a.1 – 4000x; b.1 – 2000x; a.2, b.2 – 20000x; a.3, b.3 – 40000x).

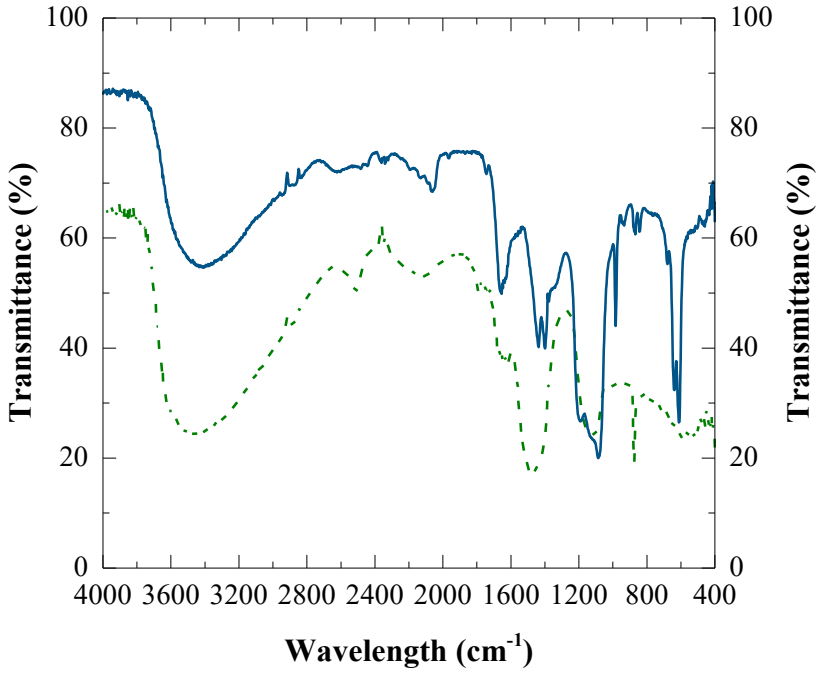

Figure 3.7 FTIR spectra for sulphate precipitates as ettringite (---) and barite (—).

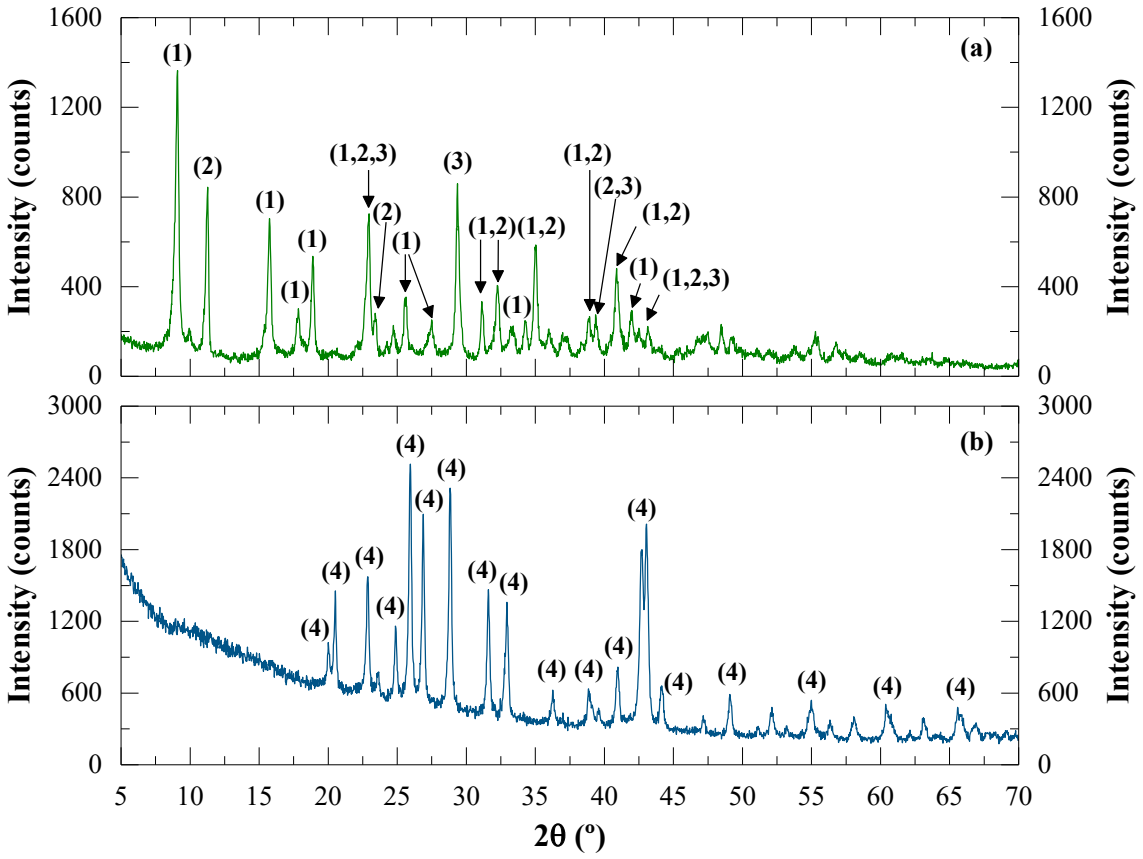

Figure 3.8 XRD paterns of the sulphate precipitates as ettringite (a) and barite (b), with indication of the identified phases (through Match! Software), presenting relative intensity higher than 10%: (1) ettringite; (2) carbonated calcium hemicarboaluminate; (3) calcite; and (4) barite.

3.4 Conclusions

The best strategy to successfully remove sulphur compounds from a HISWL leachate included: (i) catalytic oxidation of sulphide and sulphite ions at natural pH (8.7) using H_2O_2 as oxidant agent (in the molar proportions of 4 H_2O_2:S^{2-} + H_2O_2:SO_3^{2-}) and the effluent transition metals as catalysts, with partial formation of sulphate; and (ii) chemical precipitation of sulphates as pure barite under stoichiometric contents and without pH correction. This approach allowed to obtain an effluent exhibiting sulphide, sulphite and sulphate concentrations lesser than 0.1, 1.0 and 400 mg L^{-1}, fulfilling the Portuguese legal requirements. A monophasic barite precipitate with commercial value, aiming several applications, was generated. Even presenting a high salinity, the final leachate matrix proved to not completely inhibit the activated sludge activity and a high fraction of the organic load (46%) was biologically oxidised, as shown by the Zahn-Wellens test.

Moreover, the use of air in the catalytic oxidation apart from being less efficient than H_2O_2 was also unsafe due to the release of several airborne pollutants. Highly flammable VOCs, such as acetone, 2-butanone, methyl isobutyl ketone and benzene, and strongly toxic H_2S were detected at levels higher than the recommended values. XRD analysis of precipitates showed the production of a single-phase barite and the generation of a three-phase ettringite, where only 68% of the precipitate was effectively associated with the ettringite mineral.

3.5 References

[1] M.H. Gerardi, Nitrification and Denitrification in the Activated Sludge Process, Wiley, New York, 2003.

[2] P.N.L. Lens, A. Visser, A.J.H. Janssen, L.W.H. Pol, G. Lettinga, Biotechnological treatment of sulfate-rich wastewaters, Critical Reviews in Environmental Science and Technology, 28 (1998) 41-88.

[3] E. Kattel, A. Kivi, K. Klein, T. Tenno, N. Dulova, M. Trapido, Hazardous waste landfill leachate treatment by combined chemical and biological techniques, Desalination and Water Treatment, 57 (2016) 13236-13245.

[4] T.F.C.V. Silva, P.A. Soares, D.R. Manenti, A. Fonseca, I. Saraiva, R.A.R. Boaventura, V.J.P. Vilar, An innovative multistage treatment system for sanitary landfill leachate depuration: Studies at pilot-scale, Science of The Total Environment, 576 (2017) 99-117.

[5] A.Ž. Gotvajn, T. Tišler, J. Zagorc-Končan, Comparison of different treatment strategies for industrial landfill leachate, Journal of Hazardous Materials, 162 (2009) 1446-1456.

[6] F.C. Moreira, J. Soler, A. Fonseca, I. Saraiva, R.A. Boaventura, E. Brillas, V.J. Vilar, Incorporation of electrochemical advanced oxidation processes in a multistage treatment system for sanitary landfill leachate, Water Research, 81 (2015) 375-387.

[7] K.Y. Chen, J.C. Morris, Oxidation of sulfide by O 2: catalysis and inhibition, Journal of the Sanitary Engineering Division, 98 (1972) 215-227.

[8] C.E. Santo, V.J. Vilar, A. Bhatnagar, E. Kumar, C.M. Botelho, R.A. Boaventura, Sulphide removal from petroleum refinery wastewaters by catalytic oxidation, Desalination and Water Treatment, 46 (2012) 256-263.

[9] D.J. O'Brien, F.B. Birkner, Kinetics of oxygenation of reduced sulfur species in aqueous solution, Environmental Science & Technology, 11 (1977) 1114-1120.

[10] A.H. Nielsen, J. Vollertsen, T. Hvitved-Jacobsen, Determination of kinetics and stoichiometry of chemical sulfide oxidation in wastewater of sewer networks, Environmental Science & Technology, 37 (2003) 3853-3858.

[11] F.J. Millero, S. Hubinger, M. Fernandez, S. Garnett, Oxidation of H_2S in seawater as a function of temperature, pH, and ionic strength, Environmental Science & Technology, 21 (1987) 439-443.

[12] J. Lagrange, C. Pallares, G. Wenger, P. Lagrange, Kinetics of sulphur (IV) oxidation by hydrogen peroxide in basic aqueous solution, Atmospheric Environment, 30 (1996) 1013-1018.

[13] A. Kotronarou, M.R. Hoffmann, Peroxymonosulfate: An alternative to hydrogen peroxide for the control of hydrogen sulfide, Research Journal of the Water Pollution Control Federation, (1991) 965-970.

[14] A. Kotronarou, M.R. Hoffmann, Catalytic autoxidation of hydrogen sulfide in wastewater, Environmental Science Technology, 25 (1991) 1153-1160.

[15] M.R. Hoffmann, B.C. Lim, Kinetics and mechanism of the oxidation of sulfide by oxygen: catalysis by homogeneous metal-phthalocyanine complexes, Environmental Science Technology, 13 (1979) 1406-1414.

[16] M.R. Hoffmann, Kinetics and mechanism of oxidation of hydrogen sulfide by hydrogen peroxide in acidic solution, Environmental Science Technology, 11 (1977) 61-66.

[17] M. Hoffmann, J. Edwards, Kinetics of the oxidation of sulfite by hydrogen peroxide in acidic solution, The Journal of Physical Chemistry, 79 (1975) 2096-2098.

[18] H. Fischer, G. Schulz-Ekloff, D. Wöhrle, Oxidation of aqueous sulfide solutions by dioxygen part II: Catalysis by soluble and immobilized cobalt(II) phthalocyanines, Chemical Engineering & Technology: Industrial Chemistry-Plant Equipment-Process Engineering-Biotechnology, 20 (1997) 624-632.

[19] F. Cadena, R.W. Peters, Evaluation of chemical oxidizers for hydrogen sulfide control, Journal of the Water Pollution Control Federation, (1988) 1259-1263.

[20] S.D. Boyce, M.R. Hoffman, P.A. Hong, L.M. Moberly, Catalysis of the autoxidation of aquated sulfur dioxide by homogeneous metal-phthalocyanine complexes, Environmental Science Technology, 17 (1983) 602-611.

[21] N. Ahmad, S. Maitra, B.K. Dutta, F. Ahmad, Remediation of sulfidic wastewater by catalytic oxidation with hydrogen peroxide, Journal of Environmental Sciences, 21 (2009) 1735-1740.

[22] C.T. Benatti, C.R.G. Tavares, E. Lenzi, Sulfate removal from waste chemicals by precipitation, Journal of Environmental Management, 90 (2009) 504-511.

[23] W. Dou, Z. Zhou, L.-M. Jiang, A. Jiang, R. Huang, X. Tian, W. Zhang, D. Chen, Sulfate removal from wastewater using ettringite precipitation: magnesium ion inhibition and process optimization, Journal of Environmental Management, 196 (2017) 518-526.

[24] J.K. Edzwald, G.S. Kaminski, A Simple Method for Water Plant Optimization and Operation of Coagulation, Water Quality Technology Conference, American Water Works Association, 2007.

[25] J.K. Edzwald, J. Haarhoff, Seawater pretreatment for reverse osmosis: Chemistry, contaminants, and coagulation, Water Research, 45 (2011) 5428-5440.

[26] C. Sawyer, P. McCarty, G. Parkin, Chemistry for Environmental Engineering and Science, McGraw-Hill Education, 2003.

[27] OECD, Test No. 302B: Inherent Biodegradability: Zahn-Wellens/ EVPA Test, Organisation for Economic Cooperation and Development (OECD) Guidelines for the Testing of Chemicals, (1992).

[28] NP 627:1972, Portuguese Standard 627:1972, Water; Determination of true colour, *Instituto Português da Qualidade*, 1972.

[29] T.F.C.V. Silva, M.E.F. Silva, A.C. Cunha-Queda, A. Fonseca, I. Saraiva, M.A. Sousa, C. Gonçalves, M.F. Alpendurada, R.A.R. Boaventura, V.J.P. Vilar, Multistage treatment system for raw leachate from sanitary landfill combining biological nitrification–denitrification/solar photo-Fenton/biological processes, at a scale close to industrial – Biodegradability enhancement and evolution profile of trace pollutants, Water Research, 47 (2013) 6167-6186.

[30] A.H. Truesdell, B.F. Jones, WATEQ, a computer program for calculating chemical equilibria of natural waters, Journal of Research of the U. S. Geological Survey, 2 (1974) 233-248.

[31] J. Kielland, Individual activity coefficients of ions in aqueous solutions, Journal of the American Chemical Society, 59 (1937) 1675-1678.

[32] W. Stumm, J.J. Morgan, Aquatic Chemistry: Chemical Equilibria and Rates in Natural Waters, Wiley, New York, 2013.

[33] Directive 2009/161/EU of 17 December 2009 establishing a third list of indicative occupational exposure limit values in implementation of Council Directive 98/24/EC and amending Commission Directive 2000/39/EC.

[34] R. Wanek, Monitoring H_2S to Meet New Exposure Standards, Occupational Health & Safety, https://ohsonline.com/articles/2011/09/01/monitoring-h2s-to-meet-new-exposure-standards.aspx, 2011.

[35] NCBI, National Center of Biotechnology Information, PubChem - Open Chemistry Database, https://pubchem.ncbi.nlm.nih.gov/compound/4-Methyl-2-pentanone#section=Top, 2018.

[36] NIOSH, National Institute for Occupational Safety and Health, International Chemical Safety Cards, https://www.cdc.gov/niosh/ipcs/default.html, 2012.

[37] A.M. Cody, H. Lee, R.D. Cody, P.G. Spry, The effects of chemical environment on the nucleation, growth, and stability of ettringite $[Ca_3Al(OH)_6]_2(SO_4)_3 \cdot 26H_2O$, Cement and Concrete Research, 34 (2004) 869-881.

[38] C. Ruiz-Agudo, C.V. Putnis, E. Ruiz-Agudo, A. Putnis, The influence of pH on barite nucleation and growth, Chemical Geology, 391 (2015) 7-18.

[39] D.N. Kartic, B.C.A. Narayana, M. Arivazhagan, Removal of high concentration of sulfate from pigment industry effluent by chemical precipitation using barium chloride: RSM and ANN modeling approach, Journal of Environmental Management, 206 (2018) 69-76.

[40] M. Zhang, B. Zhang, X. Li, Z. Yin, X. Guo, Synthesis and surface properties of submicron barium sulfate particles, Applied Surface Science, 258 (2011) 24-29.

[41] T. Opravil, P. Ptáček, F. Šoukal, J. Havlica, J. Brandštetr, The synthesis and characterization of an expansive admixture for M-type cements I. The influence of free CaO to the formation of ettringite, Journal of Thermal Analysis Calorimetry, 111 (2013) 517-526.

[42] R. Ylmén, U. Jäglid, B.-M. Steenari, I. Panas, Early hydration and setting of Portland cement monitored by IR, SEM and Vicat techniques, Cement and Concrete Research, 39 (2009) 433-439.

[43] COD, Crystallography Open Database, http://www.crystallography.net/cod/, 2018.

[44] F. Goetz-Neunhoeffer, J. Neubauer, Refined ettringite $(Ca_6Al_2(SO_4)_3(OH)_{12} \cdot 26H_2O)$ structure for quantitative X-ray diffraction analysis, Powder Diffraction., 21 (2006) 4-11.

[45] R. Kresse, U. Baudis, P. Jäger, H.H. Riechers, H. Wagner, J. Winkler, H.U. Wolf, Barium and Barium Compounds, Ullmann's Encyclopedia of Industrial Chemistry, Wiley, New York, 2000.

4 Development of a treatment train for the remediation of a hazardous industrial solid waste landfill leachate

This chapter focuses on the development of a treatment train for the HISWL leachate previously treated in Chapter 3 by: (i) catalytic oxidation with H_2O_2 for sulphide and sulphite conversion into oxidized sulphur species, including sulphate, and (ii) chemical precipitation of sulphate as barite. The complete treatment line counted on four more stages: (iii) 1st biological oxidation for removal of biodegradable organic compounds and nitrogen species, (iv) coagulation with ferric chloride (coagulant dose of 100 mg Fe L^{-1}, pH 2.8) for removal of a fraction of recalcitrant organics and suspended solids, (v) PF-UVA (pH 2.8, initial total dissolved iron content of 140 mg L^{-1}, treatment time of ~4 h) for recalcitrant organics degradation and biodegradability improvement, and (vi) 2nd biological oxidation for removal of the biodegradable organic matter resulting from the PF-UVA process. The use of AO or PEF processes in stage (v) demonstrated to be unfeasible. A COD below 1000 mg O_2 L^{-1}, a common limit imposed by municipal wastewater treatment plants (MWWTPs) to effluents discharged into the municipal sewer, was achieved after a feasible treatment time (~4 h) using the multistep approach. The remediation of the HISWL leachate proved to be a big challenge.

This chapter is based on the following research article: "Barbosa Segundo, I.D., Moreira, F.C., Silva, T.F.C.V., Webler, A. D., Boaventura, R.A.R., Vilar, V.J.P., Development of a treatment train for the remediation of a hazardous industrial waste landfill leachate: A big challenge, Science of The Total Environment, 741 (2020) 140-165, DOI: 10.1016/j.scitotenv.2020.140165".

4.1 Introduction

Due to the complexity of landfill leachates, the implementation of multistage treatment strategies based on biological/physical/chemical processes has been gaining increasing significance. There are many studies on the development of treatment trains for leachates from MSWLs [1-10]. In contrast, few treatment strategies have been developed for leachates from ISWLs [11-14], and there is only one study on leachates from HISWLs [15] according to the best of the authors' knowledge.

The work carried out within the current chapter aimed at developing a multistep approach for a leachate from a HISWL receiving waste from steelworks and mining and metallurgy industries, soils contaminated with heavy hydrocarbons and sludge from MWWTPs. This HISWL leachate was already treated, as described in Chapter 3, by: (i) catalytic oxidation with H_2O_2 for sulphide and sulphite conversion into oxidized sulphur species, including sulphate, and (ii) chemical precipitation of sulphate as barite. The following treatment technologies were applied to the pre-treated leachate: biological oxidation, coagulation, and different AOPs/EAOPs, such as H_2O_2/UVC, AO, PF-UVA, PF-UVC and PEF-UVA. These technologies were incorporated in three different treatment trains.

4.2 Material and methods

All the chemicals, experimental units and procedures, analytical determinations, and modeling of removal kinetics used within this chapter are described in Chapter 2.

Table 4.1 exhibits the pre-treated HISWL leachate main physicochemical characteristics.

4.3 Results and discussion

4.3.1 Considerations on the pre-treated HISWL leachate

From Table 4.1, one can highlight the following characteristics of the pre-treated HISWL leachate: (i) null/low content of inorganic sulphur compounds as a result of the previous treatment stages, (ii) high content of organics (COD of 6100 mg O_2 L^{-1} and DOC of 2107 mg L^{-1}), with a medium biodegradability (46% according to the Zahn-Wellens test and a (BOD_5)/COD ratio of 0.36), (iii) high amount of suspended solids (TSS of 607 mg L^{-1}), (iv) perceptible colour, (v) total nitrogen content above the discharge limits for MWWTPs final effluents, attributed to the presence of ammonium (N-NH_4^+ of 323 mg L^{-1}), and (vi) high conductivity/salinity (70 mS cm^{-1}/48 g L^{-1}) mainly related to the presence of high amounts of Cl^- (26 g L^{-1}). The content of total aluminium, arsenic, barium, cadmium, chromium, copper, lead, manganese, nickel and zinc was lower than 0.03-0.6 mg L^{-1}. Thus, these metals were not monitored

during the current study. Total iron was an exception since it was present in a greater content in the raw and in the pre-treated HISWL leachate (1.9 mg L^{-1}) and was added in some treatment stages.

According to the pre-treated HISWL leachate characteristics, its treatment should include: (i) removal of organic compounds (biodegradable and recalcitrant), which may come along with suspended solids and colour removal, and (ii) NH_4^+ decrease or elimination. With this aim in view, three treatment strategies were tested: (i) biological oxidation followed by an AOP/EAOP at natural pH, or (ii) at acidic pH (2.8), and (iii) followed by a coagulation process and an AOP/EAOP at pH 2.8. Biological processes can be able to remove biodegradable organics and NH_4^+ under appropriate conditions [16, 17]; AOPs/EAOPs are used to remove recalcitrant organics [10, 18-20]; Coagulation is a separation process widely applied to remove suspended and colloidal particles and also some dissolved compounds of organic nature [21].

4.3.2 Biological oxidation followed by an AOP/EAOP at natural pH

4.3.2.1 Biological oxidation

The pH, temperature and DO values registered in the course of the biological process were as follows: pH of 8.4-8.7, temperature of 21.1-22.2 ºC and DO of 2.0-2.2 mg L^{-1} up to ~7 days of treatment and of 2.8 and 4.2 mg L^{-1} at ~8 and ~9 days, respectively (Figure 4.1). These conditions were indicative of a proper system functioning since Metcalf & Eddy [22] and Gerardi [23] refer that aerobic biological oxidation and nitrification processes tolerate pH values in the range 6.0-9.0 and temperatures of 10-45 ºC, and also that a DO of around 2.0 mg L^{-1} is commonly found in these processes. The DO increase in the last ~2 days of treatment can be attributed to the microbial activity weakening due to the lack of biodegradable organic matter. Moreover, the average sludge volume index (SVI) was 52 mL g^{-1}, pointing to excellent sludge settling and compaction characteristics, typically in the range 50-100 mL g^{-1} [24].

The biological process was able to provide the oxidation of almost all biodegradable organic compounds. A continuous DOC decay was registered up to stabilization from ~8 days of treatment (Figure 4.1) and DOC, COD and BOD_5 removals of 39%, 41% and 80%, respectively, were achieved at the end of the biological treatment (Table 4.1).

Table 4.1 Physicochemical characteristics of the pre-treated HISWL leachate and of the HISWL leachate along the various treatment stages.

Parameter (unit)	Pre-treated HISWL	Biological oxidation[a]	Acidification to pH 2.8[b]	Coagulation[c]	PF-UVA (4 h)[d]	2nd biological oxidation[e]	ELV[f]
Colour	Light brown	Light brown	Light brown	Light brown	Medium brown	Light yellow	
Colour (diluted 1:20)	d.	d.	d.	d.	d.	n.d.	n.d.[1] or n.c.
Colour (Pt-Co units)	1300	1250	1300	1400	1600	n.m.	
Odour	Low	Low	Low	Very Low	Null	Null	
Odour (diluted 1:20)	d.	d.	d.	n.d.	n.d.	n.d.	n.d.[1] or n.c.
pH	8.4	8.6	2.8	2.8	7.0	7.1	6.0-9.0 or n.c.
Conductivity (mS cm^{-1})	70	65	66	66	n.m.	n.m.	
Salinity (g L^{-1})	48	44	45	45	n.m.	n.m.	
Alkalinity (mg $CaCO_3$ L^{-1})	3971	3752	n.d.	n.d.	n.d.	n.d.	
Redox potential (mV)	-7.5	-12	n.m.	n.m.	n.m.	n.m.	
Turbidity (NTU)	80	65	190	50	1.2	n.m.	
Total suspended solids – TSS (mg L^{-1})	607	354	950	147	23	30	60 or 35
Total volatile solids – VSS (mg L^{-1})	67	189	530	36	10	14	
Total dissolved carbon – TDC (mg L^{-1})	3060	2137	1024	743	544	429	
Dissolved inorganic carbon – DIC (mg L^{-1})	953	857	24	18	9	7	
Dissolved organic carbon – DOC (mg L^{-1})	2107	1280	1000	725	535	422	
Chemical oxygen demand – COD (mg O_2 L^{-1})	6100	3580	3000	1838	1550	910	150 or 125
COD/DOC	2.9	2.8	3.0	2.5	2.9	2.2	
Biochemical oxygen demand – BOD_5 (mg O_2 L^{-1})	2200	440	n.m.	n.m.	n.m	12	40 or 25
BOD_5/COD	0.36	0.12	-	-	-	n.m.	
Biodegradability - Zhan-Wellens test (%)	46	14	13	11	20	n.m.	
Absorbance at 254 nm (AU) (diluted 1:50)	1.3	1.0	1.1	0.68	0.33	n.m.	
$SUVA_{254}$ (L mg^{-1} m^{-1})	3.1	3.9	5.5	4.7	3.1	n.m.	
Total nitrogen – N_T (mg L^{-1})	427	340	348	340	345	298	15 or 10
Ammonium – N-NH_4^+ (mg L^{-1})	323	245	241	237	257	188	7.8 or n.c.

Table 4.1 Physicochemical characteristics of the pre-treated HISWL leachate and of the HISWL leachate along the various treatment stages.

Parameter (unit)	Pre-treated HISWL	Biological oxidation[a]	Acidification to pH 2.8[b]	Coagulation[c]	PF-UVA (4 h)[d]	2nd biological oxidation[e]	ELV[f]
Nitrite – N-NO_2^- (mg L^{-1})	<4.9[g]	<4.9[g]	<4.9[g]	<4.9[g]	<4.9[g]	<4.9[g]	
Nitrate – N-NO_3^- (mg L^{-1})	<8.0[g]	<8.0[g]	<8.0[g]	<8.0[g]	<8.0[g]	<8.0[g]	11 or n.c.
Sulphate – SO_4^{2-} (g L^{-1})	0.3	0.3	0.3	0.3	0.5	0.5	2.0 or n.c.
Sulphite – SO_3^{2-} (mg L^{-1})	<1.0[g]	<1.0[g]	<1.0[g]	<1.0[g]	<1.0[g]	<1.0[g]	1.0 or n.c.
Sulphide – S^{2-} (mg L^{-1})	<0.1[g]	<0.1[g]	<0.1[g]	<0.1[g]	<0.1[g]	<1.0[g]	1.0 or n.c.
Chloride – Cl^- (g L^{-1})	26	26	30	30	30	n.m.	
Total phosphorous - P_T (mg L^{-1})	5.0	4.5	4.1	3.2	2.8	1.0	10 or 1
Calcium – Ca^{2+} (mg L^{-1})	<32[g]	n.m.	n.m.	n.m.	n.m.	n.m.	
Lithium – Li^+ (mg L^{-1})	<3.3[g]	n.m.	n.m.	n.m.	n.m.	n.m.	
Magnesium – Mg^{2+} (mg L^{-1})	<12[g]	n.m.	n.m.	n.m.	n.m.	n.m.	
Potassium – K^+ (g L^{-1})	3.1	n.m.	n.m.	n.m.	n.m.	n.m.	
Sodium – Na^+ (g L^{-1})	18	n.m.	n.m.	n.m.	n.m.	n.m.	
Total barium – Ba (mg L^{-1})	<0.6[g]	n.m.	n.m.	n.m.	n.m.	n.m.	
Total iron – Fe (mg L^{-1})	1.9	1.9	1.9	80	154	1.9	2.0 or n.c.
Total dissolved iron – TDI (mg L^{-1})	0.46	0.44	0.50	60	140	1.5	

d. – detected; n.d. – not detected; n.d.[1] (diluted 1:20); n.c. – not covered; n.m. – not measured;

[a] Using the pre-treated HISWL leachate. Biological oxidation conditions: Activated sludge batch reactor, pH = 8.4-8.7, Temperature = 21.1-22.2 ºC, DO = 2.0-2.2 mg L^{-1}, Treatment time = 9 d, subsequent sedimentation for 2 h and removal of biological treatment sludge;

[b] Using the HISWL leachate after biological oxidation. Acidification with HCl 37% (w/w) without subsequent clarification;

[c] Using the HISWL leachate previously subjected to biological oxidation. Coagulation conditions: pH = 2.8, 100 mg Fe L^{-1} from $FeCl_3$ coagulant, subsequent sedimentation for 2 h and removal of coagulation/flocculation sludge;

[d] Using the HISWL leachate previously subjected to biological oxidation and coagulation. PF-UVA conditions: H_2O_2 = 200-400 mg L^{-1}, pH = 2.8, TDI_0 = 140 mg L^{-1}, Temperature = 20±1 ºC, Treatment time of 4 h (240 min), subsequent neutralization to pH 7.0, sedimentation for 3 h and removal of PF-UVA sludge;

[e] Using the HISWL leachate previously subjected to biological oxidation, coagulation and PF-UVA process for 4 h (240 min). Biological oxidation conditions: 28 days Zhan-Wellens test, subsequent sedimentation for 2 h and removal of the biological treatment sludge;

[f] ELV - Emission limit value according to Decree-Law 236/98 (Portuguese legislation) or Directive 91/271/CEE (European legislation);

[g] Limit of detection.

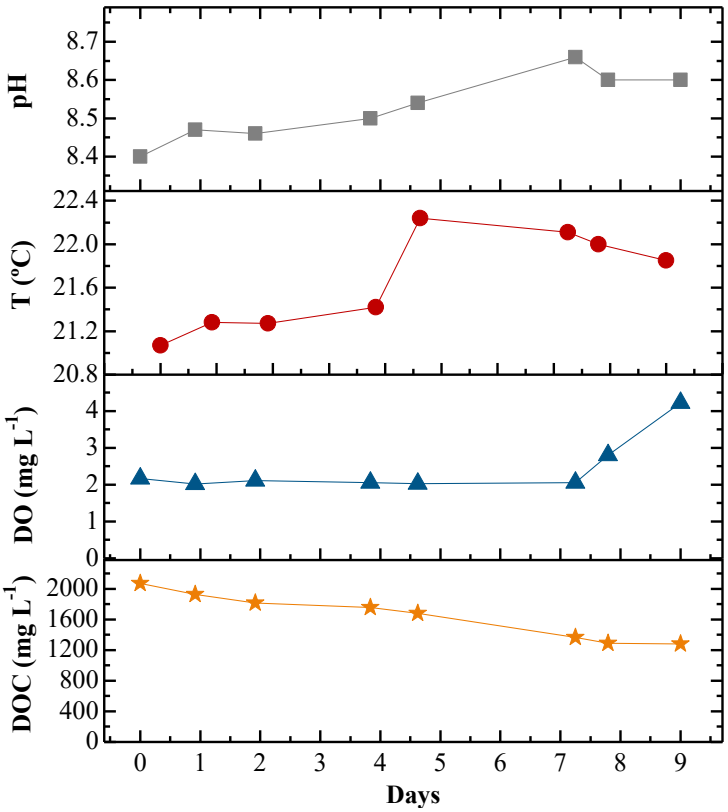

Figure 4.1 Change of pH (■), temperature (●), DO (▲) and DOC (★) during the 1st biological oxidation applied to the pre-treated HISWL leachate.

As regards inorganic compounds, ammonium was removed in 24% along with no nitrite or nitrate increase and very poor alkalinity removal (Table 4.1). This suggests the occurrence of ammonium stripping and the absence of ammonia-oxidizing bacteria in the reactor. The inhibition of ammonia-oxidizing bacteria may have occurred due to the presence of free ammonia (NH_3) contents of ~31 mg N-NH_3 L^{-1}, calculated via Eq. 4.1 as a function of total ammonia nitrogen (TAN) concentration [25], which are higher than the inhibitory contents reported in the literature, i.e. 4.1-22 mg N-NH_3 L^{-1} [26]. Furthermore, the high salinity of the leachate (48 g L^{-1}) may have caused the loss of bacterial activity [27].

$$[\text{N-NH}_3]\ (\text{mol L}^{-1}) = \frac{[\text{TAN}]\ (\text{mol L}^{-1}) \times 10^{\text{pH}}}{e^{6344/\text{T (K)}} + 10^{\text{pH}}} \qquad 4.1$$

To allow nitrification/denitrification, it would be necessary to use a low volume exchange ratio in a sequential batch biological reactor, which would provide lower ammonia contents in the reactor. Nitrification/denitrification should be instigated in this 1st biological treatment instead of in a subsequent biological oxidation step since intrinsic alkalinity and biodegradable organic matter of the pre-treated HISWL leachate can be used in nitrification and denitrification processes, respectively.

Additionally, the biological treatment provided the removal of 42% of TSS likely due to organic solids oxidation and/or solids sedimentation. Complete characterization of the bio-treated HISWL leachate can be accessed in Table 4.1.

4.3.2.2 AOPs/EAOPs at natural pH

Two AOPs/EAOPs at natural pH (8.6) were tested immediately after the application of the 1st biological oxidation: H_2O_2/UVC and AO. A blank experiment only employing the UVC light was also carried out, leading to null DOC decay as a result of null susceptibility of the organic matrix to direct photolysis. In the H_2O_2/UVC process, the H_2O_2 content was maintained in the range of 200-400 mg L^{-1} since preliminary tests showed a good balance between the oxidation rate and the H_2O_2 consumption using this H_2O_2 content. In the AO process, a current density of 200 mA cm^{-2} was applied since it is a common value for EAOPs applied to landfill leachates [28].

Figure 4.2a and 4.2a.1 show a negligible ability of H_2O_2/UVC process to remove DOC (7% DOC removal after 480 min of reaction) along with an extremely high H_2O_2 consumption (~16.5 g H_2O_2 L^{-1} after 480 min of reaction). These results suggest the occurrence of parasitic reactions besides the homolytic cleavage of the peroxide bond (–O–O–) to form hydroxyl radicals ($^{\bullet}OH$) by Eq. 1.6 [29]. These undesired reactions probably included: (i) H_2O_2 dissociation at alkaline pH with formation of perhydroxyl anions (HO_2^-) via Eq. 1.37 (pK_a = 11.6) [30] followed by HO_2^- reaction with H_2O_2 via Eq. 4.2 [31], with no generation of $^{\bullet}OH$, (ii) deactivation of $^{\bullet}OH$ by reaction with HO_2^- via Eq. 4.3, a reaction ~280 times faster than $^{\bullet}OH$ reaction with H_2O_2 (Eq. 1.21) [32], and (iii) H_2O_2 self-decomposition according to Eq. 4.4, which occurs in higher extent in alkaline solutions than in acidic solutions [33].

$$HO_2^- + H_2O_2 \rightarrow H_2O + O_2 + OH^- \quad (4.2)$$

$$^{\bullet}OH + HO_2^- \rightarrow H_2O + O_2^{\bullet -} \quad k = (7.5 \pm 1.9) \times 10^9 \text{ L mol}^{-1} \text{ s}^{-1} \quad (4.3)$$

$$2H_2O_2 \rightarrow 2H_2O + O_2 \quad (4.4)$$

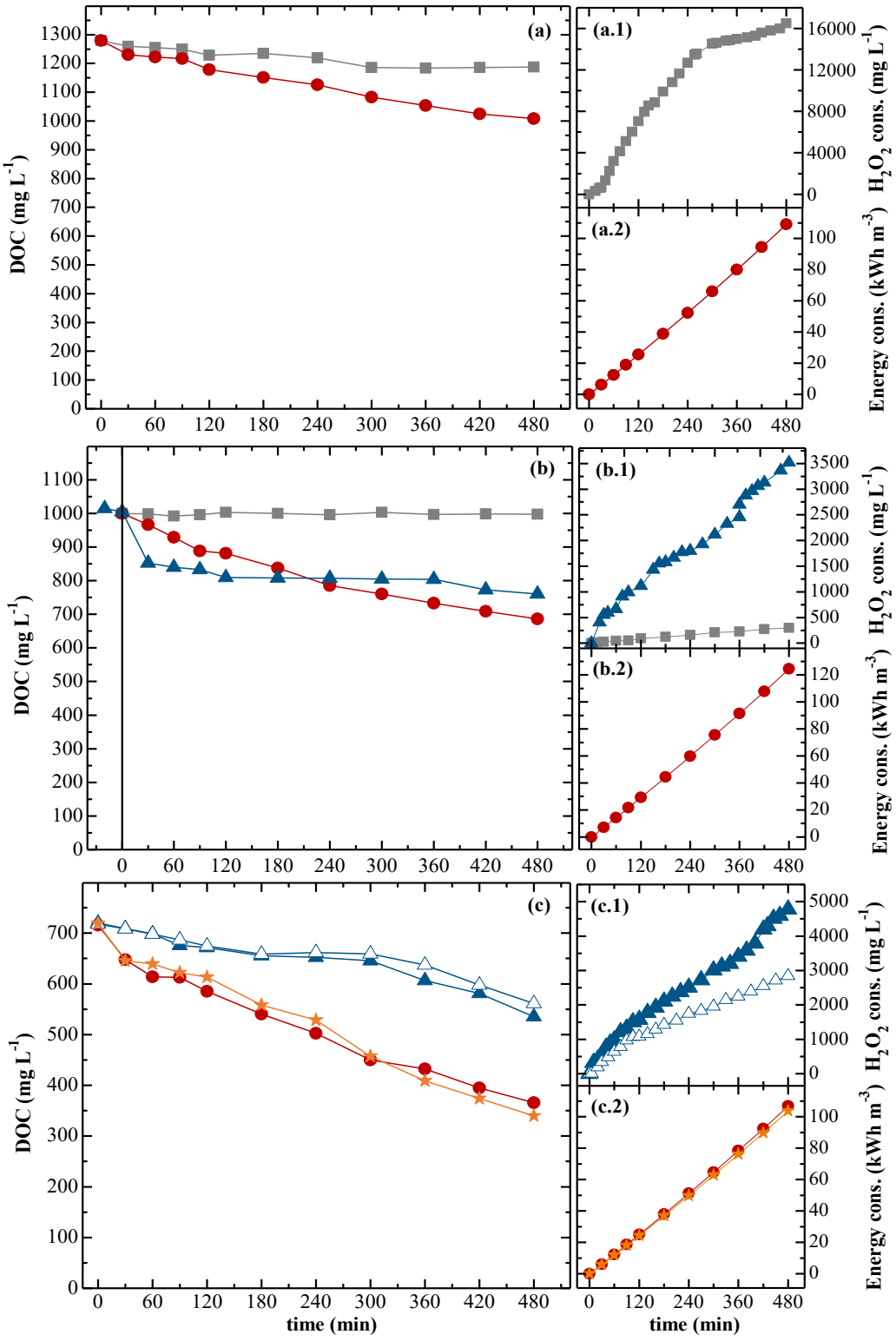

Figure 4.2 Comparison of various AOPs/EAOPs applied to different pre-treated HISWL leachates: leachate after 1st biological oxidation (a), leachate after 1st biological oxidation followed by acidification to pH 2.8 (b), and leachate after 1st biological oxidation by coagulation (c). AOP/EAOP: H_2O_2/UVC (■), AO (●), PF-UVA (▲), PF-UVC (△), PEF-UVA (★). Conditions: H_2O_2 = 200-400 mg L^{-1} for AOPs, Current density = 200 mA cm^{-2} for EAOPs, pH = 8.6 for trials using the leachate after 1st biological oxidation and pH = 2.8 for the others, TDI_0 = 60 mg L^{-1} for PF processes and trials using the leachate after coagulation and TDI_0 < 0.5 mg L^{-1} for the others, Temperature = 20±1 ºC.

The AO process provided a higher DOC removal compared to the H_2O_2/UVC process (21% DOC removal after 480 min of reaction) (Figure 4.2a). Nevertheless, this removal was poor as supported by the low pseudo-first-order kinetic constant for DOC decay (k_{DOC}) achieved for the AO process, $0.54\pm0.02 \times 10^{-3}$ min^{-1} (Table 4.2). The k_{DOC} values of all the AOPs/EAOPs carried out within this study are exhibited in Table 4.2. Electrogenerated active chlorine species must have had a crucial contribution to organic compounds oxidation in the AO process. Conversely, the generation of powerful physisorbed $^{\bullet}OH$ at the BDD anode surface, denoted BDD($^{\bullet}OH$), via Eq. 1.7 [34] may have been seriously compromised since $^{\bullet}OH$ are not expected to be electrochemically formed at pH higher than ~9 [35]. The BDD anodes have a high overvoltage for chlorine formation, not sufficient for the generation of $^{\bullet}OH$ before chlorine production [36].

Active chlorine species include chlorine-containing molecules in oxidation states other than -1, namely: (i) aqueous chlorine (Cl_2), generated thought the direct oxidation of the large amount of Cl^- in the HISWL leachate (26 g L^{-1}) via Eq. 1.10 [34], (ii) hypochlorous acid (HClO), produced from Cl_2 hydrolyzation via Eq. 1.11 [34], (iii) hypochlorite ion (ClO^-) as a result of HClO dissociation in the bulk according to Eq. 1.12 (pK_a = 7.5) [37], (iv) chlorine radical ($Cl^{\bullet}$) produced from Cl^- oxidation via Eq. 4.5 [38], (v) chlorite ion (ClO_2^-) formed according to Eqs. 1.14 and 1.15 [39], (vi) chlorate ion (ClO_3^-) generated via Eqs. 4.5 [39] and 4.6 [38], and (vii) perchlorate ion (ClO_4^-) produced via Eq. 1.17 [39], among others. At pH 8.6, the predominant active chlorine species is expected to be ClO^-, with a low redox potential (E^o = 0.81 V/SHE [32]), which can explain the low DOC removal.

$$Cl^- \rightarrow Cl^{\bullet} + e^- \quad (4.5)$$

$$2HClO + ClO^- \rightarrow ClO_3^- + 2H^+ + 2Cl^- \quad (4.6)$$

Despite the contribution of active chlorine species to organics degradation, these species can lead to the production of chlorinated organic by-products with high health-risk for living beings. Moreover, it was felt a powerful chlorine smell, mainly from 180 min of reaction, indicating the release of chlorine gas into the environment. Chlorine gas is toxic and its damages for human beings range between tolerable mild mucous membrane irritation for about 1 h at 1-3 ppm and death within only few minutes at 1000 ppm and above [40]. Finally, yet importantly, very large amounts of foam were formed during the AO process, right from the first minutes of reaction, hindering the electrochemical cell functioning. An anti-foaming agent had to be added to reduce the amount of foam. Taking into account these drawbacks, the application of AO should be taken with a high degree of caution.

Table 4.2 Pseudo-first-order kinetic constants for DOC removal (k_{DOC}), coefficient of determination (R^2) and residual variance (S^2_R).

	Time interval (min)	k_{DOC} ($\times 10^{-3}$ min^{-1})	S^2_R (mg^2 L^{-2})	R^2
HISWL leachate after 1st biological oxidation				
H_2O_2/UVC[a]	0-480	No fitting of the kinetic model to experimental data		
AO[b]	0-480	0.54±0.02	2167	0.974
HISWL leachate after 1st biological oxidation and acidification to pH 2.8				
H_2O_2/UVC[c]	0-480	No fitting of the kinetic model to experimental data		
AO[d]	0-480	0.88±0.03	4230	0.963
PF-UVA[e]	30-480	No fitting of the kinetic model to experimental data		
HISWL leachate after 1st biological oxidation and coagulation				
AO[f]	0-480	1.48±0.06	4057	0.968
PF-UVA[e]	0-480	No fitting of the kinetic model to experimental data		
PF-UVC[e]	0-480	No fitting of the kinetic model to experimental data		
PEF-UVA[f]	0-480	1.51±0.05	3338	0.979
PF-UVA[g] **- TDI_0 = 60 mg L^{-1}**	0-120, 540-960	0.84±0.02	4643	0.986
PF-UVA[g] **- TDI_0 = 100 mg L^{-1}**	0-120, 600-960	1.09±0.06	5635	0.984
PF-UVA[g] **- TDI_0 = 140 mg L^{-1}**	0-960	1.21±0.03	3384	0.991
PF-UVA[g] **- TDI_0 = 180 mg L^{-1}**	0-960	1.22±0.03	5870	0.987

[a] Conditions: H_2O_2 = 200-400 mg L^{-1}, pH = 8.6, TDI_0 < 0.5 mg L^{-1}, Temperature = 20±1 ºC;
[b] Conditions: Current density = 200 mA cm^{-2}, pH = 8.6, TDI_0 < 0.5 mg L^{-1}, Temperature = 20±1 ºC;
[c] Conditions: H_2O_2 = 200-400 mg L^{-1}, pH = 2.8, TDI_0 < 0.5 mg L^{-1}, Temperature = 20±1 ºC;
[d] Conditions: Current density = 200 mA cm^{-2}, pH = 2.8, TDI_0 < 0.5 mg L^{-1}, Temperature = 20±1 ºC;
[e] Conditions: H_2O_2 = 200-400 mg L^{-1}, pH = 2.8, TDI_0 = 60 mg L^{-1}, Temperature = 20±1 ºC;
[f] Conditions: Current density = 200 mA cm^{-2}, pH = 2.8, TDI_0 = 60 mg L^{-1}, Temperature = 20±1 ºC;
[g] Conditions: H_2O_2 = 200-400 mg L^{-1}, pH = 2.8, Temperature = 20±1 ºC.

4.3.3 Biological oxidation followed by an AOP/EAOP at acidic pH

4.3.3.1 Biological oxidation

Biological treatment was carried out as described in Section 4.3.2.1.

4.3.3.2 Acidification

A pH value of 2.8 was chosen for acidification since this was the optimum pH for Fenton's reaction based processes that were further applied, and no iron precipitation as $Fe(OH)_{3(s)}$ was expected.

Acidification of the bio-treated HISWL leachate up to pH 2.8 with no subsequent clarification provided dissolved organics removal, corresponding to a DOC decay of 22% (Table 4.1). This can be ascribed to the insolubilization of organics, such as humic substances, together with their difficult sedimentation, which was confirmed by an increase in turbidity, TSS, VSS and $SUVA_{254}$ (Table 4.1). In addition, alkalinity was removed and an increase in Cl^- of ~4 g L^{-1} was registered due to HCl addition. Complete characterization of the HISWL leachate after acidification is displayed in Table 4.1.

4.3.3.3 AOPs/EAOPs at acidic pH

The HISWL leachate after biological oxidation and acidification to pH 2.8 was subjected to three AOPs/EAOPs: H_2O_2/UVC, AO and PF-UVA. The effect of UVC or UVA light alone was also tested, leading to null organics direct UVC and UVA photolysis. An initial TDI content of 60 mg L^{-1} was used in the PF-UVA process since this was the TDI content found for the coagulated HISWL leachate (Section 4.3.4.2).

Figure 4.2b shows a null DOC decay using the H_2O_2/UVC process and Figure 4.2b.1 displays a small H_2O_2 consumption (~0.3 g H_2O_2 L^{-1} after 480 min of reaction). This H_2O_2 consumption was drastically lower than that at natural pH. These results suggest the inability of $^{\bullet}OH$ produced from H_2O_2 homolysis (Eq. 1.6) to degrade the HISWL leachate organic matter and also that parasitic reactions (Eq. 1.37, 4.2, 4.3, 1.21, 4.4) were inhibited at acidic pH.

The AO process promoted 31% DOC abatement after 480 min of reaction (Figure 4.2b), a value 10% higher than the one achieved at pH 8.6, corresponding to a 1.6-fold increase in k_{DOC} (Table 4.2). The higher DOC removal for the acidic HISWL leachate can be mainly attributed to the action of: (i) BDD($^{\bullet}OH$), which generation is favoured at acidic pH and inhibited at pH values higher than ~9 [35], and (ii) HClO, the predominant active chlorine species at acidic pH and the chlorine species with the highest redox potential (E^o = 1.48 V/SHE [30]). The effect of pH on the organics degradation ability of the AO process has been controversial, with some authors pointing to null effect, others to the superiority of acidic pH and others to best efficiencies at alkaline pH [28]. The energy consumption for electrochemical cell operation was quite similar for the HISWL leachate at acidic and alkaline pH (Figure 4.2a.2 and Figure 4.2b.2) due to the similar conductivity of the leachates. Once again, a powerful chlorine smell was felt, and large amounts of foam were produced.

The PF-UVA process was characterized by a pronounced DOC decay (~15%) in the first instants of reaction (Figure 4.2b) that can be attributed to the precipitation of complexes formed between organic compounds and Fe^{3+} generated from Fenton's reaction (Eq. 1.18) [43].

From then on, the DOC abatement was slow, with only more ~9% of DOC being removed up to the reaction end. For reaction times above 240 min, the PF-UVA process promoted even smaller DOC decays than the AO process. These results suggest that $^{\bullet}OH$ in the bulk generated from Eq.1.18, with the aid of the photoreduction of Fe(III)-hydroxy complexes, such as $FeOH^{2+}$ according to Eq. 1.23 [42], and of the direct photolysis of complexes formed between Fe^{3+} and some organics via the general Eq. 1.24 [43], were insufficient to degrade the organics that compose the acidified bio-treated HISWL leachate. Furthermore, the Cl^- salts of the leachate were likely to form complexes with Fe^{3+}, with much lower photoactivity than the above-mentioned complexes, or to act as $^{\bullet}OH$ scavengers [44].

The H_2O_2 consumption in the PF-UVA process was much higher than in the H_2O_2/UVC process (Figure 4.2b.1), suggesting the occurrence of Fenton's reaction (Eq. 1.18) in greater extent than the H_2O_2 homolysis (Eq. 1.6).

4.3.4 Biological oxidation followed by coagulation and AOP/EAOP at acidic pH

4.3.4.1 Biological oxidation

Biological treatment was performed as described in Section 4.3.2.1.

4.3.4.2 Coagulation

$FeCl_3$ was chosen as coagulant since iron salts demonstrated superiority over aluminum salts in the landfill leachates treatment [45], and, beyond that, iron can be used as a catalyst in subsequent PF experiments. Coagulation of the bio-treated HISWL leachate was carried out at pH 2.8 since it has been proved that coagulation of various landfill leachates with $FeCl_3$ coagulant is more efficient at pH ~3-5 [10, 11, 45, 46], and, furthermore, pH 2.8 is optimum for PF process, as previously discussed.

Figure 4.3 shows higher removals of DOC and accumulation of higher amounts of TDI for greater $FeCl_3$ coagulant doses, in conjunction with null colour removal or even slight colour increase, and higher turbidity for the lowest $FeCl_3$ dose (25 mg Fe L^{-1}) followed by turbidity increasing removals for greater $FeCl_3$ doses. Colour proved not to be a good parameter for the evaluation of the coagulation efficiency since even low TDI contents contributed to a reddish leachate colour. A $FeCl_3$ dose of 25 mg Fe L^{-1} was not enough to promote complete charge neutralization, contributing to colloidal stability of particles and even increasing turbidity.

A $FeCl_3$ dose of 100 mg Fe L^{-1} was selected as the optimal dose since DOC and turbidity removals were almost maximized and the TDI concentration (60 mg L^{-1}) was not large enough to hinder the efficiency

of light-assisted AOPs/EAOPs due to the occurrence of: (i) parasitic reactions, such as Eq. 1.22, (ii) inner filter effects, i.e. competitive absorption of photons between Fe^{3+} photoactive species and organics, and (iii) light attenuation along the photoreactor optical pathlength [47].

The addition of two flocculants, anionic Magnafloc 155 and cationic Ambifloc C polyacrylamide, at pH 2.8 and using 100 mg Fe L^{-1}, provided null improvements (data not shown).

From the complete characterization of the coagulated HISWL leachate presented in Table 4.1, one can highlight the following characteristics of this leachate in comparison with the bio-treated one: (i) 43% lower DOC, (ii) slightly stronger colour, likely mainly due to TDI contribution to colour, (iii) lower turbidity (23%), TSS (58%) and VSS (81%), (iv) a higher TDI content of 60 mg L^{-1} in contrast to 0.44 mg L^{-1}, (v) odour removal to comply with the discharge limit, and (vi) imperceptible Cl^- increment due to $FeCl_3$ addition. Compared to the acidified HISWL leachate, the coagulated HISWL leachate exhibited (Table 4.1): (i) DOC content 28% lower, (ii) slightly stronger colour, (iii) much lower content of solids in suspension, leading to smaller turbidity (74%), TSS (84%) and VSS (93%), and (iv) higher iron content (60 mg L^{-1} versus 0.50 mg L^{-1}).

4.3.4.3 AOPs/EAOPs at acidic pH using the coagulated HISWL leachate

The HISWL leachate after biological oxidation and chemical coagulation was subjected to four AOPs/EAOPs: AO, PF-UVA, PF-UVC and PEF-UVA. Additionally, the influence of UVA or UVC light alone was tested, revealing null organics direct photolysis. An initial TDI content of 60 mg L^{-1} was used in PF processes, corresponding to the TDI of the HISWL leachate after the coagulation step. The current density of 200 mA cm^{-2}, used in AO and PEF-UVA processes, is common in EAOPs applied to landfill leachates [28].

Figure 4.2c exhibits similar DOC removals for PF processes using either UVA or UVC light, with removals of ~24% after 480 min of reaction. Despite this, the consumption of H_2O_2 was higher for the PF-UVA (Figure 4.2c.1), which suggests a lower transmissibility of the coagulated HISWL leachate for the UVC radiation. The DOC removals were similar to those achieved for the PF-UVA process applying the acidified HISWL leachate (24%). One can then suggest that the lower content of organics and suspended particles in the coagulated HISWL leachate, with consequent increase of light-penetration, was unable to improve the susceptibility of organic matter to the attack of $^{\bullet}OH$ in the bulk, produced via Eqs. 1.18, 1.23, 1.24, and also via Eq. 1.6 in the PF-UVC process. It is worth noting that the large DOC decay found in the first instants of the PF-UVA process applied to the acidified HISWL leachate was

not observed for the coagulated HISWL leachate since the precipitation and removal Fe(III)-organic complexes had already occurred during the coagulation step.

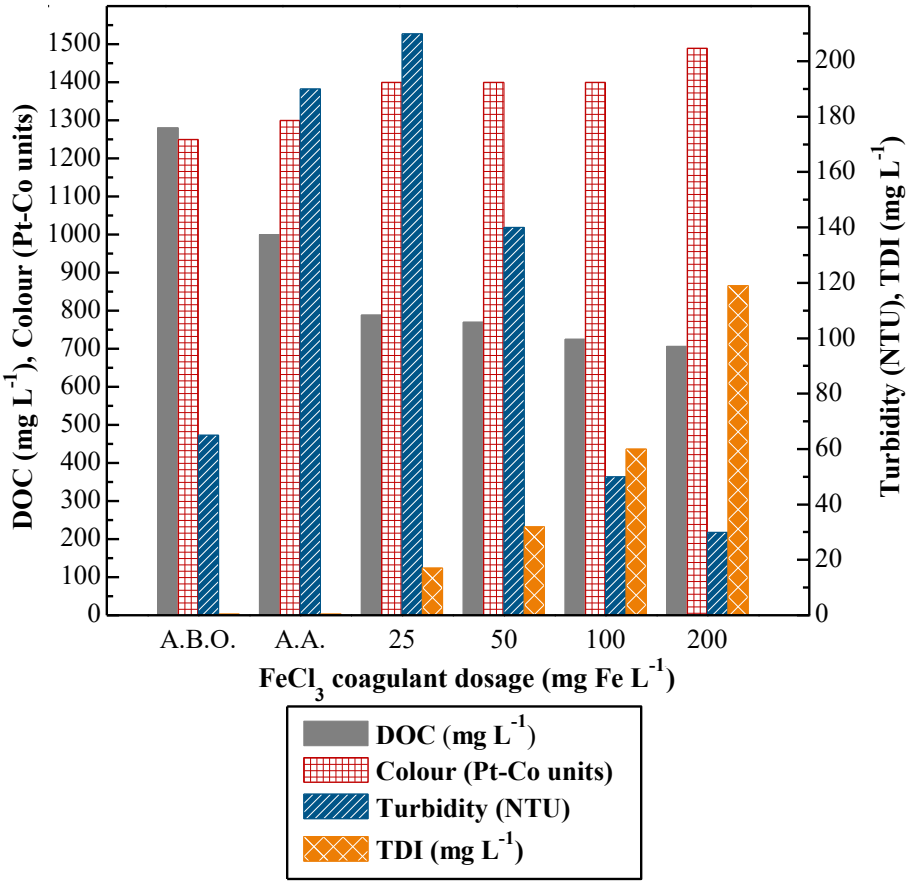

Figure 4.3 Effect of $FeCl_3$ coagulant dosage on DOC, colour, turbidity and TDI for coagulation process at pH 2.8 applied to the HISWL leachate after 1st biological oxidation. A.B.O.: After 1st biological oxidation. A.A.: After acidification to pH 2.8 (0 mg Fe L^{-1}).

AO and PEF-UVA processes achieved similar results and superiority over the PF processes (Figure 4.2c and Table 4.2). These results suggest that BDD (•OH) species played a very important role in the degradation of the organic matter since they were the common oxidizing species present in both processes. In the PEF-UVA, the accumulation of active chlorine species is expected to be avoided due to their reaction with the H_2O_2 electrochemically generated at the cathode in the presence of oxygen via Eq. 1.25 [48], which is a known dechlorination agent for free chlorine [49]. For the AO process, a powerful chlorine smell and huge amounts of foam were generated, contrasting with the absence of chlorine smell for the PEF-UVA process. Beyond BDD(•OH), the PEF-UVA process counted on •OH generated from Fenton's reaction, intensified by the Fe^{3+} regeneration to Fe^{2+} via photochemical reactions 1.23 and 1.24 and also via electrochemical reaction (Eq. 1.26) [50] at the cathode. Despite the high efficiency of the PEF-UVA process, the deposition of solids on the cathode surface (carbon-PTFE sheet) took place, with consequent stop of the H_2O_2 electrogeneration. It was necessary to interrupt the

process for three times during the experiment to clean the cathode with a concentrated HCl solution and water in abundance to ensure the proper cathode functioning.

The AO process applied to the coagulated HISWL leachate achieved 49% DOC removal after 480 min of reaction, a value 28% and 18% higher than those found for the bio-treated HISWL leachate at alkaline pH and acidic pH, respectively. The k_{DOC} value was 2.7 and 1.7 times higher, respectively. This indicates a higher ability of organics of the coagulated HISWL leachate to the attack of BDD($^{\bullet}$OH) and/or a higher availability of these oxidants in the presence of lower solids content.

4.3.5 Selecting the best treatment strategy

The application of biological oxidation followed by a chemical coagulation process and an AOP/EAOP at pH 2.8 provided the highest removal of organics, with a DOC abatement to ~353 mg L^{-1} upon the use of AO and PEF-UVA processes for 480 min (83% DOC removal), and DOC decays to ~548 mg L^{-1} by using PF-UVA and PF-UVC processes for 480 min (74% DOC removal). Despite the high efficiency of AO and PEF-UVA processes, important drawbacks derived from the application of these processes. The AO process promoted the release of chlorine gas because of the presence of an enormous amount of Cl^- in the HISWL leachate (~30 g L^{-1}), which can cause mild mucous membrane irritation or even be fatal for human beings depending on the concentration, and also the formation of large amounts of foam, which hindered the electrochemical cell operation. In addition, the generation of hazardous organochlorine compounds during AO should also be considered, irrespective of their amount has not actually been assessed. The PEF-UVA process revealed some important operational complications related to the deposition of particles on the cathode surface that inhibited the electrochemical generation of H_2O_2. As a result, the sequential application of a biological treatment, a coagulation with $FeCl_3$ and a PF oxidation process can be considered the best treatment strategy for the pre-treated HISWL leachate. Since the PF-UVC process did not show any superiority over the traditional PF-UVA process, this latter PF process can be selected as the best one.

The effect of TDI on the efficiency of the PF-UVA process was then assessed in an attempt to improve this process. Figure 4.4a and Table 4.2 show increasing DOC removal rates for initial TDI contents from 60 to 140 mg L^{-1}. This can be ascribed to the occurrence of Fenton's reaction in higher extent due to the presence of larger amounts of Fe^{2+} at the reaction beginning and their regeneration. The slightly higher H_2O_2 consumptions for increasing TDI concentrations (Figure 4.4a.1) corroborate this assumption. For TDI contents above 140 mg L^{-1}, the rate of DOC removal was not enhanced, suggesting the occurrence of parasitic reactions, inner filter effects, and light attenuation along the photoreactor optical pathlength. Furthermore, some iron precipitation took place for the highest TDI content (Figure 4.4a.2). An initial

TDI content of 140 mg L^{-1} can be chosen as optimum for the PF-UVA process applied to the coagulated HISWL leachate. This PF-UVA process displayed a k_{DOC} value only ~1.2 times lower than the k_{DOC} values attained for AO and PEF-UVA processes (Table 4.2), leading to a DOC decay to ~415 mg L^{-1} after 480 min of reaction (80% DOC removal).

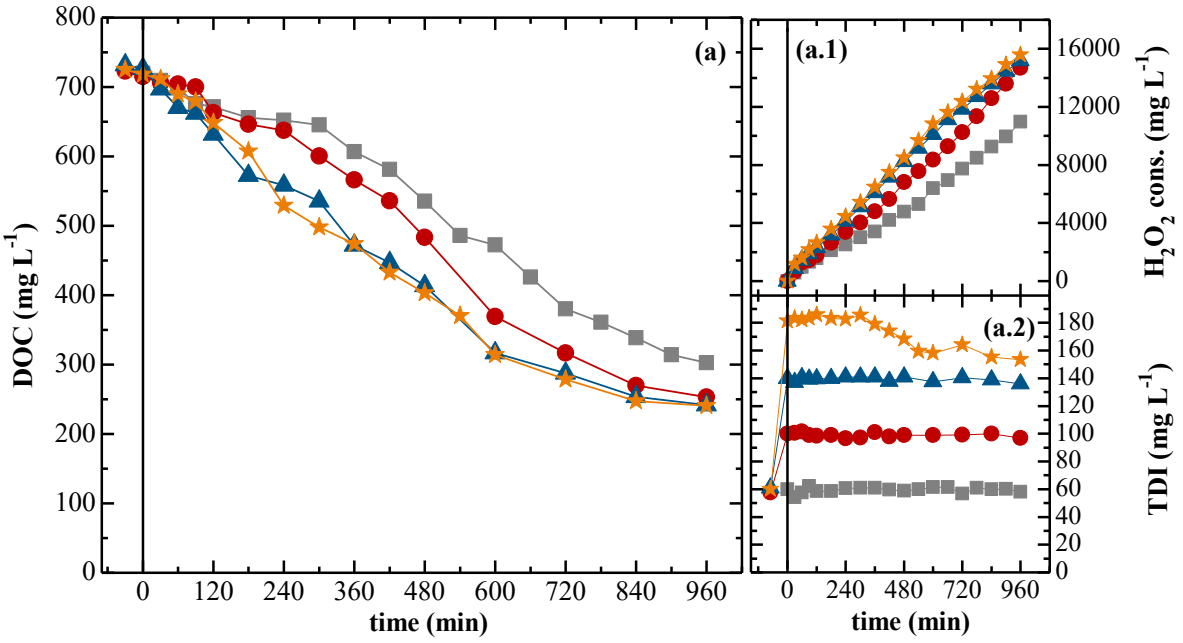

Figure 4.4 Effect of initial TDI concentration on PF-UVA process applied to the HISWL leachate after coagulation. TDI_0 (mg L^{-1}): 60 (■), 100 (●), 140 (▲), 180 (★). Conditions: H_2O_2 = 200-400 mg L^{-1}, pH = 2.8, Temperature = 20±1 ºC.

It should be noted that colour changes were observed in the course of all PF processes. The leachate became darker right upon the addition of H_2O_2 and started to become lighter only around after 5 h of reaction. This suggests the formation of darker by-products, such as phenol intermediates, known by their dark brown colour, mainly the quinone-type compounds [51].

The obtained k_{DOC} value for the PF-UVA process under optimal conditions, (1.21±0.03)×10^{-3} min^{-1}, was slightly greater than the k_{DOC} values achieved by Webler et al., [11], (0.9±0.1)×10^{-3} min^{-1}, for PF-UVA processes carried out in the same experimental system under quite similar optimum conditions applied to a non-hazardous ISWL leachate. This leachate had been previously treated by a biological process comprising nitrification/denitrification followed by a coagulation/flocculation process, starting from a DOC content of 897 mg L^{-1}. On the other hand, Moreira et al., [10] found a higher k_{DOC} value of (3.7±0.1)×10^{-3} min^{-1} for a PF-UVA process performed in a quite similar experimental unit under comparable optimal conditions applied to leachate from a MSWL previously treated by biological oxidation and coagulation, exhibiting a DOC of ~384 mg L^{-1}. Comparison can also be performed for the PEF-UVA process, for which the current HISWL leachate achieved a slower DOC decay (k_{DOC} of

1.51±0.05 min^{-1}) compared to the MSWL leachate (k_{DOC} of (4.3±0.3)×10^{-3} min^{-1}) [10] and the non-hazardous ISWL leachate (k_{DOC} of 2.22±0.07 min^{-1}) [11]. These results suggest the presence of very recalcitrant organics in the HISWL and non-hazardous ISWL leachates. Furthermore, adverse effects coming from the high salinity of the HISWL leachate (45 g L^{-1}) are likely to have occurred, mainly due to the enormous Cl^- content (30 g L^{-1}). The non-hazardous ISWL leachate and the MSWL leachate exhibited lower salinities (5.7 g L^{-1} and ~12 g L^{-1}, respectively) along with Cl^- contents of 2.1 and ~3.4 g L^{-1}, respectively.

Finally, a PF-UVA process under optimal conditions was applied to the coagulated HISWL leachate for 24 h to collect samples for a Zahn-Wellens test (Table 4.3). The aim was to define the best organics oxidation state to stop the process so that a 2nd biological treatment could provide a leachate with a COD value in line with the limit for discharge into waterbodies. Table 4.3 reveals biodegradability improvement for longer treatment times up to 20 h. However, not even the application of the PF-UVA process for 24 h was able to promote a COD value below 125 mg O_2 L^{-1} (European legislation) or 150 mg O_2 L^{-1} (Portuguese legislation). In virtue of the high cost assigned to the application of the PF-UVA for very long times (higher than 24 h), an alternative strategy can be the reduction of the COD content up to the limit imposed by MWWTPs to receive industrial effluents to be treated there, which commonly is around 1000 mg O_2 L^{-1}. The application of the PF-UVA process for 4 h (240 min) was enough to provide a COD of 910 mg O_2 L^{-1} after a secondary biological treatment. The treated leachate complied with the Portuguese and European discharge limits, except for COD, total nitrogen and ammonium (Table 4.1). Nitrification/denitrification should be promoted in the 1st biological treatment.

Table 4.3 Characterization of Zahn-Wellens test samples of the coagulated HISWL leachate subjected to different treatment times of the PF-UVA process (conditions: H_2O_2 = 200-400 mg L^{-1}, pH = 2.8, TDI_0 = 140 mg L^{-1}, Temperature = 20±1 ºC).

	Coagulated HISWL leachate	**Coagulated HISWL leachate subjected to the PF-UVA process for a given time**					
		4 h	**8 h**	**12 h**	**16 h**	**20 h**	**24 h**
D_{t28} **(%)**	11	20	22	28	42	49	41
DOC_0 **(mg L^{-1})**	711	530	415	279	242	180	145
DOC_{28} **(mg L^{-1})**	632	422	322	200	140	91	85
COD_0 **(mg L^{-1})**	1830	1358	900	661	503	481	462
COD_{28} **(mg L^{-1})**	1681	910	610	451	280	271	250

4.4 Conclusions

The complete remediation of the HISWL leachate encompassed the following six-stage treatment line: (i) catalytic oxidation of sulphide and sulphite using H_2O_2 (H_2O_2:S^{2-} and H_2O_2:SO_3^{2-} molar ratios of 4:1 and 1:1, respectively), with partial formation of sulphate, (ii) chemical precipitation of sulphate as pure barite, (Ba^{2+}:SO_4^{2-} molar ratio of 1:1), (iii) 1st biological oxidation for biodegradable organics removal and nitrification/denitrification, (iv) coagulation with $FeCl_3$ (dose of 100 mg Fe L^{-1}) at acidic pH (2.8) for removal of a fraction of recalcitrant organics and suspended solids, (v) PF-UVA process for ~4 h at pH 2.8 and initial TDI content of 140 mg L^{-1} for recalcitrant organics degradation and biodegradability enhancement, and (vi) 2nd biological oxidation for removal of the biodegradable fraction generated during the PF-UVA process. The application of AO and PEF-UVA processes as a stage (v) proved to be unfeasible mainly due to the occurrence of operational constraints.

The treatment strategy allowed to reach a COD value below 1000 mg O_2 L^{-1}, a common limit imposed by MWWTPs to receive pre-treated industrial effluents, but not the Portuguese and European COD legal requirements for the discharge of wastewaters into waterbodies (150 and 125 mg O_2 L^{-1}). It would be needed to apply the PF-UVA process for more than 24 h to achieve a final COD removal in accordance with the discharge limits into waterbodies.

4.5 References

[1] A.I. Gomes, M.L.R. Foco, E. Vieira, J. Cassidy, T.F.C.V. Silva, A. Fonseca, I. Saraiva, R.A.R. Boaventura, V.J.P. Vilar, Multistage treatment technology for leachate from mature urban landfill: Full scale operation performance and challenges, Chemical Engineering Journal, 376 (2019) 120573.

[2] T.F.C.V. Silva, P.A. Soares, D.R. Manenti, A. Fonseca, I. Saraiva, R.A.R. Boaventura, V.J.P. Vilar, An innovative multistage treatment system for sanitary landfill leachate depuration: Studies at pilot-scale, Science of the Total Environment, 576 (2017) 99-117.

[3] A. Urtiaga, A. Rueda, Á. Anglada, I. Ortiz, Integrated treatment of landfill leachates including electrooxidation at pilot plant scale, Journal of Hazardous Materials, 166 (2009) 1530-1534.

[4] G. Del Moro, L. Prieto-Rodríguez, M. De Sanctis, C. Di Iaconi, S. Malato, G. Mascolo, Landfill leachate treatment: Comparison of standalone electrochemical degradation and combined with a novel biofilter, Chemical Engineering Journal, 288 (2016) 87-98.

[5] K. Klein, A. Kivi, N. Dulova, I. Zekker, E. Mölder, T. Tenno, M. Trapido, T. Tenno, A pilot study of three-stage biological-chemical treatment of landfill leachate applying continuous ferric sludge reuse in Fenton-like process, Clean Technologies Environmental Policy, 19 (2017) 541-551.

[6] M. Peyravi, M. Jahanshahi, M. Alimoradi, E. Ganjian, Old landfill leachate treatment through multistage process: Membrane adsorption bioreactor and nanofitration, Bioprocess and Biosystem Engineering, 39 (2016) 1803-1816.

[7] E. Torres-Socías, L. Prieto-Rodríguez, A. Zapata, I. Fernández-Calderero, I. Oller, S. Malato, Detailed treatment line for a specific landfill leachate remediation. Brief economic assessment, Chemical Engineering Journal, 261 (2015) 60-66.

[8] A. Anfruns, J. Gabarró, R. Gonzalez-Olmos, S. Puig, M.D. Balaguer, J. Colprim, Coupling anammox and advanced oxidation-based technologies for mature landfill leachate treatment, Journal of Hazardous Materials, 258-259 (2013) 27-34.

[9] J.-S. Guo, A.A. Abbas, Y.-P. Chen, Z.-P. Liu, F. Fang, P. Chen, Treatment of landfill leachate using a combined stripping, Fenton, SBR, and coagulation process, Journal of Hazardous Matererials, 178 (2010) 699-705.

[10] F.C. Moreira, J. Soler, A. Fonseca, I. Saraiva, R.A.R. Boaventura, E. Brillas, V.J.P. Vilar, Incorporation of electrochemical advanced oxidation processes in a multistage treatment system for sanitary landfill leachate, Water Research, 81 (2015) 375-387.

[11] A.D. Webler, F.C. Moreira, M.W.C. Dezotti, C.F. Mahler, I.D.B. Segundo, R.A.R. Boaventura, V.J.P. Vilar, Development of an integrated treatment strategy for a leather tannery landfill leachate, Waste Management, 89 (2019) 114-128.

[12] L. Di Palma, P. Ferrantelli, C. Merli, E. Petrucci, Treatment of industrial landfill leachate by means of evaporation and reverse osmosis, Waste Management, 22 (2002) 951-955.

[13] A.Ž. Gotvajn, T. Tišler, J. Zagorc-Končan, Comparison of different treatment strategies for industrial landfill leachate, Journal of Hazardous Materials, 162 (2009) 1446-1456.

[14] P. Haapea, S. Korhonen, T. Tuhkanen, Treatment of industrial landfill leachates by chemical and biological methods: ozonation, ozonation + hydrogen peroxide, hydrogen peroxide and biological post-treatment for ozonated water, ozone, Science & Engineering, 24 (2002) 369-378.

[15] E. Kattel, A. Kivi, K. Klein, T. Tenno, N. Dulova, M. Trapido, Hazardous waste landfill leachate treatment by combined chemical and biological techniques, Desalination and Water Treatent, 57 (2016) 13236-13245.

[16] F.A. El-Gohary, G. Kamel, Characterization and biological treatment of pre-treated landfill leachate, Ecological Engineering, 94 (2016) 268-274.

[17] F. Zhang, Y. Peng, L. Miao, Z. Wang, S. Wang, B. Li, A novel simultaneous partial nitrification anammox and denitrification (SNAD) with intermittent aeration for cost-effective nitrogen removal from mature landfill leachate, Chemical Engineering Journal, 313 (2017) 619-628.

[18] E.M.R. Rocha, V.J.P. Vilar, A. Fonseca, I. Saraiva, R.A.R. Boaventura, Landfill leachate treatment by solar-driven AOPs, Solar Energy, 85 (2011) 46-56.

[19] C.A. Martínez-Huitle, M. Panizza, Electrochemical oxidation of organic pollutants for wastewater treatment, Current Opinion in Electrochemistry, 11 (2018) 62-71.

[20] C.A. Martínez-Huitle, M.A. Rodrigo, I. Sirés, O. Scialdone, Single and coupled electrochemical processes and reactors for the abatement of organic water pollutants: A critical review, Chemical Reviews, 115 (2015) 13362-13407.

[21] H. Bakraouy, S. Souabi, K. Digua, O. Dkhissi, M. Sabar, M. Fadil, Optimization of the treatment of an anaerobic pretreated landfill leachate by a coagulation-flocculation process using experimental design methodology, Process Safety and Environmental Protection, 109 (2017) 621-630.

[22] I. Metcalf & Eddy, Wastewater engineering, treatment and reuse, 4th ed., McGraw-Hill, New York, 2004.

[23] M.H. Gerardi, Nitrification and denitrification in the activated sludge process, John Wiley & Sons, Inc., New York, 2002.

[24] N.P. Cheremisinoff, Handbook of Water and Wastewater Treatment Technology, Marcel Dekker, Inc., New York, 1994.

[25] A.C. Anthonisen, R.C. Loehr, T.B.S. Prakasam, E.G. Srinath, Inhibition of nitrification by ammonia and nitrous acid, Journal Water Pollution Control Federation, 48 (1976) 835-852.

[26] S. Park, W. Bae, Modeling kinetics of ammonium oxidation and nitrite oxidation under simultaneous inhibition by free ammonia and free nitrous acid, Process Biochemistry., 44 (2009) 631-640.

[27] T. Hülsen, K. Hsieh, D.J. Batstone, Saline wastewater treatment with purple phototrophic bacteria, Water Research, 160 (2019) 259-267.

[28] F.C. Moreira, R.A.R. Boaventura, E. Brillas, V.J.P. Vilar, Electrochemical advanced oxidation processes: A review on their application to synthetic and real wastewaters, Applied Catalysis B: Environmental, 202 (2017) 217-261.

[29] J.H. Baxendale, J.A. Wilson, The photolysis of hydrogen peroxide at high light intensities, The Transactions of The Faraday Society, 53 (1957) 344-356.

[30] D.R. Lide, Handbook of Chemistry and Physics, 84th edition, CRC Press, Boca Raton, 2004.

[31] F.J. Beltrán, M. González, J.F. González, Industrial wastewater advanced oxidation. Part 1. UV radiation in the presence and absence of hydrogen peroxide, Water Research, 31 (1997) 2405-2414.

[32] H. Christensen, K. Sehested, H. Corfitzen, Reactions of hydroxyl radicals with hydrogen peroxide at ambient and elevated temperatures, The Journal of Physical Chemistry, 86 (1982) 1588-1590.

[33] W.D. Nicoll, A.F. Smith, Stability of dilute alkaline solutions of hydrogen peroxide, Industrial & Engineering Chemistry , 47 (1955) 2548-2554.

[34] M. Panizza, G. Cerisola, Direct And Mediated Anodic Oxidation of Organic Pollutants, Chemical Reviews, 109 (2009) 6541-6569.

[35] T. Enache, A.M.C. Paquim, O. Fatibello-Filho, A. Oliveira-Brett, Hydroxyl radicals electrochemically generated in situ on a boron-doped diamond electrode, Electrochemistry Communications., 11 (2009) 1342.

[36] T. Muddemann, A. Bulan, M. Sievers, U. Kunz, Avoidance of chlorine formation during electrolysis at boron-doped diamond anodes in highly sodium chloride containing and organic-polluted wastewater, Journal of The Electrochemical Society, 165 (2018) J3281-J3287.

[37] D.C. Harris, Exploring Chemical Analysis, 4rd ed., W. H. Freeman and Company, New York, 2009.

[38] E. Mostafa, P. Reinsberg, S. Garcia-Segura, H. Baltruschat, Chlorine species evolution during electrochlorination on boron-doped diamond anodes: In-situ electrogeneration of Cl_2, Cl_2O and ClO_2, Electrochimica Acta, 281 (2018) 831-840.

[39] A. Sánchez-Carretero, C. Sáez, P. Cañizares, M.A. Rodrigo, Electrochemical production of perchlorates using conductive diamond electrolyses, Chemical Engineering Journal, 166 (2011) 710-714.

[40] C.W. White, J.G. Martin, Chlorine gas inhalation: Human clinical evidence of toxicity and experience in animal models, Proceedings of the American Thoracic Society, 7 (2010) 257-263.

[41] F. Haber, J. Weiss, The catalytic decomposition of hydrogen peroxide by iron salts, Proceedings of the Royal Society of London. Series A, Mathematical and Physical Sciences, 147 (1934) 332-351.

[42] Y. Sun, J.J. Pignatello, Photochemical reactions involved in the total mineralization of 2,4-D by $Fe^{3+}/H_2O_2/UV$, Environmental Science & Technology, 27 (1993) 304-310.

[43] O. Horváth, K.L. Stevenson, Charge transfer photochemistry of coordination compounds, VCH, New York, 1992.

[44] M.M. Micó, J. Bacardit, J. Malfeito, C. Sans, Enhancement of pesticide photo-Fenton oxidation at high salinities, Applied Catalysis B: Environmental, 132-133 (2013) 162-169.

[45] E. Diamadopoulos, Characterization and treatment of recirculation-stabilized leachate, Water Research, 28 (1994) 2439-2445.

[46] C. Amor, E.D. Torres-Socías, J.A. Peres, M.I. Maldonado, I. Oller, S. Malato, M.S. Lucas, Mature landfill leachate treatment by coagulation/flocculation combined with Fenton and solar photo-Fenton processes, Journal of Hazardous Materials, 286 (2015) 261-268.

[47] S. Malato, P. Fernández-Ibáñez, M.I. Maldonado, J. Blanco, W. Gernjak, Decontamination and disinfection of water by solar photocatalysis: Recent overview and trends, Catalysis Today, 147 (2009) 1-59.

[48] P.C. Foller, R.T. Bombard, Processes for the production of mixtures of caustic soda and hydrogen peroxide via the reduction of oxygen, Journal of Applied Electrochemistry, 25 (1995) 613-627.

[49] S. Goldstein, D. Aschengrau, Y. Diamant, J. Rabani, Photolysis of aqueous H_2O_2: Quantum yield and applications for polychromatic UV actinometry in photoreactors, Environmental Science & Technology, 41 (2007) 7486-7490.

[50] E. Brillas, I. Sirés, M.A. Oturan, Electro-Fenton process and related electrochemical technologies based on Fenton's reaction chemistry, Chemical Reviews, 109 (2009) 6570-6631.

[51] F. Mijangos, F. Varona, N. Villota, Changes in solution color during phenol oxidation by Fenton reagent, Environmental Science & Technology, 40 (2006) 5538-5543.

5 Incorporation of ozone-driven processes in a treatment line for a leachate from a HISWL: Impact on the bio-refractory character and dissolved organic matter distribution

The current chapter aimed to evaluate the impact of an ozone (O_3)-based AOP in the treatment of a non-biodegradable sulphur-rich leachate from a hazardous industrial solid waste landfill (HISWL). O_3-based AOPs have encompassed: perozonation (O_3/H_2O_2) and photo-assisted ozonation (O_3/UVC) and perozonation (O_3/H_2O_2/UVC). All O_3-driven processes were applied to the HISWL leachate directly after sulphur compounds removal. Moreover, ozonation technology after coagulation with ferric or aluminium salts was also tested (O_3/Fe^{2+} or O_3/Al^{3+}) and O_3/H_2O_2/UVC system after Fe-mediated coagulation was likewise tried targeting a photo-Fenton-assisted ozonation (O_3/PF). The best treatment train encompassed: (i) catalytic oxidation (CO) with H_2O_2 (stoichiometric molar amount) under free pH, to convert sulphite and sulphide ions into oxidized sulphur species, including sulphate; (ii) chemical precipitation of sulphate anions as barite mineral without pH correction; (iii) O_3/H_2O_2 process for ca. 2.1 h (natural pH; room temperature; 3.5 kg O_3 per m^3 leachate; 1.1 kg H_2O_2 per m^3 leachate) with an associated unitary operating cost of 9.1 € m^{-3}, to degrade refractory organic matter and improve biodegradability; and (iv) biological oxidation to remove the remaining bioavailable organics fraction. This four-stage approach allowed shifting from a highly recalcitrant wastewater to an effluent in full agreement with the regulation for industrial wastewater discharge into the municipal sewer network. Furthermore, the unfeasibility of the coagulation process, as well as the effectiveness of the O_3/H_2O_2 process over the dissolved organic matter transformation were corroborated by the fluorescence excitation-emission matrix (EEM) and size exclusion chromatography (SEC) analysis.

This chapter is based on the following research article: "Barbosa Segundo, I.D., Gomes, A.I., Santos, Souza-Chaves, B.M., Park, M., dos Santos, A.B., Boaventura, R.A.R., Moreira, F.C., Silva, T.F.C.V., Vilar, V.J.P., Incorporation of ozone-driven processes in a treatment line for a leachate from a hazardous industrial waste landfill: Impact on the bio refractory character and dissolved organic matter distribution. Journal of Environmental Chemical Engineering, 9 (2021) 105554, DOI: 10.1016/j.jece.2021.105554".

5.1 Introduction

Chapters 3 and 4 conducted with this high-complexity HISWL leachate have revealed the need for a six-stage treatment system composed of the following processes: (i) catalytic oxidation (CO); (ii) chemical precipitation (CP); (iii) aerobic/anoxic biological oxidation; (iv) coagulation; (v) photo-Fenton (PF) reaction mediated by UVA radiation (PF-UVA); and (vi) aerobic biological oxidation. However, despite the promising results, it was found that to attain an effluent in compliance with the legal requirements for the discharge into water bodies, the PF-UVA process should have been performed for more than 24 h, which is an unrealistic treatment time. On the other hand, the running of the PF-UVA process for ca. 4 hours provided a treated leachate able to be released into the sewerage system. Moreover, even though their superiority, the application of electrochemical processes, such as anodic oxidation or photoelectro-Fenton oxidation, in substitution of the PF-UVA reaction, has demonstrated to be unfeasible, mostly due to operational constraints related to the release of chlorine gas into the environment and generation of high amounts of foam, or the pore-clogging at the cathode surface.

In turn, ozone (O_3)-based processes have become increasingly attractive with regard to the pre- or post-treatment of MSWL leachates [1-7], owing to the: (i) high oxidative power of the molecular O_3; (ii) particularly high effectiveness in colour removal; (iii) high reactivity and selectivity towards organic compounds containing electron-rich moieties; (iv) high efficiency under alkaline conditions (in contrast to the PF reaction), as the generation of the highly-reactive and non-selective hydroxyl radicals ($HO^{\bullet}$) is favoured; and (v) possible combination with hydrogen peroxide (H_2O_2) and/or UVC radiation, which also induce the production of $HO^{\bullet}$.

Accordingly, this chapter is mainly focused on the integration of ozonation and O_3-based AOPs (O_3/H_2O_2, O_3/UVC and O_3/H_2O_2/UVC) in the multistage treatment system aforementioned for the de-pollution of the HISWL leachate. Firstly, a detailed physicochemical characterization was performed to define the preliminary sequence of the integrated treatment strategy. The influence of inlet O_3 dosage on the ozonation and O_3/H_2O_2 processes was further assessed, using HISWL leachate after sulphur compounds removal, followed by the evaluation of the addition of UVC radiation to those systems, under the more appropriate conditions. Afterward, the impact of an upstream coagulation process (with ferric or aluminium salts) on the ozonation (O_3/Fe^{2+} or O_3/Al^{3+}) and O_3/H_2O_2/UVC (O_3/PF) systems was also addressed. Moreover, the biodegradability enhancement along the best process, and under the best conditions, was determined by means of a Zahn-Wellens test. Finally, the heterogeneous character of the dissolved organic matter [8] of the

HISWL leachate along the different treatment steps was also explored by means of emerging technics, namely fluorescence excitation-emission matrix (3D-EEM) and size-exclusion chromatography coupled with organic carbon detection (SEC-OCD).

5.2 Material and methods

All the chemicals, experimental units and procedures, analytical determinations and modeling of removal kinetics used within this chapter are described in Chapter 2.

The leachate was collected from the same HISWL as the leachate used in Chapters 3 and 4 but at a different time. It was collected in May 2018 from the non-aerated stabilization lagoon and stored at 4 °C until use. The main physicochemical characteristics of the raw leachate used in this work are displayed in Table 5.1.

5.3 Results and discussion

5.3.1 Considerations on the raw and desulphurised HISWL leachate

The raw HISWL leachate used in the current work exhibited the following major features (see Table 5.1): (i) light brown colour, apparently related to a low humic substances content; (ii) very strong odour, closely associated with the presence of hydrogen sulphide (total dissolved free sulphides concentration of 0.45 g L^{-1}) and volatile organic compounds (as discussed in Chapter 3); (iii) high alkalinity (2.4 g $CaCO_3$ L^{-1}), mainly in the form of bicarbonates (ca. 98%), as pH is very close to 8.3; (iv) high chloride ions content (14.5 g L^{-1}); (v) moderate organic matter content (DOC of 1.0 g L^{-1} and COD of 2.8 g O_2 L^{-1}); (vi) low biodegradability (biodegradation percentage of 12% and BOD_5/COD ratio of 0.13); (vii) moderate-to-low level of total nitrogen (0.26 g N L^{-1}), predominantly under the form of ammonium (85%); (viii) high content of inorganic sulphur compounds (concentration of sulphates, sulphites, and sulphides equal to 4.9 g SO_4^{2-} L^{-1}, 2.6 g SO_3^{2-} L^{-1}, and 0.5 g HS^- L^{-1}); (ix) moderate amount of suspended solids (TSS of 131 mg L^{-1}); and (x) low content of heavy metals (< 2.2 mg L^{-1}).

Table 5.1 Physicochemical characteristics of the HISWL leachate throughout the various stages of the best treatment strategy.

Parameter (unit)	Raw Leachate	After CO[a]	After CP[b]	After O_3/H_2O_2[c]	After BO[d]	EVL[e]	MCV[f]
Colour	Light brown	Light brown	Light *y*ellow	n.d.	n.d.		
Colour (diluted 1:20)	d.	d.	d.	n.d.	n.d.	n.d. (dil. 1:20) or n.c.	n.c.
Colour (Pt-Co units)	760	760	500	<15[g]	<15[g]		
Odour	Very strong	Strong	Low	n.d.	n.d.		
Odour (diluted 1:20)	d.	d.	d.	n.d.	n.d.	n.d. (dil. 1:20) or n.c.	n.c.
pH	8.4	8.6	8.9	8.1	7.0	6.0–9.0 or n.c.	5.5-9.5
Alkalinity (mg $CaCO_3$ L^{-1})	2427	2139	1921	1664	1016		
Turbidity (NTU)	29	22	19	1.2	1.5		
Total suspended solids – TSS (mg L^{-1})	157	n.m.	131	n.m.	31	60 or 35	1000
Total volatile solids – VSS (mg L^{-1})	87	n.m.	68	n.m.	13		
Total dissolved carbon – TDC (mg L^{-1})	1548	1214	1085	768	508		
Dissolved inorganic carbon – DIC (mg L^{-1})	582	508	448	405	304		
Dissolved organic carbon – DOC (mg L^{-1})	966	706	637	363	276		
Chemical oxygen demand – COD (mg O_2 L^{-1})	2809	2127	1970	980	708	150 or 125	1000
COD/DOC	2.9	3.0	3.1	2.7	2.6		
5-day biochemical oxygen demand – BOD_5 (mg O_2 L^{-1})	360	250	250	n.m.	n.m.	40 or 25	500
BOD_5/COD	0.13	0.12	0.13	n.m.	n.m.		
Biodegradability - Zhan-Wellens test (%)	12	n.m.	11	24	n.m.		
Absorbance at 254 nm (AU) (diluted 1:50)	0.75	0.72	0.54	0.011	0.013		
$SUVA_{254}$ (L mg^{-1} m^{-1})	3.88	5.12	4.26	0.15	0.24		
Total nitrogen – N_T (mg L^{-1})	260	n.m.	165	105	80	15 or 10	90
Ammonium – N-NH_4^+ (mg L^{-1})	220	n.m.	140	75	50	7.8 or n.c.	77
Nitrate – N-NO_3^- (mg L^{-1})	20	n.m.	13	15	10	11 or n.c.	11
Nitrite – N-NO_2^- (mg L^{-1})	<0.05[g]	n.m.	<0.05[g]	<0.05[g]	<0.05[g]		
Sulphate – SO_4^{2-} (mg L^{-1})	4943	6404	548	558	565	2000 or n.c.	1000
Sulphite – SO_3^{2-} (mg L^{-1})	2575	<1.0[g]	<1.0[g]	<1.0[g]	<1.0[g]	1.0 or n.c.	n.c.
Sulphide – S^{2-} (mg L^{-1})	450	<0.1[g]	<0.1[g]	<0.1[g]	<0.1[g]	1.0 or n.c.	1.0
Chloride – Cl^- (g L^{-1})	14.5	13.8	19.7	19.3	19.0		
Total phosphorous - P_T (mg L^{-1})	2.25	n.m.	n.m.	n.m.	0.85	10 or 1.0	20

Parameter (unit)	Raw Leachate	After CO[a]	After CP[b]	After O_3/H_2O_2[c]	After BO[d]	EVL[e]	MCV[f]
Total aluminium - Al (mg L^{-1})	< 5.0[g]	n.m.	n.m.	n.m.	n.m.	10 or n.c.	10
Total barium - Ba (mg L^{-1})	< 0.61[g]	n.m.	n.m.	n.m.	n.m.		
Total cadmium - Cd (mg L^{-1})	< 0.05[g]	n.m.	n.m.	n.m.	n.m.	0.2 or n.c.	n.c.
Total copper - Cu (mg L^{-1})	0.14	n.m.	n.m.	n.m.	n.m.	1.0 or n.c.	1.0
Total iron - Fe (mg L^{-1})	1.26	n.m.	n.m.	n.m.	n.m.	2.0 or n.c.	2.5
Total lead - Pb (mg L^{-1})	< 0.21[g]	n.m.	n.m.	n.m.	n.m.	1.0 or n.c.	1.0
Total manganese - Mn (mg L^{-1})	0.17	n.m.	n.m.	n.m.	n.m.		
Total nickel - Ni (mg L^{-1})	< 0.15[g]	n.m.	n.m.	n.m.	n.m.		
Total zinc - Zn (mg L^{-1})	0.23	n.m.	n.m.	n.m.	n.m.	2.0 or n.c.	5.0

d. – detected; n.d. – not detected; n.c. – not covered; n.m. – not measured; dil. – diluted;

[a] Using the raw HISWL leachate. Catalytic oxidation (CO) conditions: room temperature; natural pH; stirring time of 5 min; $[H_2O_2]:[S^{2-}]$ molar ratio = 4:1; $[H_2O_2]:[SO_3^{2-}]$ molar ratio = 1:1, subsequent sedimentation overnight and removal chemical sludge;

[b] Using the HISWL leachate after CO. Chemical precipitation (CP) conditions: room temperature; natural pH; stirring time of 30 min; $[Ba^{2+}]:[SO4^{2-}]$ molar ratio of 1:1; subsequent sedimentation overnight and removal barite precipitate;

[c] Using the HISWL leachate after sequential CO and CP. Perozonation process (O_3/H_2O_2) conditions: room temperature; natural pH; OD_{inlet} of 40 mg O_3 L^{-1}; $[H_2O_2]$ = 200-500 mg L^{-1}; contacting time of 3 h; subsequent sedimentation for 3 h and removal of O_3/H_2O_2 sludge (when required);

[d] Using the HISWL leachate after sequential CO, CP and O_3/H_2O_2 process. Biological oxidation (BO) conditions: 28 days Zhan-Wellens test, subsequent sedimentation for 2 h and removal of the biological treatment sludge;

[e] ELV - Emission limit value for discharge into water bodies according to Decree-Law 236/98 (Portuguese legislation) or Directive 91/271/CEE (European legislation);

[f] MCV - Maximum concentration values for the rejection of industrial wastewater into the municipal sewage system of the Vila Nova de Gaia municipality (Regulation no. 143/2018 published in Diário da República no. 46/2018, series II of 2018-03-06);

[g] Limit of detection.

Despite being collected from the same HISWL, the raw leachate used in the current work presented a higher quality when compared to the one that was used in Chapters 3 and 4, especially at the level of the: (i) colour, being about 63% clearer; (ii) alkalinity, which was 57% inferior; (iii) organic matter content, as the DOC and COD was 58% and 60% lower, respectively; (iv) nitrogen amount, being total and ammonium nitrogen 52% and 33% minor, respectively; and (v) sulphates, whose concentration was 61% lesser. Notwithstanding, taking into account the raw HISWL leachate characteristics and emission limit values [11] imposed by the Decree-Law no. 236/98 or European Directive no. 91/271/CEE, it can be concluded that the treatment strategy has to include the removal of: (i) sulphur compounds (with sulphates, sulphites and sulphides concentrations 2.5-, 2575- and 450-fold higher than ELV, respectively); (ii) organic matter (with COD and BOD_5 values 19- or 22- and 9- or 14- fold higher than ELV, respectively), accompanied by colour, odour and suspended solids impairment; and (iii) nitrogen substances (with total and ammonium nitrogen concentrations 17- or 26- and 28-fold higher than ELV, respectively). Therefore, an effluent in compliance with the current legislation could only be achieved by combining conventional chemical (to sulphur compounds and/or colloidal particles) and biological (to nitrogen and biodegradable organic matter) processes with AOPs (to recalcitrant organics), as already demonstrated for both industrial and urban landfill leachates [8, 12-15].

The elimination of the high sulphur compounds amount from the leachate is crucial prior to subject it to a subsequent O_3-based or biological oxidation stage, in order to minimize the O_3 consumption [16, 17] or bacteria inhibition/inactivation [18, 19], respectively. So, analogous to what was previously done, the first two steps of the treatment train for this HISWL leachate were: (i) CO, to convert more than 99.9% of sulphites and sulphides into oxidised sulphur species (see Table 5.1), with partial formation of sulphate (c.a. 33% of the reduced sulphur species was oxidised into sulphate), using the stoichiometric amount of H_2O_2 (considering full oxidation into sulphates [20, 21]) and the leachate transition metals themselves as catalysts at natural pH; and (ii) CP, to remove more than 90% of sulphates (see Table 5.1) under the form of barite mineral, with potential commercial value, using the stoichiometric amount of barium salt at natural pH. However, it is worth to mention that, conversely to what was formerly reported, this time, after the CO process: (i) a milky-white precipitate was generated, along with a 12% alkalinity reduction (see Table 5.1), suggesting the formation of carbonate/calcium salts; and (ii) a 27% DOC decreased was noticed (see Table 5.1), suggesting that a fraction of the dissolved organic compounds could have been (i) arrested by the precipitate and/or (ii)

volatilised, as larger leachate volumes have been handled. Moreover, another major difference was spotted regarding leachate biodegradability, which was not increased after the sequential CO and CP processes (see Table 5.1), making the application of a biological oxidation downstream unfeasible. Such behaviour was most probably related to the differences observed in the raw leachate physicochemical characteristics. Overall, at the end of the 2-step approach, the desulphurised HISWL leachate presented concentrations of sulphate, sulphite, and sulphide ions below 600, 1.0, and 0.1 mg L^{-1}, thus fulfilling the Portuguese legal requirements, and low biodegradability. Accordingly, the next treatment step went through an O_3-based process, with the potential incorporation of a conventional coagulation process upstream.

5.3.2 Ozonation and O_3-driven processes

Regardless of the variable in study, all O_3-based reactions followed a pseudo-first-order kinetic model (determination coefficient (R^2) > 0.98 and residual variance (S^2_R) < 3.6×10^{-4} mg^2 L^{-2}) in terms of DOC degradation. On the other side, the amount of DOC removed as a function of the oxidant consumed, either O_3 or H_2O_2, was always fitted to a pseudo-zero-order kinetic model (R^2 > 0.99). All the correspondent kinetic constants are displayed in the Table 5.2.

5.3.2.1 Effect of the inlet O_3 dose

O_3 dose is a key issue when economic viability is envisioned, mainly dealing with the treatment of high-polluted industrial wastewater. With this priority in mind, the experiments were started by changing the inlet O_3 dose (OD_{inlet}), which was achieved through the manipulation of the gas flow rate (Q_{gas}) and the inlet O_3 gas concentration ($[O_3]_{in}$). Figure 5.1 and Table 5.2 show that the increase of the OD_{inlet} from 20 to 30 mg min^{-1} in ozonation process, by keeping Q_{gas} in 0.15 L min^{-1} and rising $[O_3]_{in}$ from 134 to 200 mg O_3 L^{-1}, led to a DOC degradation rate 1.5-fold higher (Figure 5.1c), which was directly proportional to the available O_3 content, resulting in 10% more DOC removed after 3-h reaction. Moreover, in both reactions (i) very low O_3 concentrations were detected in the off-gas stream, being the O_3 utilization ratios equal to 0.96 (Figure 5.1a: inset), and (ii) a similar O_3 specific consumption was found (Figure 5.1e), being the amount of DOC removed per gram of O_3 transferred about 55±4-56±4 mg C g^{-1} O_3. These results are consistent with the work reported by Moslemi et al. [22], where it was reported that the dissolved O_3 concentration was proportional to the inlet O_3 gas concentration when the gas flow rate was kept constant.

Table 5.2 Operating conditions and kinetic parameters in terms of DOC degradation for each O_3-driven reaction.

#	Experiment[a]	OD_{inlet} (mg O_3 min^{-1})	TOD[b] (g O_3 L^{-1})	H_2O_2[b] (g L^{-1})	$DOC_{rem.}$[b] (%)	Kinetics (Time)			Kinetics (TOD)		Kinetics (H_2O_2)	
						k[c] ($\times10^{-3}$ min^{-1})	R^2	S^2_R (mg^2 L^{-2})	k_{TOD}[d] (mg C g O_3^{-1})	R^2	$k_{H_2O_2}$[d] (mg C g $H_2O_2^{-1}$)	R^2
Effect of the inlet O_3 dose (Figure 5.1)												
1.1	Ozonation_20 mg O_3 min^{-1}	20	2.42	-	19.7	1.3±0.1	0.990	5.30×10^{-5}	55±4	0.994	-	-
1.2	Ozonation _30 mg O_3 min^{-1}	30	3.61	-	29.6	2.0±0.1	0.995	5.79×10^{-5}	56±4	0.997	-	-
1.3	Ozonation _40 mg O_3 min^{-1}	40	4.38	-	34.5	2.3±0.2	0.992	1.16×10^{-4}	52±3	0.996	-	-
1.4	Ozonation _50 mg O_3 min^{-1}	50	5.06	-	31.7	2.1±0.1	0.996	4.95×10^{-5}	40±2	0.998	-	-
Effect of the H_2O_2 addition (Figure 5.1)												
2.1	$O_3/H_2O_{2(SD)}$_30 mg O_3 min^{-1}	30	3.76	1.42	34.1	2.3±0.2	0.991	1.39×10^{-4}	57±3	0.996	127±8	0.996
2.2	O_3/H_2O_2_30 mg O_3 min^{-1}	30	3.72	1.26	36.9	2.4±0.2	0.987	2.27×10^{-4}	64±4	0.997	182±9	0.997
2.3	O_3/H_2O_2_40 mg O_3 min^{-1}	40	4.97	1.71	43.0	3.0±0.1	0.997	6.22×10^{-5}	57±3	0.995	(17±2)×10	0.989
2.4	O_3/H_2O_2_50 mg O_3 min^{-1}	50	6.24	1.82	45.2	3.1±0.3	0.987	3.51×10^{-4}	47±3	0.998	(17±1)×10	0.995
Effect of the UVC irradiation exposure (Figure 5.2)												
1.2	Ozonation	30	3.61	-	29.6	2.0±0.1	0.995	5.79×10^{-5}	56±3	0.997	-	-
2.2	O_3/H_2O_2	30	3.72	1.26	36.9	2.4±0.2	0.987	2.27×10^{-4}	64±4	0.997	182±9	0.997
3.1	O_3/UVC	30	3.58	-	30.7	2.0±0.1	0.994	6.77×10^{-5}	56±2	0.996	-	-
3.2	O_3/H_2O_2/UVC	30	3.71	1.62	37.9	2.5±0.2	0.984	3.04×10^{-4}	66±2	0.997	149±8	0.997
3.3	H_2O_2/UVC	-	-	0.32	-	-	-	-	-	-	-	-
Effect of the HISWL leachate pre-treatment (Figure 5.3)												
1.2	Ozonation	30	3.61	-	29.6	2.0±0.1	0.995	5.79×10^{-5}	56±3	0.997	-	-
3.2	O_3/H_2O_2/UVC	30	3.71	1.62	37.9	2.5±0.2	0.984	3.04×10^{-4}	66±2	0.997	149±8	0.997
4.1	Al-Coag./ozonation	30	2.94	-	16.6	1.02±0.06	0.991	3.07×10^{-5}	27±3	0.997	-	-
4.2	Fe-Coag./ozonation	30	2.51	-	16.2	1.01±0.04	0.996	1.26×10^{-5}	31±3	0.996	-	-
4.3	Fe-Coag./O_3/H_2O_2/UVC	30	3.70	1.71	23.9	1.5±0.1	0.993	5.55×10^{-5}	33±2	0.998	74±4	0.996
4.4	Fe-Coag./H_2O_2/UVC	-	-	1.01	14.1	0.61±0.04	0.991	1.19×10^{-5}	-	-	50±3	0.996

[a] All experiments were performed for 3 h, at room temperature and without pH correction. Initial pH was 8.9, except for trials #4.1 and #4.2-"4.4 that was 4.8 and 2.7, respectively. Initial DOC was 637±24 mg L^{-1}, except for trials #4.1-#4.4 that was 499±6 mg L^{-1}. In trials #3.1-#3.3 and #4.3-#4.4, an 11 W UVC lamp was used. During the trials #2.3-#2.4, #3.2-#3.3 and #4.3-#4.4, H_2O_2 several doses were periodically added to keep its concentration in the range 0.2-0.5 g L^{-1}. In trial #2.1, H_2O_2 was added as a single dose (SD) of 1.5 g L^{-1};

[b] TOD, H_2O_2, and $DOC_{rem.}$ are the total (i) transferred O_3 dose, (ii) consumed H_2O_2 content, and (iii) removed DOC percentage, after 3-h reaction;

[c] Pseudo-first-order kinetic constant (k) for DOC degradation, determined though nonlinear regression method by minimizing the sum of the squared deviations between the experimental and the predicted values. The goodness of fitting was evaluated by the coefficient of determination (R^2) and residual variance (S^2_R);

[d] DOC degradation reaction rates expressed in terms of O_3 transferred and H_2O_2 consumed.

The enhancement in the O_3 dissolution as a result of higher inlet O_3 concentrations was attributed to the O_3 deficit term of the mass transfer rate since, over the range studied, the O_3 mass transfer coefficient was not considerably affected.

On the other hand, for inlet dosages above 30 mg O_3 min^{-1}, established by lowering the $[O_3]_{in}$ to ca. 168 mg O_3 L^{-1} and rising the Q_{gas} to 0.24 and 0.30 L min^{-1} (correspondent to 40 and 50 mg O_3 min^{-1}, respectively), it was verified that, there was: (i) no significant improvement in the DOC removal rate (with a confidence level of 95%), obtaining pseudo-first-order kinetic constants around 2.3±0.2 and 2.1±0.1 min^{-1} (Figure 5.1a,c); (ii) a considerably increase in the unused O_3 concentration (Figure 5.1: inset), which led to O_3 utilization ratios of 0.88 and 0.81, for OD_{inlet} of 40 and 50 mg O_3 min^{-1}, respectively; and (iii) a decreasing in the O_3 consumption efficiency from 52±3 to 40±2 mg C g^{-1} O_3, when the OD_{inlet} was raised from 40 to 50 mg O_3 min^{-1} (Figure 5.1e). This behaviour may be closely related to O_3 mass transfer limitations [23]. Under fixed conditions of contaminants load and inlet O_3 concentration, when the Q_{gas} is increased the O_3 dosage in the same period of time is also increased, which boosts the ozonation process, until a certain point. Nevertheless, when the O_3 consumed by the ozonation reactions is exceeded by the O_3 input rate, the DOC removal efficiencies became independent of the Q_{gas}, since the rate-limiting-step, i.e. the O_3 mass transfer, is turned into a kinetically controlled regime [23]. Besides, as the Q_{gas} rises O_3 losses also rise, suggesting that, for this reactional system, the use of lower inlet gas flow rates could be more suitable [22].

It is well established that, in an aqueous solution, O_3 reacts with organic and inorganic subtracts according to two kinetic regimes [24-26]: (i) direct reaction of molecular O_3 (redox potential (E^o) of 2.08 V/SHE), mainly under acidic conditions (pH < 4), with high selectivity for unsaturated electron-rich bonds of specific functional groups, such as aromatics, amines, and olefins, but relatively slow; and (ii) indirect reaction of secondary oxidisers generated by O_3 decomposition via Eqs. 1.27-1.40, such as the H_2O_2 and, most important, the powerful and non-selective hydroxyl radicals ($HO^{\bullet}$) (E^o of 2.73 V/SHE), which are rapidly and preferentially yielded at alkaline conditions (pH > 9).

Considering that all the single ozonation reactions (Figure 5.1a) have occurred under a slightly alkaline environment, following a similar descending pH profile (data not shown) with start at pH 8.9 (average) and end at pH 7.6 (average), it can be concluded that both direct and indirect pathways had contributed for the organic matter degradation. This slight deviation of less than 1.5 pH units can be ascribed to the buffering capacity of leachate intrinsic bicarbonates. It should also be noted

that, while the DOC removals varied from 20% to 35%, after a 3-h reaction, the degradation of aromatic compounds, estimated through the specific ultraviolet absorbance (SUVA) at 254 nm (data not shown), was substantially higher (around 72-95%), reaching to SUVA values between 1.5 and 0.2 L mg^{-1} m^{-1} (from 20 to 50 mg O_3 L^{-1}), right after 1-h reaction. These results endorse the fact that molecular O_3 and/or reactive by-products resulting from its decomposition has the ability to promptly attack aromatic compounds and unsaturated carbon bonds, promoting the decrement of the aromatic character of the dissolved organic matter, conducting to the formation of side products that are harder to mineralize, such as the carboxylic acids and aldehydes [4]. Higher mineralization degrees could have been attained if longer contacting times were applied.

5.3.2.2 Effect of the H_2O_2 addition

As aforementioned, O_3 alone has been found to achieve limited mineralization kinetics (see Table 5.2), with very close DOC degradation profiles when OD_{inlet} is augmented to values among 30 and 50 mg O_3 min^{-1}. Since it was not possible to significantly improve the ozonation efficiency by the increase of O_3 dosage, a strategy to optimize the ozonation overall process might involve boosting the indirect reaction mechanism, either by raising the pH (O_3/HO^-) or by adding H_2O_2 (O_3/H_2O_2) [7]. These two O_3-based AOPs have the ability to propitiate the generation of the highly reactive $HO^{\bullet}$, as a result of O_3 decomposition (Eqs. 1.27-1.40), which is enhanced by a sequence of radical type reactions initiated by HO^- or H_2O_2, according to the following routes [7, 27, 28]: (i) reaction of O_3 with HO^- to produce superoxide anions radicals ($O_2^{\bullet -}$), which undergo a series of reactions that leads to $HO^{\bullet}$, presenting a yield of 1 mol $HO^{\bullet}$ per 1.5 mol of O_3; and (ii) partial dissociation of H_2O_2 into hydroperoxide ion (HO_2^-), its conjugated base (pKa = 11.8), which quickly react with O_3 to initiate a radical chain mechanism that guides to $HO^{\bullet}$, rendering a yield of 1 mol $HO^{\bullet}$ per 1 mol of O_3. Besides the lower yield of the first approach, the increase in pH could hinder the ozonation reaction by the increase of the carbonates fraction, which are stronger $HO^{\bullet}$ scavengers than bicarbonates [7, 28]. Beyond that, as regards the second approach, in addition to being an initiator, H_2O_2 is also a promoter, or chain carrier, of the O_3 decomposition, thus maximizing the production of $HO^{\bullet}$ [28]. Taking all the above into concern, it was decided upon to follow the assays through the second approach, and perozonation (O_3/H_2O_2) process was appraised for inlet O_3 dosages of 30, 40 and 50 mg O_3 min^{-1}.

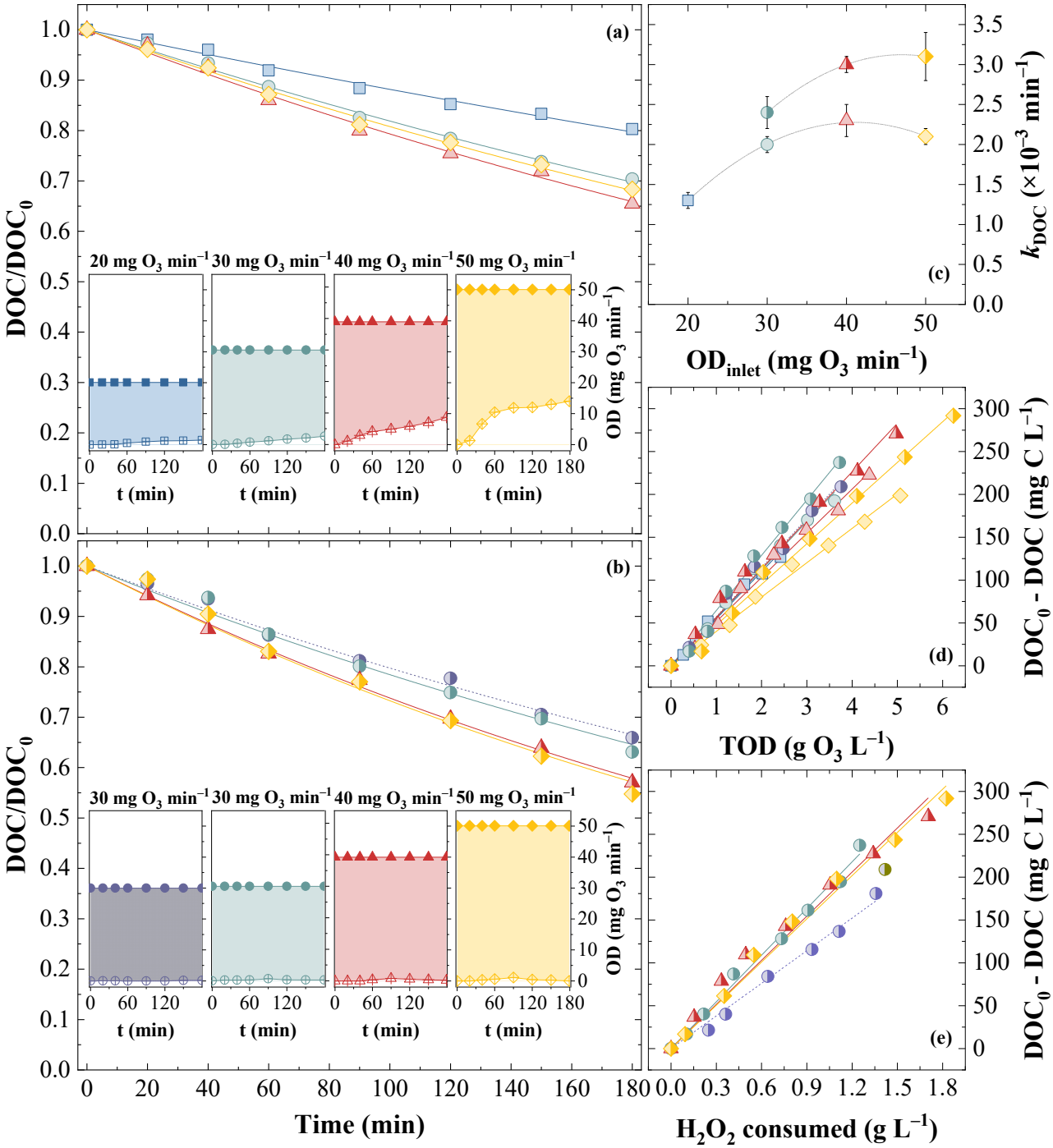

Figure 5.1 Evolution of the: (a, b) normalized DOC reduction (symbols) over time, along with the respective pseudo-first-order fitting curves (lines); (c) kinetic constants for each inlet O_3 dose (OD_{inlet}) tested; and total DOC removed as a function of the (d) transferred O_3 dose (TOD) and (e) H_2O_2 consumed; during the ozonation process (a; filled symbols) and the O_3/H_2O_2 process (b; semi-filled symbols), using different OD_{inlet}: 20 (□), 30 (○,◑,◑), 40 (△,◭), and 50 (◇,◈) mg O_3 min^{-1}. Inset: Representation of the inlet (solid symbols) and outlet (crossed symbols) O_3 dose over time, where the shaded areas correspond to the total amount of O_3 available for the reaction. Experimental conditions: $[DOC]_0$ = 637±24 mg L^{-1}; V = 1.5 L; room temperature; pH_0 = 8.9±0.2; $[H_2O_2]$ = 200–500 mg L^{-1} (periodic addition) (solid line) or $[H_2O_2]$ = 1500 mg L^{-1} (single addition) (dotted line and patterned area) – except when indicated.

In order to understand the influence of the H_2O_2 dosing method, two experiments using an OD_{inlet} of 30 mg O_3 min^{-1} were initially performed, in which the H_2O_2 was fed to the system: (i) periodically, by adding the required volumes to maintain its content amongst 200 and 500 mg L^{-1} throughout the 3-h reaction, and (ii) as a single dose right at the reaction beginning, by adding the total volume that was added in the periodic mode. The only noteworthy differences observed between these two experiments were at the level of the H_2O_2 consumption and availability. When the single dose method was used, the amount of DOC removed per gram of H_2O_2 consumed was lowered from 182±9 to 127±8 mg C g^{-1} H_2O_2, and H_2O_2 was depleted between the 150- and 180-min of reaction. This behaviour suggests that H_2O_2 was being used in parasitic reactions. Therefore, in the view of an H_2O_2 saving, periodic addition mode was chosen to pursue the trials.

As can be seen from Figure 5.1a-c and Table 5.2, the addition of H_2O_2 was effectively able to provide faster DOC decays than ozonation as the O_3 content fed to the system increased, due to the extra amount of $HO^{\bullet}$ available to react with the organic matter, indicating that the indirect kinetic regime was indeed boosted. In fact, the integration of O_3 with H_2O_2 has led to a synergy (Syn.) of 20±2%, 30±3%, and 48±6% for OD_{inlet} of 30, 40, and 50 mg O_3 min^{-1}, respectively, which was estimated considering the pseudo-first-order kinetic constants for each OD_{inlet} condition, in the presence and absence of H_2O_2 (Syn. (%) = (k_{O_3/H_2O_2}/(k_{O_3}+$k_{H_2O_2}$)-1)×100), and that the H_2O_2 alone has been responsible for null DOC removal (data not shown). Likewise, the efficiency in terms of O_3 consumption was also improved when H_2O_2 was supplied (see Figure 5.1b: inlet), being detected, at maximum, O_3 concentrations of 4 mg O_3 L^{-1} in the off-gas stream, while during the single ozonation trials, the outlet O_3 content has reached to values of one order of magnitude higher. Accordingly, the total amount of O_3 transferred over the 3-h reaction was also higher when H_2O_2 was added, fundamentally for OD_{inlet} of 40 and 50 mg O_3 min^{-1}. Overall, the O_3/H_2O_2 process has allowed achieving O_3 utilization ratios above 0.99 regardless of the amount of O_3 introduced into the reaction medium, together with an enhancement of the specific relation between the carbon removed and O_3 transferred by about 10-18% (Figure 5.1d and Table 5.2). Moreover, despite presenting similar profiles, pH dropping was slightly slower (on average, the pH decayed from 9.0 to 8.0 after a 3-h reaction) when H_2O_2 was added, indicating that the organics oxidation reactions happened preferentially by the $HO^{\bullet}$ attack and molecular O_3 reactions were, to some extent, impaired.

Regarding the O_3/H_2O_2 process alone, it was noted that, keeping H_2O_2 continuously available within a concentration range of 200-500 mg L^{-1}: (i) the H_2O_2 specific consumption was not

statistically different regardless of the OD_{inlet} applied, being the quantity of DOC depleted per gram of H_2O_2 consumed in average (17±2)×10 mg C g^{-1} H_2O_2 (see Figure 5.1e and Table 5.2); (ii) the DOC degradation rate was increased about 25% as the OD_{inlet} was increased from 30 to 40 mg O_3 min^{-1}, with a consistent $[H_2O_2]$:$[O_3]$ molar ratio of 0.47:1 (total amount of the H_2O_2 consumed over O_3 transferred during the 3-h reaction), which is very close to optimum molar ratio for peroxone process reported elsewhere ($[H_2O_2]$:$[O_3]$ molar ratio of 0.5:1) [29]; and (iii) the mineralization kinetics were not affected by the increment of the OD_{inlet} from 40 to 50 mg O_3 min^{-1} and the decrement of the $[H_2O_2]$:$[O_3]$ molar ratio from 0.47:1 to 0.41:1 (Figure 5.1b,c). These results, along with the low dissolved O_3 concentrations detected (data not shown), suggest that for OD_{inlet} above 40 mg O_3 min^{-1}, $HO^{\bullet}$ generation is quenching by the O_3 in excess, possibly by the occurrence of parallel side reactions not conducting to $HO^{\bullet}$ production [30, 31]. Despite the OD_{inlet} of 40 mg O_3 min^{-1} has provided the best performance regarding the O_3/H_2O_2 process, an OD_{inlet} of 30 mg O_3 min^{-1} was selected to evaluate de remaining experimental conditions since showed the most efficient results in the single ozonation. Besides that, under this dosage, virtual no O_3 was detected in the off-gas stream and similar TOD values were obtained in spite of the H_2O_2 attendance or not.

5.3.2.3 Effect of the UVC irradiation

Another approach to potentially improve the O_3 oxidizing power is its combination with UVC radiation. In aqueous solution, the introduction of UVC photons can induce the photolysis of O_3 into H_2O_2, according to Eq. 1.41. In sequence, the newly-generated H_2O_2 can also undergo photolysis (Eq. 1.6), which gives rise to the direct production of additional $HO^{\bullet}$, and/or, under alkaline conditions, dissociate into HO_2^-, which in turn reacts with O_3, thus initiating the radical chain mechanism by electron transfer, which can also result in the generation of free $HO^{\bullet}$ [24].

With the prospect to achieve higher synergy levels, two photo-assisted reactions were carried out, applying an OD_{inlet} of 30 mg O_3 min^{-1} at natural pH: (i) UVC-driven ozonation (O_3/UVC); and (ii) UVC-driven perozonation (O_3/H_2O_2/UVC). Furthermore, a UVC/H_2O_2 blank experiment was also performed, leading to null DOC decay along with a low H_2O_2 consumption (~0.32 g L^{-1}) within a 3-h interval (Figure 5.2 and Table 5.2). These results suggest that neither the organic matrix was susceptible to direct photolysis nor the photolytic cleavage of H_2O_2 into two $HO^{\bullet}$ occurred in a significant way, most probably due to the low UV transmissibility of the leachate and the presence of light-absorbing species acting as inner-filters. Notwithstanding, although in very low extent, the H_2O_2 consumption could potentially be attributed to the: (i) homolytic cleavage of the peroxide bond (–O–O–) to form $HO^{\bullet}$ (Eq. 1.6); (ii) reaction of H_2O_2 with its conjugated base (Eq. 5.1) [32], with no production of $HO^{\bullet}$; (iii) quenching of

$HO^{\bullet}$ by reaction with H_2O_2 (Eq. 1.39), k = (2.7±0.3) × 10^7 L mol^{-1} s^{-1}) and/or HO_2^- (Eq. 1.40), k = (7.5±1.9) × 10^9 L mol^{-1} s^{-1}) [33]; and (iv) self-decomposition of H_2O_2 (Eq. 5.2), preferentially under alkaline conditions [34].

$$HO_2^- + H_2O_2 \rightarrow H_2O + O_2 + OH^- \quad 5.1$$

$$2H_2O_2 \rightarrow 2H_2O + O_2 \quad 5.2$$

Contrary to the expected, the addition of UVC radiation was not able to enhance the efficiency of O_3 and O_3/H_2O_2 processes. Figure 5.2a and Table 5.2 reveal that the kinetic constants regarding DOC degradation were not statistically different (with a confidence level of 95%) for O_3 and O_3/UVC processes and for O_3/H_2O_2 and O_3/H_2O_2/UVC processes. The same trend was found as regards the pH profile (data not shown) and the amount of DOC removed as a function of TOD (see Figure 5.2c and Table 5.2), with virtually no unused O_3 for all trials (data not shown), being reached O_3 utilization ratios among 0.96 and 0.99.

The major dissimilarity was spotted concerning the H_2O_2-assisted reactions, where it was found an H_2O_2 consumption for O_3/H_2O_2/UVC process about 29% higher than for O_3/H_2O_2 process (see Figure 5.2b and Table 5.2), which is the equivalent to a difference of 0.36 g H_2O_2 L^{-1}. Such outcomes are in good agreement with the H_2O_2/UVC blank trial, where a H_2O_2 consumption of 0.32 g L^{-1} was noticed along with no mineralization, suggesting the occurrence of H_2O_2 consuming parasitic reactions. Therefore, the failure of the UVC light to boost the O_3 and O_3/H_2O_2 processes can potentially be ascribed to the low leachate UV-transmittance and the presence of some chromophore groups which strongly absorbed the UVC photons, thus blocking the generation of additional $HO^{\bullet}$ [24].

Accordingly, taking all these results into consideration, the different O_3-driven processes applied to the desulphurised HISWL leachate (using an OD_{inlet} of 30 mg O_3 min^{-1}) may be ordered from the least to the most efficient, in terms of mineralization kinetic constants, as follows: ozonation (2.0±0.1 × 10^{-3} min^{-1}) ≈ O_3/UVC (2.0±0.1 × 10^{-3} min^{-1}) < O_3/H_2O_2 (2.4±0.2 × 10^{-3} min^{-1}) ≈ O_3/H_2O_2/UVC (2.5±0.2 × 10^{-3} min^{-1}).

5.3.2.4 Effect of the HISWL leachate pre-treatment

The last endeavour to upgrade ozonation and O_3-based processes passed through the application of an upstream coagulation process. With this pre-treatment, it is envisioned the removal of part of the DOM and total suspended solids, thus increasing the transmissibility of the HISWL leachate. On the one hand,

light absorption by photoactive species is enhanced, which is of utmost importance when photo-driven reactions are intended. On the other hand, undesired competitive O_3 reactions with particulate matter are avoided, which have shown themselves to be as sharp as the ones with highly reactive DOM moieties [35].

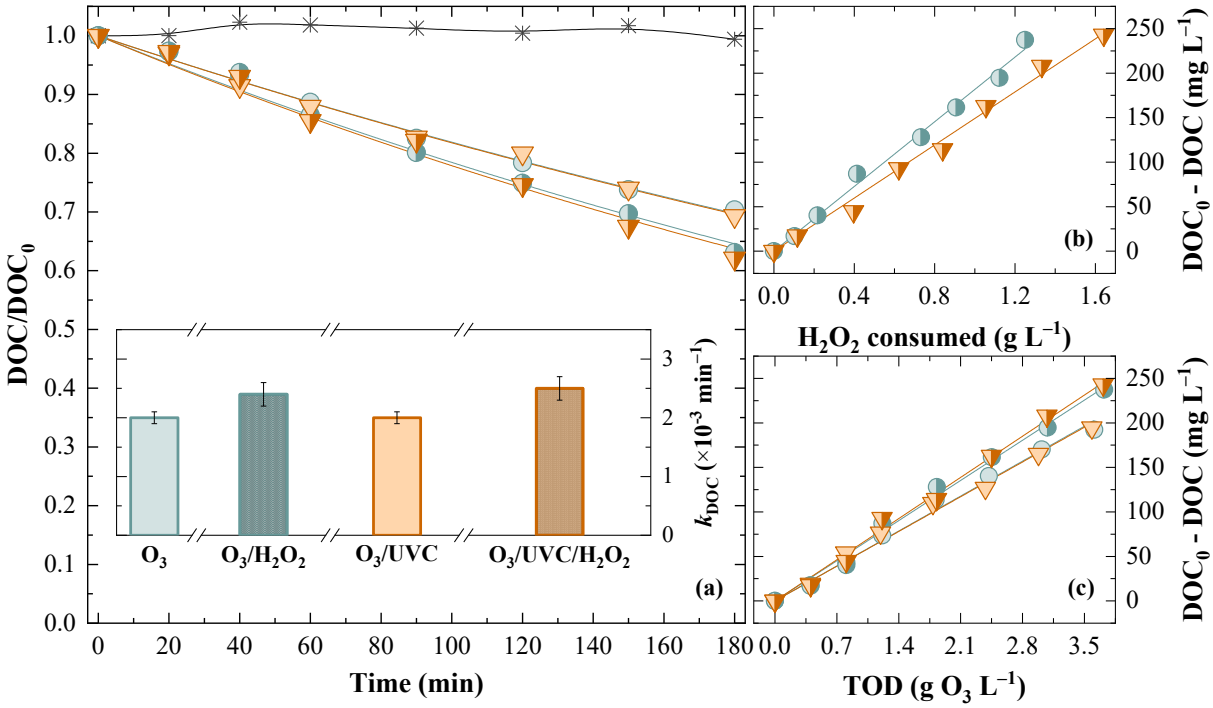

Figure 5.2 Evolution of the: (a) normalized DOC reduction (symbols) over time, along with the respective pseudo-first-order fitting curves (lines); and total DOC removed as a function of the (b) H_2O_2 consumed and (c) transferred O_3 dose (TOD), during the different O_3- and/or photo-based processes: ozonation (◯), O_3/H_2O_2 (◑), O_3/UVC (▽), O_3/UVC/H_2O_2 (▼), and UVC/H_2O_2 (✳). Inset: Representation of the kinetic constants (bars) for each experiment. Experimental conditions: $[DOC]_0 = 637\pm24$ mg L^{-1}; $V = 1.5$ L; room temperature; $pH_0 = 8.9\pm0.2$; OD_{inlet} = 30 mg O_3 min^{-1}; $[H_2O_2]$ = 200–500 mg L^{-1} (except when indicated); 11W UVC lamp (except when indicated).

The desulphurised HISWL leachate was subjected to coagulation with: (i) ferric salts at acidic medium, aiming at further Fe-catalysed- or PF-assisted ozonation (O_3/Fe^{2+} or O_3/PF); and (ii) aluminium salts at near-neutral pH (O_3/Al^{3+}), to benefit from the alkaline pH and buffer capacity of the leachate, as well as from both direct electrophilic attack by molecular O_3 and indirect attack by $HO^{\bullet}$ resulting from O_3 decomposition. The coagulated leachate was then subjected to O_3 or O_3/H_2O_2/UVC processes.

Fe-driven coagulation was performed under the best conditions (100 mg Fe^{3+} L^{-1}; pH of 2.8) reported in Chapter 3, using a leachate from the same HISWL, and Al-driven coagulation was optimized regarding the solution pH and the coagulant dosage (data not shown). The best compromise in terms of DOC and turbidity removal was attained for an aluminium content of 400 mg Al^{3+} L^{-1} at free pH. Regardless of the coagulant used, a DOC removal of 21-22% and a turbidity raise of 163-189% were obtained.

Nevertheless, as anticipated, two main differences were noticed with reference to the Fe- and Al-coagulated leachate, respectively: (i) the solution pH was 2.7 against 4.8; and (ii) residual Fe (total dissolved iron) and Al (total aluminium) concentrations were 61 mg Fe L^{-1} (56 mg Fe^{2+} L^{-1} + 5 mg Fe^{3+} L^{-1}) and 6.8 mg Al L^{-1}, accompanied by an increase in the content of the respective co-anions (about more 0.500 g Cl^- L^{-1} and 2.2 g SO_4^{2-} L^{-1}). In spite of the coagulation has accounted for DOM removal, although low, the same was not true for suspended particulate matter, even caused it to worsen. Such behaviour could be related to the molecular composition of the HISWL leachate, indicating that the main constituents of the dissolved and colloidal matter were not susceptible to the charge neutralization mechanism and further micro-flocs aggregation, either by the preponderance of positively charged sites instead of the negative ones or by the lack of charged groups. Hence, the main goals towards the implementation of this pre-treatment were not fully achieved.

As concerns the O_3-mediated reactions, Figure 5.3a,b and Table 5.2 depict that the mineralization rates were about 40% or 49% slower when coagulated leachates were subjected to ozonation, in the presence or absence of UVC/H_2O_2, respectively. This lower performance can conceivably be associated with the: (i) higher turbidity (53±3 NTU *vs.* 19±2 NTU), and consequent suspended solids; (ii) lower DOC (499±6 mg L^{-1} *vs.* 637±24 mg L^{-1}); (iii) greater concentration of chloride (20.2 g L^{-1} *vs.* 19.7 g L^{-1}, as a result of $FeCl_3$ addition) or sulphate (0.5 g L^{-1} *vs.* 2.7 g L^{-1}, as a result of $Al_2(SO_4)_2$ addition), which can act as O_3/$HO^{\bullet}$ or $HO^{\bullet}$ scavengers, respectively [7]; and (iv) minor pH (2.7-4.8 *vs.* 8.9) (see Figure 5.1c); of the coagulated HISWL leachate, at the beginning of the O_3-driven process, in contrast with the desulphurised HISWL leachate. Conducting the reaction under a considerably acidic pH range (4.8-1.7) rather than a slightly alkaline (8.9-7.6) dictated the prevalence of the direct O_3 reaction mechanism over the indirect one, which led to a lesser production of the powerful and non-selective $HO^{\bullet}$. As molecular O_3 presents lower redox potential than free $HO^{\bullet}$, the mineralization kinetic was slower. These results, together with the better performance of the O_3/H_2O_2 process faced to O_3 only (showed in Section 5.3.2.2), might confirm that the leachate molecules, as well as the respective intermediates, are more susceptible to the attack of the $HO^{\bullet}$ than of the O_3.

Similar to the reported in the previous sections, the fraction of unused O_3 was higher in the absence of UVC and H_2O_2, especially whenever employed after coagulation (see Figure 5.3a,b: inset). Besides that, the mineralization efficiency in terms of O_3 or H_2O_2 consumption was about 50% lower when coagulated leachates were used, rather than the desulphurised one, whatever the remaining experimental conditions (Figure 5.3d,e), suggesting the incidence of parasitic reactions that consume O_3 and H_2O_2, either with particulate organic or soluble inorganic compounds, which impaired the degradation of the dissolved

organic pollutants. In the absence of UVC light and H_2O_2, and even at a low extent, the production of $HO^{\bullet}$ as a result of O_3 decomposition could also take place in the acidic O_3/Al^{3+} and O_3/Fe^{2+} systems by the reaction with the: (i) HO^-, since initial pH is higher than 4 (Figure 5.3c), as shown in section 3.2.1; and (ii) Fe^{2+}, either through the generation of O_3^- anion or through the generation of ferryl ion ($(FeO)^{2+}$) oxidant, according to Eqs. 5.3-5.7 [24, 36].

In turn, contributing to the low mineralization degrees, in the O_3/Al^{3+} and O_3/Fe^{2+} systems, the free $HO^{\bullet}$ and $HO^{\bullet}/(FeO)^{2+}$ oxidants can have been scavenged by the reaction with the: (i) SO_4^{2-}, whose concentration ascended to 2.7 g L^{-1} (in contrast with 0.5 g L^{-1}), giving the radical $SO_4^{\bullet-}$ (E^o of 2.60 V/SHE), which can further react with SO_4^{2-}, to produce persulphate (E^o of 2.12 V/SHE) as stated by Eqs. 5.8 and 5.9 [7]; and (ii) Fe^{2+} (Eqs. 1.22 and 5.10), whose concentration ranged between 56 and 42 mg L^{-1} during the reaction [24].

$$Fe^{2+} + O_3 \rightarrow Fe^{3+} + O_3^- \quad (5.3)$$

$$O_3^- + H^+ \leftrightarrow HO_3 \quad (5.4)$$

$$HO_3 \rightarrow HO^{\bullet} + O_2 \quad (5.5)$$

$$Fe^{2+} + O_3 \rightarrow (FeO)^{2+} + O_2 \quad (5.6)$$

$$(FeO)^{2+} + H_2O \rightarrow Fe^{3+} + HO^{\bullet} + OH^- \quad (5.7)$$

$$SO_4^{2-} + HO^{\bullet} \rightarrow SO_4^{\bullet-} + OH^- \quad (5.8)$$

$$SO_4^{2-} + SO_4^{\bullet-} \rightarrow S_2O_8^{2-} + e^- \quad (5.9)$$

$$(FeO)^{2+} + Fe^{2+} + 2H^+ \rightarrow 2Fe^{3+} + H_2O \quad (5.10)$$

Additionally, under acidic conditions and UVC light, O_3 and H_2O_2 can react with $HO^{\bullet}$ producing the less reactive perhydroxyl radical ($HO_2^{\bullet}$) (E^o of 1.70 V/SCE [24]), as displayed in Eqs. 1.35 and 1.39. Notwithstanding, for all systems considered till here (including those addressed in the previous sections), only DOC removals among 16%-45% were attained over a 3-h reaction time. These general low mineralization yields might well be related to the high chloride content (> 19 g Cl^- L^{-1}) of the HISWL leachate since these species can quench both O_3 and $HO^{\bullet}$, according to Eqs. 5.11 ($k = 8.9 \times 10^7$ L mol^{-1} s^{-1}) and 5.12 ($k = 0.003$ L mol^{-1} s^{-1}), respectively [7]. Given the continuous availability of molecular O_3, it is very plausible that chlorides quickly reappear in the solution as shown in Eq. 5.13 ($k = 110$ L mol^{-1} s^{-1}), once its rate constant is higher than the one of the reaction represented by Eq. 5.12 [7].

$$HO^{\bullet} + Cl^{-} \rightarrow ClOH^{\bullet -} \quad 5.11$$

$$O_3 + Cl^{-} \rightarrow O_2 + OCl^{-} \quad 5.12$$

$$O_3 + OCl^{-} \rightarrow 2O_2 + Cl^{-} \quad 5.13$$

Looking at the single ozonation process (Figure 5.3a,c), it can be observed that there was no significant difference in using Al- or Fe-coagulated leachate regarding the kinetic constants for DOC degradation ($k \approx 1 \times 10^{-3}$ min^{-1}) and final pH (1.7-1.8). Excepting O_3 concentration in the off-gas that was slightly different (Figure 5.3a: inset), reaching to O_3 utilization ratios of 0.67 and 0.78 for O_3/Fe^{3+} and O_3/Al^{3+} systems. The higher consumption perceived for the second system can be explained by the higher initial pH (4.8 vs. 2.7), which apparently had more influence on the O_3 decomposition chain reactions than the presence of Fe^{2+} ion. From Figure 5.3a,b and Table 5.2, it was also possible to disclose that the introduction of UVC light and H_2O_2 into the O_3 reaction system led to a reaction rate improvement of (i) 25%, when Fe^{2+} was absent, and (ii) 50%, when Fe^{2+} was present. Such a tendency can be accounted for several parallel pathways capable to produce greater amounts of highly reactive species, besides the former mentioned $HO^{\bullet}$-generating reactions regarding the ozonation, O_3/H_2O_2, O_3/UVC, O_3/H_2O_2/UVC, and O_3/Fe^{2+} systems. Under Fe^{2+} attendance, the different parallel pathways could include: (i) classical Fenton's reaction via Eq. 1.18 [37]; (ii) photoreduction of Fe(III)-hydroxy complexes to Fe^{2+}, according to Eq. 1.23 [37]; (iii) direct photolysis of Fe(III)-carboxylate complexes as stated by the general Eq. 1.24 [38]; and (vi) reaction of resulting Fe^{3+} with O_3, in line with Eq. 5.14 [24]. Furthermore, aside from Eqs. 1.23 and 1.24, Fe^{2+} could also be regenerated from the chemical reduction of Fe^{3+} with H_2O_2 and $HO_2^{\bullet}$, even to a low extent, conforming to Eqs. 1.19 and 1.25 [39]. So, continuous generation of $HO^{\bullet}$ could be maximized by the occurrence of the reactions 1.23-1.24 and 1.19-1.20 that guarantee the catalytic loop of the Fe^{3+}/Fe^{2+}, allowing a Fe^{2+} content enough to propagate the reactions 5.3-5.8 and 1.18.

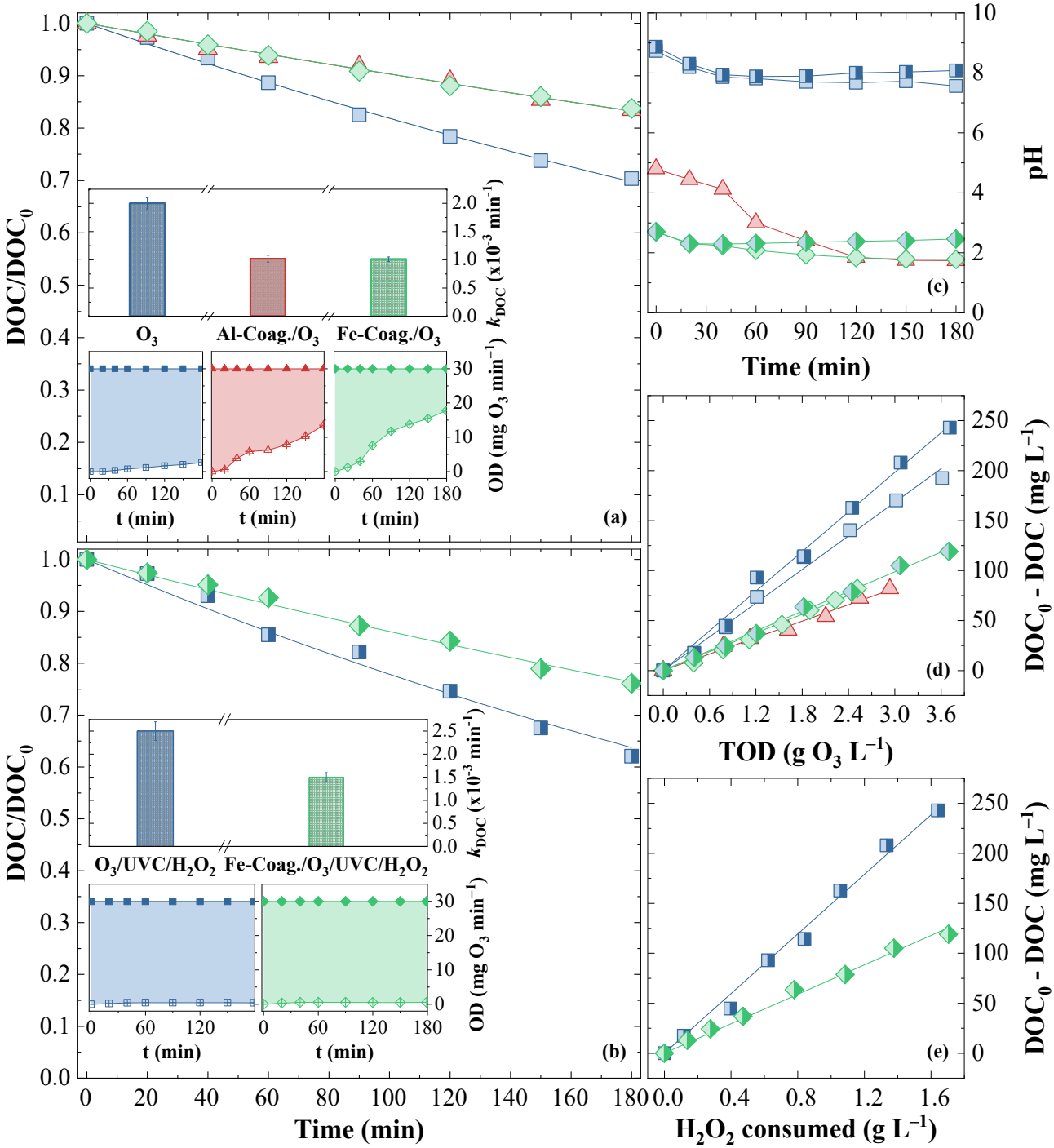

Figure 5.3 Evolution of the: (a, b) normalized DOC reduction (symbols) over time, along with the respective pseudo-first-order fitting curves (lines); (c) pH over time; and total DOC removed as a function of the (d) transferred O_3 dose (TOD) and (e) H_2O_2 consumed; during the ozonation process (filled symbols), the O_3/H_2O_2 process and the $O_3/UVC/H_2O_2$ process (semi-filled symbols), using desulphurised (◻,◼), Fe-coagulated (◇, ◈) or Al-coagulated (△) HISWL leachate. Inset: Representation of (i) kinetic constants for each experiment and (ii) inlet (solid symbols) and outlet (crossed symbols) O_3 dose over time, where the shaded areas correspond to the total amount of O_3 available for the reaction. Experimental conditions: $[DOC]_0$ = 637±24 mg L^{-1} (desulphurised leachate) or 499±6 mg L^{-1} (coagulated leachate); V = 1.5 L; room temperature; OD_{inlet} = 30 mg O_3 min^{-1}; $[H_2O_2]$ = 200–500 mg L^{-1} (except when indicated); 11W UVC lamp (except when indicated).

$$Fe^{3+} + O_3 \rightarrow (FeO)^{2+} + H^+ + O_2 + HO^{\bullet} \quad 5.14$$

Also, the slower decrease in pH for O_3/PF than for O_3/Fe^{2+} system supports the fact that this leachate is preferentiality attacked by free $HO^{\bullet}$ instead of the O_3 molecular. It is worthy to mention that a blank UVC/H_2O_2 experiment using the Fe-coagulated HISWL leachate (see Table 5.2) at an average pH of 2.8, the so-called PF reaction, was also performed, showing a DOC removal rate 40% and 59% lower than the O_3/Fe^{2+} and O_3/PF processes under the same conditions. Although a quicker organics removal had been achieved, synergy was not accomplished by the integrated O_3/PF system, as its kinetic constant was lower than the sum of the kinetic constants for the individual O_3/Fe^{2+} and PF processes, as could be realised in Table 5.2.

As a final remark, it was found that even though higher reaction rates were reached for O_3-based systems using the HISWL leachate right after the CO and CP stages, in absolute terms, the DOC reduction was higher when the desulphurised HISWL leachate undergone treatment by coagulation combined with O_3-based processes (34% or 40% *vs*. 30% or 38% for O_3/Fe^{2+} or O_3/PF *vs.* ozonation or O_3/H_2O_2/UVC, respectively). However, the inclusion of a coagulation stage would also imply the addition of one more neutralization step after the O_3-driven process. So, it was decided to exclude the coagulation from the treatment line and pursue the biodegradability assessment using desulphurised HISWL leachate along the O_3/H_2O_2 process under an OD_{inlet} of 40 mg O_3 min^{-1}, since it was the condition that conducted to the best results.

5.3.3 Biodegradability assessment

One of the most important indicators to appraise the effectiveness of O_3-based systems, especially when treating high-polluted wastewater whose total mineralization is too difficult and economically not viable, is the alteration on the biodegradability in the course of the reaction. In order to attest the applicability of a biological oxidation process downstream of the O_3-based AOP and define the best organics oxidation state to end it, the Zahn-Wellens test was performed on samples collected at 0-, 3-, 6- and 9-h of the O_3/H_2O_2 process with an OD_{inlet} of 40 mg O_3 min^{-1} (Figure 5.4). The overall purpose is cost reduction, which means that the O_3/H_2O_2 process should take a short time as possible yet sufficient so that an ensuing biological oxidation process is able to provide a COD in compliance with legal discharge requirements.

As expected, the ozonation reaction promotes a progressive enhancement in the biodegradation rate [40] from 11%, at time 0, up to 38%, after a 9-h reaction, which is equivalent to an O_3 dose of 14.9 g L^{-1}

leachate and an H_2O_2 consumption of 6.6 g L^{-1} leachate as depicted in Figure 5.4. Nevertheless, to achieved COD values below 125 mg O_2 L^{-1} (European legislation) or 150 mg O_2 L^{-1} (Portuguese legislation) after a biological oxidation, it would be necessary to carry out the O_3/H_2O_2 process for more than 9-h, which is not economically feasible. In fact, the unitary operating cost assigned only to O_3/H_2O_2 stage was estimated at 40.4 € m^{-3}, considering the: (i) total O_3 dose (14.9 g L^{-1}) and H_2O_2 consumption (6.6 g L^{-1}) after a 9-h contacting time; (ii) O_3 energy consumption and electric energy price (15 kWh kg^{-1} O_3 [40] and 0.10 € kWh^{-1}, the average market price for a sanitary landfill); (iii) cost related to the O_2 flow rate (15 L h^{-1}) fed to the O_3 generator (0.14 € m^{-3}, the market price of a Portuguese company); and (iv) price of an H_2O_2 solution at 50% (w/v) (375 € ton^{-1}, the market price of a Portuguese company).

In view of the high operating costs associated with the O_3/H_2O_2 process, when the discharge of the HISWL leachate into aquatic systems is aimed, a second approach can be its discharge into the municipal sewerage system, whose emission limited value for COD is usually 1000 mg O_2 L^{-1} (Portuguese municipality legislation). Given this alternative, and based on the Zahn-Wellens test profile together with O_3/H_2O_2 experiment results (Figure 5.4), it was estimated that the O_3/H_2O_2 process should be carried out until an O_3 dose of 3.5 g O_3 per litre of leachate is attained and 1.1 g of H_2O_2 per litre of leachate is consumed (which corresponds to a 2.1-h reaction in this experimental facility), considering an initial DOC and COD of 637 mg L^{-1} and 1970 mg O_2 L^{-1}, respectively. Under these conditions, the HISWL leachate would be featured a DOC and COD of: (i) 433 mg L^{-1} and 1250 mg O_2 L^{-1}, respectively, after the O_3/H_2O_2 process, presenting a substantially lower unitary operating cost of 9.1 € m^{-3}; and (ii) 354 mg L^{-1} and 978 mg O_2 L^{-1}, respectively, after the subsequent biological oxidation process.

5.3.4 Dissolved organic matter characterization

To better understand the nature and proprieties of the DOM (quantified until here by means DOC analysis) that constitutes the HISWL leachate, as well as its structural and compositional changes suffered throughout the chemical-based stages of the best treatment train, 3D-EEM and SEC-OCD analysis were performed to the following samples: (i) raw leachate; (ii) leachate after CO; (iii) leachate after CP; and (iv) leachate after O_3/H_2O_2 process (OD_{inlet} of 40 mg O_3 L^{-1}; contacting time of 3-h) (Figure 5.5).

3D-EEM fluorescence spectra was divided into five regions, as could be seen from Figure 6a), according to the classification adopted by Chen et al. [41] regarding the type and location of the fluorescent material, namely: (i) region I, comprising tyrosine-like aromatic proteins (Ex < 250 nm, Em < 330 nm); (ii) region II, encompassing tryptophan-like aromatic proteins (Ex < 250 nm, 330 nm < Em < 380 nm);

(iii) region III, containing fulvic-like acids (Ex < 250 nm, Em > 380 nm); (iv) region IV, covering soluble microbial metabolic products (Ex > 250 nm, Em < 380 nm); and (v) region V, consisting of humic-like acids (Ex > 250 nm, Em > 380 nm). Total fluorescence intensity for each region along with relative fluorescence intensity integrated at each region are depicted in Figure 5.5b. Contrary to what is usual for urban leachates, 3D-EEM contour (Figure 5.5a) together with relative fluorescence intensity data (Figure 5.5b) for raw HISWL leachate discloses that tryptophan-like (45%), tyrosine-like (23%) aromatic proteins and soluble microbial metabolic products (23%) were found to be the main fluorophores, whose the sum of the integrated regional volume accounted for more than 90% of the DOM.

This distribution remained constant along the next CO and CP stages, being only noticed a slight reduction in the total fluorescence intensity, suggesting that there was no significant difference in the fluorophores physicochemical characteristics. Such performance was already anticipated since during both processes just sulphur compounds were meaningfully removed and only a low DOC depletion was observed. Interestingly, despite the relative fluorescence associated with recalcitrant humic- and fulvic-like matter have just counted for less than 10% of the total fluorescence, the HISWL leachate biodegradability, either raw or along CO and CP process was very low (around 11-12%), suggesting that the biomass activity could have been inhibited by the presence of other refractory organic (e.g. non-fluorescent DOM) or inorganic (besides the known and depleted sulphur compounds) constituents. Furthermore, in industrial wastewater matrices other than sanitary landfill leachates, regions I and IV were related to polyphenolic compounds (that could be resultant from lignin), DNA fragments, organic acids, benzene, and their derivates, and region II was associated with some nitrogen heterocyclic compounds (e.g. indole), recognised as refractory pollutants [42, 43].

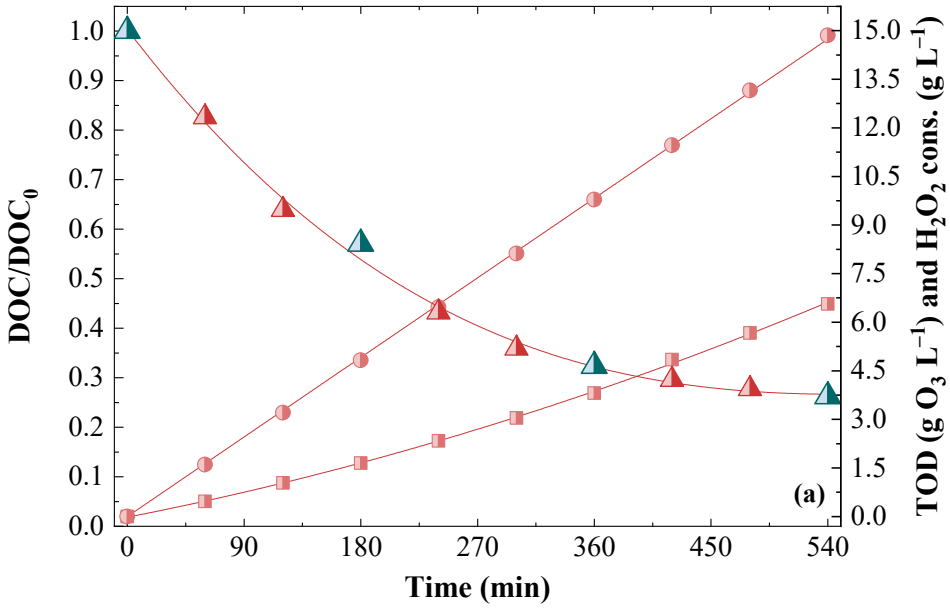

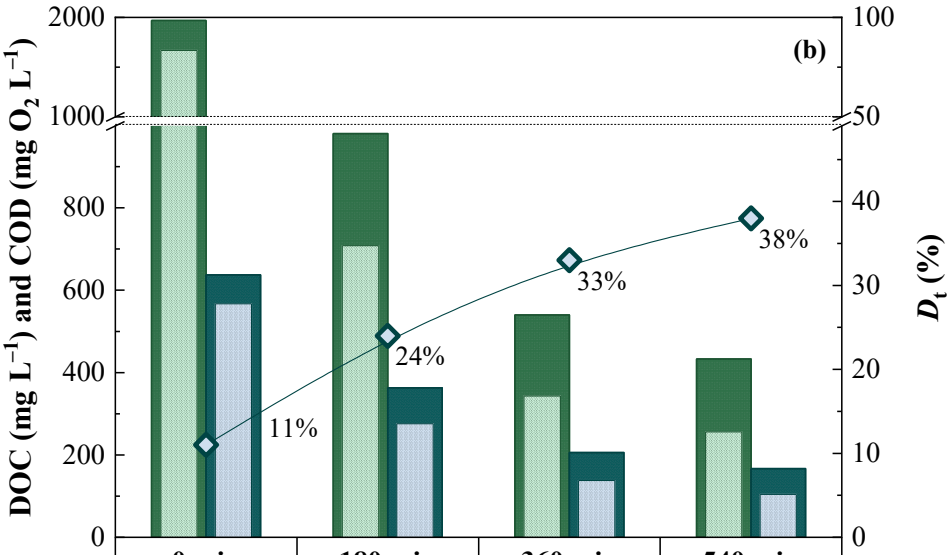

	0 min	180 min	360 min	540 min
DOC (day 0)	637	363	206	167
DOC (day 28)	567	276	138	104
COD (day 0)	1970	980	540	433
COD (day 28)	1667	708	343	256

Figure 5.4 Evolution of the: (a) normalized DOC reduction (▲,▲), whose the symbols highlighted in green correspond to the samples submitted to the Zahn-Wellens test, transferred O3 dose (TOD) (●) and H_2O_2 consumed (■) over time, during the treatment of desulphurised HISWL leachate by O_3/H_2O_2 process; and (b) DOC and COD at day 0 and 28 (bars) of the Zahn-Wellens test, as well as the biodegradation percentage at day 28 (symbols), considering the samples collected at 0, 180, 360 and 540 min of the O_3/H_2O_2 process. Experimental conditions: $[DOC]_0$ = 637±24 mg L^{-1}; V = 1.5 L; room temperature; pH_0 = 8.9±0.2; OD_{inlet} = 40 mg O_3 min^{-1}; $[H_2O_2]$ = 200-500 mg L^{-1}.

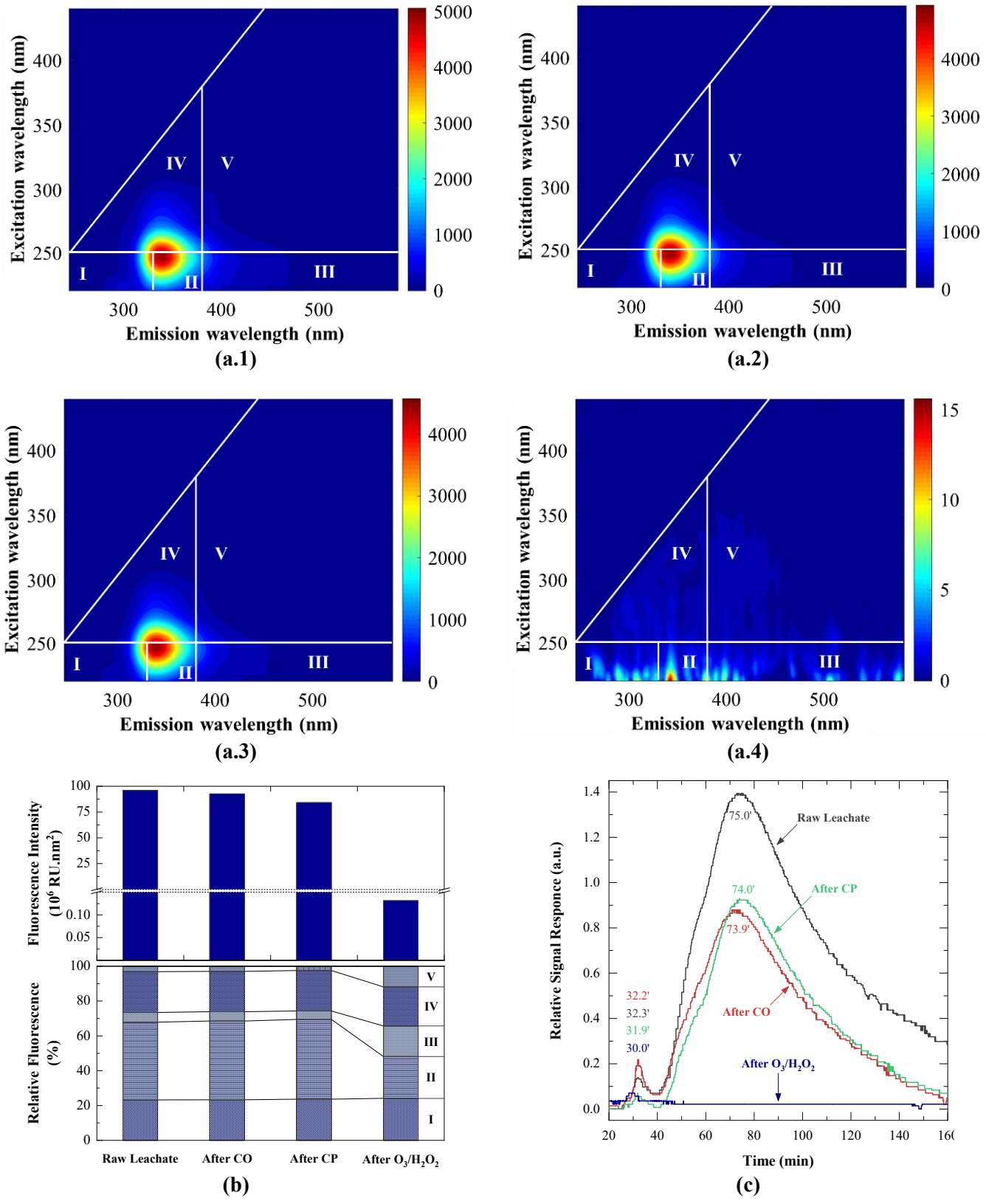

Figure 5.5 Illustration of the (a) 3D-EEM spectra for (.1) raw HISWL leachate and for HISWL leachate after (.2) catalytic oxidation (CO), (.3) chemical precipitation (CP) and (.4) O_3/H_2O_2 process ($[DOC]_0$ = 637±24 mg L^{-1}, V = 1.5 L, room temperature, pH_0 = 8.9±0.2, OD_{inlet} = 40 mg O_3 min^{-1}, $[H_2O_2]$ = 200–500 mg L^{-1}, 3-h contacting time), as well as the (b) total fluorescence intensity and relative fluorescence by region, and (c) SEC-OCD chromatograms.

Therefore, the presence of tryptophan/tyrosine-like aromatic proteins and soluble microbial by-products are in agreement with a former analysis of the volatile organic carbon compounds of a leachate collected from the same HISWL, and might be ascribed to the type of waste deposited in the landfill, which includes sludge from MWWTPs, soils containing heavy hydrocarbons, and residues from steelworks and mining and metallurgical industries.

The 3D-EEM results (Figure 5.5a,b) were confirmed by the SEC-OCD chromatograms (Figure 5.5c) for raw and desulphurised leachate, which exhibit one peak around 31.9-32.3 min, representing about 0.8-2.8% of the total area, and a second peak around 73.9-75.0 min, corresponding to about 97.1-99.2%. While the first peak is assigned to large size biopolymers (e.g. polysaccharides), the second peak is not clearly differentiable among the humic and low molecular weight (LMW) fractions, such as building blocks and LMW neutral/acids, yet it may primarily be contributed by LMW fractions [44, 45]. Also, the slender decrease in the retention time of the second peak for the desulphurised HISWL leachate suggests the selective removal of LMW substances. In any case, the predominance of LMW substances is in agreement with the low DOC decays (20-21%) observed for the coagulation process.

As expected, the application of the O_3/H_2O_2 system led to a drastic decrease in both total fluorescence intensity (>99.8%) and total SEC-OCD area (>99.5%), as can be seen in Figure 6. Regarding the remaining fluorescent DOM, it is possible to infer that the physicochemical characteristics of the ozonised HISWL leachate (Figure 5.5a.4) have obviously diverged from those of the desulphurised one (Figure 5.5a.3). Whereas the relative fluorescence of the tyrosine-like aromatic proteins (region I) and soluble microbial metabolic by-products (region IV) remained approximately constant, the proportions of the fulvic/humic-like acids have increased to 18/12% (region III/V), at the same time than of the tryptophan-like aromatic proteins (region II) has oppositely decreased to 24% (Figure 5.5b). In contrast, from the SEC-OCD chromatogram for the ozonised HISWL leachate, only the high molecular weight biopolymers were noticed (Figure 5.5c). This discrepancy amongst 3D-EEM and SEC-OCD data can be explained in terms of the analytical sensitivity of the two technics since, for 3D-EEM analysis, all samples were diluted to present the same DOC due to instrumental issues, and for SEC-OCD analysis, all samples were injected without further dilution for the better conceptualization of the treatment effectiveness. Such behaviour points toward a preferential attack of the $O_3/HO^{\bullet}$ to the simpler molecular structures. Notwithstanding, the DOM profile of the treated HISWL leachate supported its low bioavailability. In spite of the biodegradability having increased during O_3-based AOP its final value was still small (24%), as this sample was collected with only 3-h contact time (Figure 5.5).

5.4 Conclusions

The best treatment strategy to de-pollute a high-strength HISWL leachate, mainly presenting high sulphur content, moderate organic load, moderate-to-low nitrogen level, and low biodegradability, should comprise the following processes: (i) catalytic oxidation of sulphites and sulphides at natural pH using H_2O_2 as oxidant (H_2O_2:SO_3^{2-} and [H_2O_2]:[S^{2-}] molar ratios of 1:1 and 4:1, respectively) and leachate transition metals as catalysts, with the partial formation of sulphate (~33%); (ii) chemical precipitation of sulphates as barite mineral ($BaSO_4$) without pH correction and stoichiometric conditions; (iii) O_3/H_2O_2 for 2.1 h under free pH, being transferred about 3.5 kg O_3 per m^3 leachate and consumed ca. 1.1 kg H_2O_2 per m^3 leachate, in order to degrade the recalcitrant organics while enhancing the biodegradability (even though at a low extent); and (iv) biological oxidation to remove the biodegradable organics fraction resulting from the O_3/H_2O_2. The application of this treatment line, with an O_3-stage-associated unitary operating cost of 9.1 € m^{-3}, would allow attaining an effluent in full compliance with the legal municipal requirements for the discharge of industrial wastewater into the sewage system, but not with Portuguese and European legislation targeting the discharge of wastewaters into waterbodies. The DOM distribution in the hazardous leachate matrix obtained by the 3D-EEM and SEC-OCD analysis was found to be in agreement with the multistage treatment strategy performed, being the O_3-based AOPs step the one which had more influence on the DOM composition changes. Also, the prevalence of low molecular weight matter might justify the low performance spotted for the coagulation process. Finally, it was also established that neither the addition of UVC irradiation nor a preliminary coagulation step had a positive effect on O_3-based reactions.

5.5 References

[1] N. Amaral-Silva, R.C. Martins, S. Castro-Silva, R.M. Quinta-Ferreira, Ozonation and perozonation on the biodegradability improvement of a landfill leachate, Journal of Environmental Chemical Engineering, 4 (2016) 527-533.

[2] P. Asaithambi, B. Sajjadi, A.R.A. Aziz, W.M.A.B.W. Daud, Ozone (O_3) and sono (US) based advanced oxidation processes for the removal of color, COD and determination of electrical energy from landfill leachate, Separation and Purification Technology, 172 (2017) 442-449.

[3] S. Cortez, P. Teixeira, R. Oliveira, M. Mota, Ozonation as polishing treatment of mature landfill leachate, Journal of Hazardous Materials, 182 (2010) 730-734.

[4] S. Cortez, P. Teixeira, R. Oliveira, M. Mota, Evaluation of Fenton and ozone-based advanced oxidation processes as mature landfill leachate pre-treatments, Journal of Environmental Management, 92 (2011) 749-755.

[5] X. Ntampou, A.I. Zouboulis, P. Samaras, Appropriate combination of physico-chemical methods (coagulation/flocculation and ozonation) for the efficient treatment of landfill leachates, Chemosphere, 62 (2006) 722-730.

[6] C. Tizaoui, L. Bouselmi, L. Mansouri, A. Ghrabi, Landfill leachate treatment with ozone and ozone/hydrogen peroxide systems, Journal of Hazardous Materials, 140 (2007) 316-324.

[7] A.I. Gomes, T.F. Soares, T.F.C.V. Silva, R.A.R. Boaventura, V.J.P. Vilar, Ozone-driven processes for mature urban landfill leachate treatment: Organic matter degradation, biodegradability enhancement and treatment costs for different reactors configuration, Science of The Total Environment, 724 (2020) 138083.

[8] U. Kingdom, Waste water treatment works: treatment monitoring and compliance limits, in: U.K.E. Agency (Ed.), 2019.

[9] Portuguese Ministry of the Environment, Decree Law 236/98 of 1 August - Appendix XVIII. Official Gazette of Portugal - Series I-A, 1998.

[10] The Council of the European Union, Council Directive 91/271/EEC of 21st May 1991 concerning urban waste-water treatment, Official Journal of the European Communities., 1991.

[11] F.C. Moreira, E. Bocos, A.G.F. Faria, J.B.L. Pereira, C.P. Fonte, R.J. Santos, J.C.B. Lopes, M.M. Dias, M.A. Sanromán, M. Pazos, R.A.R. Boaventura, V.J.P. Vilar, Selecting the best piping arrangement for scaling-up an annular channel reactor: An experimental and computational fluid dynamics study, Science of The Total Environment, 667 (2019) 821-832.

[12] A.I. Gomes, M.L.R. Foco, E. Vieira, J. Cassidy, T.F.C.V. Silva, A. Fonseca, I. Saraiva, R.A.R. Boaventura, V.J.P. Vilar, Multistage treatment technology for leachate from mature urban landfill: Full scale operation performance and challenges, Chemical Engineering Journal, 376 (2019) 120573.

[13] F.C. Moreira, J. Soler, A. Fonseca, I. Saraiva, R.A.R. Boaventura, E. Brillas, V.J.P. Vilar, Incorporation of electrochemical advanced oxidation processes in a multistage treatment system for sanitary landfill leachate, Water Research, 81 (2015) 375-387.

[14] T.F.C.V. Silva, P.A. Soares, D.R. Manenti, A. Fonseca, I. Saraiva, R.A.R. Boaventura, V.J.P. Vilar, An innovative multistage treatment system for sanitary landfill leachate depuration: Studies at pilot-scale, Science of The Total Environment, 576 (2017) 99-117.

[15] A.D. Webler, F.C. Moreira, M.W.C. Dezotti, C.F. Mahler, I.D. Barbosa Segundo, R.A.R. Boaventura, V.J.P. Vilar, Development of an integrated treatment strategy for a leather tannery landfill leachate, Waste Management, 89 (2019) 114-128.

[16] J. Hoigné, The Chemistry of Ozone in Water, in: S. Stucki (Ed.) Process Technologies for Water Treatment, Springer US, Boston, MA, 1988, pp. 121-141.

[17] J. Hoigné, H. Bader, W.R. Haag, J. Staehelin, Rate constants of reactions of ozone with organic and inorganic compounds in water—III. Inorganic compounds and radicals, Water Research, 19 (1985) 993-1004.

[18] M.H. Gerardi, Nitrification and denitrification in the activated sludge process, John Wiley & Sons, New York, 2003.

[19] P.N.L. Lens, A. Visser, A.J.H. Janssen, L.W.H. Pol, G. Lettinga, Biotechnological Treatment of Sulfate-Rich Wastewaters, Critical Reviews in Environmental Science and Technology, 28 (1998) 41-88.

[20] M.R. Hoffmann, Kinetics and mechanism of oxidation of hydrogen sulfide by hydrogen peroxide in acidic solution, Environmental Science & Technology, 11 (1977) 61-66.

[21] J. Lagrange, C. Pallares, G. Wenger, P. Lagrange, Kinetics of sulphur(IV) oxidation by hydrogen peroxide in basic aqueous solution, Atmospheric Environment, 30 (1996) 1013-1018.

[22] M. Moslemi, S.H. Davies, S.J. Masten, Ozone mass transfer in a recirculating loop semibatch reactor operated at high pressure, Journal of Advanced Oxidation Technologies, 13 (2010) 79-88.

[23] X. Quan, D. Luo, J. Wu, R. Li, W. Cheng, s. Ge, Ozonation of acid red 18 wastewater using $O_3/Ca(OH)_2$ system in a micro bubble gas-liquid reactor, Journal of Environmental Chemical Engineering, 5 (2017) 283-291.

[24] K. Chandrasekara Pillai, T.O. Kwon, I.S. Moon, Degradation of wastewater from terephthalic acid manufacturing process by ozonation catalyzed with Fe^{2+}, H_2O_2 and UV light: Direct versus indirect ozonation reactions, Applied Catalysis B: Environmental, 91 (2009) 319-328.

[25] J. Hoigné, H. Bader, Rate constants of reactions of ozone with organic and inorganic compounds in water—II: Dissociating organic compounds, Water Research, 17 (1983) 185-194.

[26] H. Tomiyasu, H. Fukutomi, G. Gordon, Kinetics and mechanism of ozone decomposition in basic aqueous solution, Inorganic Chemistry, 24 (1985) 2962-2966.

[27] J. Staehelin, J. Hoigne, Decomposition of ozone in water: rate of initiation by hydroxide ions and hydrogen peroxide, Environmental Science & Technology, 16 (1982) 676-681.

[28] D. Gardoni, A. Vailati, R. Canziani, Decay of Ozone in Water: A Review, Ozone: Science & Engineering, 34 (2012) 233-242.

[29] D.B. Miklos, C. Remy, M. Jekel, K.G. Linden, J.E. Drewes, U. Hübner, Evaluation of advanced oxidation processes for water and wastewater treatment–A critical review, Water Research, 139 (2018) 118-131.

[30] A. Cruz-Alcalde, S. Esplugas, C. Sans, Continuous versus single H_2O_2 addition in peroxone process: Performance improvement and modelling in wastewater effluents, Journal of Hazardous Materials, 387 (2020) 121993.

[31] S. Naumov, G. Mark, A. Jarocki, C. von Sonntag, The Reactions of Nitrite Ion with Ozone in Aqueous Solution – New Experimental Data and Quantum-Chemical Considerations, Ozone: Science & Engineering, 32 (2010) 430-434.

[32] F.J. Beltrán, M. González, J.F. González, Industrial wastewater advanced oxidation. Part 1. UV radiation in the presence and absence of hydrogen peroxide, Water Research, 31 (1997) 2405-2414.

[33] H. Christensen, K. Sehested, H. Corfitzen, Reactions of hydroxyl radicals with hydrogen peroxide at ambient and elevated temperatures, The Journal of Physical Chemistry, 86 (1982) 1588-1590.

[34] W.D. Nicoll, A.F. Smith, Stability of dilute alkaline solutions of hydrogen peroxide, Industrial & Engineering Chemistry, 47 (1955) 2548-2554.

[35] I. Zucker, Y. Lester, D. Avisar, U. Hübner, M. Jekel, Y. Weinberger, H. Mamane, Influence of Wastewater Particles on Ozone Degradation of Trace Organic Contaminants, Environmental Science & Technology, 49 (2015) 301-308.

[36] B. Legube, N.K.V. Leitner, Catalytic ozonation: a promising advanced oxidation technology for water treatment, Catalysis Today, 53 (1999) 61-72.

[37] Y. Sun, J.J. Pignatello, Photochemical reactions involved in the total mineralization of 2,4-D by $Fe^{3+}/H_2O_2/UV$, Environmental Science & Technology, 27 (1993) 304-310.

[38] O. Horváth, K.L. Stevenson, Charge Transfer Photochemistry of Coordination Compounds, VCH, New York, 1992.

[39] E. Brillas, P.-L.s. Cabot, R.M.a. Rodríguez, C. Arias, J.A. Garrido, R. Oliver, Degradation of the herbicide 2,4-DP by catalyzed ozonation using the $O_3/Fe^{2+}/UVA$ system, Applied Catalysis B: Environmental, 51 (2004) 117-127.

[40] A.C. Twort, D.D. Ratnayaka, M.J. Brandt, Water supply, Elsevier, Oxford, 2000.

[41] W. Chen, P. Westerhoff, J.A. Leenheer, K. Booksh, Fluorescence excitation− emission matrix regional integration to quantify spectra for dissolved organic matter, Environmental Science & Technology, 37 (2003) 5701-5710.

[42] Z. Chen, D. Li, Q. Wen, Investigation of hydrolysis acidification process during anaerobic treatment of coal gasification wastewater (CGW): Evolution of dissolved organic matter and biotoxicity, Science of The Total Environment, 723 (2020) 137995.

[43] D.M. Reynolds, The differentiation of biodegradable and non-biodegradable dissolved organic matter in wastewaters using fluorescence spectroscopy, Journal of Chemical Technology & Biotechnology, 77 (2002) 965-972.

[44] S.A. Huber, A. Balz, M. Abert, W. Pronk, Characterisation of aquatic humic and non-humic matter with size-exclusion chromatography–organic carbon detection–organic nitrogen detection (LC-OCD-OND), Water Research, 45 (2011) 879-885.

[45] V.L. Quang, I. Choi, J. Hur, Tracking the behavior of different size fractions of dissolved organic matter in a full-scale advanced drinking water treatment plant, Environmental Science and Pollution Research, 22 (2015) 18176-18184.

6 Finding a suitable treatment solution for a leachate from a non-hazardous industrial solid waste landfill

This chapter aimed at tackling the lack of effective treatment solutions for leachates from industrial solid waste landfills, through the development of a treatment train for a non-hazardous ISWL (NHISWL) leachate with low/moderate content of organics and salts and low biodegradability. The following technologies were tested: (i) coagulation using ferric chloride ($FeCl_3$) or aluminium sulphate ($Al_2(SO_4)_3$), (ii) biological oxidation, and (iii) chemical and electrochemical advanced oxidation processes (AOPs/EAOPs), including photo-Fenton oxidation using ultraviolet C (UVC) or ultraviolet A (UVA) radiation (PF-UVC or PF-UVA), anodic oxidation (AO), ozonation process and ozone (O_3)-based processes. The best multistage treatment strategy included: (i) coagulation with $FeCl_3$ for partial removal of organics (with direct impact on colour, odour and turbidity removal and biodegradability enhancement) and phosphorous, (ii) PF-UVC process for recalcitrant organics oxidation (with direct impact on colour and odour removal and biodegradability enhancement) coupled to a clarification step for removal of suspended solids, turbidity, iron and phosphorous, and (iii) biological process for removal of the generated biodegradable organics and of nitrogen compounds. Upon treatment, the NHISWL leachate fulfilled European and Portuguese requirements for discharge into aquatic systems, except for ammonium (and consequently for total nitrogen), pointing to the need to change the biological process conditions or add an air stripping step. The application of coagulation before the PF-UVC process has proved to be crucial for the fulfilment of the legislation requirements.

This chapter is based on the following research article: "Barbosa Segundo, I.D., Martins, R.J.E., Boaventura, R.A.R., Silva, T.F.C.V., Moreira, F.C., Vilar, V.J.P., Finding a suitable treatment solution for a leachate from a non-hazardous industrial solid waste landfill. Journal of Environmental Chemical Engineering, 9 (2021) 105168, DOI: https://doi.org/10.1016/j.jece.2021.105168".

6.1 Introduction

The current study aimed at tackling the lack of effective treatment solutions for ISWL leachates by developing a multistage treatment strategy for a NHISWL leachate with low biodegradability and moderate content of organics and salts. To the best of the knowledge, this was the first time that an ISWL leachate with these characteristics was object of study.

The application of conventional physicochemical, separation and biological processes was appraised as well as of the following AOPs and EAOPs: PF oxidation using UVC or UVA radiation (PF-UVC or PF-UVA), anodic oxidation (AO), ozonation process and ozone (O_3)-based technologies, such as O_3 combined with hydrogen peroxide (O_3/H_2O_2), with UVC radiation (O_3/UVC) and with PF-UVC oxidation (O_3/H_2O_2/UVC). The developed treatment strategy might be suitable for the remediation of other ISWL leachates with quite similar features.

6.2 Material and methods

All the chemicals, experimental units and procedures, analytical determinations and modeling of removal kinetics used within this chapter are described in Chapter 2.

The leachate (120 L sample) was directly collected in a plastic container from the landfill cell exit of a NHISWL located in Northern mainland Portugal, without any treatment. The NHISWL receives large amounts of waste resulting from industrial activities, such as textile waste, plastic waste, metal, biodegradable waste, paper, cardboard and wood, fiber cement and ashes, and also sludge from MWWTPs. It has a capacity for more than 2 million m^3 and produces on average a volume of 12 m^3 of leachate per day. After collection, the leachate was refrigerated at 4 ºC until the start of each assay.

Table 6.1 Physicochemical characteristics of the raw NHISWL leachate and of the NHISWL leachate at different treatment stages.

Parameter (unit)	Raw NHISWL leachate	After ozonation [a]	After ozonation + Biological treatment [b]	After coagulation with $FeCl_3$ [c]	After coagulation with $Al_2(SO_4)_3$ [d]	After coagulation with $FeCl_3$ + PF-UVC [e]	After coagulation with $FeCl_3$ + PF-UVC + Biological treatment [f]	ELV [g]
Colour	Dark brown	Very light yellow	Very light brown	Light brown	Light brown	Light yellow	Light brown	
Colour (diluted 1:20)	d.	n.d.	n.d.	n.d.	n.d.	n.d.	n.d.	n.c. or n.d. (diluted 1:20)
Colour (Pt-Co units)	3800	280	320	470	800	350	380	
Odour	Strong	Null	Null	Moderate	Moderate	Null	Null	
Odour (diluted 1:20)	d.	n.d.	n.d.	d.	d.	n.d.	n.d.	n.c. or n.d. (diluted 1:20)
pH	8.2	7.8	7.0	4.0	4.8	7.0	7.1	n.c. or 6.0-9.0
Conductivity (mS cm^{-1})	15	n.m.	n.m.	22	23	n.m.	n.m.	
Salinity (g L^{-1})	8.9	n.m.	n.m.	14	14	n.m.	n.m.	
Alkalinity (mg $CaCO_3$ L^{-1})	6100	3380	615	60	35	n.d.	n.d.	
Turbidity (NTU)	90	3.0	n.m.	30	38	10	10	
Total suspended solids – TSS (mg L^{-1})	219	20	32	212	220	33	30	35 or 60
Total volatile solids – VSS (mg L^{-1})	68	5	10	48	52	15	12	
Total dissolved carbon – TDC (mg L^{-1})	2482	1221	287	349	448	157	31	
Dissolved inorganic carbon – DIC (mg L^{-1})	1460	809	147	14	9.0	7.0	<0.3 [g]	
Dissolved organic carbon – DOC (mg L^{-1})	1022	412	140	335	439	150	31	
Chemical oxygen demand – COD (mg O_2 L^{-1})	2667	1311	349	922	1381	560	122	125 or 150
COD/DOC	2.6	3.2	2.5	2.8	3.1	3.7	3.9	

Parameter (unit)	Raw NHISWL leachate	After ozonation [a]	After ozonation + Biological treatment [b]	After coagulation with $FeCl_3$ [c]	After coagulation with $Al_2(SO_4)_3$ [d]	After coagulation with $FeCl_3$ + PF-UVC [e]	After coagulation with $FeCl_3$ + PF-UVC + Biological treatment [f]	ELV [g]
Biochemical oxygen demand – BOD_5 (mg O_2 L^{-1})	245	310	10	270	280	300	8.0	25 or 40
BOD_5/COD	0.09	0.24	0.03	0.29	0.20	0.54	0.06	
Biodegradability - Zhan-Wellens test (%)	18	67	Null	32	25	85	Null	
Transmittance at 254 nm (%) (diluted 1:50)	30	94	n.m.	65	69	90	n.m.	
$SUVA_{254}$ (L mg^{-1} m^{-1})	2.5	0.3	n.m.	2.8	1.8	1.5	n.m.	
Total fluorescence (R.U. nm^2)	3.7×10^7	1.3×10^6	n.m.	2.2×10^7	n.m.	2.2×10^5	n.m.	
Total nitrogen – N_T (mg L^{-1})	1160	675	501	901	788	870	820	10 or 15
Dissolved inorganic nitrogen (mg L^{-1})	844	655	487	802	782	786	762	
Ammonium – N-NH_4^+ (mg L^{-1})	834	380	210	802	782	786	762	n.c. or 7.8
Nitrite – N-NO_2^- (mg L^{-1})	<4.9 [g]	<4.9 [g]	<4.9 [g]	<4.9 [g]	<4.9 [g]	<4.9 [g]	<4.9 [g]	
Nitrate – N-NO_3^- (mg L^{-1})	10	275	277	<8.0 [g]	<8.0 [g]	<8.0 [g]	<8.0 [g]	n.c. or 11
Chloride – Cl^- (mg L^{-1})	1247	1280	1375	5259	4164	5359	5144	
Sulphate – SO_4^{2-} (mg L^{-1})	289	317	340	271	1908	305	287	n.c. or 2000
Total phosphorous – P_T (mg L^{-1})	4.3	2.0	0.5	2.3	1.5	0.9	0.3	1 or 10
Calcium – Ca^{2+} (mg L^{-1})	861	n.m.	n.m.	n.m.	n.m.	n.m.	n.m.	
Lithium – Li^+ (mg L^{-1})	<3.3 [g]	n.m.	n.m.	n.m.	n.m.	n.m.	n.m.	
Magnesium – Mg^{2+} (mg L^{-1})	192	n.m.	n.m.	n.m.	n.m.	n.m.	n.m.	
Potassium – K^+ (mg L^{-1})	519	n.m.	n.m.	n.m.	n.m.	n.m.	n.m.	
Sodium – Na^+ (mg L^{-1})	982	n.m.	n.m.	n.m.	n.m.	n.m.	n.m.	
Total aluminium – Al (mg L^{-1})	<0.6 [g]	n.m.	n.m.	n.m.	6.8	n.m.	n.m.	
Total cadmium – Cd (mg L^{-1})	<0.05 [g]	n.m.	n.m.	n.m.	n.m.	n.m.	n.m.	
Total copper – Cu (mg L^{-1})	0.14	n.m.	n.m.	n.m.	n.m.	n.m.	n.m.	

Parameter (unit)	Raw NHISWL leachate	After ozonation [a]	After ozonation + Biological treatment [b]	After coagulation with $FeCl_3$ [c]	After coagulation with $Al_2(SO_4)_3$ [d]	After coagulation with $FeCl_3$ + PF-UVC [e]	After coagulation with $FeCl_3$ + PF-UVC + Biological treatment [f]	ELV [g]
Total lead – Pb (mg L^{-1})	<0.21 [g]	n.m.	n.m.	n.m.	n.m.	n.m.	n.m.	
Total manganese – Mn (mg L^{-1})	<0.35 [g]	n.m.	n.m.	n.m.	n.m.	n.m.	n.m.	
Total nickel – Ni (mg L^{-1})	<0.15 [g]	n.m.	n.m.	n.m.	n.m.	n.m.	n.m.	
Total zinc – Zn (mg L^{-1})	0.23	n.m.	n.m.	n.m.	n.m.	n.m.	n.m.	
Total iron – Fe (mg L^{-1})	2.3	1.8	1.8	116	1.1	1.9	<0.5 [g]	n.c. or 2.0
Total dissolved iron – TDI (mg L^{-1})	1.8	1.7	1.6	115	<0.4 [g]	1.2	<0.4 [g]	

d. – detected; n.c. – not covered; n.d. – not detected; n.m. – not measured;

[a] Using the raw NHISWL leachate. Ozonation conditions: O_3 dose = 30 mg min^{-1}, pH = 8.2, Temperature = 20±1 ºC, Treatment time = 7 h, sedimentation for 2 h and removal of O_3 sludge;

[b] Using the NHISWL leachate subjected to ozonation . Biological treatment conditions: 28 days Zhan-Wellens test, subsequent sedimentation for 2 h and removal of the biological treatment sludge;

[c] Using the raw NHISWL leachate. Coagulation conditions: pH = 4.0, 300 mg Fe L^{-1} from $FeCl_3$ coagulant, sedimentation for 2 h and removal of coagulation sludge;

[d] Using the raw NHISWL leachate. Coagulation conditions: pH = 5.0, 300 mg Al L^{-1} from $Al_2(SO_4)_3$ coagulant, sedimentation for 2 h and removal of coagulation sludge;

[e] Using the NHISWL leachate subjected to coagulation with $FeCl_3$. PF-UVC conditions: pH = 4.0, H_2O_2 = ~100-500 mg L^{-1}, 11 W UVC lamp, TDI_0 = 115 mg L^{-1}, Temperature = 20±1 ºC, Treatment time = 4 h, neutralization to pH 7.0, sedimentation for 2 h and removal of PF-UVC sludge;

[f] Using the NHISWL leachate subjected to coagulation with $FeCl_3$ and PF-UVC process. Biological treatment conditions: 28 days Zhan-Wellens test, subsequent sedimentation for 2 h and removal of the biological treatment sludge;

[g] ELV - Emission limit value according to Directive 91/271/CEE (European legislation) or Decree-Law 236/98 (Portuguese legislation);

[h] Limit of detection.

6.3 Results and discussion

Table 6.1 exhibits the leachate main physicochemical characteristics. The organic load of the current NHISWL leachate (DOC of 1022 mg L^{-1}, COD of 2667 mg O_2 L^{-1}) was (i) lower than that of the majority of leachates from NHISWLs [1-3] (DOC of 5244-19303 mg L^{-1}, COD of 19900-64000 mg O_2 L^{-1}), the HISWL leachate studied in the previous chapters (DOC of 2318 mg L^{-1}, COD of 7063 mg O_2 L^{-1}), and some leachates from MSWLs [4-6] (DOC of 1222-15000 mg L^{-1}, COD of 3106-43000 mg O_2 L^{-1}), (ii) higher than that of the HISWL leachate used by Kattel et al. [7] (DOC of 352 mg L^{-1}, COD of 1446 mg O_2 L^{-1}), and (iii) similar to that of the NHISWL leachate used in the work from Gotvajn et al. [8] (DOC of 955 mg L^{-1}, COD of 2463 mg O_2 L^{-1}). The level of organic compounds of the current NHISWL leachate can then be qualified as low/moderate in relation to a large part of the ISWL leachates studied so far. As regards organics biodegradability, the current leachate exhibited a much lower value (biodegradability of 18%, BOD_5/COD of 0.09) compared to the leachates covered in the studies from Di Palma et al. [1], Schoeman et al. [2], Gotvajn et al. [8], Kattel et al. [7] and Webler et al. [3] and in the previous chapters (BOD_5/COD or BOD_7/COD of 0.20, 0.26, 0.24, 0.32, 0.31 and 0.16, respectively). In terms of conductivity/salinity, the ISWL leachates used by Di Palma et al. [1], Schoeman et al. [2] and Webler et al. [3] and that used in the previous chapters showed extremely higher conductivities (80, 87, 42 and 62 mS cm^{-1}) than the current NHISWL leachate (15 mS cm^{-1}), mainly due to ammonium, chloride, sodium and sulphate ions. The ammonium content of the current leachate (834 mg N-NH_4^+ L^{-1}) was low/moderate when compared to the reported studies (3.5-8403 mg N-NH_4^+ L^{-1}, average of 2694 mg N-NH_4^+ L^{-1}) [3-9]. The content of total suspended solids (TSS) and turbidity of the current NHISWL leachate (TSS of 219 mg L^{-1}, turbidity of 90 NTU) can be qualified as moderate in comparison with the ISWL leachates characterized in terms of this parameter. While the HISWL leachates used in the works from Kattel et al. [7] and in the previous chapters exhibited lower TSS contents (23 and 128 mg L^{-1}, respectively), the NHISWL leachates used by Schoeman et al. [2] and Webler et al. [3] were much richer in TSS (3778 and 1187 mg L^{-1}, respectively). The alkalinity of the current NHISWL leachate (6100 mg $CaCO_3$ L^{-1}) did not substantially differ from that of the previous chapters and of Schoeman et al. [2] (5707 and 8971 mg $CaCO_3$ L^{-1}, respectively), in contrast to the much higher value of the leachate studied by Webler et al. [3] (28800 mg $CaCO_3$ L^{-1}). The total iron content (2.3 mg L^{-1}) was low, as observed for the leachate previously studied within this thesis and for that covered in Webler et al. [3] (1.9 and 7.0 mg L^{-1}, respectively), and in contrast to the iron content of the leachate covered by Schoeman et al. [2] (96 mg L^{-1}). The iron content came along with zero or low levels of other metals. The total phosphorous content (4.3 mg L^{-1}) was in the range of values found by Webler et al. [3] and in the HISWL leachate studied in the previous chapters.

The results of size exclusion chromatography combined with organic carbon detection (SEC-OCD) (Figure 6.1) reveals a prevalence of humic substances, with no noticeable peaks for lower molecular weight matter, such as low molecular weight acids/neutrals or building blocks. This was confirmed by the relative fluorescence intensities integrated at each fluorescent region (Figure 6.1) and by the 3D-fluorescence excitation-emission matrix (EEM) contour (Figure 6.1). Region III, which comprises fulvic-like acids [9], and region V, which includes humic-like acids [9], were responsible for ~37% and ~25%, respectively, of the total fluorescence intensity. Additionally, aromatic proteins, both tyrosine-like (region I) and tryptophane-like (region II) [9], were also present, being responsible for ~24% of the total fluorescence intensity. The dominance of humic substances supports the low biodegradability of the NHISWL leachate since they are known for their recalcitrant nature and are commonly more recalcitrant than protein-like components [10].

In order to attain the European limits for discharge of wastewaters into waterbodies (Directive 91/271/CEE [11]), the content of organics, total nitrogen (on account of the ammonium ion), TSS and total phosphorous of the current leachate should be reduced. With regard to the Portuguese emission limits (Decree Law 236/98 [12]) colour, odour and total iron should be lowered in addition to the aforementioned parameters. With these required removals in mind, two multistep treatment approaches were tested. The first approach included: (i) an AOP/EAOP step for organics oxidation and biodegradability improvement (plus potential ammonium removal for certain AOPs/EAOPs), with possible impact on colour and odour removal, and (ii) a biological process stage for removal of the resulting biodegradable organics and, if needed, nitrogen species and total phosphorous. The second approach comprised: (i) a coagulation stage for decreasing organic and inorganic levels in order to boost the efficiency of a subsequent AOP/EAOP step, with likely impact on colour, odour, turbidity, TSS, total phosphorous and/or biodegradability, (ii) an AOP/EAOP step for recalcitrant organics oxidation and biodegradability enhancement (plus potential ammonium removal for certain AOPs/EAOPs), with probable colour and odour abatement, and (iii) a biological process stage for removal of the previously generated biodegradable organics and, if necessary, nitrogen species and total phosphorous. In both approaches, an additional clarification intermediate step taking place after the AOP/EAOP stage can be needed, aiming at the decrease of turbidity, TSS, total iron and total phosphorous. By default, coagulation and biological processes already include a clarification step.

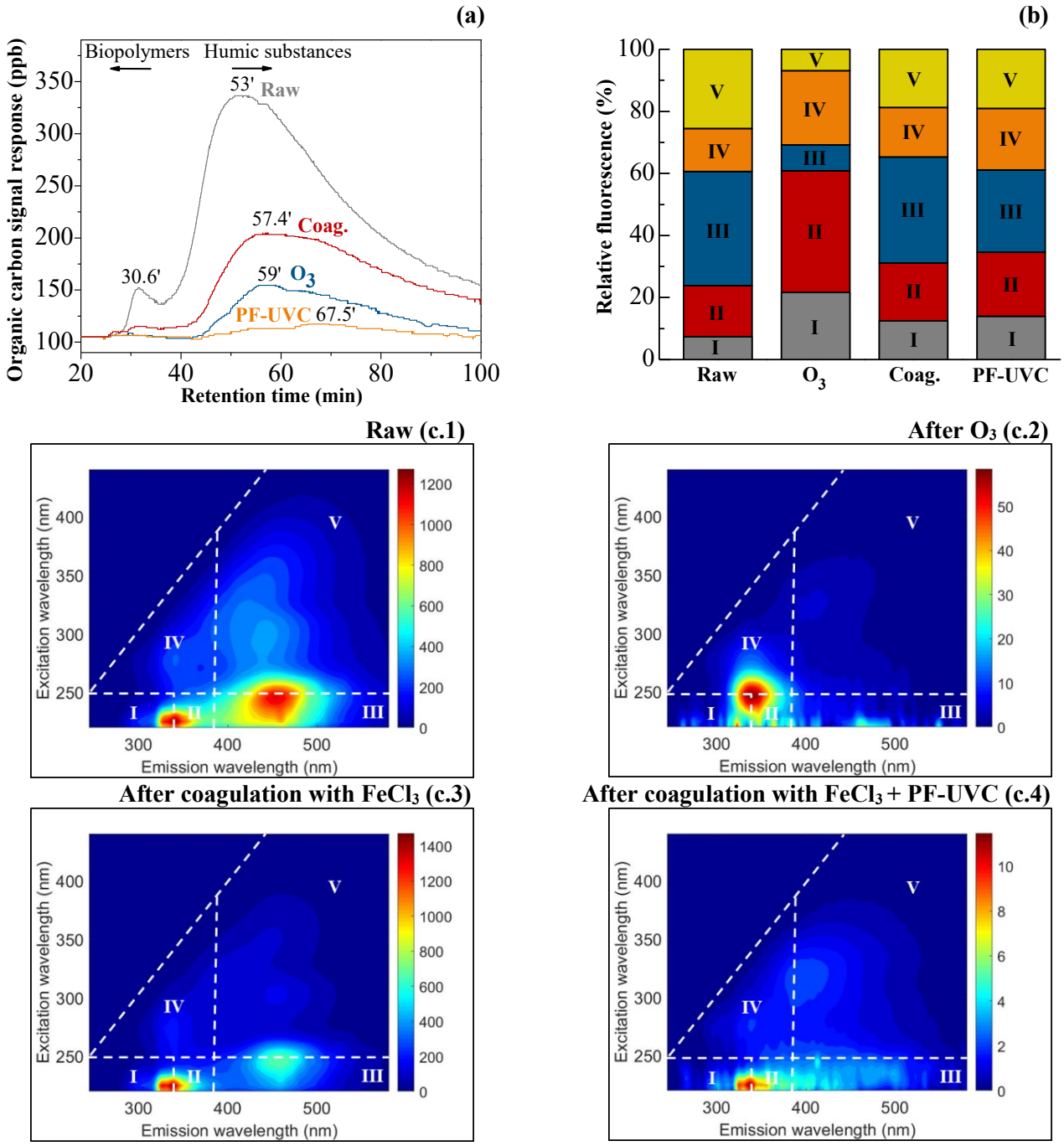

Figure 6.1 SEC-OCD chromatograms (a), relative fluorescence (b) and 3D-EEM spectra (c) for: the raw NHISWL leachate, the NHISWL leachate after ozonation process (conditions: O3 dose = 30 mg min-1, pH = 8.2, Temperature = 20±1 ºC, Treatment time = 7 h, sedimentation for 2 h and removal of O_3 sludge), the NHISWL leachate after coagulation with $FeCl_3$ (conditions: pH = 4.0, 300 mg Fe L^{-1} from $FeCl_3$ coagulant, sedimentation for 2 h, removal of coagulation sludge and neutralization to pH 7.0), and the NHISWL leachate after coagulation with $FeCl_3$ + PF-UVC process (conditions: pH = 4.0, H_2O_2 = ~100-500 mg L^{-1}, 11 W UVC lamp, TDI_0 = 115 mg L^{-1}, Temperature = 20±1 ºC, Treatment time = 4 h, neutralization to pH 7.0.

6.3.1 First approach: AOP/EAOP + biological process

6.3.1.1 AOP/EAOP

Six AOPs/EAOPs were applied to the raw NHISWL leachate: PF-UVC, AO, ozonation, O_3/H_2O_2, O_3/UVC and O_3/H_2O_2/UVC. Figure 6.2 shows the results of DOC decay, EC and TOD of these reactions and Table 6.2 shows the respective k_{DOC} values. An UVC blank experiment was also carried out (data not shown), providing no changes in the leachate and thus indicating null susceptibility of organics to direct UVC photolysis.

The PF-UVC process led to null organics mineralization (Figure 6.2a) but provided a visual change in the leachate colour to a darker shade after some minutes of reaction that persisted until the reaction end. This suggests that the oxidizing species available in the PF-UVC process were unable to mineralize organics but able to oxidize them to more colourful compounds, which is likely to have inhibited UVC light penetration through the solution. Oxidizing species may have included hydroxyl radicals ($HO^{\bullet}$) (E^{o} of 2.730 V/SHE) [13]) mainly generated by the homolytic cleavage of the peroxide bond (–O–O–) under UVC radiation via Eq. 1.6 [14]. The occurrence of H_2O_2 homolysis was evidenced by a large H_2O_2 consumption (1340 mg L^{-1} after 240 min of reaction – data not shown).

The production of $HO^{\bullet}$ via Fenton's reaction (Eq. 1.18), photoreduction of Fe(III)-hydroxy complexes via Eq. 1.23 [15] and direct photolysis of Fe^{3+}-organics complexes via general Eq. 1.24 [16] may not have occurred or occurred in very low extent taking into account the alkaline pH (~8.2) and the very small amount of TDI (1.8 mg L^{-1}) of the NHISWL leachate. It is known that Fenton's reaction is favoured at acidic pH (usually ~3) and higher TDI contents [15]. Probably, it should be about H_2O_2/UVC process instead of PF-UVC.

Conversely, the AO process promoted some organics mineralization (Fig. 6.2a, Table 6.2), which was more pronounced for a higher current density of 200 mA cm^{-2} compared to 50 mA cm^{-2} (24% *versus* 13% DOC removal after 240 min of reaction; k_{DOC} 1.9-fold higher). A similar effect of the current density on the AO process mineralization efficiency has been achieved for other landfill leachates [17, 18]. The AO process may have benefited from electrochemically generated $HO^{\bullet}$ [19], physisorbed at the BDD anode surface and denoted BDD($HO^{\bullet}$), and from electrochemically generated active chlorine species as a result of the leachate chloride content (1247 mg L^{-1}). At the pH of the AO process (~8.2), the predictable predominant active chlorine species corresponds to the weak hypochlorite ion (ClO^{-}) (E^{o} of 0.81 V/SHE [20]) produced via Eqs. 1.10-1.12 [21]. However, other active chlorine species may have been available, such as: aqueous chlorine (Cl_2) (Eq. 1.10 [19]), hypochlorous acid (HClO) (Eq. 1.11)

[19]), chlorine radical ($Cl^{\bullet}$) (Eq. 4.5 [22]), chlorite ion (ClO_2^-) (Eqs. 1.14 and 1.15 [23]), chlorate ion (ClO_3^-) (Eqs. 1.16 [23] and 4.6 [22]) and perchlorate ion (ClO_4^-) (Eq. 6.1 [23]). Despite the primarily presence of the weak ClO^-, the role played by active chlorine species in organics degradation may have been more critical than that of BDD($HO^{\bullet}$). This is because the production of the latter oxidant is expected to be hindered for alkaline pH close to 9 [24] and BDD anodes have a high overvoltage for chlorine formation that does not allow $HO^{\bullet}$ production prior to chlorine generation [25].

$$ClO_3^- + HO^{\bullet} \rightarrow ClO_4^- + H^+ + e^- \qquad 6.1$$

The higher mineralization rate for 200 mA cm^{-2} compared to 50 mA cm^{-2}, sustained by the larger rates of electrochemical reactions (Eqs. 6.1, 6.2, 1.10, 1.14-1.17), for higher current densities, brought with it much larger EC (Figure 6.2a.1) and less efficient use of energy, as given by the DOC decay data as a function of specific charge (data not shown). For the AO process with 50 and 200 mA cm^{-2}, a specific charge of 2.0 Ah L^{-1} (attained after 240 and 60 min of reaction, respectively) provided DOC removals of 13% and 6%, respectively, and a specific charge of ~18 Ah L^{-1} (reached after 1920 and 520 min of reaction, respectively - extended reactions) promoted DOC removals of 68% and 51%, respectively.

The ozonation process with an inlet O_3 dose of 30 mg min^{-1} provided an even higher DOC removal compared to the AO process with 200 mA cm^{-2} – 34% *versus* 20% DOC removal after 180 min of reaction (Figure 6.2a) and 1.9-fold higher k_{DOC} value (Table 6.2). This inlet O_3 dose promoted the fastest DOC removal among a set of three doses – 10, 20 and 30 mg min^{-1} (Figure 6.2a, Table 6.2). Higher mineralization values were achieved for higher O_3 doses, as reported by Gomes et al. [26] in the ozonation of a MSWL leachate using quite similar O_3 doses. Two main mechanisms should have caused the high ozonation process efficiency: (i) direct reaction pathway involving O_3 on account of its high redox potential (E^o of 2.076 V/SHE) [20]), which may have preferentially impacted unsaturated electron-rich bonds of specific functional groups (e.g. aromatics, olefins and amines) due to the selectivity of the O_3 attack [27], and (ii) indirect route involving various highly reactive species generated by O_3 decomposition at alkaline pH via Eqs. 1.27-1.40 [28], among which the powerful $HO^{\bullet}$ and also H_2O_2.

Despite the higher DOC removals for greater inlet O_3 doses, the O_3 consumption in terms of TOD was also superior (Figure 6.2a.2). Furthermore, while no O_3 was detected in the off-gas during reactions with 10 and 20 mg min^{-1}, the reaction with 30 mg min^{-1} brought along with the presence of O_3 in the off-gas from 60 min, reaching an O_3 off-gas content that represented 16% of the total O_3 fed to the system after 180 min (data not shown). It should also be mentioned that large amounts of foam were generated for

all the inlet O_3 doses and even larger quantities were formed for inlet O_3 doses above 30 mg min^{-1}, making it impossible to apply them.

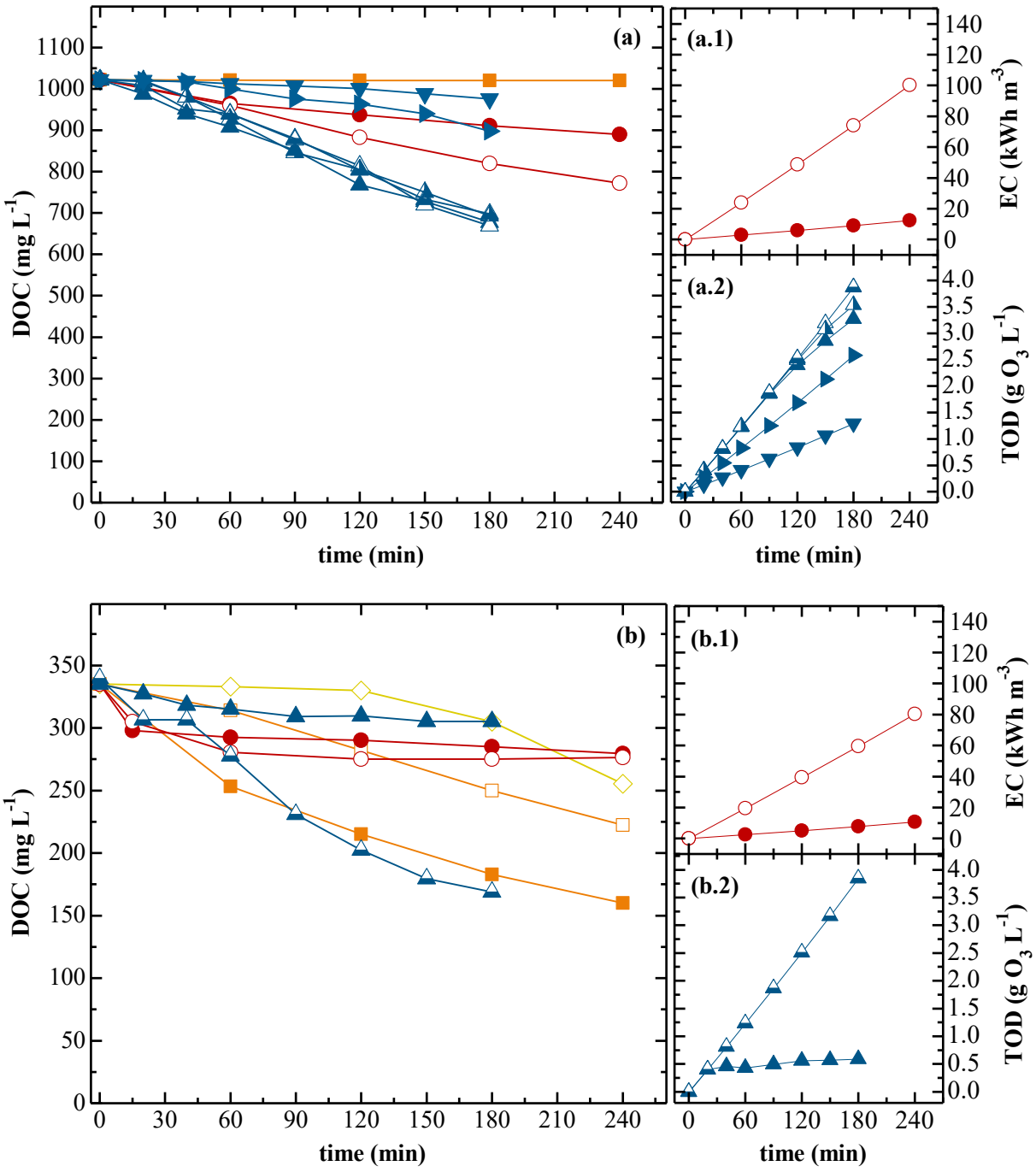

Figure 6.2 Comparison of various AOPs/EAOPs applied to the raw NHISWL leachate (a) and to the NHISWL leachate after coagulation with $FeCl_3$ (b). AOP/EAOP: PF-UVC (■), AO with current density = 50 mA cm^{-2} (●), AO with current density = 200 mA cm^{-2} (○), ozonation with inlet O_3 dose = 10 mg min^{-1} (▼), ozonation with inlet O_3 dose = 20 mg min^{-1} (▶), ozonation with inlet O_3 dose = 30 mg min^{-1} (▲), O_3/H_2O_2 (△), O_3/UVC (◭), O_3/H_2O_2/UVC (△), PF-UVC with 6 W UVC lamp (□), PF-UVA with 6 W UVA lamp (◇). Conditions: pH = 8.2 for the raw NHISWL leachate and pH = 4.0 for the NHISWL leachate after coagulation with $FeCl_3$; H_2O_2 = ~100-500 mg L^{-1}; TDI_0 = 1.8 mg L^{-1} for the raw NHISWL leachate and TDI_0 = 115 mg L^{-1} for the NHISWL leachate after coagulation with $FeCl_3$; 11 W UVC lamp (except when indicated); Inlet O_3 dose = 30 mg min^{-1} (except when indicated); Temperature = 20±1 ºC. EC: Energy consumption for electrochemical cell operation. TOD: Transferred O_3 dose.

Table 6.2 Pseudo-first-order kinetic constants for DOC removal (k_{DOC}) along with the time interval of reaction selected for fitting, coefficient of determination (R^2) and residual variance (S^2_R).

	Time (min)	k_{DOC} (x10^{-3} min^{-1})	S^2_R (mg^2 L^{-2})	R^2
Raw NHISWL leachate				
PF-UVC [a]	0-240	No fitting of a pseudo-first-order kinetic model to experimental data		
AO - 50 mA/cm² [b]	0-240	0.63±0.04	594	0.944
AO - 200 mA/cm² [c]	0-240	1.19±0.02	121	0.997
Ozonation - 10 mg/min [d]	0-180	0.22±0.02	135	0.928
Ozonation - 20 mg/min [e]	0-180	0.58±0.05	1258	0.909
Ozonation - 30 mg/min [f]	0-180	2.23±0.05	801	0.993
O_3/H_2O_2 - 30 mg/min [g]	0-180	2.1±0.1	7520	0.941
O_3/UVC - 30 mg/min [h]	0-180	2.0±0.1	3758	0.966
O_3/H_2O_2/UVC - 30 mg/min [i]	0-180	2.0±0.1	3306	0.969
NHISWL leachate after coagulation with $FeCl_3$				
PF-UVC [j]	0-240	3.4±0.2	602	0.968
PF-UVC - 6W UVC lamp [k]	0-240	1.60±0.08	160	0.981
PF-UVA - 6W UVA lamp [l]	0-240	No fitting of a pseudo-first-order kinetic model to experimental data		
AO - 50 mA/cm² [m]	0-240	No fitting of a pseudo-first-order kinetic model to experimental data		
AO - 200 mA/cm² [n]	0-240	No fitting of a pseudo-first-order kinetic model to experimental data		
Ozonation - 30 mg/min [o]	0-180	No fitting of a pseudo-first-order kinetic model to experimental data		
O_3/H_2O_2/UVC - 30 mg/min [p]	0-180	3.9±0.2	722	0.975

[a] Conditions: pH = 8.1, H_2O_2 = ~100-500 mg L^{-1}, 11W UVC lamp, TDI_0 = 1.8 mg L^{-1}, T = 20±1 ºC;
[b] Conditions: pH = 8.1, Current density = 50 mA cm^{-2}, TDI_0 = 1.8 mg L^{-1}, T = 20±1 ºC;
[c] Conditions: pH = 8.1, Current density = 200 mA cm^{-2}, TDI_0 = 1.8 mg L^{-1}, T = 20±1 ºC;
[d] Conditions: pH = 8.1, Inlet O_3 dose = 10 mg min^{-1}, TDI_0 = 1.8 mg L^{-1}, T = 20±1 ºC;
[e] Conditions: pH = 8.1, Inlet O_3 dose = 20 mg min^{-1}, TDI_0 = 1.8 mg L^{-1}, T = 20±1 ºC;
[f] Conditions: pH = 8.1, Inlet O_3 dose = 30 mg min^{-1}, TDI_0 = 1.8 mg L^{-1}, T = 20±1 ºC;
[g] Conditions: pH = 8.1, Inlet O_3 dose = 30 mg min^{-1}, H_2O_2 = ~100-500 mg L^{-1},TDI_0 = 1.8 mg L^{-1}, T = 20±1 ºC;
[h] Conditions: pH = 8.1, Inlet O_3 dose = 30 mg min^{-1}, 11 W UVC lamp,TDI_0 = 1.8 mg L^{-1}, T = 20±1 ºC;
[i] Conditions: pH = 8.1, Inlet O_3 = 30 mg min^{-1}, H_2O_2 = ~100-500 mg L^{-1}, 11W UVC lamp,TDI_0 = 1.8 mg L^{-1}, T = 20±1 ºC;
[j] Conditions: pH = 4.0, H_2O_2 = ~100-500 mg L^{-1}, 11 W UVC lamp, TDI_0 = 115 mg L^{-1}, T = 20±1 ºC;
[k] Conditions: pH = 4.0, H_2O_2 = ~100-500 mg L^{-1}, 6 W UVC lamp, TDI_0 = 115 mg L^{-1}, T = 20±1 ºC;
[l] Conditions: pH = 4.0, H_2O_2 = ~100-500 mg L^{-1}, 6 W UVA lamp, TDI_0 = 115 mg L^{-1}, T = 20±1 ºC;
[m] Conditions: pH = 4.0, Current density = 50 mA cm^{-2}, TDI_0 = 115 mg L^{-1}, T = 20±1 ºC;
[n] Conditions: pH = 4.0, Current density = 200 mA cm^{-2}, TDI_0 = 115 mg L^{-1}, T = 20±1 ºC;
[o] Conditions: pH = 4.0, Inlet O_3 dose = 30 mg min^{-1}, TDI_0 = 115 mg L^{-1}, T = 20±1 ºC;
[p] Conditions: pH = 4.0, Inlet O_3 = 30 mg min^{-1}, H_2O_2 = ~100-500 L^{-1}, 11 W UVC lamp,TDI_0 = 115 mg L^{-1}, T = 20±1 ºC.

O_3-based processes were carried out with an inlet O_3 dose of 30 mg min^{-1}. The three tested O_3-based processes – O_3/H_2O_2, O_3/UVC and O_3/H_2O_2/UVC – achieved similar DOC decays compared to the ozonation process (Figure 6.2a and Table 6.2) and also similar $SUVA_{254}$ and turbidity decays ($SUVA_{254}$ of ~0.6 L mg^{-1} m^{-1} and turbidity of ~5.5 NTU after 180 min of reaction – data not shown). This stands for similar degree of organics oxidation. In terms of O_3 content in the off-gas, the results differed: (i) while in the ozonation process the O_3 in the off-gas was detected from 60 min of reaction and the content of O_3 in the off-gas represented 16% of the total O_3 fed to the system at the reaction end, (ii) in the

O_3/UVC process the O_3 in the off-gas was detected only from 90 min of reaction and represented 8.6% of the total O_3 fed to the system at the reaction end, and (iii) in the O_3/H_2O_2 and O_3/H_2O_2/UVC processes there was no O_3 in the off-gas over the course of whole reactions (data not shown). Accordingly, O_3-driven processes can be ordered as follows in terms of O_3 consumption (Figure 6.2a.2): O_3/H_2O_2 = O_3/H_2O_2/UVC > O_3/UVC > ozonation. This means that some O_3-consuming reactions took place on a larger scale in the O_3-based processes than in the ozonation process. In fact, there may have been various reactions occurring on larger scale and the occurrence of some additional reactions. The totality of reactions taking place on larger scale may have included: (i) Eqs. 1.37 and 1.38, initiated by H_2O_2, (ii) the chain reactions comprising Eqs. 1.28-1.36, promoted by the higher rate of Eq. 1.37, and (iii) Eqs. 1.39 and 1.40, initiated/promoted by H_2O_2. New reactions may have included: (i) Eq. 1.6, initiated by UVC radiation, and (ii) the photodecomposition of O_3 under UVC light via Eq. 1.41 [29].

The enhancement of the rate of parasitic Eqs. 1.33-1.35, 1.39 and 1.40 in O_3-based processes may have caused the lack of oxidation improvement due to the waste of powerful oxidants to produce less powerful ones. Beyond that, in the presence of H_2O_2 the oxidative reactions may have preferentially occurred by $HO^{\bullet}$ attack and the O_3 oxidation reactions may have been hindered. The efficiency of the O_3-based processes depends on the composition of the landfill leachate, as evidenced by the distinct results attained by Gomes et al. [26] in the treatment of a MSWL leachate. For that leachate, the O_3/H_2O_2 process promoted a slightly higher DOC removal compared to ozonation process and the O_3/UVC process contributed to an even slightly higher DOC decay than the O_3/H_2O_2 process.

Taking into consideration all the results, the ozonation process with an inlet O_3 dose of 30 mg min^{-1} could be selected as the best AOP/EAOP for application to the raw NHISWL leachate. The physicochemical characteristics of the leachate upon the application of an extended 7-h duration ozonation process followed by sedimentation for 2 h and removal of the generated sludge can be accessed in Table 6.1. Organics oxidation came along with the reduction of colour, odour and TSS to levels below European and Portuguese discharge limits (Directive 91/271/CEE and Decree Law 236/98) and biodegradability improvement (49% increase according to the Zhan-Wellens test). Beyond that, Table 6.1 discloses an ammonium decay along with a nitrate raise upon the ozonation process, likely due to the occurrence of Eq. 6.2 [30]. This reaction may have occurred at low rate at the reaction pH (~8). Additionally, the removal of some organic nitrogen, total phosphorous and total iron occurred (total phosphorous and total iron reduced to values below the Portuguese discharge limits).

$$NH_4^+ + 4O_3 \rightarrow NO_3^- + 4O_2 + H_2O + 2H^+ \qquad 6.2$$

Figure 6.1a shows a drastic reduction of humic substances content upon the ozonation process application. This was corroborated by a reduction of total fluorescence in ~96% (from $3.7x10^7$ to $1.3x10^6$ R.U. nm^2) and also by the relative fluorescence intensities (Figure 6.1b) and the 3D-EEM contour (Figure 6.1c.2), which reveal a severe decrease of fulvic-like acids (regions III) and humic-like acids (region V). With the decrease of fulvic-like and humic-like acids content, the relative content of aromatic proteins (regions I and II) and soluble microbial metabolic by-products (region IV, according to Chen et al. [9]) has increased.

6.3.1.2 Biological process

Samples collected after 4, 5 and 7 h of the ozonation process with an inlet O_3 dose of 30 mg min^{-1} were used to assess the feasibility of an ensuing biological process. To this end, a Zhan-Wellens test was conducted. Table 6.3 displays the data of organic load before (day 0) and after (day 28) the Zhan-Wellens test and of D_t upon the Zhan-Wellens. Decreasing organic loads at day 0 for longer O_3 treatment times were accompanied by slightly higher D_t upon 28 days of Zhan-Wellens test, giving rise to increasingly lower organic loads after the biological treatment as the ozonation process progressed. But even the application of the ozonation process for 7 h was unable to provide a low COD value after biological treatment (COD of 349 mg O_2 L^{-1}). Since European and Portuguese legislation for discharge of wastewaters into waterbodies (Directive 91/271/CEE and Decree Law 236/98) demand COD values of 125 and 150 mg O_2 L^{-1}, respectively, it would be necessary to extend the ozonation process for more than 7 h to fulfil the legislation requirements. This confers unsuitability to the application of a treatment approach comprising an ozonation process followed by a biological process for the current NHISWL leachate. Nevertheless, this approach was able to provide the fulfilment of colour, odour, TSS, sulphate, total phosphorous and total iron requirements (see the detailed physicochemical characterization of leachate after 7-h duration ozonation process followed by biological treatment in Table 6.1). It should also be highlighted that the imposed discharge limits of ammonium, nitrate and total nitrogen have not been met. This can be achieved through the optimization of the biological process operating conditions to enable nitrification/denitrification, which can encompass the provision of an external carbon source to ensure a favourable C/N ratio [31]. Furthermore, the inclusion of an air stripping step for ammonium removal prior to the biological treatment can be considered [32].

6.3.2 Second approach: Coagulation process + AOP/EAOP + biological process

6.3.2.1 Coagulation process

Two coagulants were tested: $FeCl_3$ and $Al_2(SO_4)_3$. $FeCl_3$ was chosen due to the good results that have been achieved with this salt in the treatment of landfill leachates [33] and, in addition, iron can be used as catalyst in subsequent Fenton's reaction based processes. $Al_2(SO_4)_3$ corresponds to the most commonly used coagulant in the world. For both coagulants, the optimum pH and the optimum coagulant dosage were determined taking due account of changes in DOC, colour and turbidity (and also in TDI for the $FeCl_3$ coagulant). Looking at the $FeCl_3$ coagulant results, Figure 6.3a.1 and a.2 show maximum DOC, colour and turbidity abatements for pH 4.0 and 300 mg Fe L^{-1} together with a moderate TDI content (115 mg L^{-1}), proposing these pH and coagulant dose as optimum.

Table 6.3 Results of the Zahn-Wellens test for samples from the ozonation process applied to the raw NHISWL leachate and for samples from the PF-UVC process applied to the NHISWL leachate after coagulation with $FeCl_3$.

	Raw NHISWL leachate	**Raw NHISWL leachate subjected to ozonation process for a given time**		
		4 h (240 min)	**5 h (300 min)**	**7 h (420 min)**
D_t (day 28) (%)	18	58	61	67
DOC (day 0) (mg L^{-1})	1012	630	550	410
DOC (day 28) (mg L^{-1})	822	273	180	140
COD (day 0) (mg L^{-1})	2513	1941	1704	1299
COD (day 28) (mg L^{-1})	2149	696	566	349
	Coagulated NHISWL leachate	**NHISWL leachate after coagulation with $FeCl_3$ subjected to PF-UVC process for a given time**		
		4 h (240 min)	**6 h (360 min)**	**8 h (480 min)**
D_t (day 28) (%)	32	85	83	78
DOC (day 0) (mg L^{-1})	330	147	110	90
DOC (day 28) (mg L^{-1})	245	31	27	27
COD (day 0) (mg L^{-1})	911	563	375	328
COD (day 28) (mg L^{-1})	696	122	107	109

Note 1: Some DOC and COD values are slightly lower than those in Table 1 and Fig. 6.2 due to subtle samples dilution for Zhan-Wellens test execution;
Note 2: Both day 0 and day 28 samples were subjected to sedimentation for 2 h followed by removal of the generated sludge prior to characterization.

A TDI of 115 mg L^{-1} content may not be high enough to hinder the efficiency of light-assisted AOPs/EAOPs due to the occurrence of: (i) undesirable reactions, such as Eq. 1.22 [34], (ii) inner filter effects, i.e. competition for photons between photo-activators and light-absorbing compounds, including some iron species, and/or (iii) light attenuation through the optical pathlength of the photoreactor. Analysing the $Al_2(SO_4)_3$ coagulant results, Figure 6.3b.1 indicates maximum and identical DOC and turbidity removals for pH 4.5 and 5.0 together with a slightly higher colour decay for pH 5.0 in

comparison to pH 4.5. Thus, pH 5.0 was selected as optimum. Figure 6.3b.2 shows a maximum DOC decay for 300 mg Al L^{-1} along with only slightly larger colour and turbidity removals for 400 mg Al L^{-1}, pointing to the choice of a $Al_2(SO_4)_3$ coagulant dosage of 300 mg Al L^{-1} as optimum.

For both coagulants, the feasibility of using a flocculant was assessed under optimum coagulation conditions (pH 4.0 and 300 mg Fe L^{-1} for $FeCl_3$ and pH 5.0 and 300 mg Al L^{-1} for $Al_2(SO_4)_3$). Dosages of 2-10 mg L^{-1} of cationic polyacrylamide Ambifloc C 58 and of anionic polyacrylamide Magnafloc 155 had no influence on the NHISWL leachate physicochemical characteristics for both coagulants (data not shown).

Particular emphasis can be given to the following effects of coagulation with $FeCl_3$ and $Al_2(SO_4)_3$ under optimum conditions on the NHISWL leachate (Table 6.1): (i) removal of a fraction of organics, more sharply for the $FeCl_3$ coagulant (DOC removal of 67% *versus* 57% (>10%), COD removal of 65% *versus* 48% (>17%)), (ii) removal of colour, more pronounced for the $FeCl_3$ coagulant (88% *versus* 79% (>9%)), although colour has not been detected for a 1:20 dilution for both coagulants, (iii) reduction of odour from strong to moderate for both coagulants, but still detected for a 1:20 dilution, (iv) increase in biodegradability to a greater extent for the $FeCl_3$ coagulant (14% *versus* 7% (>7%)), (v) reduction of turbidity, slightly greater for the $FeCl_3$ coagulant (67% *versus* 58% (>9%)), along with no change in TSS content for both coagulants, (vi) increase of ~52% in conductivity/salinity for both coagulants, mainly due to chloride increment for the $FeCl_3$ coagulant (because of acidification with HCl and chloride from the coagulant itself) and due to chloride and sulphate increase for the $Al_2(SO_4)_3$ coagulant (because of acidification with HCl and sulphate from the coagulant itself), (vii) sharp alkalinity decay for both coagulants in virtue of acidification, and (viii) removal of phosphorous, more pronounced for the $Al_2(SO_4)_3$ coagulant (65% *versus* 47% (>18%)).

The greater removal of organics, colour and turbidity for the $FeCl_3$ coagulant along with a steeper biodegradability increase suggests a better charge neutralization of the negatively charged sites of the humic acids in the presence of Fe^{3+} ions instead of Al^{3+} ions. On the other hand, the slightly higher phosphorous removal for the $Al_2(SO_4)_3$ coagulant proposes a better charge neutralization of phosphorous compounds and/or the removal of higher amounts of organics with attached phosphorous in the presence of Al^{3+} ions. The fact that the removal of turbidity has not been accompanied by the removal of TSS indicates that the coagulation process was able to remove dissolved coloured material, such as humic substances, but not particles larger than 1.2 μm (filter size), or that some large insoluble particles may have been generated by chemical addition, counteracting the removal of solids initially present in the NHISWL leachate.

On the basis of the achieved results, the $FeCl_3$ coagulant was chosen as the best coagulant. It provided not only greater removal of organics, colour and turbidity and more pronounced biodegradability increment, but also a content of TDI that can be used in further AOPs/EAOPs based on Fenton's reaction. Superiority of the $FeCl_3$ coagulant over the $Al_2(SO_4)_3$ coagulant was also achieved for other landfill leachates [35, 36].

The SEC-OCD chromatogram of the NHISWL leachate after coagulation with $FeCl_3$ (Figure 6.1a) shows that humic substances still prevail in the leachate but in much lower amount. This was corroborated by a total fluorescence decay of ~40% (from $3.7x10^7$ to $2.2x10^7$ R.U. nm^2), the relative fluorescence intensities (Figure 6.1b) and the 3D-EEM contour (Figure 6.1c.3), in which a reduction of humic-like acids (region V) and fulvic-like acids (region III) was more evident.

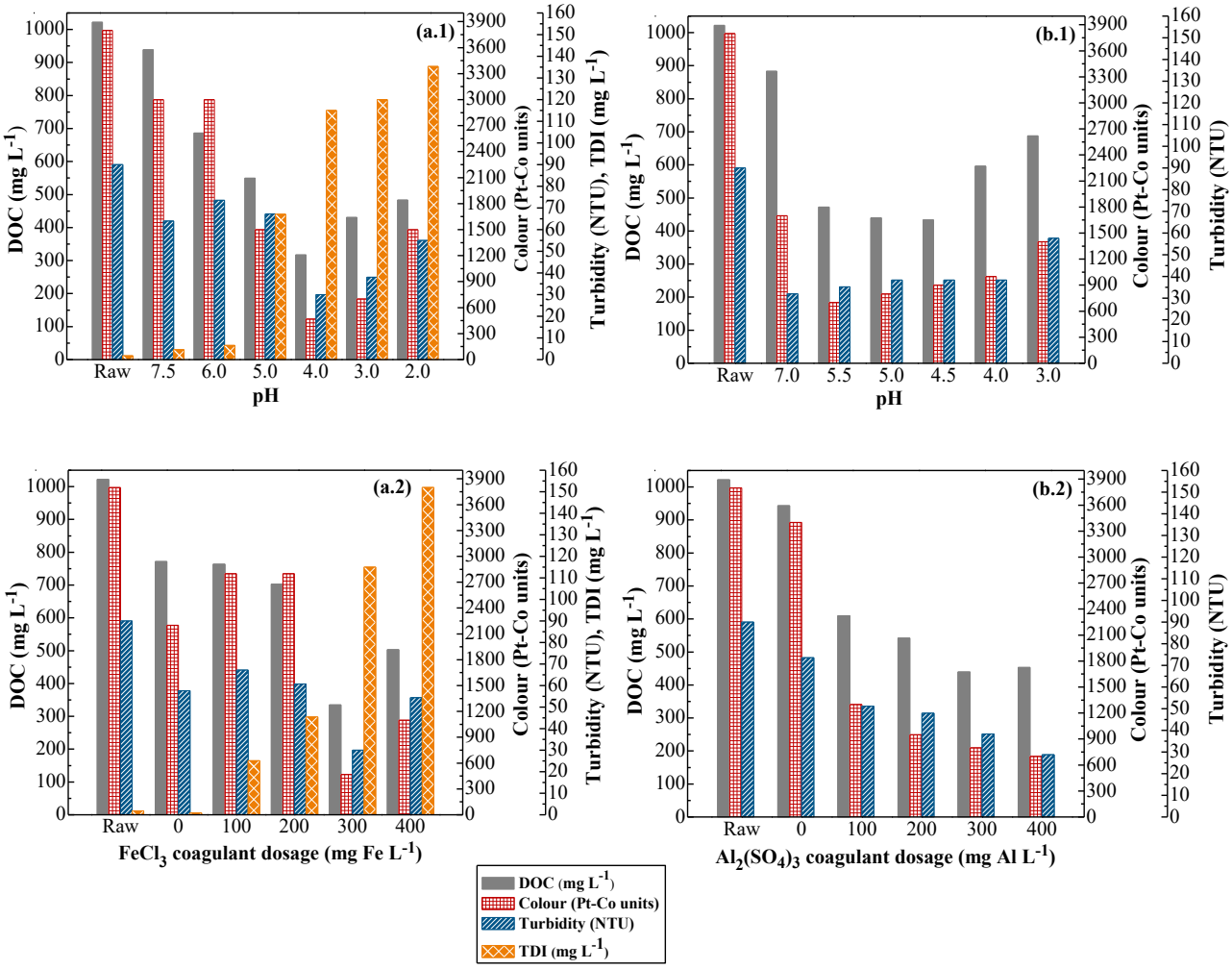

Figure 6.3 Effect of pH and coagulant dosage on the coagulation process applied to the raw NHISWL leachate using $FeCl_3$ (a) or $Al_2(SO_4)_3$ (b) coagulant. Conditions: effect of pH assessed for a coagulant dosage of 300 mg L^{-1} of Fe or Al; effect of $FeCl_3$ coagulant dosage assessed for pH 4.0; effect of $Al_2(SO_4)_3$ coagulant dosage assessed for pH 5.0. Raw: without any treatment.

6.3.2.2 AOP/EAOP

Five AOPs/EAOPs were applied to the NHISWL leachate upon coagulation with $FeCl_3$ (Figure 6.3b): PF-UVC, AO, ozonation, O_3/H_2O_2/UVC and PF-UVA. Figure 6.3 displays the results of DOC decay, EC and TOD of these processes and Table 6.2 shows the respective k_{DOC} values. Additional UVC and UVA blank experiments promoted null organics degradation (data not shown), pointing to absence of UVC and UVC direct photolysis.

Figure 6.2b shows that the ozonation process with an inlet O_3 dose of 30 mg min^{-1} provided almost null DOC removal. This can be mainly attributed to the hindering of indirect oxidation routes from O_3 decomposition (Eqs. 1.27-1.40)q\aq at the leachate acidic pH. Additionally, O_3, as a selective oxidant, may have been unable to directly oxidize the organics of the coagulated NHISWL leachate, and the reaction of Fe^{3+} (TDI content of the coagulated NHISWL leachate of 115 mg L^{-1}) with O_3 via Eq. 5.14 [37] along with the production of $HO^{\bullet}$ and ferryl ion ($(FeO)^{2+}$) oxidant may have been negligible. The low reactivity of O_3 was confirmed by the poor O_3 consumption along the reaction (Figure 6.2b.2). Although in very low extent, in consideration of the low reactivity of O_3, this oxidant may have been quenched by chloride according to Eqs. 5.12 and 5.13 [38] taking into account the high chloride content of the coagulated leachate (5259 mg L^{-1}).

The AO process using current densities of 50 and 200 mA cm^{-2} provided 6-11% DOC decay during the first 15 min of reaction (Figure 6.2b), probably due to mineralization of simple organics and/or organics precipitation because of pH reduction from 4.0 to ~3.5 (data not shown) likely in virtue of carboxylic acids formation. Afterwards, mineralization remained very slight until the reaction end (~17% after 240 min of reaction for both current densities). From the obtained results, one can instigate that BDD($HO^{\bullet}$) produced via Eq. 6.1, and the estimated large amount of active chlorine species obtained from leachate chloride content (5259 mg L^{-1}) were unable to largely degrade the organics of the NHISWL leachate. Note that the predominant active chlorine species at the reaction pH (3.4-4.0) was the highly powerful HClO (E^{o} of 1.49 V/SHE [20]) generated via Eqs. 1.10 and 1.11.

By contrast, PF-UVC and O_3/H_2O_2/UVC processes employing an 11 W UVC lamp provided sharp and similar DOC decays (45% and 50% after 180 min of reaction) (Fig. 6.2b, Table 6.2). Organics may have been degraded mainly by $HO^{\bullet}$ in the bulk produced by two main mechanisms: H_2O_2 homolysis (Eq. 1.6 and Fenton's reaction (Eq. 1.18, enhanced by light via Eqs. 1.23 and 1.24. Note that the amount of TDI was much higher for the coagulated NHISWL leachate (115 mg L^{-1}) compared to the raw NHISWL leachate (1.8 mg L^{-1}) and the pH was acidic for the coagulated leachate (4.0) in contrast to the alkaline

pH of the raw leachate (8.2). Thus, the occurrence of Fenton's reaction (Eq. 1.18, 1.23, and 1.24) is expected to have occurred in much greater extent for the coagulated leachate. The participation of O_3 in organics oxidation must have been negligible, mainly due to the impairing of indirect oxidation routes from O_3 decomposition (Eqs. 1.27-1.40) at the leachate acidic pH, in corroboration with the results achieved for ozonation. Despite this, the photodecomposition of O_3 under UVC light via Eq. 1.41 may have occurred, explaining the high O_3 consumption for the O_3/PF-UVC process (Figure 6.2b2). The reaction of Fe^{2+}, generated from Fe^{3+} in the presence of light mainly via Eqs. 1.23 and 1.24, with O_3 together with the production of $HO^{\bullet}$ and $(FeO)^{2+}$, according to Eqs. 5.3-5.7 [37, 39], may have been negligible taking into account the inability of O_3 in improving the PF-UVC process.

Additional PF-UVC and PF-UVA processes carried out with 6 W lamps achieved much lower DOC decays. This was more evident for the PF-UVA process, which was characterized by an initial induction period of ~120 min with no DOC decay (Figure 6.2b). This reveals: (i) the generation of insufficient photons by the 6 W UVC lamp to maximize H_2O_2 homolysis (Eq. 1.6) and Fenton's reaction (Eq. 1.18) (ii) the hindering of H_2O_2 photolysis under UVA light, and/or (iii) difficulty of UVA photons to penetrate the leachate.

All the aforementioned results point to the selection of PF-UVC process as the best AOP/EAOP for application to the coagulated NHISWL leachate. The physicochemical characteristics of the leachate upon the application of coagulation with $FeCl_3$ followed by PF-UVC process for 4 h, neutralization to pH 7.0, sedimentation for 2 h and removal of PF-UVC sludge can be accessed in Table 6.1. The removal of organic compounds was accompanied by odour and TSS removal to levels below European and Portuguese discharge limits (Directive 91/271/CEE and Decree Law 236/98) and biodegradability enhancement (53% increase according to the Zhan-Wellens test). Colour was also reduced but was already in agreement with legislation requirements before PF-UVC application. Additionally, total iron was successfully removed by precipitation to a value below 2.0 mg L^{-1} (Portuguese discharge limit) and total phosphorous was removed to a value below 1 mg L^{-1} (European discharge limit). Nitrogen species remained almost unaffected upon PF-UVC application. Figure 6.1a discloses a large drop in the organic content upon PF-UVC process application and the total fluorescence corroborates this finding since it was reduced in ~99% (from $2.2x10^7$ to $2.2x10^5$ R.U. nm^2). With regard to the physicochemical characteristics of the remaining fluorescent organics, they did not substantially differ from those of the coagulated leachate (Figure 6.2b and Figure 6.2c.4).

Differences between AOPs/EAOPs applied to the raw and the coagulated NHISWL leachate mainly refer to PF-UVC, ozonation and AO processes and can be easily related to the leachates intrinsic

properties. The PF-UVC process provided a highly deeper DOC decay for the coagulated leachate in virtue of the leachate pH (4.0 versus 8.2) and TDI (115 versus 1.8 mg L^{-1}). Acidic pH and high TDI are known for being contributors to Fenton's reaction (Eq. 1.18). The ozonation process promoted a higher degree of mineralization for the raw leachate that can be mainly attributed to the alkaline leachate pH since it favours O_3 decomposition with consequent generation of reactive species (Eqs. 1.27-1.40) The AO process provided higher DOC removal for the raw leachate likely due to the presence of easily degradable organic compounds in this leachate. The EC for the raw leachate was, however, a little bit higher (Figure 6.2b.1) as a result of the lower leachate conductivity/salinity (15 mS cm^{-1}/8.9 g L^{-1} *versus* 22 mS cm^{-1}/14 g L^{-1}). With regard to the best AOP/EAOP for each leachate (ozonation process for the raw leachate and PF-UVC process for the coagulated leachate), one can highlight the more pronounced DOC decay for the coagulated leachate (k_{DOC} 1.7-fold higher - Table 6.2).

6.3.2.3 Biological process

Samples collected after 4, 6 and 8 h of the PF-UVC process were subjected to a Zhan-Wellens test in order to assess the feasibility of applying a biological process. Table 6.3 collects the data of organic load before (day 0) and after (day 28) the Zhan-Wellens test and of D_t at day 28. Organic loads at day 0 decreased for longer PF-UVC treatment times and came along with slightly decreasing D_t after 28 days of Zhan-Wellens. This resulted in quite similar final organic loads for the different treatment times (COD of 107-122 mg O_2 L^{-1}). The achieved COD values were all below the European and Portuguese requirements for discharge of wastewaters into waterbodies - 125 and 150 mg O_2 L^{-1}, respectively (Directive 91/271/CEE and Decree Law 236/98) and thus the application of a 4-h duration PF-UVC process followed by a biological process had proved sufficient for the fulfilment of the legislation requirements as regards organics. The detailed physicochemical characterization of the leachate after 4 h of PF-UVC process followed by biological treatment can be accessed in Table 6.1. The discharge limit of ammonium, and consequently of total nitrogen, has not been met, pointing to the need to change the biological treatment operational conditions in order to enable nitrification/denitrification reactions or to carry out air stripping prior to the biological treatment. The fulfilment of all the other parameters imposed by the legislation had been met in previous stages.

6.4 Conclusions

The best treatment train for the NHISWL leachate included: (i) coagulation with $FeCl_3$ (conditions: pH 4.0, coagulant dosage of 300 mg Fe L^{-1}) for partial removal of organics, along with direct impact on colour, odour and turbidity removal and biodegradability enhancement, and also for partial removal of

phosphorous, (ii) PF-UVC process (conditions: pH 4.0, TDI of 115 mg L^{-1} provided by $FeCl_3$ coagulant, 4-h duration) for recalcitrant organics oxidation, with consequent colour and odour abatement and biodegradability enhancement, coupled to a subsequent clarification stage for removal of TSS, turbidity, iron and phosphorous, and (iii) biological process for removal of the previously generated biodegradable organics and nitrogen compounds. Upon treatment, the leachate fulfilled European and Portuguese requirements for discharge into aquatic systems except for ammonium, and thus for total nitrogen. This points to the need to change biological treatment operational conditions in order to enable nitrification/denitrification or to add an air stripping stage for ammonium removal prior to the biological treatment. The use of coagulation prior to the AOP/EAOP stage has proved indispensable for the fulfilment of the legislation demands. The developed treatment strategy can be suitable for the remediation of a wide range of ISWL leachates with low biodegradability and low/moderate content of organics and salts.

6.5 References

[1] L. Di Palma, P. Ferrantelli, C. Merli, E. Petrucci, Treatment of industrial landfill leachate by means of evaporation and reverse osmosis, Waste Management, 22 (2002) 951-955.

[2] J.J. Schoeman, A. Steyn, M. Makgae, Evaluation of electrodialysis for the treatment of an industrial solid waste leachate, Desalination, 186 (2005) 273-289.

[3] A.D. Webler, F.C. Moreira, M.W.C. Dezotti, C.F. Mahler, I.D.B. Segundo, R.A.R. Boaventura, V.J.P. Vilar, Development of an integrated treatment strategy for a leather tannery landfill leachate, Waste Management, 89 (2019) 114-128.

[4] F.C. Moreira, J. Soler, A. Fonseca, I. Saraiva, R.A.R. Boaventura, E. Brillas, V.J.P. Vilar, Incorporation of electrochemical advanced oxidation processes in a multistage treatment system for sanitary landfill leachate, Water Research, 81 (2015) 375-387.

[5] O. Primo, M.J. Rivero, I. Ortiz, Photo-Fenton process as an efficient alternative to the treatment of landfill leachates, Journal of Hazardous Materials, 153 (2008) 834-842.

[6] E. Torres-Socías, L. Prieto-Rodríguez, A. Zapata, I. Fernández-Calderero, I. Oller, S. Malato, Detailed treatment line for a specific landfill leachate remediation. Brief economic assessment, Chemical Engineering Journal, 261 (2015) 60-66.

[7] E. Kattel, A. Kivi, K. Klein, T. Tenno, N. Dulova, M. Trapido, Hazardous waste landfill leachate treatment by combined chemical and biological techniques, Desalination and Water Treatment, 57 (2016) 13236-13245.

[8] A.Ž. Gotvajn, T. Tišler, J. Zagorc-Končan, Comparison of different treatment strategies for industrial landfill leachate, Journal of Hazardous Materials, 162 (2009) 1446-1456.

[9] W. Chen, P. Westerhoff, J.A. Leenheer, K. Booksh, Fluorescence excitation−emission matrix regional integration to quantify spectra for dissolved organic matter, Environmental Science & Technology, 37 (2003) 5701-5710.

[10] L. Yang, H.S. Shin, J. Hur, Estimating the concentration and biodegradability of organic matter in 22 wastewater treatment plants using fluorescence excitation emission matrices and parallel factor analysis, Sensors (Basel, Switzerland), 14 (2014) 1771-1786.

[11] The Council of the European Union, Council Directive 91/271/EEC of 21 May 1991 concerning urban waste-water treatment, Official Journal of the European Communities., 1991.

[12] Portuguese Ministry of the Environment, Decree Law 236/98 of 1st August - Appendix XVIII, Official Gazette of Portugal, Series I-A (1995).

[13] D.A. Armstrong, R.E. Huie, W.H. Koppenol, S.V. Lymar, G. Merényi, P. Neta, B. Ruscic, D.M. Stanbury, S. Steenken, P. Wardman, Standard electrode potentials involving radicals in aqueous solution: Inorganic radicals (IUPAC Technical Report), pac, 87 (2015) 1139-1150.

[14] J.H. Baxendale, J.A. Wilson, The photolysis of hydrogen peroxide at high light intensities, Transactions of the Faraday Society, 53 (1957) 344-356.

[15] Y. Sun, J.J. Pignatello, Photochemical reactions involved in the total mineralization of 2,4-D by $Fe^{3+}/H_2O_2/UV$, Environmental Science & Technology, 27 (1993) 304-310.

[16] O. Horváth, K.L. Stevenson, Charge Transfer Photochemistry of Coordination Compounds, VCH, New York, 1992.

[17] A. Fernandes, M.J. Pacheco, L. Ciríaco, A. Lopes, Anodic oxidation of a biologically treated leachate on a boron-doped diamond anode, Journal of Hazardous Materials, 199-200 (2012) 82-87.

[18] Á. Anglada, A. Urtiaga, I. Ortiz, D. Mantzavinos, E. Diamadopoulos, Boron-doped diamond anodic treatment of landfill leachate: Evaluation of operating variables and formation of oxidation by-products, Water Research, 45 (2011) 828-838.

[19] M. Panizza, G. Cerisola, Direct And mediated anodic oxidation of organic pollutants, Chemical Reviews, 109 (2009) 6541-6569.

[20] D.R. Lide, Handbook of Chemistry and Physics, 84th edition, CRC Press, Boca Raton, 2004.

[21] D.C. Harris, Exploring Chemical Analysis, 4rd edition, W. H. Freeman and Company, New York, 2009.

[22] E. Mostafa, P. Reinsberg, S. Garcia-Segura, H. Baltruschat, Chlorine species evolution during electrochlorination on boron-doped diamond anodes: In-situ electrogeneration of Cl_2, Cl_2O and ClO_2, Electrochimica Acta, 281 (2018) 831-840.

[23] A. Sánchez-Carretero, C. Sáez, P. Cañizares, M.A. Rodrigo, Electrochemical production of perchlorates using conductive diamond electrolyses, Chemical Engineering Journal, 166 (2011) 710-714.

[24] T. Enache, A.M.C. Paquim, O. Fatibello-Filho, A. Oliveira-Brett, Hydroxyl radicals electrochemically generated in situ on a boron-doped diamond electrode, Electrochemistry Communications, 11 (2009) 1342.

[25] T. Muddemann, A. Bulan, M. Sievers, U. Kunz, Avoidance of chlorine formation during electrolysis at boron-doped diamond anodes in highly sodium chloride containing and organic-polluted wastewater, Journal of The Electrochemical Society, 165 (2018) J3281-J3287.

[26] A.I. Gomes, T.F. Soares, T.F.C.V. Silva, R.A.R. Boaventura, V.J.P. Vilar, Ozone-driven processes for mature urban landfill leachate treatment: Organic matter degradation, biodegradability enhancement and treatment costs for different reactors configuration, Science of The Total Environment, 724 (2020) 138083.

[27] J. Hoigné, H. Bader, Rate constants of reactions of ozone with organic and inorganic compounds in water-II: Dissociating organic compounds, Water Research, 17 (1983) 185-194.

[28] H. Tomiyasu, H. Fukutomi, G. Gordon, Kinetics and mechanism of ozone decomposition in basic aqueous solution, Inorganic Chemistry, 24 (1985) 2962-2966.

[29] F.J. Beltran, Ozone–UV radiation–hydrogen peroxide oxidation technologies, in: M.A. Tarr (Ed.) Chemical Degradation Methods for Wastes and Pollutants - Environmental and Industrial Applications, Marcel Dekker, Inc., New York, 2003, pp. 1-77.

[30] S.H. Lin, Y.L. Yen, Ammonia and nitrite removal from sea water by ozonation, Environmental Technology, 18 (1997) 65-73.

[31] J.-J. Her, J.-S. Huang, Influences of carbon source and C/N ratio on nitrate/nitrite denitrification and carbon breakthrough, Bioresource Technology, 54 (1995) 45-51.

[32] M. de Carluccio, A. Fiorentino, L. Rizzo, Multi-barrier treatment of mature landfill leachate: effect of Fenton oxidation and air stripping on activated sludge process and cost analysis, Journal of Environmental Chemical Engineering, 8 (2020) 104444.

[33] E. Diamadopoulos, Characterization and treatment of recirculation-stabilized leachate, Water Research, 28 (1994) 2439-2445.

[34] S. Malato, P. Fernández-Ibáñez, M.I. Maldonado, J. Blanco, W. Gernjak, Decontamination and disinfection of water by solar photocatalysis: Recent overview and trends, Catalysis Today, 147 (2009) 1-59.

[35] H.A. Aziz, S. Alias, M.N. Adlan, Faridah, A.H. Asaari, M.S. Zahari, Colour removal from landfill leachate by coagulation and flocculation processes, Bioresource Technology, 98 (2007) 218-220.

[36] E. Marañón, L. Castrillón, Y. Fernández-Nava, A. Fernández-Méndez, A. Fernández-Sánchez, Coagulation–flocculation as a pretreatment process at a landfill leachate nitrification–denitrification plant, Journal of Hazardous Materials, 156 (2008) 538-544.

[37] K. Chandrasekara Pillai, T.O. Kwon, I.S. Moon, Degradation of wastewater from terephthalic acid manufacturing process by ozonation catalyzed with Fe^{2+}, H_2O_2 and UV light: Direct versus indirect ozonation reactions, Applied Catalysis B: Environmental, 91 (2009) 319-328.

[38] C. Tizaoui, L. Bouselmi, L. Mansouri, A. Ghrabi, Landfill leachate treatment with ozone and ozone/hydrogen peroxide systems, Journal of Hazardous Materials, 140 (2007) 316-324.

[39] B. Legube, N. Karpel Vel Leitner, Catalytic ozonation: a promising advanced oxidation technology for water treatment, Catal. Today, 53 (1999) 61-72.

7 Final Remarks

This last chapter presents the most relevant results and conclusions reported in the previous chapters, as well as some suggestions for future work.

7.1 Conclusions

It was remarkably challenging to develop suitable treatment strategies for both HISWL and NHISWL leachates towards final satisfactory effluents. The HISWL leachate exhibited large/moderate amounts of organic matter with low biodegradability and was notably rich in sulphur compounds (sulphate, sulphite and sulphide) and chloride ions (Table 7.1). The NHISWL leachate presented moderate content of organics with low biodegradability and moderate content of salts (Table 7.1). Furthermore, the organic matter composition in the two leachates was distinct: while in the raw HISWL leachate there was a prevalence of aromatic proteins (~68%), with humic substances representing less than 10% of the total organics, in the NHISWL leachate there was a predominance of humic substances (~68%), and aromatic proteins contributed to ~24% of total organics (Table 7.1).

Table 7.1 Comparison of some physico-chemical characteristics of the HISWL and NHISWL leachates.

Parameters	Leachate		
	HISWL (Chapters 3 and 4)	**HISWL (Chapter 5)**	**NHISWL (Chapter 6)**
DOC (mg L^{-1})	2318	966	1022
COD (mg O_2 L^{-1})	7063	2809	2667
Biodegradability – Zhan-Wellens (%)	15	12	18
Fulvic-like acids (%)	-	6	37
Humic-like acids (%)	-	3	25
Tryptophan-like aromatic proteins (%)	-	45	16
Tyrosine-like aromatic proteins (%)	-	23	8
Soluble microbial metabolic products (%)	-	23	14
TSS (mg L^{-1})	128	157	219
Total nitrogen – T_N (mg L^{-1})	540	260	1160
Sulphate – SO_4^{2-} (g L^{-1})	12.7	4.9	0.29
Sulphite – SO_3^{2-} (mg L^{-1})	2500	2575	-
Sulphide – S^{2-} (mg L^{-1})	500	450	-
Chloride – Cl^- (g L^{-1})	15.4	14.5	1.2

The developed treatment strategy for the HISWL leachate was complex, encompassing six treatment stages for the leachate collected in a first time (Chapters 3 and 4) and a four treatment stages for the leachate collected in a second time (Chapter 5), and allowed reaching a COD value below 1000 mg O_2 L^{-1}, a common limit imposed by MWWTPs to receive pre-treated effluents, but not the European and Portuguese COD legal requirements for the discharge of wastewaters into waterbodies (150 and 125 mg O_2 L^{-1}). In turn, the developed treatment line for the NHISWL leachate only included three stages and permitted achieving a final effluent in agreement with both European and Portuguese regulations for the discharge of treated effluents into aquatic systems. This sustains a higher complexity for the HISWL leachate matrix.

The six-stage treatment line for the HISWL leachate collected in a first time included: (i) catalytic oxidation of sulphide and sulphite using H_2O_2 (H_2O_2:S^{2-} and H_2O_2:SO_3^{2-} molar ratios of 4:1 and 1:1, respectively), with partial formation of sulphate, (ii) chemical precipitation of sulphate as pure barite, (Ba^{2+}:SO_4^{2-} molar ratio of 1:1), (iii) 1st biological oxidation for biodegradable organics removal and nitrification/denitrification, (iv) coagulation with $FeCl_3$ (dose of 100 mg Fe L^{-1}) at acidic pH (2.8) for removal of a fraction of recalcitrant organics and suspended solids, (v) PF-UVA process for ~4 h at pH 2.8 and initial TDI content of 140 mg L^{-1} in order to degrade the recalcitrant organics while enhancing the biodegradability, and (vi) 2nd biological oxidation for removal of the biodegradable fraction generated during the AOP. Catalytic oxidation using H_2O_2 for the removal of sulphide and sulphite was preferable to O_2-driven catalytic oxidation because of the release of high amounts of VOCs and toxic substances during the latter process. The removal of the high sulphur content before biological treatment was crucial for avoiding the inhibition of the activated sludge activity. On the other hand, the high values of remaining salinity in the HISWL leachate did not totally inhibit the activated sludge activity using well acclimatized bacteria. But the same did not occurr when applying the AO process since high amounts of the hazardous chlorine gas were released due to the presence of the high amounts of chloride. Beyond that, high amounts of foam were generated during the AO process. The PEF process also revealed some important operational drawbacks related to the deposition of particles on the cathode surface that inhibited the electrochemical generation of H_2O_2. A special highlight must be given to the formation of a monophasic barite precipitate with commercial value at the second stage of treatment of the hazardous effluent.

The four-stage integrated treatment for the HISWL leachate collected in a second time encompassed similar stages (i) and (ii) followed by (iii) O_3/H_2O_2 process for ~2 h under free pH, transfer of ~3.5 kg O_3 per m^3 leachate and consumption of ~1.1 kg H_2O_2 per m^3 leachate, and (iv) a similar 2nd biological oxidation for removal of the biodegradable fraction generated during the AOP. This HISWL leachate did not contain biodegradable compounds to justify the application of biological oxidation after chemical precipitation.

The three-stage de-pollution approach for the NHISWL leachate comprised: (i) coagulation with $FeCl_3$ (dose of 300 mg Fe L^{-1}) at acidic pH (4.0) for partial removal of organics and phosphorous, (ii) PF-UVC process for ~4 h at pH 4.0 and initial TDI of 115 mg L^{-1} for recalcitrant organics oxidation and biodegradability enhancement, and (iii) biological process for removal of the previously generated biodegradable organics (and nitrogen compounds in the case of optimized operational conditions). The

application of coagulation prior to the AOP/EAOP stage has proved indispensable for the fulfilment of legislation demands.

The two developed treatment strategies can be suitable for the remediation of a wide range of ISWL leachates with quite similar characteristics.

7.2 Suggestions for future work

The application of biological processes must be better investigated, aiming for faster and more efficient organics degradation and nitrification/denitrification processes. In particular, it would be valuable to study the biota in detail, quantifying and qualifying the bacteria communities, and also test other technologies, as the granular biomass, which application has been increasing in the last years. Considering granule's high size and structure, it can be expected that: (i) in the aerobic outer layer containing autotrophic and heterotrophic organisms, the ammonium will be oxidized to nitrate/nitrite (NOx) and biodegradable organic matter will be degraded, during aerobic stage; and (ii) in the anaerobic/anoxic core containing anaerobic/denitrifying organisms, sulphate/NOx will be heterotrophically reduced to sulphide/nitrogen, if biodegradable organic matter is present, during anaerobic/anoxic stage. On the other hand, even in the aerobic stage, nitrogen can be removed at granule's core, via: (i) autotrophic sulphide oxidation with NOx as electron acceptor; and (ii) autotrophic ammonium oxidation with nitrite as electron acceptor. This could translate into reductions in the external carbon source needs.

For the improvement of the ozonation process, innovative reactors can be tested in order to break barriers as: high ozone supply demands, extended contact times, and equipment bulky size. Hence, it is intended to explore this underdeveloped area by incorporating an inverted cone (a very efficient oxygen contactor) in ozonation processes, as a down-flow gas-liquid contactor to enhance ozone mass transfer, resulting in a highly compact reaction vessel.